

**The 2nd-Order Smooth Variable Structure Filter (2nd-SVSF)
for State Estimation: Theory and Applications**

**The 2nd-Order Smooth Variable Structure Filter (2nd-SVSF) for State
Estimation: Theory and Applications**

By

Hamed Hossein Afshari, B.Sc., M.Sc.,

A Thesis

Submitted to the School of Graduate Studies
in Partial Fulfilment of the Requirements
for the Degree of Doctor of Philosophy
in Mechanical Engineering
at McMaster University, Hamilton, ON,
Canada

Doctor of Philosophy (2014)

McMaster University

(Mechanical Engineering)

Hamilton, Ontario

TITLE: The 2nd-Order Smooth Variable Structure Filter (2nd-SVSF) for State Estimation: Theory and Applications

AUTHOR: Hamed Hossein Afshari, B.Sc., M.Sc., (K. N. Toosi University)

SUPERVISOR: Dr. Saeid R. Habibi

NUMBER OF PAGES: XX, 241

Permission to Use

In presenting this thesis in partial fulfillment of the requirements for a Postgraduate degree from McMaster University, I agree that the Libraries of this University may take it freely available for inspection. I further agree that the permission for copying this thesis in any manner, in whole or in part for scholarly purposes, may be granted by the professors who supervised my thesis work or, in their absence, by the head of the Department or the Faculty Dean in which my thesis work was conducted. It is understood that any copying or publication or use of this thesis or parts thereof for financial gain shall not be allowed without my writing permission. It is also understood that due recognition shall be given to me and McMaster University in any scholarly use which may be made of any material in my thesis. Requests for permission to copy or to make other use of material in this thesis, in whole or part, should be addressed to:

Head of Department of Mechanical Engineering

McMaster University

Faculty of Engineering

1280 Main Street West

Hamilton, Ontario L8S 4L6

Canada

Abstract

Kalman-type filtering methods are mostly designed based on exact knowledge of the system's model with known parameters. In real applications, there may be considerable amount of uncertainties about the model structure, physical parameters, level of noise, and initial conditions. In order to overcome such difficulties, robust state estimation techniques are recommended. This PhD thesis presents a novel robust state estimation method that is referred to as the 2nd-order smooth variable structure filter (2nd-order SVSF) and satisfies the first and second order sliding conditions. It is an extension to the 1st-order SVSF introduced in 2007. In the 1st-order SVSF chattering is reduced by using a smoothing boundary layer; however, the 2nd-order SVSF alleviates chattering by preserving the second order sliding condition. It reduces the estimation error and its first difference until the existence boundary layer is reached. Thereafter, it is presented that the estimation error and its difference remain norm-bounded given bounded noise and modeling uncertainties. As such, the 2nd-order SVSF produces more accurate and smoother state estimates under uncertain conditions than the 1st-order version. The main issue with the 2nd-order SVSF is that it is not optimal in the mean square error sense.

In order to overcome this issue, the dynamic 2nd-order SVSF is initially presented based on a dynamic sliding mode manifold. This manifold introduces a variable cut-off frequency coefficient that adjusts the filter bandwidth. An optimal derivation of the 2nd-order SVSF is then obtained by minimizing the trace of the state error covariance matrix with respect to the cut-off frequency matrix. An experimental setup of an electro-hydrostatic actuator is used to compare the performance of the 2nd-order SVSF and its optimal version with other estimation methods such as the Kalman filter and the 1st-order SVSF. Experiments confirm the superior performance of the 2nd-order SVSF given modeling uncertainties.

Acknowledgements

The author would like to express his gratitude to his supervisor, Dr. Saied R. Habibi, for his guidance, advice, and support during the course of his research and the writing of this dissertation. Special thanks must be conveyed to the committee members; Dr. G. Bone, Dr. S. Veldhuis, and Dr. T. Kirubarajan for their kindness, encouragement, support during committee meetings. Furthermore, special gratitude to fellow graduate students Andrew Gadsden, Ali Gorji, Mina Attatri, and Xiang Hu for their kind assistance, technical expertise, and support during this PhD research.

Financial support provided by the School of Graduate Studies, the Department of Mechanical Engineering, and the Ontario Graduate Scholarship (OGS) program is acknowledged and greatly appreciated.

I would also like to convey my gratitude to my parents, Khadijeh and Sadrollah, and siblings, Abbass, and Maryam, for their encouragement and support throughout my entire academic career.

Table of Contents

Abstract.....	IV
Acknowledgments.....	V
Table of Contents.....	VI
List of Figures.....	X
List of Tables.....	XIIV
List of Abbreviations.....	XV
List of Nomenclature.....	XVII
Chapter 1: Introduction.....	1
1.1. Problem Statement.....	2
1.2. Hypotheses and Objectives.....	8
1.3. Organization of the Thesis.....	11
Chapter 2: Literature Review on Gaussian State Estimation.....	13
2.1. Introduction.....	14
2.2. State Estimation of Stochastic Dynamic Systems.....	17
2.2.1. Bayesian Paradigm for State Estimation.....	18
2.2.2. Gaussian Assumption for the Bayesian Estimation Paradigm.....	20
2.3. Gaussian Filters for Linear Systems.....	25
2.3.1. Linear Optimal State Estimation.....	26
2.3.1.1. The Wiener-Kolmogorov Filter (WF).....	25
2.3.1.2. The Kalman Filter (KF).....	27
2.3.1.3. Extensions to the Kalman Filter.....	30

2.3.2. Linear Robust Kalman Filter.....	34
2.4. Gaussian Filters for Nonlinear State Estimation.....	39
2.4.1. Linearization-Based Filtering.....	41
2.4.1.1. The Extended Kalman Filter (EKF).....	41
2.4.2. Numerical Integration-Based Filtering.....	43
2.4.2.1. The Unscented Kalman Filter (UKF).....	46
2.4.2.2. The Gauss-Hermite Filter (GHF).....	50
2.4.2.3. The Quadrature Kalman Filter (QKF).....	52
2.4.2.4. The Cubature Kalman Filter (CKF).....	55
2.4.2.5. The Monte Carlo Kalman Filter (MCKF).....	60
2.4.2.6. The Gaussian Particle Filter (GPF).....	63
2.4.3. Adaptive Filtering.....	66
2.4.3.1. Adaptive Filtering with Gain Adaptation.....	67
2.4.3.2. Kalman Filtering with Adaptive Noise Estimation.....	68
2.4.3.3. The Multiple Models (MM) Filtering.....	69
2.4.3.3.1. Static versus Dynamic MM Filters.....	72
2.4.3.3.2. The Interacting Multiple Model (IMM) Strategy.....	75
2.4.3.3.3. The Multiple Models Adaptive Estimation (MMAE).....	80
2.4.4. The Nonlinear Robust Filtering.....	83
2.4.4.1. The Variable Structure-Type Filtering.....	83
2.4.4.1.1. The Variable Structure Filtering (VSF).....	85
2.4.4.1.2. The Smooth Variable Structure Filter (SVSF).....	87

2.4.4.1.3. The SVSF with Variable Boundary Layer (SVSF-VBL).....	91
2.4.4.2. The H_{∞} Filtering.....	94
2.5. Summary.....	98
Chapter 3: The Novel 2nd-Order SVSF for State Estimation.....	99
3.1. Introduction.....	100
3.2. Sliding Mode Control Theory.....	102
3.3. The 2 nd -Order SVSF Estimation Process.....	109
3.4. A New Stability Rule for Second-Order Sliding Mode Systems.....	113
3.5. Derivation of the 2 nd -Order SVSF Corrective Gain.....	118
3.6. The 2 nd -Order SVSF for Linear Systems with Fewer Measurements than States...	126
3.7. Comparative Analysis of the 2 nd -Order SVSF.....	129
3.8. Summary.....	138
Chapter 4: The Optimal 2nd-Order SVSF Based on a Dynamic Sliding Manifold..	140
4.1. Introduction.....	141
4.2. The Optimal 2 nd -Order SVSF Estimation Process.....	143
4.3. Corrective Gain for the 2 nd -Order SVSF Method.....	152
4.4. Derivation of an Optimal Cut-Off Frequency Matrix.....	156
4.5. Geometrical Interpretation of the Cut-Off Frequency Matrix.....	164
4.6. The Optimal 2 nd -SVSF for Systems with Fewer Measurements than States.....	165
4.7. Comparative Analysis of Combined Method (Dynamic & Optimal 2 nd -SVSF)	167
4.8. Robustness Analysis with an Explicit Consideration of Uncertainties.....	176
4.9. Summary.....	180

Chapter 5: Application to Fault Detection and Diagnosis.....	182
5.1. Introduction.....	183
5.2. State Estimation-Based FDI Task.....	184
5.3. The Experimental Electro-Hydrostatic Actuator (EHA) Setup.....	186
5.4. State Estimation under the Normal and Faulty Conditions.....	191
5.5. FDI of the EHA Setup Using the State Estimation Approach.....	200
5.5.1. FDI Structure Using the Dynamic 2 nd -order SVSF and the IMM Filter.....	200
5.5.2. Comparative Analysis Using the Experimental EHA Setup.....	205
5.6. Summary.....	213
Chapter 6: Summary and Concluding Remarks.....	214
6.1. Summary of the PhD Research.....	215
6.2. Concluding Remarks.....	217
6.3. Recommendations and Future Research.....	219
Bibliography.....	221
Appendix.....	237

List of Figures

Figure 1.1: Block-diagram scheme of a model-based state estimation process.....	3
Figure 1.2: Flow-diagram representation of the PhD research.....	7
Figure 2.1: The 200 year history of main contributions to the estimation theory.....	16
Figure 2.2: Effects of the probability distribution on point state estimation.....	20
Figure 2.3: A block-diagram scheme of a one-cycle Gaussian filtering.....	23
Figure 2.4: A general classification of main Gaussian filters for state estimation.....	25
Figure 2.5: Block-diagram scheme of the Wiener-Kolmogorov filter.....	27
Figure 2.6: Block-diagram scheme of a one cycle Kalman filter.....	29
Figure 2.7: Schematic of the unscented transformation used in the UKF.....	47
Figure 2.8: Comparison of the 2-D point set distribution in UKF and CKF.....	57
Figure 2.9: Block-diagram scheme of a one-cycle GPF estimation process.....	65
Figure 2.10: Schematic of adaptive noise filtering applied to the KF process.....	70
Figure 2.11: Block-diagram scheme of one cycle of a static MM filter.....	74
Figure 2.12: Block-diagram scheme of the interacting multiple model (IMM) strategy...	79
Figure 2.13: Diagram of the multiple model adaptive estimation (MMAE).....	81
Figure 2.14: Combination of MMAE with residual correlation KF bank.....	83
Figure 2.15: Representation of the SVSF estimation concept.....	88
Figure 2.16: Effect of the smoothing layer width ψ on the SVSF performance.....	91
Figure 2.17: Concept of SVSF-VBL for a system in normal and faulty conditions.....	92
Figure 3.1: Main concept of system trajectories under a sliding mode control.....	103
Figure 3.2: A scheme of the 2 nd -order sliding mode regime.....	107

Figure 3.3: Block diagram representation of the 2nd-order SVSF estimation process....123

Figure 3.4: Main concept of the 2nd-order SVSF method for state estimation.....124

Figure 3.5: Main concept of increasing accuracy via the 2nd-order SVSF.....125

Figure 3.6: State estimations by the Kalman filter and 2nd-order SVSF for the normal EHA system.....135

Figure 3.7: State estimations by the Kalman filter and 2nd-order SVSF for the faulty EHA system.....135

Figure 3.8: Profiles of measurement errors by different estimators for normal and faulty EHA.....136

Figure 3.9: Phase portrait of the measurement error and its difference obtained by the 1st-order SVSF.....137

Figure 3.10: Phase portrait of the measurement error and its difference obtained by the 2nd-order SVSF.....137

Figure 4.1: Main concept of the 2nd-order SVSF under the linear sliding manifold.....151

Figure 4.2: A block-diagram of the optimal 2nd-order SVSF estimation process.....161

Figure 4.3: Main concept of combined strategy based on the dynamic and optimal 2nd-order SVSF.....163

Figure 4.4: A geometrical depiction of the cut-off frequency matrix with its entries.....164

Figure 4.5: State estimations by the Kalman filter and the combined strategy (optimal 2nd-order SVSF for the normal condition and dynamic 2nd-order SVSF for the uncertain condition).....173

Figure 4.6: State estimations by the Kalman filter and the combined strategy (optimal 2nd-order SVSF for the normal condition and dynamic 2nd-order SVSF for the uncertain condition).....174

Figure 4.7: Profiles of the measurement error by the Kalman filter and the combined strategy (optimal 2nd-order SVSF for the normal condition and dynamic 2nd-order SVSF for the uncertain condition).....175

Figure 4.8: Phase portrait of the measurement error and its difference produced by the combined strategy (optimal 2nd-order SVSF for the normal condition and dynamic 2nd-order SVSF for the uncertain condition).....175

Figure 4.9: Profiles of the sliding variable and the dynamic sliding mode manifold produced by the combined strategy (optimal 2nd-order SVSF for the normal condition and dynamic 2nd-order SVSF for the uncertain condition).....176

Figure 4.10: Profiles of the cut-off frequency coefficients produced by the combined strategy (optimal 2nd-order SVSF for the normal condition and dynamic 2nd-order SVSF for the uncertain condition).....176

Figure 5.1: A block-diagram scheme of the state estimation-based FDI task.....185

Figure 5.2: Experimental setup of the electro-hydrostatic actuator prototype.....187

Figure 5.3: The circuit diagram of the EHA experimental setup.....188

Figure 5.4: State estimate profiles by different estimators for the normal EHA.....196

Figure 5.5: State estimate profiles by different estimators for the EHA under friction...196

Figure 5.6: State estimate profiles by different estimators for the EHA under leakage...197

Figure 5.7: Phase portrait of the sliding variable and its difference for the normal EHA setup.....197

Figure 5.8: Phase portrait of the sliding variable and its difference for the EHA under friction.....198

Figure 5.9: Phase portrait of the sliding variable and its difference for the EHA under leakage.....198

Figure 5.10: Measurement noise profiles for the normal and faulty EHA setups.....199

Figure 5.11: Block-diagram of the IMM-based dynamic 2nd-order SVSF structure.....204

Figure 5.12: Profile of the input into the EHA setup (motor velocity).....207

Figure 5.13: Measurement profile of the EHA setup (actuator position).....207

Figure 5.14: Total mode probability detections by different methods.....210

Figure 5.15: Mode probability estimate generated by the IMM-based EKF.....211

Figure 5.16: Mode probability estimate generated by the IMM-based 1st-order SVSF...211

Figure 5.17: Mode probability estimate given by the IMM-dynamic 2nd-order SVSF...212

Figure 5.18: Actual and estimated state trajectories using the IMM-based dynamic 2nd-order SVSF method.....212

Figure A.1: Total mode probability detections by different methods.....239

Figure A.2: Normal mode probability results by different methods.....240

Figure A.3: Leakage fault mode probability results by different methods.....241

Figure A.4: Friction fault mode probability results by different methods.....241

List of Tables

Table 3.1: Comparison between RMSE of three estimation methods applied to the EHA model.....	134
Table 3.2: Comparison between Biases of the three estimation methods applied to the EHA model.....	134
Table 3.3: Comparison between STD of the estimation methods applied on the EHA model.....	134
Table 4.1: Comparison between RMSE values of the four estimation methods applied to the EHA model.....	171
Table 4.2: Comparison between bias values of the four estimation methods applied to the EHA model.....	172
Table 4.3: Comparison between STD of the four estimation methods applied to the EHA model.....	172
Table 4.4: Numeric values of the robustness index α for each filter.....	180
Table 5.1: Numeric values of the EHA parameters.....	190
Table 5.2: Numeric values of the friction coefficients.....	191
Table 5.3: Numeric values of the leakage coefficients and flow rate offsets.....	191
Table 5.4: Indicators of different filters under the normal and faulty scenarios.....	195
Table 5.5: Confusion matrix for the IMM-based EKF.....	209
Table 5.6: Confusion matrix for the IMM-based 1 st -order SVSF.....	209
Table 5.7: Confusion matrix for the IMM-based dynamic 2 nd -order SVSF.....	209
Table 5.8: RMSE values of different state estimators for the EHA setup.....	213
Table A.1: Confusion matrix for the IMM-based UKF.....	238
Table A.2: Confusion matrix for the IMM-based CKF.....	238
Table A.3: Confusion matrix for the IMM-based PF.....	238

List of Abbreviations

CDF	Central Difference Filter
CKF	Cubature Kalman Filter
DDF	Divided Difference Filter
EHA	Electro-Hydraulic Actuator
EKF	Extended Kalman Filter
GHF	Gauss-Hermite Filter
GPB	Generalized Pseudo Bayesian
GPF	Gaussian Particle Filter
GSF	Gaussian Sum Filter
H_∞	H-infinity Filter
IIR	Infinite Impulse Response
IMM	Interacting Multiple Models
KF	Kalman Filter
LQG	Linear Quadratic Gaussian
MAP	Maximum <i>A Posteriori</i>
MCKF	Monte Carlo Kalman Filter
MHTA	Multiple Hypothesis Testing Algorithm
MKF	Mixture Kalman Filter
MLE	Maximum Likelihood Estimator
MM	Multiple Models
MMAE	Multiple Models Adaptive Estimation
MMSE	Minimum Mean Square Error
MSE	Mean Square Error
PDAF	Probability Data Association Filter
PDF	Probability Density Function
PF	Particle Filter
QKF	Quadrature Kalman Filter

RKF	Robust Kalman Filter
RMSE	Root Mean-Square Error
SPKF	Sigma-Point Kalman Filter
SVSF	Smooth Variable Structure Filter
SVSF-VBL	SVSF with a Variable Boundary Layer
STD	Standard Deviation
UKF	Unscented Kalman Filter
VSF	Variable Structure Filter
VSM	Variable Structure Multiple Model
WF	Wiener-Kolmogorov Filter

List of Nomenclature

A	Linear state matrix
A_E	EHA piston area
B	Linear control matrix
B_E	EHA load friction
C	Linear measurement matrix
D_P	EHA pump displacement
F	Linearized state matrix
G	Linearized control matrix
H	Linearized measurement matrix
I	Identity matrix
J	Fisher information matrix
K	Filter's gain
L	EHA leakage coefficient
M	EHA load mass
N	Sample size
$\mathcal{N}(\boldsymbol{\mu}, \boldsymbol{\Sigma})$	Gaussian distribution
P_{xx}	Covariance
P_{xy}	Cross covariance
P_{k k}	Conditional Probability
Q	Process noise covariance matrix
R	Measurement noise covariance matrix
S	Vector of sliding variables
S_{rc}	Residual covariance matrix
T	Sample rate
Tr	Trace of a matrix
V	Lyapunov function
V₀	EHA initial cylinder volume

W	Weights used by filters
e_x	State error
e_y	Artificial measurement
e_z	Measurement error
f	Nonlinear state model
g	Nonlinear control model
i, j	Index value
k	Sample time
m	Mode number in the MM filters
n	Number of states
p_{ij}	Mode transition matrix
s	Sliding mode variable
u	Control vector
v	Measurement noise
w	Process noise
x	State vector
y	Artificial measurement vector
z	Measurement vector
\square	Absolute value
$\ \square\$	Euclidean norm
$\bar{\square}$	Mean value
$\hat{\square}$	Estimated value
$\tilde{\square}$	Error (residual) value
$(\square)^T$	Transpose operator
$(\square)^{-1}$	Inverse operator
$(\square)^+$	Pseudo inverse operator
diag(\square)	Creation of a square matrix with diagonal elements
$E\{\square\}$	Expected value

Pr (□)	Probability function
p (□)	Probability distribution function
sat (□)	Saturation function
sign (□)	Signum function
$\square_{k+1 k}$	<i>a priori</i> value
$\square_{k+1 k+1}$	<i>a posteriori</i> value
○	Schur product
*	Convolution operator
β	Existence subspace
β_e	EHA effective bulk modulus
γ	Convergence rate
Θ	H_∞ performance bound
π	Markovian transition probability
μ	Mean value
μ_i	Mixing probability of the i^{th} mode in the IMM filter
Λ	Likelihood function
Σ	Variance
ξ	Sigma points of the UKF
δ	Kronecker delta
ψ	Smoothing boundary layer

Chapter 1

Introduction

This chapter presents an introduction to the PhD thesis. It initially explains the state estimation task and the two concepts of optimality and robustness in state estimation. Thereafter, it discusses the main hypotheses and objectives of this research as well as the main contributions. For more clarity, a flow-diagram of the research is provided in Figure 1.2.

1.1. Problem Statement

Real-time control systems can benefit from reliable parameter and state estimates for better performance. Estimation is the process of extracting information pertaining to a state variable or a parameter from measurements. In general, the term *parameter* refers to a time-invariant physical quantity that may be a scalar, a vector, or a matrix. The term *state* usually refers to a vector that evolves over time by the use of an equation which describes the dynamics of a system [1]. In this context, there exist two different classes of estimators which include the parameter estimator and the state estimator. The main goal of the estimation task is to minimize the state or parameter estimation error while being robust to uncertainties and perturbations. Noise and perturbations are inherently present in the measurement process, and are caused by instruments and environmental factors. System uncertainties are usually caused by inaccuracies in modeling the process, approximations, nonlinearities, and variations in physical parameters of the system.

The conventional state estimation approaches are mainly based on the well-known Bayesian rule of statistics. In these approaches, the *a posteriori* probability density function (PDF) of the states is recursively calculated based on the known *a priori* PDF and newer measurements. The calculation includes two main steps: prediction and update. In the prediction stage, the system model is used to predict state values. The predicted values of states are then refined and updated based on measurements from the system. There are three concepts that include smoothing, filtering, and prediction. Smoothing uses the measurements beyond the desired time of interest, $t_{obs} > t_{est}$, to refine the estimates further. Filtering uses measurements up to and including the time of interest, $t_{obs} \leq t_{est}$. Prediction only uses measurements prior to the time of interest and thus predicts the future of the system's state, $t_{obs} < t_{est}$ [1]. A model-based state estimation process is

generally constructed based on the available knowledge of the system summarized in four items:

1. The state transition model;
2. The measurement model;
3. The input or its probabilistic characterization;
4. The prior knowledge of the system.

Figure 1.1 shows a block-diagram scheme of a model-based state estimation process.

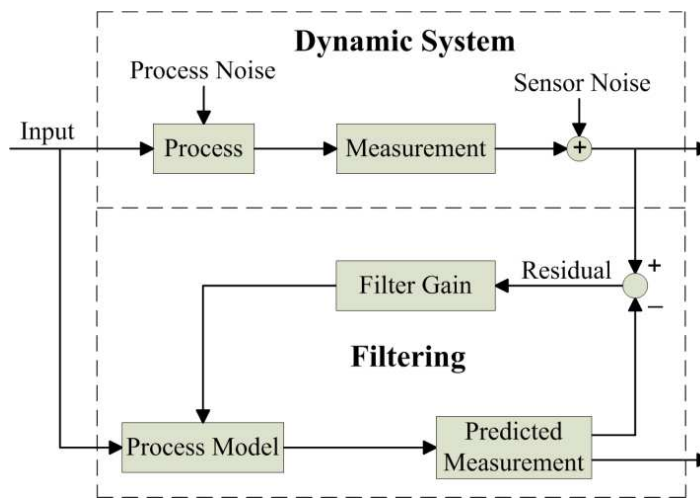


Figure 1.1: Block-diagram scheme of a model-based state estimation process

The recursive equation of an estimated posteriori PDF may be calculated in an optimal form with linear state transition and measurement models subjected to Gaussian white additive noise. In such cases, the *a posteriori* PDF is expressed by simply using the mean and the covariance terms. Thereafter, the *a posteriori* mean and covariance are predicted and updated. The most popular method used to solve linear Gaussian state estimation problems is the Kalman filter. For general nonlinear and non-Gaussian systems, several techniques using linearization (e.g., the Extended Kalman filter) or PDF

approximation (e.g., the Unscented Kalman filter, or the Cubature Kalman filter) have been proposed. More recently and with increasing computational power, the Particle Filters (PF) are increasingly being used in nonlinear or non-Gaussian estimation problems. The PF technique uses a set of weighted particles which approximates the state *a posteriori* PDF. The main disadvantages of particle filtering are its high computational complexity and long running time.

The Kalman-type filtering methods are primarily designed based on the assumptions that noise is white and the system's model is known. In real applications, noise may be non-Gaussian and there may be considerable uncertainties in the model structure, physical parameters, and initial conditions. In some situations, the system dynamic may be too complex to model; or, the system structure or parameters may change thus causing uncertainties.

Two filtering strategies for dealing with uncertainties are referred to as the robust state estimation and the adaptive state estimation. The main objective of robust estimation is designing a filter that would not be affected or minimized the impact of uncertainties [2]. The prevalent forms of robust state estimation methods are the robust Kalman (or H_2) filter, the H_∞ filter, and the new Smooth Variable Structure Filter (SVSF). Otherwise, the adaptive estimation approach is primarily used to estimate both the states and the unknown parameters that may change with time.

A new robust estimation strategy based on the variable structure system's concept was introduced in 2007, referred to as the Smooth Variable Structure Filter (SVSF) [3]. The SVSF has a predictor-corrector structure and uses a discontinuous corrective gain to push the state estimates towards their true values. The discontinuous corrective action of the SVSF method satisfies the first sliding condition and hence achieves robustness to

bounded uncertainties. This filter alleviates the need for tuning by trial and error and presents a mechanism for an explicit consideration of modeling uncertainties within the filter formulations. The main concern of this type of filter is eliminating the unwanted chattering effects from state estimates. The chattering phenomenon arises from discontinuous corrective actions inherent in sliding mode control systems [3].

A smoothing boundary layer is commonly used to suppress chattering in sliding mode control systems [4,5], and also applied to the SVSF's gain formulation. The implementation of the smoothing action is through a saturation function that interpolates the discontinuous corrective action within a smoothing boundary layer around the switching hyperplane. Outside the smoothing boundary layer the discontinuous correction is fully applied to maintain stability. The width of the smoothing boundary layer is defined as a function of the upper bound of noise, uncertainties, and perturbations [3]. Note that by interpolating the switching function within the smoothing boundary layer, the accuracy and robustness of the sliding mode are compromised [6,7].

The SVSF state estimation method has been used in a number of applications including target tracking [8,9], control as well as in parameter estimation for fault detection in an Electro-Hydrostatic Actuation (EHA) system [10]. Gadsden extended the SVSF by deriving a state error covariance term for it and using that for obtaining an optimal smoothing boundary layer [11,12,10]. The SVSF with an optimal time-varying boundary layer results in an optimal filter within the smoothing boundary layer when applied to linear Gaussian problems. However, the method still uses a smoothing boundary layer that interpolates the discontinuous corrective action in the vicinity of the switching hyperplane at the expense of robustness.

The higher order sliding mode concept is a strong alternative to the smoothing boundary layer for chatter avoidance. This concept is based on forcing the higher order time-derivatives of the sliding variable to satisfy additional constraints related to sliding motion. Along with keeping the main advantages of the variable structure systems, this concept is capable of reducing and in some cases removing the chattering effect completely. The higher order sliding mode concept provides better accuracy without compromising robustness and without the need to approximate or relax the discontinuous corrective action. The sliding mode order implies the degree of dynamic smoothness in the vicinity of the switching surface [6,7,13]. There are many publications on the second-order sliding mode control method [14,15,16,17]. Other research on higher order sliding mode systems includes Sira-Ramirez's dynamic sliding mode technique based on augmenting the differential algebraic approach to system formulations. This approach presents switching surfaces that produce chatter-free sliding mode for a special class of nonlinear systems [16,17].

In this thesis, a 2nd-order SVSF state estimation method is firstly proposed and formulated. It can satisfy both the first and second sliding mode conditions. It is capable of estimating state variables both for linear and nonlinear systems in noisy and uncertain conditions in which the level, source and occurrence of uncertainties are unknown. The main advantage of the 2nd-order SVSF is that it alleviates chattering without the needs for approximation or interpolation. This capability leads to better accuracy and robustness in uncertain conditions. The 2nd-order SVSF derivation is based on a discrete Lyapunov function that contains the first and second-order derivatives of the sliding variable.

Optimal derivation of the 2nd-order SVSF, referred to as the optimal 2nd-order SVSF method, is one of the contributions of this research. This method is applied to systems

with linear state and measurement models that are subject to white additive noise. A new formulation for the corrective gain is calculated based on the dynamic sliding mode concept. A linear sliding mode manifold is defined in terms of the sliding variable and its first difference. It is later proven that the slope of this linear manifold is effectively a cut-off frequency that filters chattering and can dynamically be updated at each time step. In order to formulate the optimal 2nd-order SVSF, the *a posteriori* state error covariance needs to be minimized by finding the optimal value of the cut-off frequency at each step.

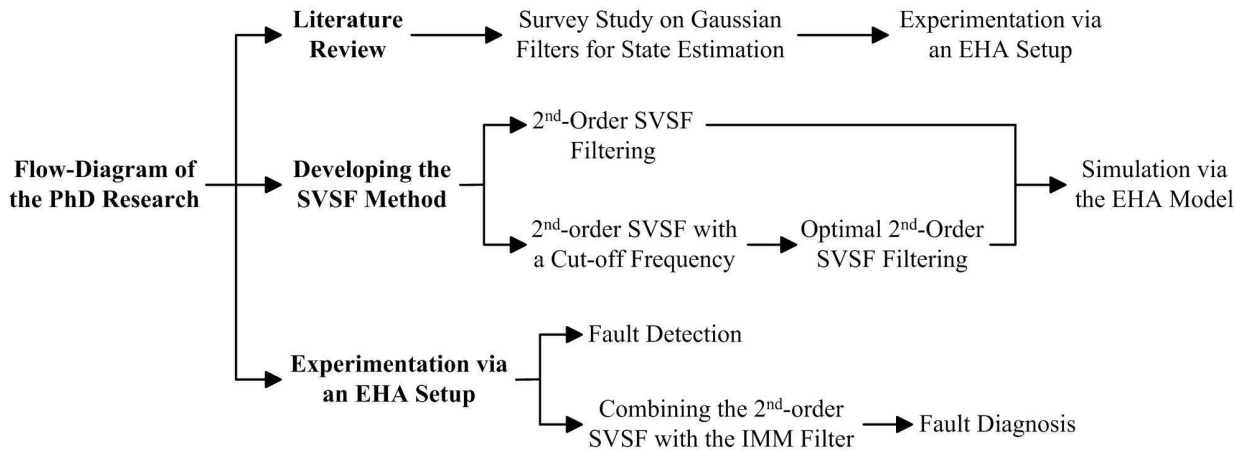


Figure 1.2: Flow-diagram representation of the PhD research

In order to verify robustness and accuracy of the 2nd-order SVSF and its optimal version, they are implemented on an experimental EHA setup for the fault detection and diagnosis purpose. Fault detection is performed by comparing the RMSE of state estimates with ones under normal condition. Moreover, fault diagnosis is performed by combining the 2nd-order SVSF with the Interacting Multiple Models (IMM) filter. The mode probability estimate represents the current operating regime (normal or faulty) of the system. The IMM-based 2nd-order SVSF successfully identified the correct operating regime with smaller values of RMSE and higher values of the mode probability.

Experimentations confirm the superior performance of the 2nd-order SVSF method in comparison to other state estimators such as the Kalman filter and the 1st-order SVSF. Figure 1.2 shows a flow-diagram of the PhD research that represents sequence of the main steps of the research.

1.2. Hypotheses and Objectives

The smooth variable structure filter (SVSF) formulation stems from a stability theorem that can result in an algorithm with an inherent switching action that preserves convergence of estimates to within a neighborhood of actual states. This research will initially concentrate on designing the 2nd-order SVSF state estimation method that satisfies the first and second order sliding mode conditions. A dynamic 2nd-order SVSF method is then formulated using a dynamic sliding mode manifold. An optimal derivation of the dynamic 2nd-order SVSF is then presented by minimizing the trace of the error covariance matrix. The main hypotheses of this PhD research are as follows:

1. Dynamic systems are described using mathematical equations in the state-space form. This form uses a set of first-order differential equations in order to provide a mathematical model of the system as a function of input, output and state variables. A discrete realization of the state space model is used in the linear and/or nonlinear form for designing the state estimator and control rules.
2. The 2nd-order SVSF method provides more accurate, robust and smoother state estimates in comparison to the standard SVSF method. It shows a superior performance over the Kalman filter under uncertain conditions. The 2nd-order SVSF applies constraints to the measurement error and its first difference such that they approach zero in finite time.

3. The robust 2nd-order SVSF method may not produce accurate state estimates under the normal operating condition. An optimal derivation of the 2nd-order SVSF is hence required for minimizing the trace of the state error covariance matrix. In this context, a new formulation of the 2nd-order SVSF is sought that introduces a variable cut-off frequency coefficient.
4. The 2nd-order SVSF method may be used for creating a robust fault detection and diagnosis structure. It is a combination of the Interacting Multiple Models (IMM) filter and the 2nd-order SVSF for robust state estimation. It applies to an experimental EHA setup for fault detection and identification.

The main objectives of this PhD research may be summarized as to:

1. perform a survey study on Gaussian filters for state estimation;
2. design and implementation of the 2nd-order SVSF method for robust state estimation;
3. design and implementation of the optimal 2nd-order SVSF that minimizes the error covariance matrix by automatically adjusting an optimal cut-off frequency coefficient;
4. combine the 2nd-order SVSF method with the IMM filter in order to construct state estimation under different operating modes; and
5. apply the 2nd-order SVSF and its optimal version to an experimental EHA setup for fault detection and diagnosis.

The main publications from this PhD research are:

Journal Papers:

1. **H.H. Afshari**, S.A. Gadsden, and S.R. Habibi, “Robust fault diagnosis of an electro-hydrostatic actuator using the optimal 2nd-order SVSF and the interacting multiple model (IMM)”, *International Journal of Fluid Power*, 2014, (In Press).

2. **H.H. Afshari**, and S.R. Habibi, “Second-order smooth variable structure filter for robust state estimation”, *ASME Journal of Dynamic Systems, Measurement, and Control*, (Submitted on November 2013).
3. **H.H. Afshari**, S.A. Gadsden, and S.R. Habibi, “A tutorial on Gaussian state estimation techniques: review and recent trends”, *Signal Processing*, (Submitted on October 2014).
4. H.H. Afshari, and S.R. Habibi, “Dynamic 2nd-order smooth variable structure filter based a dynamic sliding manifold”, *Automatica*, (Submitted on November 2014).
5. H.H. Afshari, and S.R. Habibi, “A new adaptive control scheme based on the interacting multiple model (IMM) estimation”, *Journal of Mechanical Science and Technology*, (Submitted on September 2014).

Conference Papers

6. **H.H. Afshari**, S.A. Gadsden, and S.R. Habibi, “A robust fault diagnosis scheme based on the interacting multiple model (IMM) and the 2nd-order SVSF methods”, *ASME International Mechanical Engineering Congress and Exposition, IMECE2014-36438*, Montreal, Canada, 2014.
7. **H.H. Afshari**, D. Al-Ani, and S.R. Habibi, “Fault prognosis of roller bearings using the adaptive auto-step reinforcement learning technique”, *ASME Dynamic Systems and Control Conference, DSCC2014-6108*, San Antonio, Texas, USA, 2014.
8. **H.H. Afshari**, and S.R. Habibi, ”Robustness analysis of some robust state estimation methods with an explicit consideration of uncertainties”, *IEEE Canadian Conference on Electrical and Computer Engineering*, Halifax, Canada, 2015.
9. **H.H. Afshari**, D. Al-Ani, and S.R. Habibi, “State estimation of faulty actuator using the second-order smooth variable structure filter (the 2nd-order SVSF)”, *IEEE Canadian Conference on Electrical and Computer Engineering*, Halifax, Canada, 2015.

1.3. Organization of the Thesis

This PhD thesis is organized in seven chapters. Chapter 2 presents a literature review on Gaussian filters with applications to state estimation. It firstly describes the Bayesian paradigm for state estimation and then introduces filtering strategies based on the Gaussian assumption of noise and uncertainties. This chapter also describes the prevalent state estimation filters based on the Gaussian assumption. These filters are categorized under two subgroups optimality or robustness. They may be classified into subgroups based on their structural characteristics including ability to estimate linear or nonlinear systems, methods used for approximating nonlinearities, robustness, and adaptation characteristics. New advances and trends relevant to each state estimation method are discussed in detail.

Chapter 3 introduces the novel 2nd-order SVSF method for state estimation. This chapter presents the main steps of this filter, the filter's corrective gain, the proof of stability under the presented gain, and furthermore, adding the Luenberger's observer for the case with lower measurements than states. A linearized model of the EHA is used for simulation under the normal and uncertain cases. The 2nd-order SVSF is also compared with some state estimation approaches such as the Kalman filter, and the former 1st-order SVSF in terms of accuracy, robustness and smoothness.

Chapter 4 presents the design and implementation of the optimal 2nd-order SVSF method applies to systems with linear state and measurement models. It shows a new formulation of the corrective gain by defining a dynamic sliding mode manifold that is a linear combination of the sliding variable and its time difference. The stability proof of the filter under this gain is obtained using a discrete-time Lyapunov stability criterion. This chapter also presents a procedure for predicting and updating the error covariance

matrix for the new derivation of the 2nd-order SVSF. In the next step, the optimal 2nd-order SVSF is obtained by minimizing the error covariance matrix (trace) at each time step. The EHA system is finally used to verify the accuracy and robustness of the optimal 2nd-order SVSF in comparison to other state estimation approaches.

Chapter 5 contains an experimental study involving the implementations of the 2nd-order SVSF and its optimal version on an EHA prototype. The EHA setup is located in the Center for Mechatronics and Hybrid Technology at McMaster University. The EHA experimental setup, its components, and possible fault conditions are briefly described in Appendix I. Chapter 5 presents applications of the 2nd-order SVSF for fault detection and diagnosis of the EHA setup. Its accuracy and robustness are then compared with the Kalman filter and the 1st-order SVSF under the normal and faulty EHA conditions. Chapter 6 summarizes the major contributions of the PhD research, concluding remarks, and some suggestions for future research.

Chapter 2

Literature Review on Gaussian State Estimation

The development of state estimation methods started nearly five centuries ago and has involved contributions from a variety of fields. This chapter presents a review of the most prevalent Gaussian filters that are used for state estimation of stochastic dynamic systems. Gaussian filters are used in applications where the measurement noise and modeling uncertainties can be characterized with a Gaussian distribution. The main concept of state estimation is firstly described based on the Bayesian paradigm and Gaussian assumption of the noise. The various forms of this type of filter are then categorized into optimality and robustness subgroups. Each category itself includes linear and nonlinear filtering; the nonlinear filtering methods often involve linearization or approximations. New advances and trends are discussed in detail.

2.1. Introduction

Estimation is the process of extracting the value of a state or parameter from indirect, inaccurate and uncertain measurements. In this context, there exist two different classes of estimators which include the parameter estimator and the state estimator. The main goals of the estimation task are to minimize the state or parameter estimation error while being robust to uncertainties and perturbations. Noise and perturbations are inherently present in the measurement process, and are caused by instruments and environmental factors. System uncertainties are usually caused by inaccuracy in modeling the process, and small variations of physical parameters due to the aging phenomenon.

Major contributions to the probability field began in the fifteen century, and included a large number of contributors from a variety of backgrounds. Girolamo Cardano (1564-1642), as the first major contributor to this field, introduced an accurate analysis of probabilities. His book about games of chance, “*Liber de ludo aleae*”, published in 1663, contains the first systematic treatment of probability [18]. Later on, Jakob Bernoulli (1654-1705) presented the first rigorous proof of the law of large numbers for repeated independent trials called the Bernoulli trials. Thomas Bayes (1701-1761) introduced the famous Bayesian rule for statistical inference that provides the basic formula for Bayesian estimation methods [19]. Pierre de Laplace (1749-1827) developed probability and statistics and used them specifically to solve problems in celestial mechanics [19]. During the nineteenth century, it became apparent that probabilistic theory should be used to study and even model the behavior of some natural phenomena and systems.

The pioneering study that provides an optimal estimate from noisy data was performed by Carl Friedrich Gauss (1777-1855). He invented the famous least square estimation method in 1795 and used it to solve nonlinear estimation problems in

mathematical astronomy [20]. Andrei Markov (1856-1922) introduced the Markov process and Markov chain theories based on probability and statistical methods [20]. The Markov theories formulate transitions in random processes from one state to another, between a finite or countable number of possible states. He proved that the probability distribution of states may be calculated using its current distribution that contains the effects of all the past events of the system [21]. Andrei Kolmogorov (1903-1987) published his well-known book, *Foundations of the Theory of Probability*, in 1933 laying the modern axiomatic foundations of probability theory. In 1938, Kolmogorov published his basic theorems for smoothing and predicting stationary stochastic processes that would have major military applications during the Cold War. Sydney Chapman (1888-1970) continued the research on the Markov processes. Chapman and Kolmogorov independently presented the Chapman-Kolmogorov equations used for solving basic equations in the estimation field [20].

Ronald Aylmer Fisher (1890-1962) became famous for his major contribution, the so-called Fisher information matrix. It represents a measure of the amount of information extracted from a sample of values with a given probability distribution [20]. Norbert Wiener (1894-1964) introduced the so-called Wiener filter formulation in 1949 for signal processing applications. This filter reduces the amount of noise present in a signal in comparison with an estimation of the desired noiseless signal [22]. Kolmogorov (1903-1987), along with Wiener, made the foundation of estimation theories that were used later to develop the theory of prediction, filtering, and smoothing. His research ultimately led to the derivation of an optimal estimator, which was formulated for continuous-time systems [23]. Meanwhile, Kolmogorov independently derived an optimal linear predictor for discrete-time systems [24]. Their research would later become famous, known as the Wiener-Kolmogorov filter (WF), a predecessor to the Kalman filter [18].

In 1960, Rudolf Kalman, building on the work of others, introduced a new approach to linear filtering and prediction problems; later referred to as the Kalman filter [21]. The Kalman filter was successfully applied by NASA for the Apollo onboard guidance and quickly became popular as the most practical method for state estimation [18,21,25]. The Kalman filter (KF) uses a linear dynamic model and sequential measurements of the system to provide an optimal state estimate in the presence of Gaussian noise. A continuous version of the KF was later developed by Kalman and Bucy which later became known as the Kalman-Bucy filter [26].

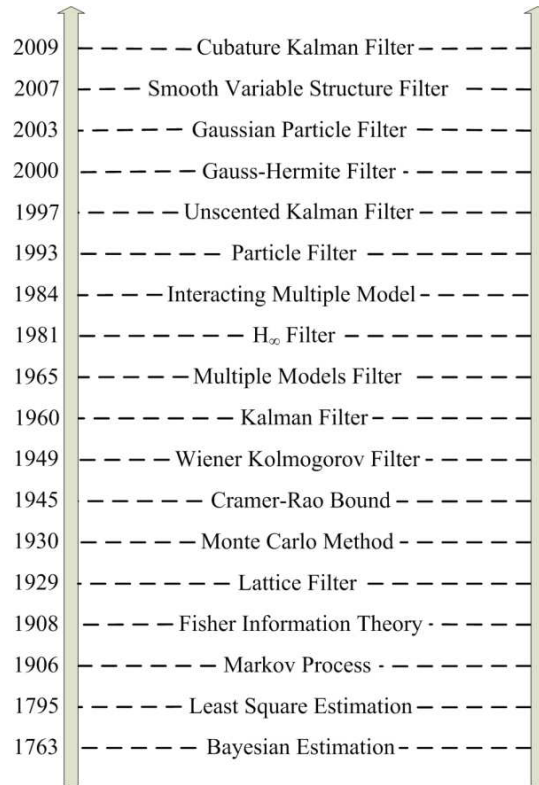


Figure 2.1: The 200 year history of main contributions to the estimation theory

Some extensions to the KF formulation, such as linearization and approximation, led to the extended Kalman filter (EKF) and the unscented Kalman filter (UKF), respectively.

These extensions allowed the KF strategy to be implemented on nonlinear systems for the purpose of state and parameter estimation. Other advanced variants of the Kalman filter include the quadrature Kalman filter (QKF) [27,28], mixture Kalman filter (MKF) [29], and the cubature Kalman filter (CKF) [30]. Figure 2.1 presents the progression of a number of main contributions to the estimation theory from the eighteenth century to present. State estimation methods are extensively used in modern engineering applications. These include control systems, tracking, communications, fault diagnosis and prognosis, biomedical engineering, and economic systems. Depending on the different case studies, linear or nonlinear, full-order or reduced-order, fixed or adaptive filters may be applied. During recent years, this field has attracted a significant amount of attention in both theory and applications [31,32,33,34,35,36].

2.2. State Estimation of Stochastic Dynamic Systems

The task of extracting state variables from inaccurate, uncertain, and noisy measurements is referred to as state estimation. The main objective is to minimize the estimation error when projected to the output space. This error is referred to as the residual or innovation vector. It is important to note that due to the presence of noise and uncertainties (caused by the measurement process, instrumentation, and environment), the measurements cannot reflect exact values of the state variables. In order to construct a framework for the state estimation of stochastic dynamic systems, one may assume a first-order Markov process that is modeled as follows:

$$x_{k+1} = f(x_k, u_k, w_k), \quad (2.1)$$

$$z_{k+1} = h(x_k, v_k), \quad (2.2)$$

where x_k , u_k , and z_k are the state, input, and measurement vectors, respectively, and, w_k and v_k are the process uncertainty and measurement noise at time step k , respectively. It is assumed that f , h , and u_k are known, when w_k and v_k are mutually independent white stochastic processes. The filtering problem is formulated by recursively calculating an estimate of the state vector x_k . This can be achieved by constructing a Bayesian paradigm based on the sequence of measurements Z_k up to time k . Note that there are two main concepts in statistics that help to computationally simplify the process of state estimation. They are the Bayesian paradigm and the Gaussian distribution of states, which will be explained in the subsequent subsections.

2.2.1. Bayesian Paradigm for State Estimation

The main purpose of using a Bayesian paradigm in state estimation is to calculate the conditional *a posteriori* state PDF $p(x_{k+1}|Z_{k+1})$, where $Z_{k+1} = \{z_1, z_2, \dots, z_{k+1}\}$ is the vector of noisy measurements. In order to formulate the state's *a posterior* PDF, a two stage recursive algorithm can be used, when the state *a priori* PDF $p(x_k|z_k)$ is available. It is assumed that the initial PDF of the state is $p(x_0) = p(x_0|z_0)$. The filtering process contains two stages including prediction and update. The Chapman-Kolmogorov equation can be used for the prediction stage using the system model of (2.1) as follows [37]:

$$p(x_{k+1}|Z_k) = \int p(x_{k+1}|x_k)p(x_k|Z_k)dx_k \quad (2.3)$$

where the state transition probability $p(x_{k+1}|x_k)$ is obtained from the state equation (2.1). The Bayesian rule is used to provide the basis for the update stage given by [37]:

$$p(x_{k+1} | Z_{k+1}) = \frac{p(z_{k+1} | x_{k+1}) p(x_{k+1} | Z_k)}{p(z_{k+1} | Z_k)}, \quad (2.4)$$

where $p(z_{k+1} | Z_k)$ is the normalizing constant, and is obtained by [37]:

$$p(z_{k+1} | Z_k) = \int p(z_{k+1} | x_{k+1}) p(x_{k+1} | Z_k) dx_{k+1}, \quad (2.5)$$

This value depends on the likelihood function $p(z_{k+1} | x_{k+1})$ that is obtained from the measurement equation (2.2). From the *a posteriori* PDF, a theoretically optimal state estimate may be computed using an approach such as the minimum mean square error (MMSE), which is as follows [37]:

$$\hat{x}_{k+1|k+1}^{MMSE} \triangleq \int x_{k+1} p(x_{k+1} | Z_{k+1}) dx_{k+1}, \quad (2.6)$$

Alternatively, the maximum *a posteriori* (MAP) method may be used, as follows [37]:

$$\hat{x}_{k|k}^{MAP} \triangleq \arg \max_{x_k} p(x_{k+1} | Z_{k+1}), \quad (2.7)$$

The above calculations are based on two assumptions:

- 1- The state transitions follow a first order Markov process, i.e.,

$$p(x_{k+1} | X_k, Z_{k+1}) = p(x_{k+1} | x_k), \text{ where } X_k = \{x_0, \dots, x_k\};$$

- 2- The measurements are conditionally independent given the states, i.e.,

$$p(z_{k+1} | X_{k+1}, Z_k) = p(z_{k+1} | x_{k+1}) \text{ [38]}.$$

The main purpose of filtering is to construct an accurate posterior PDF of the state based on all available information. Equations (2.3) through (2.5) provide the basis for recursive estimation schemes; with emphasis that they present only a conceptual solution,

which in some scenarios cannot be calculated analytically. It is possible to solve the recursive equation of the estimated posteriori PDF analytically for the estimation problem with a linear state transition and measurement model, subjected to additive noise and uncertainties with Gaussian PDF. As a statistical point of view, in linear systems with Gaussian uncertainties, $p(x_k | Z_k)$ contains all statistical information about x_k . In this way, it is expected to convert the estimation problem to the point estimation in which the mode, mean, or median are estimated. In such cases, the *a posteriori* PDF can be expressed with simply the mean and covariance terms; the *a posteriori* mean and covariance can be predicted and updated recursively. However, this approach is not applicable to nonlinear systems or systems with non-Gaussian uncertainties. Figure 2.2 compares the main concept of point estimation for systems with the Gaussian and non-Gaussian uncertainties. For systems with Gaussian distributions, the mode, mean and median are the same. The most popular method used to solve the linear estimation problem when subjected to the white Gaussian noise is the Kalman filter (KF) [37,25].

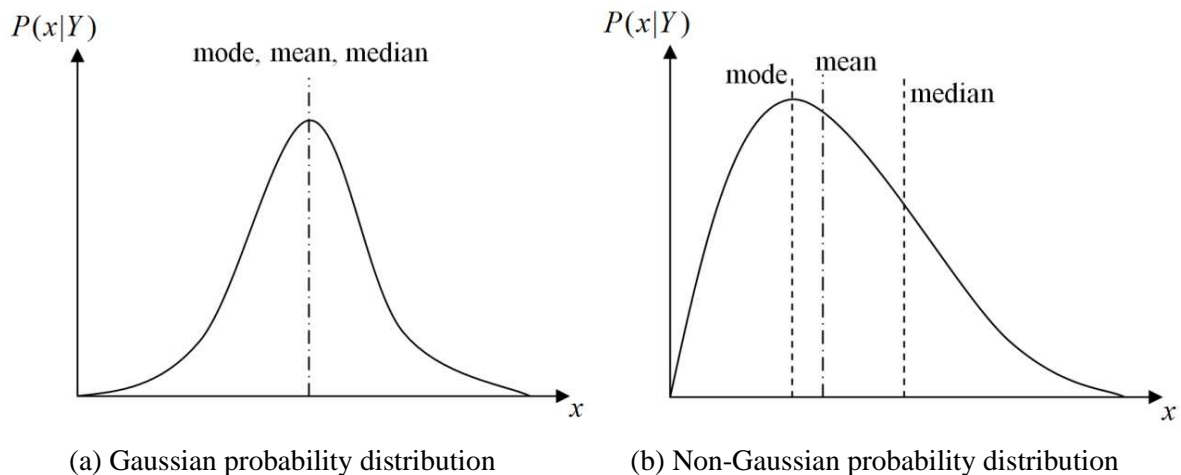


Figure 2.2: Effects of the probability distribution on point state estimation [38]

2.2. Gaussian Assumption for the Bayesian Estimation Paradigm

In order to simplify complex equations of the Bayesian filtering paradigm, Gaussian distributions for the noise and uncertainties are assumed. This assumption provides a Gaussian distribution for the state *a priori* PDF $p(x_{k+1} | Z_k)$ and the filter likelihood density $p(z_{k+1} | Z_k)$ which alternatively results in a Gaussian distribution for the state *a posteriori* PDF $p(x_{k+1} | Z_{k+1})$. In this context, a class of Bayesian filters is formulated under the Gaussian assumption and is referred to as the Gaussian filters. Following this formulation, recursive computations of the former Bayesian filter convert to recursive algebraic computations of the first moment (mean) and the second moment (covariance) of existing conditional PDFs. This procedure is followed for both time and measurement updates, which follow [30].

A. Time Update [30]: In this step, the state's *a priori* mean $\hat{x}_{k+1|k}$ and the state estimation error's *a priori* covariance $P_{k+1|k}$ of the Gaussian distribution are calculated using the expectation operator as follows [30]:

$$\begin{aligned}\hat{x}_{k+1|k} &= E \{ f(x_k, u_k) | Z_k \} \\ &= \int_{\mathbb{R}^{n_x}} f(x_k, u_k) \times N(x_k; \hat{x}_{k|k}, P_{k|k}) dx_k,\end{aligned}\tag{2.8}$$

$$\begin{aligned}P_{k+1|k} &= E \{ (x_{k+1} - \hat{x}_{k+1|k})(x_{k+1} - \hat{x}_{k+1|k})^T | Z_k \} \\ &= \int_{\mathbb{R}^{n_x}} f(x_k, u_k) f^T(x_k, u_k) \times N(x_k; \hat{x}_{k|k}, P_{k|k}) dx_k - \hat{x}_{k+1|k} \hat{x}_{k+1|k}^T + Q_k.\end{aligned}\tag{2.9}$$

where $N(.,.)$ denotes the Gaussian density function.

B. Measurement Update [30]: Since the error in the *a priori* measurement is a zero-mean white stochastic process [39], it is possible to approximate the error to be Gaussian and restate the filter likelihood density as follows [30]:

$$p(z_{k+1} | Z_k) = N(z_{k+1}; \hat{z}_{k+1|k}, P_{zz,k+1|k}), \quad (2.10)$$

where the *a priori* measurement is given by [30]:

$$\hat{z}_{k+1|k} = \int_{\mathbb{R}^{n_x}} h(x_{k+1}, u_{k+1}) \times N(x_{k+1}; \hat{x}_{k+1|k}, P_{k+1|k}) dx_k, \quad (2.11)$$

and the *a priori* covariance and cross-covariance are respectively calculated as [30]:

$$P_{zz,k+1|k} = \int_{\mathbb{R}^{n_x}} h(x_{k+1}, u_{k+1}) h^T(x_{k+1}, u_{k+1}) \times N(x_{k+1}; \hat{x}_{k+1|k}, P_{k+1|k}) dx_k - \hat{z}_{k+1|k} \hat{z}_{k+1|k}^T + R_{k+1}. \quad (2.12)$$

$$P_{xz,k+1|k} = \int_{\mathbb{R}^{n_x}} x_{k+1} h^T(x_{k+1}, u_{k+1}) \times N(x_{k+1}; \hat{x}_{k+1|k}, P_{k+1|k}) dx_k - \hat{x}_{k+1|k} \hat{z}_{k+1|k}^T. \quad (2.13)$$

The Gaussian filter concept then supports the calculation of the state *a posteriori* PDF based on the new measurement z_{k+1} [30]:

$$p(x_{k+1} | Z_{k+1}) = N(x_{k+1}; \hat{x}_{k+1|k+1}, P_{k+1|k+1}), \quad (2.14)$$

and hence, the *a posteriori* state and error covariance may be calculated by [30]:

$$\hat{x}_{k+1|k+1} = \hat{x}_{k+1|k} + W_{k+1}(z_{k+1} - \hat{z}_{k+1|k}), \quad (2.15)$$

$$P_{k+1|k+1} = P_{k+1|k} - W_{k+1} P_{zz,k+1|k} W_{k+1}^T, \quad (2.16)$$

$$W_{k+1} = P_{xz,k+1|k} P_{zz,k+1|k}^{-1}. \quad (2.17)$$

Note that for the case with linear state and measurement functions subjected to an additive zero-mean white Gaussian noise, the above formulation reduces to the Kalman filter. However, the main basis of the Gaussian filter is concentrated on how to calculate the Gaussian weighted integrals that are all formulated as nonlinear functions with Gaussian densities [30]. Figure 2.3 presents a block-diagram concept of a one-cycle Gaussian filtering process.

In the case of nonlinear systems with non-Gaussian noise and disturbances, however, it is impossible to obtain an exact analytical solution. Techniques such as linearization or PDF approximation may be considered to solve the estimation problem. The extended Kalman filter (EKF) technique is the most common Gaussian method for solving recursive nonlinear estimation problems through linearization [20,19,40]. The unscented Kalman filter (UKF) is an extension to the Kalman filter. It uses an unscented transform to approximate the posterior distribution by capturing its mean and covariance accurately to the second order. The corresponding approximation error will be in the third order or higher [20,19,40]. It is important to note that both the EKF and the UKF are recursive MMSE estimators that approximate the posterior distribution as a Gaussian distribution. In the past decade, due to increased computational power, the Particle filter (PF) has attracted considerable interest as a powerful tool for solving nonlinear estimation problems. The PF technique uses a random set of weighted particles that approximate nonlinear characteristics or distributions in the state *a posteriori* PDF.

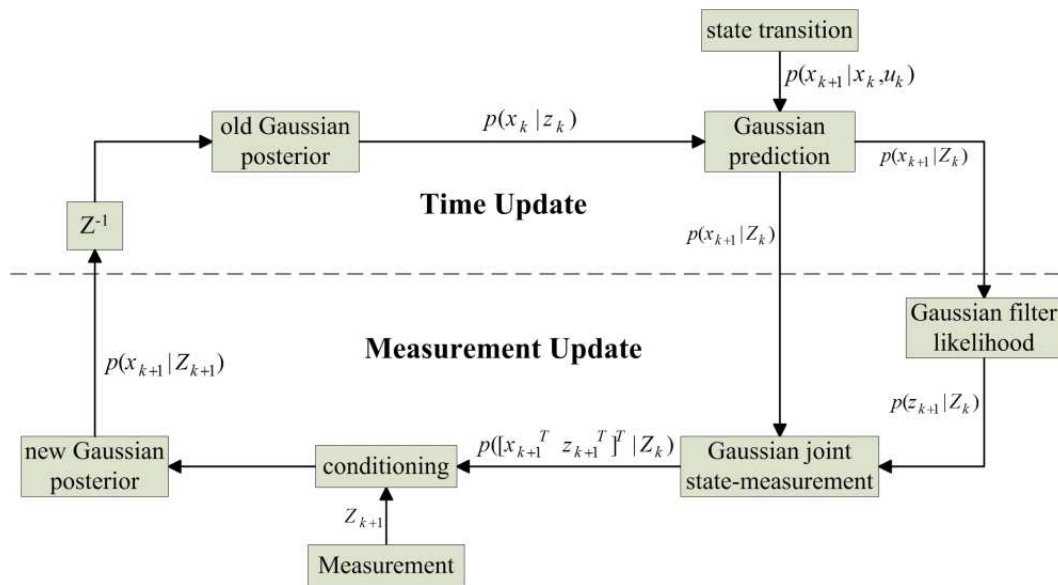


Figure 2.3: A block-diagram scheme of a one-cycle Gaussian filtering [30]

The Kalman-type filtering methods are primarily designed based on the assumption that the system model is known and that noise is white. In real applications, there may be considerable uncertainties about the model structure, physical parameters, level and distribution of noise, and initial conditions. In some situations, the system dynamic is too complex to be modeled exactly, or *a priori* knowledge is not available about parameters such as noise levels or distributions. In other situations, the system structure or parameters may change with time unpredictably. In order to overcome such potential difficulties, there are two approaches in state estimation, when the Kalman-type filtering methods diverge or present unacceptable performance. These two approaches are referred to as the robust state estimation and the adaptive state estimation.

The main objective of robust estimation is designing a fixed filter that presents an acceptable performance for a wide range of modeling uncertainties [81]. The main robust state estimation methods found in the literature are the robust Kalman (or H_2) filter, the H_∞ filter and the variable structure filter (VSF). Otherwise, the adaptive estimation approach is primarily used to estimate both the unknown state and the unknown noise parameters, when in some cases they may considerably change over time. There are two main approaches for adaptive estimation that include the adaptive filter with gain adaptation approach and the multiple models (MM) approach.

In the first approach, the filter gain and parameters are adjusted based on statistical characteristics of noise and uncertainties. This approach includes several techniques such as the joint filtering of state and parameters, the on-line noise tuning, and batch estimation of parameters [81]. In the MM approach, several models of the system, each representing a particular operating regime, are stored and used for state estimation. The final state and covariance estimates are then calculated through a weighted summation of each filter

output. Figure 2.4 shows a general classification of main Gaussian filters that are used for state estimation of stochastic dynamic systems.

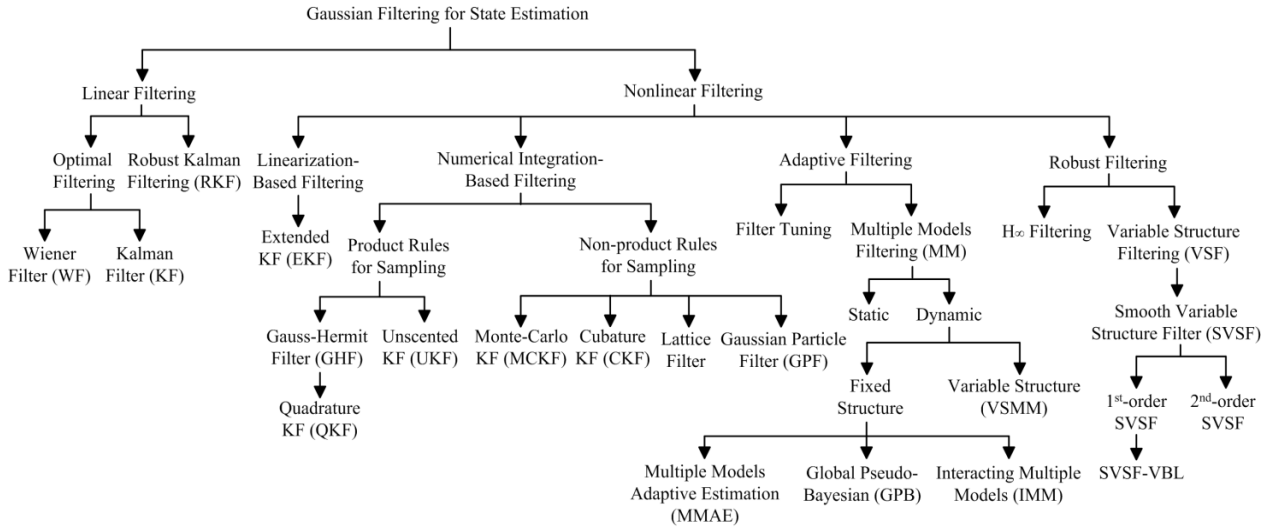


Figure 2.4: A general classification of main Gaussian filters for state estimation

2.3. Gaussian Filters for Linear Systems

Gaussian filters may be used to estimate states of systems with linear or nonlinear state transition models. For linear systems, there are two main approaches including optimal filtering and robust filtering. In the linear optimal filtering, the main purpose is minimizing the estimation error. In robust filtering, the main objective is designing a filter that presents an acceptable performance for a wider range of modeling uncertainties. The optimal filtering for linear Gaussian systems leads to the Wiener-Kolmogorov filter (WF) and its extension, the well-known Kalman filter (KF). In the subsequent sections, these two approaches are reviewed in detail.

2.3.1. Linear Optimal State Estimation

The optimal state estimation is the task of extracting state values from system measurements by minimizing the mean square error (MSE). The Wiener-Kolmogorov filter (WF) is the first contribution into the optimal filtering field and is only applicable to stationary signals. The Kalman filter (KF) is an extension of the WF filter and is applied to linear systems with non-stationary Gaussian signals.

2.3.1.1. The Wiener-Kolmogorov Filter (WF)

The Wiener-Kolmogorov filter (WF) is a statistical estimation method that was independently invented by Norbert Wiener and Andrei Kolmogorov in the 1940's. The major contribution of this filter was the use of a statistical model approach based on the famous Bayesian inference formulation. This statistical estimation method contributed to the development of many other filters including the Kalman filter and particle filter for example. The WF estimates stationary signals with known spectral properties subjected to white noise. The goal of the WF is to filter out the undesirable noise from the measurement signal by minimizing the mean square error (MSE) [20,22].

To formulate the Wiener-Kolmogorov filter, consider the measurement $z(t)$ that is a function of the process signal $x(t)$ that itself contains the noise signal $v(t)$ as follows:

$$z(t) = x(t) + v(t). \quad (2.18)$$

The WF provides an estimate of the signal $\hat{x}(t)$ using a gain K_{WF} as follows:

$$\hat{x}(t) = K_{WF}(t) * z(t), \quad (2.19)$$

where $*$ denotes the convolution operator. The solution to this equation that produces the estimate $\hat{x}(t)$ is obtained in the frequency domain. The WF gain is actually a transfer function formulated by using the Fourier transforms [21]. Note that the WF estimation process minimizes the mean squared error based on the gain given by [41]:

$$K_{WF}(t) = F^{-1} \left[\frac{S_z - S_v}{S_z} \right], \quad (2.20)$$

where F^{-1} denotes the inverse Fourier transforms, S_z and S_v denote the Fourier transforms of the measurement and noise auto-correlations, respectively [41]. NASA implemented the WF for estimation in its space navigation system. Figure 2.5 presents a block-diagram scheme of the WF estimation process.

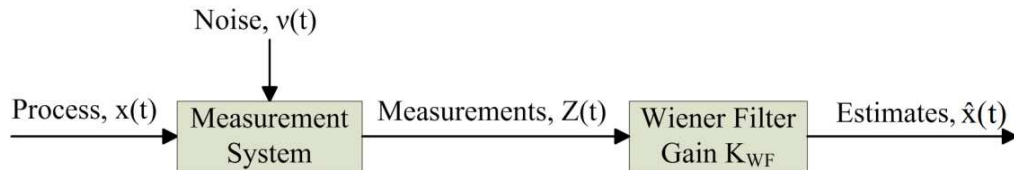


Figure 2.5: Block-diagram scheme of the Wiener-Kolmogorov filter [21]

2.3.1.2. The Kalman Filter (KF)

Rudolf Kalman introduced a new approach to the linear estimation and prediction problem more than 50 years ago that later became famous as the Kalman filter (KF) [42]. It is an optimal recursive Bayesian filter restricted to the class of linear Gaussian estimation problems. The KF is a generalization of the WF and by using a state transition model, adapts itself to non-stationary signals. It was successfully utilized by NASA in the Lunar and Apollo missions. The KF requires a dynamic model of the system, known control inputs, and measurements containing white noise. Under these strict assumptions,

it provides optimal state estimates by recursively predicting the states, estimating the uncertainty of the predicted states, computing a weighted average of the predicted and measured values, and refining the predicted states. There has been a significant amount of research on the KF theory as applied to engineering applications.

A one cycle KF has two main stages: prediction, and update. The prediction step uses the state estimate from the previous time step to produce an estimate at the current time step. This predicted state estimate is also known as the *a priori* state estimate. In the update stage, the current *a priori* prediction is combined with current measurement for refining the state estimate into the *a posteriori* state estimate. To formulate the KF, assume the linearized form of system equations of (2.1) and (2.2) as follows [21]:

$$x_{k+1} = F_k x_k + G_k u_k + w_k, \quad (2.21)$$

$$z_{k+1} = H_{k+1} x_{k+1} + v_{k+1}. \quad (2.22)$$

The KF process for state estimation is now summarized as follows [21]:

1. Prediction Step:

- Calculation of the predicted (*a priori*) state and covariance estimates [21]:

$$\hat{x}_{k+1|k} = F_k \hat{x}_{k|k} + G_k u_k, \quad (2.23)$$

$$P_{k+1|k} = F_k P_{k|k} F_k^T + Q_k. \quad (2.24)$$

2. Update Step

- Calculation of the innovation (or measurement error) and its covariance [21]:

$$V_{k+1} = z_{k+1} - \hat{z}_{k+1|k}, \quad (2.25)$$

$$S_{rc,k+1} = R_{k+1} + H_{k+1} P_{k+1|k} H_{k+1}^T. \quad (2.26)$$

- Calculation of the optimal Kalman gain [21]:

$$K_{k+1} = P_{k+1|k} H_{k+1}^T S_{rc,k+1}^{-1}. \quad (2.27)$$

- Calculation of the update (*a posteriori*) state and covariance estimates [21]:

$$\hat{x}_{k+1|k+1} = \hat{x}_{k+1|k} + K_{k+1} V_{k+1}, \quad (2.28)$$

$$P_{k+1|k+1} = P_{k+1|k} - K_{k+1} S_{rc,k+1} K_{k+1}^T. \quad (2.29)$$

Note that Q and R refer to the system and measurement noise covariance matrices, respectively [21]. Figure 2.6 presents a block-diagram scheme of a one cycle Kalman filtering process.

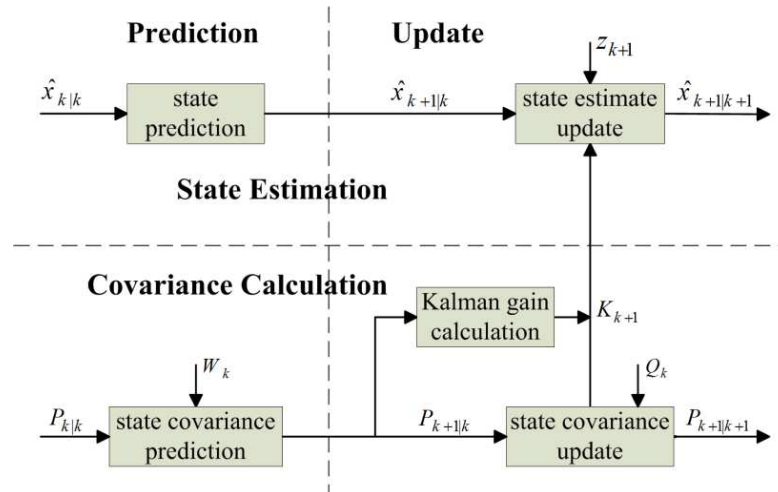


Figure 2.6: Block-diagram scheme of a one cycle Kalman filter [20]

A large number of references exist that describe KF derivation in detail [42,40,8]. Important to note is that the optimality of the KF comes at the price of stability and robustness. In the KF derivation process, it is assumed that the system model is known and linear, as well as the system and measurement noises being white, and the states have initial conditions with known means and variances [18,21]. However, in real engineering applications, these assumptions are not always preserved or true. In such situations, the KF not only results in suboptimal state estimates, but also in some cases it may become unstable [43,8]. The convergence of the KF is dependent on the computer precision and mathematical operations required for calculating matrix inversions [20,8].

The main aspects of the KF method are summarized as follows:

1. It provides a real-time recursive estimator that minimizes the RMSE of the estimation. It produces unbiased and minimum variance estimates of system states. This illustrates that the expected value of the error between estimates and real states is zero and the expected value of the root-mean-squared of the error is minimum [44].
2. It operates like an adaptive low-pass infinite impulse response (IIR) filter and its cut-off frequency is related on the ratio between the system uncertainties and measurement noise, as well as the estimate covariance [44].
3. When covariance matrices are symmetric, the recursive computation of the Kalman filtering may diverge which leads to numerical instability in the estimation process. Furthermore, if both the process uncertainties and measurement noise covariance matrices are assumed to be very small, then the covariance of the estimation error will reduce quickly and it may also lead to the numerical instability [40].

2.3.1.3. Extensions to the Kalman Filter

An important issue with the Kalman filter is its numerical stability. In simulations with small values of the process noise covariance Q_k , the round-off error equation may have a small positive eigenvalue. This makes the numeric form of the state covariance matrix be indefinite, in spite of its true form that is positive-definite. However, positive definite matrixes have a triangular matrix square root $P = S_{rc} .S_{rc}^T$. Squared-form (or the factored-form) derivation helps the estimation filter to preserve numerical stability [45]. The square-root formulation of the filter is obtained by using three techniques in the linear algebra including QR decomposition, Cholesky factor updating, and efficient least squares [46]. In this context, the covariance matrix is decomposed into factored terms that are propagated forward and updated at each measurement sample time.

There exist two main factored-form filters including the Potter's square-root filter and Bierman-Thornton's U-D filter [47]. The U - D decomposition form is obtained by $P=U.D.U^T$, where U is a unit triangular matrix and D is a diagonal matrix. The Bierman-Thornton's U-D filter has similar accuracy to Potter's filter and has less computational cost. It is obtained by using transformation techniques that involve an upper triangle covariance factorization [47]. Grewal and Andrews have presented a number of different techniques to construct the U and D matrices and the application of the U - D decomposition [20].

Numerical stability of filtering methods may be increased by decomposing the covariance matrix into Cholesky factors, specifically when dealing with finite precision arithmetic [48]. Another way to increase the KF stability is to impose boundaries on the state estimates that are based on the prior knowledge of the system [49]. In this context,

upper bounds may be defined on the level of parametric or modeling uncertainties. This provides a bound on the KF that increases estimation stability. Formulations of the *a priori* and the *a posteriori* error covariance may be also modified such that they explicitly contain effects of modeling uncertainties. For instance, one may define the *a priori* error covariance matrix $P_{k+1|k}$ as follows [21]:

$$P_{k+1|k} = \hat{F} P_{k|k} \hat{F}^T + \tilde{F} X_k \tilde{F}^T + \hat{F} Y_{k|k} \hat{F}^T + \tilde{F} Y_{k|k} \tilde{F}^T + Q_k, \quad (2.30)$$

where it contains the modeling error explicitly. Matrix X_k denotes the mean square value matrix (or a correlation matrix, namely $E\{x_k x_k^T\}$), matrix $Y_{k|k}$ denotes the cross term between the true states x_k and the error \tilde{x}_k , namely $E\{x_k \tilde{x}_k^T\}$. The *a posteriori* error covariance matrix may also be defined as [21]:

$$P_{k+1|k+1} = (I - K_{k+1} \hat{H}) P_{k+1|k} (I - K_{k+1} \hat{H})^T + K_{k+1} R_{k+1} K_{k+1}^T + K_{k+1} \tilde{H} X_{k+1} \hat{H}^T K_{k+1}^T - (I - K_{k+1} \hat{H}) Y_{k+1|k} \tilde{H}^T K_{k+1}^T - K_{k+1} \tilde{H} Y_{k+1|k}^T (I - K_{k+1} \hat{H}). \quad (2.31)$$

In order to update the error covariance matrix, the matrices X_k and $H_{k|k}$ are also required to be calculated recursively [21].

Another strategy for increasing the KF stability includes the addition of fictitious process noise and consideration of a fading memory to the KF formulation [41]. Using a fading memory in the filter formulation results in neglecting measurements in the distant past and putting more emphasis on the current information. Although this modification leads to a partial loss to the optimality via the new formulation, it helps to improve the robustness and stability of the filter. In this way, the *a priori* state error covariance is restated in the following form [41]:

$$P_{k+1|k} = \alpha F P_{k+1|k} F^T + Q_k, \quad (2.32)$$

where α denotes the forgetting factor which is a positive, typically slightly larger than 1 (i.e., $\alpha=1.01$). Its value is chosen based on how much the past measurements are desired [41]. In some applications, a time-varying value for α is proposed to improve the filter performance [21].

The KF performance may be improved numerically by introducing the “Joseph form” of the *a posteriori* state error covariance matrix as follows [20,41]:

$$P_{k+1|k+1} = (I - K_{k+1}H)P_{k+1|k}(I - K_{k+1}H)^T + K_{k+1}R_{k+1}K_{k+1}^T. \quad (2.33)$$

This form was firstly proposed and implemented by Peter Joseph in the 1960s [22]. This form is proven to be more stable and robust over the former formulation presented in equation (29). Using the Joseph form in the *a posteriori* error covariance matrix ensures that it will always be symmetric positive definite at the cost of increasing the computational complexity [20,41]. Another approach that helps to increase the numerical stability of the KF is to force the covariance matrix to be symmetric and to initialize it accordingly [41]. In order to provide a symmetric covariance matrix, the *a posteriori* covariance matrix may be restated as follows [41]:

$$P_{k+1|k+1} = (P_{k+1|k+1} + P_{k+1|k+1}^T)/2. \quad (2.34)$$

Another approach to this context is to equalize off-diagonal entries to each other (i.e., $P_{ij} = P_{ji}$), or making the eigenvalues of $P_{k+1|k+1}$ to be positive. Using an appropriate initial value for the covariance improves the filter performance and prevents large or abrupt changes in the covariance throughout the estimation process [41].

The information filter is another variant of the KF in which the estimated error covariance and the estimated state are replaced with the information matrix and the information vector, respectively. They are defined as follows [21]:

$$Y_{k|k} = P_{k|k}^{-1}, \quad (2.35)$$

$$\hat{y}_{k|k} = P_{k|k}^{-1} \hat{x}_{k|k}. \quad (2.36)$$

In this way, the measurement covariance and measurement vector are stated as [21]:

$$I_k = H_k^T R_k^{-1} H_k, \quad (2.37)$$

$$i_k = H_k^T R_k^{-1} z_k. \quad (2.38)$$

Now, the information is simply updated through a summation as [21]:

$$Y_{k+1|k+1} = Y_{k+1|k} + I_{k+1}, \quad (2.39)$$

$$\hat{y}_{k+1|k+1} = \hat{y}_{k+1|k} + i_{k+1}. \quad (2.40)$$

The main advantage of using the information filter is that it can easily filter N measurements at each step by only summing their Information matrices,

$Y_{k+1|k+1} = Y_{k+1|k} + \sum_{j=1}^N I_{k+1,j}$, and their information vectors that are represented as:

$$\hat{y}_{k+1|k+1} = \hat{y}_{k+1|k} + \sum_{j=1}^N i_{k+1,j} \quad [21].$$

2.3.2. Linear Robust Kalman Filter

Robust state estimation is one of the main aspects of filtering in which the objective is to design a filter that limits the effect of modeling uncertainties or environmental noise

on filter performance. Robust state estimation has attracted significant amounts of research in some specific areas such as control systems, target tracking, fault diagnosis and health monitoring systems. There are several approaches for increasing robustness of the discrete-time Kalman filter against norm-bounded parameter uncertainties [50,51,52,53] or unknown initial conditions [54]. The other main approaches include the H_∞ filtering [41,55,56], the robust Kalman filtering [50,57], the set-valued estimation [58], the guaranteed-cost design [59], and the smooth variable structure filter (SVSF) [3]. Sayed has presented a general framework for robust state estimation of dynamic systems with modeling uncertainties [2].

The main idea of the KF design is minimizing the trace of the estimation error covariance. However, the KF is only accurate when there are small amounts of uncertainties and noise in the process model, initial conditions and measurements. There are a large number of publications that describe the robust Kalman filter (RKF) techniques. Xie, Soh, and Souza have proposed a RKF technique for linear systems subjected to norm-bounded parametric uncertainty in the state and measurement matrices [50]. Masreliez and Martin have introduced a robust Bayesian estimator that can operate under two different scenarios [60]. The first situation is when the state x is Gaussian and the measurement z is non-Gaussian (heavy-tailed). The second scenario is when the state is non-Gaussian (heavy-tailed) and the measurement z is Gaussian [60]. Furthermore, Hsieh has proposed a RKF technique that is insensitive to unknown inputs [54]. This filter is an alternative to the Kitanidis's unbiased minimum variance filter [61].

Wang and Balakrishnan introduced a RKF algorithm as applied to linear systems with stochastic parametric uncertainties [53]. This method is designed to minimize an upper bound of the mean square estimation error at each step. Benavoli, Zaffalon, and

Miranda designed a RKF by considering the uncertainty characterizations in terms of coherent lower previsions [62]. Bertsekas and Rhodes presented the set-valued approach for state estimation that is based on defining ellipsoids around state estimates that are consistent with the measurement data [58]. Note that the centers of ellipsoids are assumed to be the estimated states. In this context, there are several recursive algorithms to account for uncertain models, particularly the one proposed by Savkin and Petersen [63]. The Guaranteed-cost design is another important approach in which the filter is designed by preserving an upper bound on the variance of the estimation error. This approach is mostly applied to quadratically stable systems in the steady-state phase of the operation [2,50]. In this section, the Sayed's robust Kalman filtering technique is reviewed as a general framework for linear robust state estimation.

Assume an uncertain dynamic model with bounded uncertainties in state and measurement models that is presented by [2]:

$$x_{k+1} = (F_k + \delta F_k)x_k + (G_k + \delta G_k)u_k, \quad (2.41)$$

$$y_k = H_k x_k + v_k, \quad (2.42)$$

where δF_k and δG_k denote small uncertainties in state transition and control matrices, when matrix H_k is assumed to be known exactly. Uncertainties in F_k and G_k may be modeled as [2]:

$$[\delta F_k \quad \delta G_k] = M_k \Delta_k [E\{F_k\} \quad E\{G_k\}], \quad (2.43)$$

where Δ_k is an arbitrary contraction, when $\|\Delta_k\| \leq 1$. In order to start the estimation process, let assume that the *a priori* state estimate $\hat{x}_{k|k}$ and covariance $P_{k|k}$ are available

along with the measurement z_{k+1} . Then, the estimate of x_k may be updated from $\hat{x}_{k|k}$ to $\hat{x}_{k+1|k}$ by solving the following criterion [2]:

$$\min_{\{x_k, u_k\}} \max_{\delta F_k, \delta G_k} \left\{ \|x_k - \hat{x}_{k|k}\|_{P_{k|k}}^2 + \|u_k\|_{Q_k}^2 + \|y_{k+1} - H_{k+1}x_{k+1}\|_{R_{k+1}}^2 \right\}. \quad (2.44)$$

Sayed has presented a solution $\{\hat{x}_{k+1|k} - \hat{u}_{k+1|k}\}$ to the above problem by solving the corresponding set of equations. Now, in order to follow his solution, one may assume the dynamic model of equations (2.41) through to (2.43), where x_0 , u_k , and v_k are uncorrelated zero-mean white stochastic processes with following variances [2]:

$$E \left(\begin{bmatrix} x_0 \\ u_i \\ v_i \end{bmatrix} \begin{bmatrix} x_0 \\ u_j \\ v_j \end{bmatrix}^T \right) = \begin{bmatrix} \Pi_0 & 0 & 0 \\ 0 & Q_i \delta_{ij} & 0 \\ 0 & 0 & R_i \delta_{ij} \end{bmatrix}, \quad (2.45)$$

where $\Pi_0 > 0$, $R_i > 0$, $Q_i > 0$ are given weighting matrices. Note that δ_{ij} is the Kronecker delta function that is equal to one when $i = j$ and equal to zero otherwise. The initial conditions for the robust filtering algorithm are set to $\hat{x}_{0|0} = P_{0|0} H_0^T R_0^{-1} y_0$, and $P_{0|0} = (\Pi_0^{-1} + H_0^T R_0^{-1} H_0)^{-1}$, alternatively. The robust filtering method is summarized into the time-update and measurement-update formulations using the following steps [2]:

Step 1: If $H_{i+1} M_i = 0$, then put $\hat{\lambda}_i = 0$. If not, calculate the function $G(\lambda)$ as [2]:

$$G(\lambda) = \|x(\lambda)\|_Q^2 + \lambda \|E_a x(\lambda) - E_b\|^2 + \|A x(\lambda) - b\|_{W(\lambda)}^2. \quad (2.46)$$

Note that the non-negative scalar parameter is determined from the optimization problem, where functions $W(\lambda), Q(\lambda), x(\lambda)$ are defined as [2]:

$$W(\lambda) \triangleq W + WH(\lambda I - H^TWH)^+H^TW, \quad (2.47)$$

$$Q(\lambda) \triangleq Q + \lambda E_a^T E_a, \quad (2.48)$$

$$x(\lambda) \triangleq [Q(\lambda) + A^T W(\lambda)A]^{-1}[A^T W(\lambda)b + \lambda E_a^T E_a]. \quad (2.49)$$

Note that $x = \text{col}\{x_k - \hat{x}_{k|k}, u_k\}$, $b = y_{k+1} - H_{k+1}F_k \hat{x}_{k|k}$, $A = H_{k+1}[F_k \ G_k]$, $Q = P_{k|k}^{-1} \oplus Q_k^{-1}$, $W = R_{k+1}^{-1}$, $H = H_{k+1}M_k$, $E_a = [E\{F_k\} \ E\{G_k\}]$, and $E_b = -E\{F_k\}\hat{x}_{k|k}$.

Note that $\hat{\lambda}_k$ is obtained by minimizing the function $G(\lambda)$ [2].

Step 2: Replace $\{Q_k, R_{k+1}, P_{k|k}, G_k, F_k\}$, by [2]:

$$\hat{Q}_k^{-1} = Q_k^{-1} + \hat{\lambda}_k E_{g,k}^T [I + \hat{\lambda}_k E_{f,k} P_{k|k} E_{f,k}^T]^{-1} E_{g,k}, \quad (2.50)$$

$$\hat{R}_{k+1} = R_{k+1} - \hat{\lambda}_k^{-1} H_{k+1} M_k M_k^T H_{k+1}^T, \quad (2.51)$$

$$\hat{P}_{k|k} = P_{k|k} - P_{k|k} E_{f,k}^T (\hat{\lambda}_k^{-1} I + E_{f,k} P_{k|k} E_{f,k}^T)^{-1} E_{f,k} P_{k|k}, \quad (2.52)$$

$$\hat{G}_k = G_k - \hat{\lambda}_k F_k \hat{P}_{k|k} E_{f,k}^T E_{g,k}, \quad (2.53)$$

$$\hat{F}_k = (F_k - \hat{\lambda}_k \hat{G}_k \hat{Q}_k E_{g,k}^T E_{f,k}) (I - \hat{\lambda}_k \hat{P}_{k|k} E_{f,k}^T E_{f,k}), \quad (2.54)$$

If $\hat{\lambda}_k = 0$, then it will be obtained that $\hat{Q}_k = Q_k$, $\hat{R}_{k+1} = R_{k+1}$, $\hat{P}_{k|k} = P_{k|k}$, $\hat{G}_k = G_k$, and $\hat{F}_k = F_k$ [46].

Step 3: Update the state estimate and state error covariance $\{\hat{x}_{k|k}, P_{k|k}\}$, as follows [2]:

$$\hat{x}_{k+1} = \hat{F}_k \hat{x}_{k|k}, \quad (2.55)$$

$$\hat{x}_{k+1|k+1} = \hat{x}_{k+1} + P_{k+1|k+1} H_{k+1}^T \hat{R}_{k+1}^{-1} e_{k+1}, \quad (2.56)$$

$$e_{k+1} = z_{k+1} - H_{k+1} \hat{x}_{k+1}, \quad (2.57)$$

$$P_{k+1} = F_k \hat{P}_{k|k} F_k^T + \hat{G}_k \hat{Q}_k \hat{G}_k^T, \quad (2.58)$$

$$\hat{P}_{k+1|k+1} = P_{k+1} - P_{k+1} H_{k+1}^T R_{e,k+1}^{-1} H_{k+1} P_{k+1}, \quad (2.59)$$

$$R_{e,k+1} = \hat{R}_{k+1} + H_{k+1} P_{k+1} H_{k+1}^T. \quad (2.60)$$

Sayed also formulated the above robust estimator in the information form in which the inverse of the error covariance matrix $P_{k|k}$ is propagated instead of $P_{k|k}$ [2]. However, the presented estimation algorithm needs to optimize the cost function $N(x;0,1)$. An approximation formula for the correction parameter $\hat{\lambda}_i$ is presented in [2].

2.4. Gaussian Filters for Nonlinear State Estimation

As explained, the Kalman-type filtering process is a special case of the Bayesian filter, when the system and measurement models are linear. Measurement noise and modeling uncertainties are also modeled by additive white Gaussian processes with zero mean and known covariance matrices. In this case, the KF provides an optimal solution to the estimation problem by minimizing the RMSE. However, for the general case of nonlinear systems with non-Gaussian noise distribution, the predicted distribution $p(x_{k+1}|Z_k)$ cannot be computed exactly. Therefore, it needs to use some kind of approximations that would sacrifice optimality for computability and hence, search for a sub-optimal nonlinear filtering approach that is computationally tractable.

In order to approximate nonlinear filtering, there are two main approaches including the local approach and the global approach as follows [30]:

- 1. Local approach:** In this approach, the distributions are assumed to be Gaussian, and then the *a posteriori* distribution is calculated using a direct numerical approximation in a local sense. This approach leads to several estimation techniques that are based on linearization such as the extended Kalman filter (EKF) [20,19], and the central difference filter (CDF) [64,65], or PDF approximation such as the unscented Kalman filter (UKF) [20,19], quadrature Kalman filter (QKF) [28], and the cubature Kalman filter (CKF) [30]. The locality approach for the filter design makes the filters to be simple and fast for implementation [30].
- 2. Global approach:** In this approach, there are no assumptions pertaining to the *a posteriori* distribution; it is calculated using an indirect numerical approximation in a global sense. This leads to new filtering techniques such as the point-mass filter that uses adaptive grids [66], the Gaussian mixture filter [67], the mixture Kalman filter [29], and the well-known particle filter (PF). The particle filtering technique uses a set of weighted particles to approximate the state *a posteriori* PDF that contains nonlinear and non-Gaussian characteristics. The main disadvantage of estimation techniques categorized in the global approach is their large computational cost that makes them useless for some on-line state estimation applications [30].

Note that based on the method of approximation, the nonlinear Gaussian filters may be classified into different categories. These categories include the linearization-based filtering, numerical integration based-filtering, and the adaptive and robust filtering.

2.4.1. Linearization-Based Filtering

In this section, main approaches for nonlinear Gaussian filtering are reviewed.

2.4.1.1. The Extended Kalman Filter (EKF)

The extended Kalman filter (EKF) is used for estimating states of a nonlinear dynamic system. Local linearization is performed in this method in order to approximate the nonlinearity of the state or measurement model at the operating point and to calculate a corrective gain. The EKF derivation is based on the Taylor series expansion of the nonlinear state transition (2.1) and measurement (2.2) with linear terms. However, these nonlinear f and h functions cannot be applied to the covariance term directly, and their Jacobian's must be computed. Similar to the KF, the EKF has two main stages as follows:

1. The Prediction Step [41]:

- Calculation of the predicted state and covariance estimates as follows [41]:

$$\hat{x}_{k+1|k} = f(\hat{x}_{k|k}, u_k, w_k), \quad (2.61)$$

$$P_{k+1|k} = F_k P_{k|k} F_k^T + Q_k. \quad (2.62)$$

2. The Update Step [41]:

- Calculation of the Jacobian of the system transition and measurement equations, F_k and H_{k+1} , respectively as follows [41]:

$$F_k = \left. \frac{\partial f}{\partial x} \right|_{\hat{x}_{k|k}, u_k}, \quad (2.63)$$

$$H_{k+1} = \left. \frac{\partial h}{\partial x} \right|_{\hat{x}_{k+1|k}}. \quad (2.64)$$

- Determination of the innovation (or measurement error) and its covariance as [41]:

$$V_{k+1} = z_{k+1} - h(\hat{x}_{k+1|k}), \quad (2.65)$$

$$S_{rc,k+1} = H_{k+1} P_{k+1|k} H_{k+1}^T + R_{k+1}. \quad (2.66)$$

- Calculation of the EKF's gain as follows [41]:

$$K_{k+1} = P_{k+1|k} H_{k+1}^T S_{rc,k+1}^{-1}. \quad (2.67)$$

- Updating the state and covariance estimates as follows [41]:

$$\hat{x}_{k+1|k+1} = \hat{x}_{k+1|k} + K_{k+1} V_{k+1}, \quad (2.68)$$

$$P_{k+1|k+1} = (I - K_{k+1} H_{k+1}) P_{k+1|k}. \quad (2.69)$$

The main aspects of the EKF estimation technique may be summarized as:

1. If the system is highly nonlinear, or a local linearization assumption does not fit the estimation problem well, a large estimation error will be produced and the EKF solution may lead to an estimate that diverges from the true state trajectory.
2. Because of the linearization process, the EKF does not provide optimal state estimates in the RMSE sense. Also, it does not guarantee unbiased state estimates and the calculated error covariance matrix does not necessarily equal to the real error covariance matrix [44].
3. EKF's parameters need to be tuned such that the convergence improves. The convergence of the EKF is also dependent on the choice of the initial state estimates [44].

2.4.2. Numerical Integration-Based Filtering

As discussed, the main difficulty produced within the EKF derivation is the local linearization at a single point in the state probability densities. In order to ameliorate this difficulty, several techniques were proposed. Some techniques use the higher-order terms of the Taylor series expansion for approximating nonlinearities and lead to the so-called higher-order filters (e.g., second-order filter [68,18]). However, due to some difficulties appearing in calculation of the Hessian matrix, these approaches have not been used in the recent state estimation strategies. In order to overcome the main drawbacks of linearization-based approaches for nonlinear state estimation, the estimation filter may be constructed based on the transformation of statistical information. In regards to the computational issues, it is understood that approximating a probability distribution is much easier than approximating an arbitrary nonlinear transformation [68]. It in turn results in using the PDF approximation techniques for solving the integrals of equations (3) through (7). The main basis for the integration-based estimation approach may be summarized in three main steps [68]:

1. Calculating the mean and covariance of a probability density via a set of selected samples
2. Propagating the samples by means of the nonlinear transformation function
3. Determining the parameters of the propagated Gaussian approximation from the transformed samples

As explained, the Bayesian filtering paradigm is mainly based on calculating Gaussian weighted integrals whose integrands are formulated as: *nonlinear function* \times *Gaussian density*. In order to make a general formulation of the numerical integration-based filtering, one may consider a multi-dimensional weighted integral stated as [30]:

$$I(f) = \int_D f(x)w(x)dx, \quad (2.70)$$

where $f(x)$ is an arbitrary function, $D \subseteq \mathbb{R}^n$ is the region of integration, and $w(x) \geq 0$ is the known weighting function applied for all $x \in D$. In Gaussian filtering, $w(x)$ has a Gaussian distribution and preserves the non-negativity condition in the entire region $D \subseteq \mathbb{R}^n$. In some cases, it may be extremely difficult to solve the integral (70) analytically. Hence, a numerical integration technique may be sought in which a set of points x_i and weights w_i is used to approximate the integral $I(f)$ through a weighted summation, as follows [30]:

$$I(f) \approx \sum_{i=1}^m w_i f(x_i). \quad (2.71)$$

In order to calculate $\{x_i, w_i\}$, there are two main approaches including the product and non-product rules that are described as follows [30]:

1- Product rules: In this approach, the quadrature rule is used to calculate the integral (70) numerically [69]. In the case of Gaussian filters, this rule is restated by the Gauss-Hermite quadrature rule, when the weighting function $w(x)$ has a Gaussian distribution. The integrand $f(x)$ is then approximated by a polynomial in terms of x , and the Gauss-Hermite quadrature rule is applied to calculate the Gaussian-weighted integral [30]. Julier and Uhlmann introduced the Unscented Kalman filter (UKF) [70] based on the unscented transform, as another example of this approach. Furthermore, Ito and Xiong [71] proposed two different techniques. The first technique is the Gauss-Hermite filter (GHF) formulated based on the Gauss-Hermite quadrature rule and the second technique is the central difference filter (CDF) formulated based on the interpolation techniques.

2- Non-product rules: This approach is used to address the dimensionality issue in the product rules approach. In this context, the integrals are numerically solved by selecting sample points from the integration domain and applying the non-product rules. Some of the main non-product rules include the Monte Carlo technique [72], quasi-Monte Carlo technique [73], Lattice rules [74], and sparse grids [75]. The randomized Monte Carlo technique calculates integrals by utilizing a set of equally weighted sample points that are selected randomly. The quasi-Monte Carlo technique and lattice rule use a deterministic approach to produce the sample points from a unit hyper-cubic region [30]. The sparse grids method is a numerical technique used to integrate or interpolate high dimensional functions based on the Smolyak's rule. The sparse grids method searches to find the more important dimensions and put more grid points there [30].

The simplest technique among numerical integration-based filters is the unscented Kalman filter (UKF) invented by Julier and Uhlmann [70]. The unscented transform is used in the UKF to transform statistical information of the probabilistic densities into a predictor-corrector form. Wu and Hu described the unscented transform as a statistical linear regression technique that uses the system information at multiple points, in spite of the local linearization (e.g., the EKF) uses information of only one point [68]. More efficient filters are obtained by developing the Gauss-Hermite rule for numerical integration, such as the Quadrature Kalman filter (QKF) [28,27]. In other research, Norgaard, Poulsen, and Ravn [65] invented the Divided Difference filter (DDF) to overcome several difficulties that appear in calculation of the derivatives in the EKF formulation. The DDF approximates the derivatives (e.g., Jacobian/Hessian matrices) and replaces them by the central divided difference. This is performed using the Sterling's polynomial interpolation criterion that makes the DDF a derivative free filter [68].

More recently, Ito and Xiong presented the mixed Gaussian filter that approximates the conditional probability density of states using a linear combination of multiple Gaussian distributions [71]. In order to update estimates in the mixed Gaussian filter, a Gaussian filter is applied to each Gaussian distribution, when each update is independent from the others and they operate in a parallel manner [71]. Kotecha and Djuric [76] invented the Gaussian Particle filter (GPF) technique. Since the GPF selects an optimal number of random samples and also benefits from the ability of analytical calculation and transformation of samples, it may be considered as a near-optimal estimation technique. The GPF is an extension to the Gaussian filter and applies the Monte Carlo integration technique to the Bayesian update rule [68]. Note the main drawback of any random-based sampling method (e.g., the GPF) is its high computational cost that makes it useless for on-line applications [77]. In the subsequent section, some of the main Gaussian filters that use the numerical integration-based approach are reviewed and compared in terms of accuracy, efficiency and computational cost.

2.4.2.1. The Unscented Kalman Filter (UKF)

The next important development to the Kalman filter is the unscented Kalman filter (UKF) [41]. Its formulation is based on a weighted statistical linear regression approach that linearizes the nonlinear state model statistically [78,8]. The UKF method produces a certain number of points called the sigma points from the projected probability distribution of the system's states. In order to provide the *a posteriori* estimate of the probability distribution, the sigma points are then mapped through the system's nonlinear model. This strategy makes any linearization unnecessary. Therefore, the calculation of the Jacobian matrices is avoided and the accuracy of the state estimation increases considerably [79,8].

The UKF utilizes a deterministic sampling approach, referred to as the unscented transform, to select a minimal set of sample points around the mean. The minimal sets of points are known as sigma points. The sigma points are propagated using the nonlinear functions. It is possible to approximately determine the mean and covariance of the density using the Monte Carlo sampling technique or Taylor series approximation [80]. The UKF can capture the *a posteriori* mean and covariance to the third order for any nonlinearity, and is therefore more accurate than the EKF. Another advantage of the UKF is that there is no need to compute the Jacobian or partial derivatives [80,70]. The UKF has a number of different forms that include the general unscented [41,81], the simplex unscented [41,81,82], and the spherical unscented [41,81,82]. Here, only the standard UKF is explained and simulated.

Figure 2.7 shows a schematic representation of the unscented transformation used in the UKF method. To formulate the UKF, assume an n -dimensional state vector of x_k , with a mean $\bar{x}_{k|k}$ and covariance $P_{k|k}$ that are approximated by $2n+1$ weighted sigma points. The UKF process is recursive, and can be formulated in two main steps of the prediction and update as follows [80]:

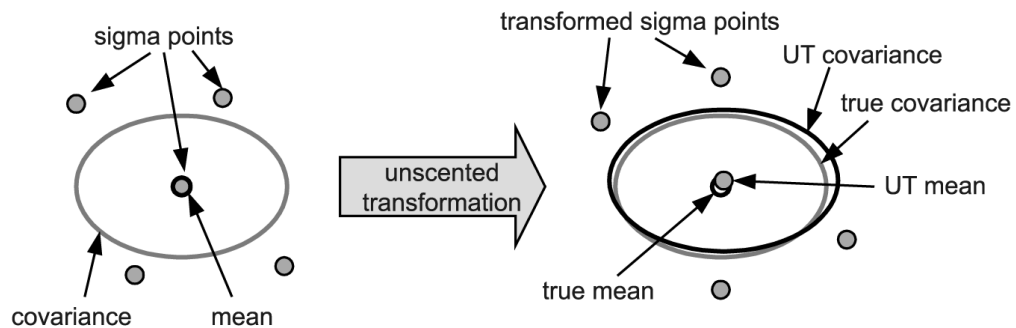


Figure 2.7: Schematic of the unscented transformation used in the UKF (Taken from [83])

1. The prediction step [80]:

- Calculation of the sigma points as follows [80]:

$$\begin{cases} \mathcal{X}_{k|k}^0 = \bar{x}_{k|k}, & i = 0 \\ \mathcal{X}_{k|k}^i = \bar{x}_{k|k} + (\gamma \sqrt{P_{k|k}})_i, & i = 1, \dots, n, \\ \mathcal{X}_{k|k}^{i+n} = \bar{x}_{k|k} - (\gamma \sqrt{P_{k|k}})_i, & i = 1, \dots, n \end{cases} \quad (2.72)$$

where the parameter $\gamma = \sqrt{n + \kappa}$ is the associated weight of samples, determined as [80]:

$$\begin{cases} w_0 = \kappa / (n + \kappa), & i = 0 \\ w_i = 1 / (2(n + \kappa)), & i = 1, \dots, 2n \end{cases}, \quad (2.73)$$

where κ is a scaling factor. Note that $(\sqrt{(n + \kappa)P_{k|k}})_i$ is the i^{th} row or column of the matrix square root of $(n + \kappa)P_{k|k}$. Furthermore, the normalized weights sum to one.

- Predicting the state mean and covariance by propagating sigma points as [80]:

$$\mathcal{X}_{k+1|k}^i = f(\mathcal{X}_{k|k}^i), \quad (2.74)$$

$$\hat{x}_{k+1|k} = \sum_{i=0}^{2n} w_i \mathcal{X}_{k+1|k}^i, \quad (2.75)$$

$$P_{k+1|k} = Q_k + \sum_{i=0}^{2n} w_i \left[\mathcal{X}_{k|k}^i - \hat{x}_{k+1|k} \right] \left[\mathcal{X}_{k|k}^i - \hat{x}_{k+1|k} \right]^T. \quad (2.76)$$

- Calculating the measurement predictions as [80]:

$$\xi_{k+1|k}^i = h(\mathcal{X}_{k+1|k}^i), \quad (2.77)$$

$$\hat{z}_{k+1|k} = \sum_{i=0}^{2n} w_i \xi_{k+1|k}^i. \quad (2.78)$$

2. The update step [80]:

- Calculating the UKF gain [80]:

$$P_z = \sum_{i=0}^{2n} w_i \left[\xi_{k+1|k}^i - \hat{z}_{k+1|k} \right] \left[\xi_{k+1|k}^i - \hat{z}_{k+1|k} \right]^T, \quad (2.79)$$

$$P_{xz} = \sum_{i=0}^{2n} w_i \left[\chi_{k+1|k}^i - \hat{x}_{k+1|k} \right] \left[\xi_{k+1|k}^i - \hat{z}_{k+1|k} \right]^T, \quad (2.80)$$

$$K_k = P_{xz} P_z^{-1}. \quad (2.81)$$

- Calculating the state mean and covariance updates [80]:

$$\hat{x}_{k+1|k+1} = \hat{x}_{k+1|k} + K_k (z_k - \hat{z}_{k+1|k}), \quad (2.82)$$

$$P_{k+1|k+1} = P_{k+1|k} - K_k P_z K_k^T. \quad (2.83)$$

The main aspects of the UKF estimation technique are summarized below:

1. The UKF is similar to Monte Carlo methods, because it uses a number of points to estimate the system's mean and covariance. But the main difference is that UKF only uses a small number of points that are not generated randomly. Hence, the computational cost decreases. The convergence of the UKF is highly dependent on the choice of sigma points [81].
2. The UKF is better than the EKF in terms of the accuracy and computational cost. Tuning the EKF can be problematic when the Jacobian matrix is not derived easily. Furthermore, the EKF can only handle limited levels of nonlinearities.
3. The UKF provides a trade-off between the particle filter and EKF in terms of accuracy and computational cost.

2.4.2.2. The Gauss-Hermite Filter (GHF)

The Gauss-Hermite quadrature rule is the main basis for constructing the Gauss-Hermite filter (GHF). The rule states the weight function is assumed to be Gaussian density with zero mean and unit variance $N(x;0,1)$, when the interval of interest is $(-\infty, \infty)$. It is difficult to calculate quadrature points q_i and weights w_i analytically for a nonlinear system. In this context, some appropriate points should be chosen as the quadratic points based on the problem under study. Thereafter, the weights w_i may be obtained by calculating the moments M_i of the integral for the m number of quadrature points as follows [28]:

$$M_i = \int_a^b x^i W(x) dx, \quad \text{for } i \in \{0, 1, \dots, m-1\}, \quad (2.84)$$

The Vandermonde system of equations is stated as follows [28]:

$$\begin{pmatrix} 1 & 1 & \dots & 1 \\ q_1 & q_2 & \dots & q_m \\ \vdots & \vdots & & \vdots \\ q_1^{m-1} & q_2^{m-1} & \dots & q_m^{m-1} \end{pmatrix} \begin{pmatrix} w_1 \\ w_2 \\ \vdots \\ w_m \end{pmatrix} = \begin{pmatrix} M_0 \\ M_1 \\ \vdots \\ M_{m-1} \end{pmatrix}. \quad (2.85)$$

The set (q_i, w_i) may be used to approximate an integral using the quadrature rule as follows [71]:

$$\int_{\mathbb{R}^n} F(x) \frac{1}{(2\pi)^{n/2}} e^{-|x|^2} dx \sim \sum_{i=1}^N w_i F(q_i), \quad (2.86)$$

where \hat{x}_0 and P_0 are starting values for the mean and covariance of the random variable $x(0)$. More details on the Gauss-Hermite quadrature rule and its applications for

numerical integration are provided in [28,71]. The GHF process is summarized in two main steps [71] as follows.

1- Prediction step [71]:

To begin, one must factor the covariance as $P_{k-1|k-1} = S^T S$, and then set $x_i = S^T q_i + x_{k-1|k-1}$. Following this, the values of state and its error covariance may be predicted [71]:

$$x_{k+1|k} = \sum_{i=1}^N f(x_i) w_i, \quad (2.87)$$

$$P_{k+1|k} = Q + \sum_{i=1}^N (f(x_i) - x_{k+1|k})(f(x_i) - x_{k+1|k})^T w_i. \quad (2.88)$$

2- Update step [71]:

The predicted state and covariance estimates may be updated as [71]:

$$x_{k+1|k+1} = x_{k+1|k} + L_k (z_k - \hat{z}_k), \quad (2.89)$$

$$P_{k+1|k+1} = P_{k+1|k} - L_k P_{xz}^T, \quad (2.90)$$

where [71]:

$$\hat{z}_k = \sum_{i=1}^N h(x_i) w_i, \quad (2.91)$$

$$P_{xz} = \sum_{i=1}^N (x_i - x_{k+1|k})(h(x_i) - \hat{z}_k)^T w_i, \quad (2.92)$$

$$P_{zz} = \sum_{i=1}^N (h(x_i) - \hat{z}_k)(h(x_i) - \hat{z}_k)^T w_i, \quad (2.93)$$

$$L_k = P_{xz} (R + P_{zz})^{-1}. \quad (2.94)$$

Note that the main advantage of using the quadrature rule for approximation is that there is no need to calculate derivatives of the state transition and measurement matrices [71].

2.4.2.3. The Quadrature Kalman Filter (QKF)

The quadrature Kalman filter (QKF) was introduced and implemented by Arasaratnam and Haykin in 2007 [28]. The QKF was firstly formulated for nonlinear systems with an additive Gaussian distribution of the noise. In this formulation, the process and measurement models are linearized by using the statistical linear regression approach that projects the Gaussian density function based on a set of Gauss-Hermite quadrature points [28,84]. The main concept of the new QKF was extended to cover discrete-time nonlinear systems with an additive non-Gaussian distribution of the noise.

In this extension, a bank of parallel QKFs referred to as the Gaussian sum-quadrature Kalman filter was used to approximate the *a priori* and *a posteriori* density functions. This approximation was alternatively performed using a finite number of weighted summations of Gaussian distributions, when the weights are calculated from the residuals of the QKFs [28]. Arasaratnam, Haykin, and Elliott reported that the Gaussian sum-quadrature Kalman filter is more accurate than other nonlinear filtering methods, such as the basic particle filters. They proposed the Gaussian-sum EKF technique for solving nonlinear non-Gaussian filtering problems [28].

In this chapter, only the general formulation of the QKF for nonlinear systems with an additive Gaussian distribution of noise is explained. Similar to the GHF, at first the *a priori* and the *a posteriori* error covariance must be factored respectively as:

$P_{k|k} = \sqrt{P_{k|k}} (\sqrt{P_{k|k}})^T$ and $P_{k+1|k} = \sqrt{P_{k+1|k}} (\sqrt{P_{k+1|k}})^T$. The QKF may be summarized in two steps that include the prediction and update steps as follows [28].

1. The prediction step [28]:

- Calculation of the quadrature points $\{X_{l,k|k}\}_{l=1}^m$ for states [28]:

$$X_{l,k|k} = \sqrt{P_{k|k}} \xi_l + \hat{x}_{k|k}. \quad (2.95)$$

- Evaluation of the predicted quadrature points $\{X_{l,k+1|k}^*\}_{l=1}^m$ for states [28]:

$$X_{l,k+1|k}^* = f(X_{l,k|k}, u_k, k). \quad (2.96)$$

- Calculation of the predicted state estimate [28]:

$$\hat{x}_{k+1|k} = \sum_{l=1}^m \omega_l X_{l,k+1|k}^*. \quad (2.97)$$

- Evaluation of the predicted error covariance [28]:

$$P_{k+1|k} = \sum_{l=1}^m \omega_l X_{l,k+1|k}^* (X_{l,k+1|k}^*)^T - \hat{x}_{k|k-1} (\hat{x}_{k|k-1})^T + Q_k. \quad (2.98)$$

At this stage, the predicted density $P(x_{k+1} | z_{1:k}) = \mathbf{N}(\hat{x}_{k+1|k}, P_{k+1|k})$ is obtained.

- Calculation of the predicted quadrature points $\{Z_{l,k+1|k}\}_{l=1}^m$ for measurement [28]:

$$Z_{l,k+1|k} = h(X_{l,k+1|k}, u_k, k). \quad (2.99)$$

- Evaluation of the predicted measurement [28]:

$$\hat{z}_{k+1|k} = \sum_{l=1}^m \omega_l Z_{l,k+1|k}. \quad (2.100)$$

- Evaluation of the predicted error covariance matrix and cross covariance matrix as follows [28]:

$$P_{zz,k+1|k} = R_{k+1} + \sum_{l=1}^m \omega_l Z_{l,k+1|k} Z_{l,k+1|k}^T - \hat{z}_{l,k+1|k} \hat{z}_{l,k+1|k}^T. \quad (2.101)$$

$$P_{xz,k+1|k} = \sum_{l=1}^m \omega_l X_{l,k+1|k} Z_{l,k+1|k}^T - \hat{x}_{k+1|k} \hat{z}_{l,k+1|k}^T. \quad (2.102)$$

2. The update step [28]:

- Evaluation of the QKF gain as [28]:

$$W_{k+1} = P_{xz,k+1|k} P_{zz,k+1|k}^{-1}. \quad (2.103)$$

- Calculation of the update state and covariance estimates [28]:

$$\hat{x}_{k+1|k+1} = \hat{x}_{k+1|k} + W_{k+1} (z_{k+1} - \hat{z}_{k+1|k}). \quad (2.104)$$

$$P_{k+1|k+1} = P_{k+1|k} - W_{k+1} P_{zz,k+1|k} W_{k+1}^T. \quad (2.105)$$

Finally, the *a posteriori* density $P(x_{k+1} | z_{1:k+1}) = N(\hat{x}_{k+1|k+1}, P_{k+1|k+1})$ is calculated.

The main aspects of the QKF estimation technique may be summarized as:

1. If the *a priori* mean is far from the *a posteriori* mean, the EKF will fail to make accurate estimates. Since the QKF needs only to calculate some functions and not

the derivatives of $f(\cdot)$ and $h(\cdot)$, it may be applied to non-smooth and non-analytical systems [28].

2. The QKF is able to estimate systems with correlated or non-additive Gaussian process and measurement noise, by adding terms to the state vector and relevant covariance [28].
3. The main disadvantage of the QKF is evident when applied to high dimensional systems, especially when the state vector size is greater than six. In high dimensional systems, the QKF's error covariance matrix may diverge from its nominal value [28].
4. Another disadvantage of the QKF is evident when applied to estimate systems. When applied to estimate systems with a limited word length for a long period of time, the round-off errors will accumulate and the QKF's accuracy may decrease. This may even cause numerical instability for the QKF in some cases [28].

2.4.2.4. The Cubature Kalman Filter (CKF)

The Cubature Kalman filter (CKF) is a nonlinear state estimation technique for large-dimensional systems. It was invented and implemented by Arasaratnam and Haykin in 2009 [30]. The CKF formulation is based on a cubature transformation [85] that makes it possible to numerically calculate the Gaussian-weighted integrals for nonlinear Bayesian filtering. In order to produce a set of cubature points that will be later mapped through the state transition model, a third-degree spherical-radial cubature rule is used [30]. The cubature transformation overcomes the divergence and dimensionality issues that are the main issues with running the EKF, UKF or QKF estimation techniques. Furthermore, the CKF provides more accurate state estimates for nonlinear systems subjected to white Gaussian noise [86]. The cubature transformation helps the CKF to

reduce the computational difficulties of calculating conditional density for some solvable multi-dimensional integrals.

As discussed previously, by assuming the conditional densities to be Gaussian, the Bayesian solution to the filtering problem leads to solving multi-dimensional integrals whose integrands are generally represented as $h(f) = \int_{\mathbb{R}^n} f(x) N(x; \bar{x}, P^{xx}) dx$, where $f(x)$ is an arbitrary nonlinear function in n -dimensional space \mathbb{R}^n , and $N(x; \bar{x}, P^{xx})$ is a normalized Gaussian function with the mean \bar{x} and covariance matrix P^{xx} . The CKF uses the cubature rule to numerically approximate these Gaussian-weighted integrals. The cubature rule used for approximating such n -dimensional integral is given by [30]:

$$\int_{\mathbb{R}^n} f(x) N(x; \bar{x}, P^{xx}) dx \approx \frac{1}{2n} f(\bar{x} + \sqrt{P^{xx}} \xi_i), \quad (2.106)$$

where the covariance is factorized as $P^{xx} = \sqrt{P^{xx}} \sqrt{P^{xx}}^T$ and a set of $2n$ cubature points that are calculated by:

$$\xi_i = \begin{cases} \sqrt{n} e_i, & i = 1, 2, \dots, n \\ -\sqrt{n} e_{i-n}, & i = n+1, n+2, \dots, 2n \end{cases}, \quad (2.107)$$

where $e_i \in \mathbb{R}^n$ represents the i^{th} elementary column vector. Arasaratnam and Haykin proposed the third degree cubature rule to approximate polynomial integrands [30].

The main structure of the CKF is similar to the UKF, but they are based on a thoroughly different set of deterministic points that provide weights for Gaussian integrals. The UKF utilizes the unscented transform to weight the selected sigma point set, whereas the CKF utilizes the cubature rule to provide weights for cubature point set.

Figure 2.8 presents a comparison of the point set distributions for the UKF and CKF estimation techniques. As illustrated, the location and the height of each point represent the sample point and its weights respectively. The main advantage of using the cubature-point set made by the CKF over the sigma-point set made by UKF is to increase the filter stability as well as its numerical accuracy. It is also possible to derive the square-root version of the CKF in spite of the UKF [30].

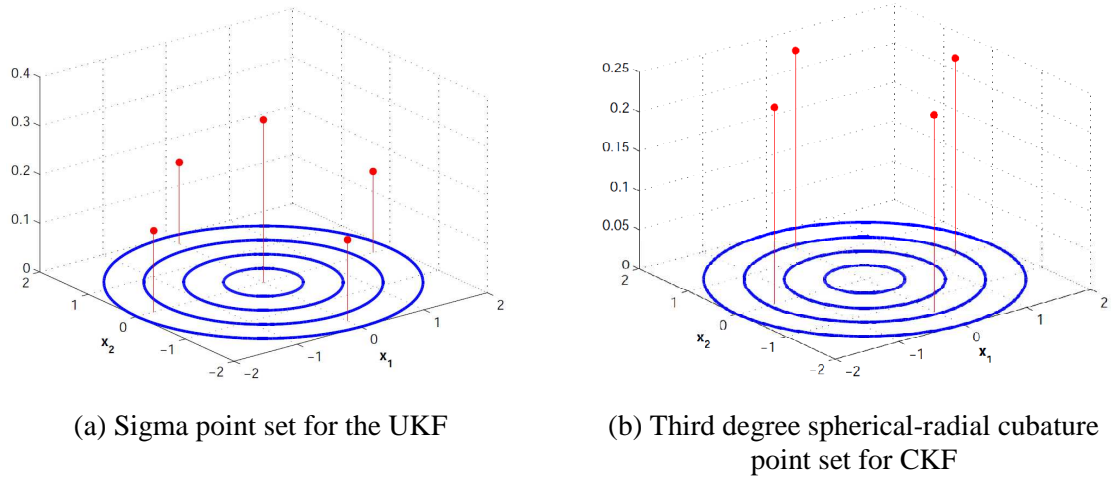


Figure 2.8: Comparison of the 2-D point set distribution in UKF and CKF (Taken from [30])

The CKF process is recursive and can be summarized in two main steps of prediction and update (like other Kalman filtering techniques) which are summarized below. It is important to note that similar to the GHF, at first the *a priori* and the *a posteriori* error covariance should be factorized respectively: $P_{k|k} = \sqrt{P_{k|k}} (\sqrt{P_{k|k}})^T$ and $P_{k+1|k} = \sqrt{P_{k+1|k}} (\sqrt{P_{k+1|k}})^T$ [30].

1. The prediction step [30]:

- Evaluation of the cubature points $\{X_{i,k|k}\}_{i=1}^m$ for states as [30]:

$$X_{i,k|k} = S_{k|k} \zeta_i + \hat{x}_{k|k}. \quad (2.108)$$

- Calculation of the predicted cubature points $\{X_{i,k+1|k}^*\}_{i=1}^m$ for states as [30]:

$$X_{i,k+1|k}^* = f(X_{i,k|k}, u_k, k). \quad (2.109)$$

- Prediction of the state values [30]:

$$\hat{x}_{k+1|k} = \frac{1}{m} \sum_{i=1}^m X_{i,k+1|k}^*. \quad (2.110)$$

- Estimation of the predicted error covariance [30]:

$$P_{k+1|k} = \frac{1}{m} \sum_{i=1}^m X_{i,k+1|k}^* (X_{i,k+1|k}^*)^T - \hat{x}_{k|k-1} (\hat{x}_{k|k-1})^T + Q_k. \quad (2.111)$$

- Calculation of the predicted cubature points $\{Z_{i,k+1|k}\}_{i=1}^m$ for measurement [30]:

$$Z_{i,k+1|k} = h(X_{i,k+1|k}, u_k, k). \quad (2.112)$$

- Evaluation of the predicted measurement [30]:

$$\hat{z}_{k+1|k} = \frac{1}{m} \sum_{i=1}^m Z_{i,k+1|k}. \quad (2.113)$$

- Evaluation of the predicted error covariance matrix and cross covariance matrix as follows [30]:

$$P_{zz,k+1|k} = R_{k+1} + \frac{1}{m} \sum_{i=1}^m Z_{i,k+1|k} Z_{i,k+1|k}^T - \hat{z}_{l,k+1|k} \hat{z}_{l,k+1|k}^T. \quad (2.114)$$

$$P_{xz,k+1|k} = \sum_{i=1}^m \omega_i X_{i,k+1|k} Z_{i,k+1|k}^T - \hat{x}_{k+1|k} \hat{z}_{l,k+1|k}^T. \quad (2.115)$$

2. The update step [30]:

- Evaluation of the CKF gain as [30]:

$$W_{k+1} = P_{xz,k+1|k} P_{zz,k+1|k}^{-1}. \quad (2.116)$$

- Calculation of the update state and covariance estimates as [30]:

$$\hat{x}_{k+1|k+1} = \hat{x}_{k+1|k} + W_{k+1} (z_{k+1} - \hat{z}_{k+1|k}). \quad (2.117)$$

$$P_{k+1|k+1} = P_{k+1|k} - W_{k+1} P_{zz,k+1|k} W_{k+1}^T. \quad (2.118)$$

The main advantages of the CKF over other estimation methods are as follows [30]:

1. Note that the cubature rule is a derivative-free transformation and hence, it removes the difficulties that may appear in the calculation of the Jacobian and Hessian of systems with complicated nonlinearities. This derivative-free characteristic allows writing the pre-packaged computer programs [30].
2. The cubature rule involves $2n$ cubature points, where n is the number of state variables. Hence, $2n$ functional computations are required at each iteration cycle. The computational complexity is linearly changing with the state vector dimension n and this makes the CKF effective for estimating high dimensional systems [30].

3. Presence of the negative weight in the CKF formulation prevents the factorization of the covariance matrix in a squared form. The CKF formulation of the filter guarantees that the sample weights are positive definite and hence the squared form of the CKF is always available [30].

In order to increase the accuracy of the CKF, Jia, Xin, and Cheng have introduced a new family of CKFs with arbitrary degrees of accuracy that calculate the spherical and radial integrals [87]. The described third-degree CKF is a special example of this family. The accuracy and performance of the high-order CKFs is similar to the Gauss-Hermite filter (GHF). To achieve $(2m+1)^{th}$ degree of accuracy, the number of points that are required for the cubature transform increases by the dimension n polynomially. Since the computational cost of CKF is a polynomial function of the point's dimension, it is computationally more efficient than the GHF [87].

2.4.2.5. The Monte Carlo Kalman Filter (MCKF)

In the Monte Carlo Kalman filter (MCKF), the Monte Carlo numerical integration technique is used for approximating the expected values in the integral forms. In this approach, N_s samples are drawn from the state Gaussian distribution $N(x; \bar{x}, P^{xx})$, where $\{x^{(i)}, i=1, \dots, N_s\}$ is a set of particles (random samples) with weights $\{w^{(i)}=1/N_s, i=1, \dots, N_s\}$. The state distribution may be approximated using the Monte Carlo technique as [88]:

$$N(x; \bar{x}, P^{xx}) \approx \sum_{i=1}^{N_s} w^{(i)} \delta(x - x^{(i)}), \quad (2.119)$$

where N_s is the number of samples and δ is the Dirac function. Note that the probability density near the sample $x^{(i)}$ is obtained by the density of points in a region around $x^{(i)}$. If $N_s \rightarrow \infty$, the approximation of the integral will converge to its true value. The MCKF estimation process is constructed based on approximating the predicted values of state, measurement, and their covariance through the Monte Carlo numerical integration technique [88].

The MCKF process is recursive and is summarized in two steps, similar to other Gaussian filters. The summary describes the two steps that address prediction and update as follows [88,89].

1- Prediction Step [88,89]:

- Generating prior samples based on Gaussian assumption and starting from $\hat{x}_{0|0}, P_{0|0}^{xx}$ as:

$$x_{k|k}^{(i)} \approx N(x_k, \bar{x}_{k|k}, P_{k|k}^{xx}). \quad (2.120)$$

- Prediction of the state and error covariance using the state transition model as:

$$\hat{x}_{k+1|k} = \frac{1}{N_s} \sum_{i=1}^{N_s} f(x_{k|k}^{(i)}), \quad (2.121)$$

$$P_{k+1|k}^{xx} = \frac{1}{N_s} \sum_{i=1}^{N_s} f(x_{k|k}^{(i)}) f^T(x_{k|k}^{(i)}) - \left[\frac{1}{N_s} \sum_{i=1}^{N_s} f(x_{k|k}^{(i)}) \right] \left[\frac{1}{N_s} \sum_{i=1}^{N_s} f(x_{k|k}^{(i)}) \right]^T + Q. \quad (2.122)$$

- Generating predictive samples:

$$x_{k+1|k}^{(i)} \approx N(x_{k+1}, \bar{x}_{k+1|k}, P_{k+1|k}^{xx}). \quad (2.123)$$

- Prediction of the measurement and its covariance and cross-covariance with the state as follows:

$$\hat{z}_{k+1|k} = \frac{1}{N_s} \sum_{i=1}^{N_s} h(x_{k+1|k}^{(i)}), \quad (2.124)$$

$$P_{k+1|k}^{zz} = \frac{1}{N_s} \sum_{i=1}^{N_s} h(x_{k+1|k}^{(i)}) h(x_{k+1|k}^{(i)}) - \left[\frac{1}{N_s} \sum_{i=1}^{N_s} h(x_{k+1|k}^{(i)}) \right] \left[\frac{1}{N_s} \sum_{i=1}^{N_s} h(x_{k+1|k}^{(i)}) \right]^T + R. \quad (2.125)$$

$$P_{k+1|k}^{xz} = \frac{1}{N_s} \sum_{i=1}^{N_s} x_{k+1|k}^{(i)} h(x_{k+1|k}^{(i)}) - \left[\frac{1}{N_s} \sum_{i=1}^{N_s} x_{k+1|k}^{(i)} \right] \left[\frac{1}{N_s} \sum_{i=1}^{N_s} h(x_{k+1|k}^{(i)}) \right]^T. \quad (2.126)$$

2- Update Step [88,89]:

- Calculating the MCKF gain as:

$$K_{k+1} = P_{k+1|k}^{xz} (P_{k+1|k}^{zz})^{-1}. \quad (2.127)$$

- Updating the state and the error covariance as:

$$\hat{x}_{k+1|k+1} = \hat{x}_{k+1|k} + K_{k+1} (z_{k+1} - \hat{z}_{k+1|k}), \quad (2.128)$$

$$P_{k+1|k+1}^{xx} = P_{k+1|k}^{xx} - K_{k+1} P_{k+1|k}^{zz} K_{k+1}^T. \quad (2.129)$$

The main issues of the MCKF are summarized below:

1. The Monte Carlo integration rule is similar to the quadrature integration rule presented previously. The two rules are similar, however, a difference between the two rules exist. In the quadrature rule, the sample points are selected at fixed intervals, while in the Monte Carlo rule they are selected randomly [88].

2. In the Monte Carlo integration process, the variance of state estimation is proportional to $1/N_s$, which means for a simulation study with 10^4 samples, the error in variance is equal to 1%. Since the numeric integration of the Monte Carlo process is recursive, it may result in increased error and the filter's divergence [90,89].
3. The computational cost of the MCKF is independent of the number of dimensions of the integrands. The GHF computational cost is proportional to M^n and therefore, by increasing the system dimension, growth occurs rapidly. Hence, for such cases with a large dimension, the MCKF is more popular than the GHF [88,90].

2.4.2.6. The Gaussian Particle Filter (GPF)

The Gaussian particle filter (GPF) was invented by Kotecha and Djuric in 2003 [76]. It uses the important sampling technique to approximate the *a posteriori* mean and covariance of Gaussian distributions. The approximation procedure of the GPF is similar to the particle filter. The only difference is that in spite of the particle filter, the GPF does not require resampling that increases filter complexity. Under the Gaussian assumptions, the GPF is optimal in the number of particles, which improves the filter performance against large nonlinearities. Alspach and Sorenson [91] introduced the Gaussian sum filter (GSF) method that approximates the posterior densities using the finite Gaussian mixtures. The approximation is performed using the Gaussian mixture and provides more accurate estimates over the techniques that are based on calculating probability densities of the grids [92].

The GPF approximates updated distribution by using a Gaussian distribution such that $p(x_k | z_{0:k}) \approx N(x_k; \bar{x}_k, P_k^{xx})$. Note that there are no general solutions for the mean \hat{x}_k and covariance P_k^{xx} of distribution $p(x_k | z_{0:k})$. The GPF technique is able to estimate the mean and covariance from the samples $x_k^{(i)}$ and their weights using the Monte Carlo numerical integration. The GPF's samples are produced using an importance sampling function $\pi(x_k | z_{0:k})$. The GPF estimation process is recursive and has two main steps [76]:

1- Measurement update [76]:

- Produce samples from the importance function $\pi(x_k | z_{0:k})$ and present them as

$$\{x_k^{(j)}\}_{j=1}^M.$$

- Calculate the corresponding weights as follows [76]:

$$\bar{w}_k^{(j)} = \frac{p(z_k | x_k^{(j)}) N(x_k = x_k^{(j)}, \bar{x}_k, P_k^{xx})}{\pi(x_k^{(j)} | z_{0:k})}. \quad (2.130)$$

- Normalize the weights as:

$$w_k^{(j)} = \bar{w}_k^{(j)} / \sum_{j=1}^M \bar{w}_k^{(j)}. \quad (2.131)$$

- Estimate the mean and covariance respectively as follows [76]:

$$\begin{aligned} \bar{x}_k &= \sum_{j=1}^M w_k^{(j)} x_k^{(j)}, \\ P_k^{xx} &= \sum_{j=1}^M w_k^{(j)} \begin{bmatrix} \bar{x}_k & x_k^{(j)} \end{bmatrix} \begin{bmatrix} \bar{x}_k & x_k^{(j)} \end{bmatrix}^H. \end{aligned} \quad (2.132)$$

2- Time update [76]:

- Produce samples from $N(x_k, \bar{x}_k, P_k^{xx})$ and present them as $\{x_k^{(j)}\}_{j=1}^M$.
- For $j=1, \dots, M$ produce samples from $p(x_{k+1} | x_k = x_k^{(j)})$ to calculate $\{x_{k+1}^{(j)}\}_{j=1}^M$.
- Update the mean and covariance respectively as follows [76]:

$$\begin{aligned} \bar{x}_{k+1} &= \frac{1}{M} \sum_{j=1}^M x_{k+1}^{(j)}, \\ P_{k+1}^{xx} &= \frac{1}{M} \sum_{j=1}^M \begin{bmatrix} \bar{x}_{k+1} & x_{k+1}^{(j)} \end{bmatrix} \begin{bmatrix} \bar{x}_{k+1} & x_{k+1}^{(j)} \end{bmatrix}^H. \end{aligned} \tag{2.133}$$

Figure 2.9 presents a block-diagram scheme of the Gaussian particle filter (GPF).

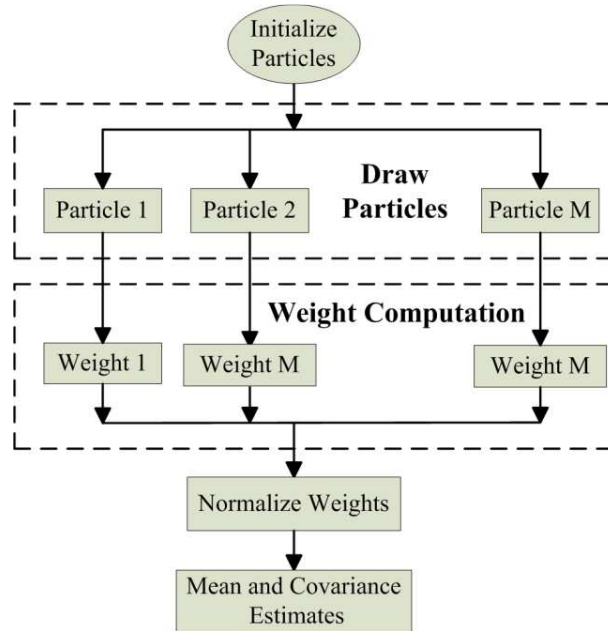


Figure 2.9: Block-diagram scheme of a one-cycle GPF estimation process

Some of the advantages and disadvantages of the Gaussian Particle Filter (GPF) may be summarized as follows [76]:

- The GPF provides more accurate state estimates than the EKF, and UKF. The additive Gaussian noise assumption may be easily alleviated without any needs to modify the filter algorithm.
- Since the GPF does not perform resampling, it has a lower computational cost in comparison to the particle filter. This makes the GPF be more suitable for real-time state estimation.
- In the GSF, the model is approximated using a weighted bank of Gaussian noise models. Alternatively, the GPF filtering and predictive distributions are only approximated based on a single Gaussian distribution. As a result, there is a decrease in the amount of complexity in GPF.

2.4.3. Adaptive Filtering

The previous state estimation techniques are all formulated under the assumption that statistics of the input and measurement noise and system parameters are known. However, in real applications, there is often some degree of uncertainty or inaccuracy in the values of physical parameters, initial conditions, or noise characteristics. Applying the filter without any modification to such cases degrades the optimality of the estimation method and increases the state estimation error. In order to alleviate such effects, one solution is to estimate the uncertain parameters and noise statistics during the filtering process and then augment an adaptation mechanism to the filter. This mechanism is referred to as an adaptive filter, which tunes the filter gain based on the parametric variations or noise statistics. Note that adaptation is considered into the filtering process such that robustness against statistical variation of parameters increases. Adaptation does not affect optimality of the filter with respect to a specific statistical model [93].

There are two main approaches for adaptive state estimation including the Multiple Models (MM) approach and the adaptive filter design based on gain adaptation. In the MM approach, several state-space models are used to cover all operating regimes of the system. Each model presents a particular operating regime of the system under certain conditions. The state and covariance estimates are calculated as a weighted summation of each filter output. In contrast, in the adaptive filter with gain adaptation approach, there is only one model of the system and some techniques are augmented to estimate the state and known parameters recursively based on statistic properties of noise and uncertainties.

2.4.3.1. Adaptive Filtering with Gain Adaptation

There are three main approaches for adapting the filter gain that include [94,95]:

- 1- Joint filtering of state and parameters:** In this approach, the system's unknown parameters are considered as new states. Hence, the new state vector contains the former states and unknown parameters and used to estimate both the states and unknown parameters. There are several techniques that may combine with estimation filters (e.g. the EKF or the particle filter) and tune their gain to jointly estimate the unknown states and unknown parameters. However, this approach is not efficient in some situations and may cause numerical instability [94].
- 2- Online noise tuning:** In this approach, when the filter starts to diverge, some techniques are applied for tuning the levels of measurement noise and or modeling uncertainties. The main symptom of the filter divergence is the characteristics of the error vector. By starting divergence, the error vector is not white and its covariance does not match with the predicted error covariance [94].
- 3- Batch estimation of parameters:** In this approach, some off-line techniques are used to estimate the system and noise parameters based on a batch of

measurements. For instance, the expectation-maximization technique may be directly used to calculate the Maximum Likelihood Estimates (MLE). Meanwhile, the noise covariance may be estimated using heuristic procedures [94]. In the next section, the Kalman filtering process with adaptive (batch) estimation of the noise parameters is presented.

2.4.3.2. Kalman Filtering with Adaptive Noise Estimation

One may begin by considering a Kalman filtering process that is applied to a linear stationary system and estimates \hat{x}_k , and P_k at each time step $k=1, \dots, N$. In this context, the KF innovation and its corresponding covariance are respectively calculated as $v_{k+1} = z_{k+1} - H x_{k+1|k}$ and $P_{k+1} = H P_{k+1|k} H^T + R_{k+1}$. The measurement covariance R may be estimated using the following off-line adaptive estimation procedure [94,95]:

- Estimate the innovation bias and its corresponding covariance as [94]:

$$\begin{aligned}\bar{v} &= \frac{1}{N} \sum_{k=1}^N v_k, \\ \hat{P} &= \frac{1}{N-1} \sum_{j=1}^N (v_k - \bar{v})(v_k - \bar{v})^T.\end{aligned}\tag{2.134}$$

- Estimate R based on the above relations as [94]:

$$\hat{R} = \hat{P} - H \left(\frac{1}{N} \sum_{k=1}^N P_{k+1|k} \right) H^T.\tag{2.135}$$

In order to estimate Q , calculate $\tilde{x}_{k+1|k}$ as: $\tilde{x}_{k+1|k} \triangleq x_{k+1} - \hat{x}_{k+1|k} = F(x_k - \hat{x}_{k|k}) + w_k$, and then Q is obtained by: $Q = F \text{cov}(\tilde{x}_{k|k}) F^T - \text{cov}(\tilde{x}_{k+1|k})$. Now, the parameter $\text{cov}(\tilde{x}_{k|k})$

may be approximated using $P_{k|k}$, but it is impossible to approximate $\text{cov}(\tilde{x}_{k+1|k})$ by $P_{k+1|k}$ through the filter. The reason is because if the filter approximates $P_{k+1|k}$ as: $P_{k+1|k} = F P_{k|k} F^T + Q_k$, then it leads to Q_k with the wrong covariance. The solution to this problem requires one to approximate x_{k+1} by $\hat{x}_{k+1|k+1}$ in the following form [94]:

$$\tilde{x}_{k+1|k} \approx \hat{x}_{k+1|k+1} - \hat{x}_{k+1|k} = d_{k+1}. \quad (2.136)$$

The estimation process continues as [94]:

- Estimate $\text{cov}(\tilde{x}_{k+1|k})$ as the empirical covariance of d_k , as follows [94]:

$$\begin{aligned} \bar{X} &= \frac{1}{N} \sum_{k=1}^N d_k, \\ \hat{P}_{k+1|k} &= \frac{1}{N-1} \sum_{k=1}^N (d_k - \bar{X})(d_k - \bar{X})^T. \end{aligned} \quad (2.137)$$

- Estimate Q using the following relation [94]:

$$\hat{Q} = \hat{P}_{k+1|k} - F \left(\frac{1}{N} \sum_{k=1}^N P_{k+1|k+1} \right) F^T. \quad (2.138)$$

It is important to note that other variants of adaptive noise filtering may be used to improve the accuracy of estimation. There are also other techniques that modify the Kalman gain directly [95]. Figure 2.10 presents a block-diagram scheme of adaptive noise filtering via the KF process.

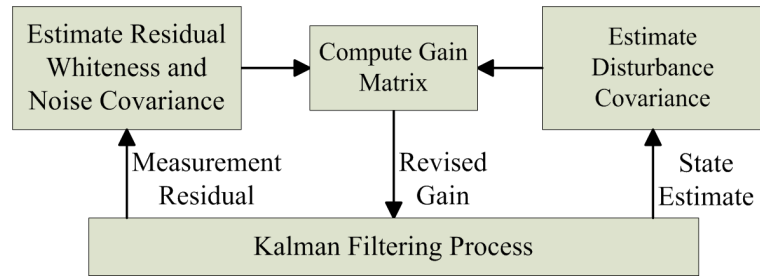


Figure 2.10: Schematic of adaptive noise filtering applied to the KF process [95]

2.4.3.3. The Multiple Models (MM) Filtering

An interesting approach for the modeling and estimation of complex nonlinear systems is to describe the system by a finite number of possible operating regimes. Such systems are generally classified as hybrid dynamical systems. A hybrid dynamical system is defined as a system that contains two types of time-varying elements [21]. The first type referred to as state variables, includes elements that vary with time. The second type includes elements that only transit from one operational mode to another. This is referred to as the mode or modal state. Note that the state variables only describe the systems dynamic behavior, while the mode states represent a possible system's regime among a finite number of possible operating regimes. These formulations are often referred to as the Markovian jump or hybrid estimation phenomenon [21]. Further studies regarding the above phenomena are found in [21,96,97,98,99].

The multiple models (MM) approach is the most well-known approach used to describe a hybrid dynamic system in which a set of models is considered that covers all of the possible operating regimes. The estimated state or parameter is then obtained by a weighted summation of each individual estimate corresponding to a particular model. The first generation of the MM algorithms were produced by Magill [98] and Lainiotis [100,101], and were widely implemented and promoted by several researchers. These

researchers included Maybeck [102,103,104,105,106], Bar-Shalom [21,107,108,109], Rong Li [110,109,111,112], and a number of other prominent researches. The MM has attracted a significant amount of attention among other estimation techniques, especially in the areas of target tracking systems [113,108,114], health monitoring systems [115,116,117,118] and adaptive multiple model control systems [119,102,120].

In the MM approach, it is assumed that the dynamic system operates according to one of a finite number of models, each corresponding to a particular operating regime. These models may differ in their mathematical structure or in their noise and uncertainty characteristics. The structural differences include dimensions of state variables, system inputs, and outputs. Noise and uncertainties may differ in the level or their probability distributions and can be represented as an additive or multiplicative term [19,21]. MM filters are generally classified into two categories: static and dynamic. Static MM estimation algorithms were introduced in the 1960s. In the static MM method, the system follows a fixed operating mode and no switching occurred from one mode to another during the estimation process.

In contrast, the dynamic MM estimator switches from one mode to another automatically in order to provide the most accurate estimate of the operating situation [21]. Tugnait presented a survey on suboptimal MM methods for discrete dynamic systems with abruptly changing structures [97]. Since the performance of the MM estimation strategy is directly related to the model sets selection, the primary difficulty in the implementation of MM methods lies in the correct identification of the model set. It has been proven that the use of too many models (i.e., over-designing the solution) may have as bad an effect on the solution as the use of too few models (i.e., under-designing) [112].

2.4.3.3.1. Static versus Dynamic MM Filters

In the static MM filter, it is assumed that the operating mode is constant and unknown. Thus, as the system follows one of the possible modes, the number of components in the mixture combination is fixed. The main problem is to identify which model should be in effect during the estimation process. However, in the dynamic MM method, the dynamic system can switch different operating modes to locate the most accurate regime, based on the overall estimated mean and covariance. The design process of MM filters has four main stages: model set design, filter selection, estimation fusion, and filter re-initialization [21]. In the model set design stage, several mathematical models, each describe a particular operating regime, are defined. Along with each mathematical model an estimation filter (e.g. Kalman filter) is set [21].

In the filter selection stage of the MM filtering, the best model-based filter that fits with the input-output data is selected among the bank of filters. Thereafter, in the estimation fusion stage, the final values of the estimated state and covariance are calculated through a weighted summation of the calculated mode condition properties. In this way, three kinds of decisions are proposed: soft, hard, and random decisions [99]. Filter re-initialization is an important stage, and reinitializes each single model-based filter at the beginning of each time step. Essentially, each filter uses its previous state and covariance estimate at the current cycle [21]. It provides a non-interacting MM estimator such as the multiple model adaptive estimation (MMAE), while some filters work in parallel without any direct interactions. The most efficient and popular way to reinitialize the state and covariance estimates is based on the IMM filter method [99].

In order to formulate a MM dynamic filter, assume a general form of system state transition and measurement models, respectively [21]:

$$x(k+1) = F(k, m_k)x(k) + G(k, m_k)u(k, m_k) + \Gamma(k, m_k)w(k, m_k), \quad (2.139)$$

$$z(k) = H(k, m_k)x(k) + v(k, m_k), \quad (2.140)$$

where m_k and M denote the current model and the set of all possible modes respectively.

In this context, the event that model m_i is operating at time k is presented as:

$M_i(k) = \{m(k) = m_i\}$. It is assumed that the system model sequence is a homogenous

Markov chain with transition probabilities calculated as follows [21]:

$$P\{m_j(k+1) | m_i(k)\} = \pi_{ij}(k), \quad \forall i, j \in M \quad (2.141)$$

where π_{ij} is the Markovian transition probability from mode i to mode j , where [21]:

$$\sum_{j=1}^r \pi_{ij}(k) = 1. \quad (2.142)$$

The mode probabilities are updated at each new measurement and the resulting weights are used for estimating state variables. Figure 2.11 presents a block-diagram scheme of one cycle of a static MM filter.

As long as each mode sequence is matched to a filter, the number of filters required for the state estimation process will grow exponentially. In order to avoid this numerical problem, suboptimal techniques should be considered. A simple technique for obtaining a suboptimal solution is to keep the N samples of histories with the largest probabilities, ignore the rest, and renormalize the selected N probabilities in a way their summation will equal to unity. Within this approach, there are three methods: the 1st-order Generalized Pseudo Bayesian (GPB1), the 2nd-order version (GPB2), and the Interacting Multiple Model (IMM) strategy.

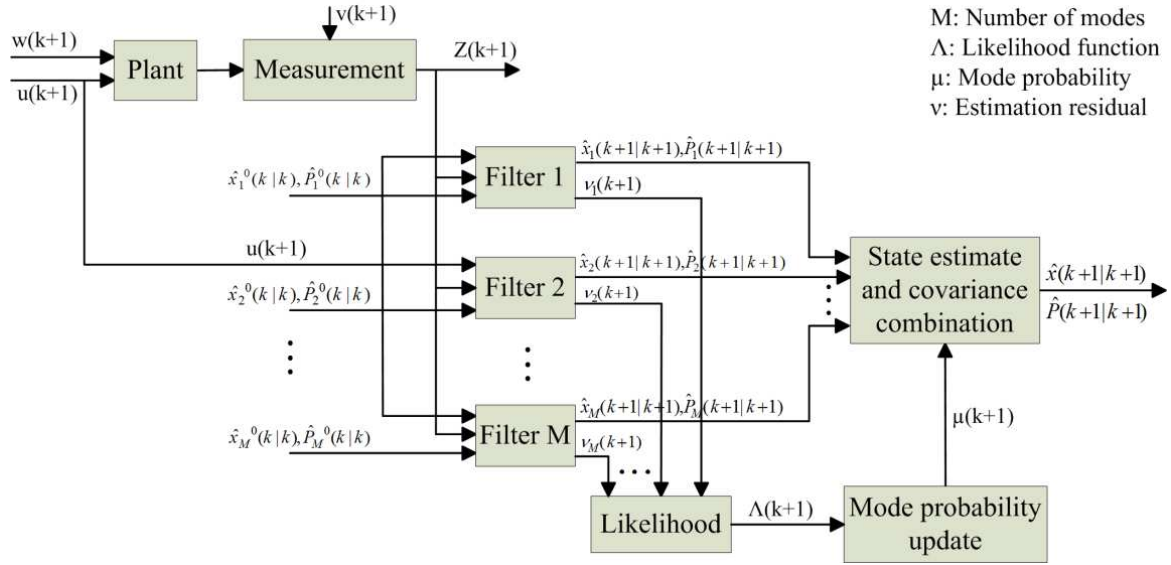


Figure 2.11: Block-diagram scheme of one cycle of a static MM filter

In the GPB1 method, only the possible models in the last sampling period are taken into account. The algorithm will only need to run r parallel filters to formulate the best estimate. The GPB2 method uses the last two sampling periods, and hence r^2 filters are required. The IMM algorithm is computationally more efficient than the GPB1 and GPB2 algorithms [21]. For the IMM strategy, with r hypotheses, each filter utilizes a different weighted combination of the previous model conditioned estimates. This model condition is referred to as the mixed initial condition. Based on this, there is an interaction between different possible modes of the system at each period of time. In addition to the reduction of the computational cost of the IMM filter, the accuracy of the overall estimate and the convergence rate is increased significantly [21].

2.4.3.3.2. The Interacting Multiple Model (IMM) Strategy

The interacting multiple model (IMM) algorithm is the most popular type of MM filter, and is capable of estimating the system state variables among several switching

modes. Bloom is among the first researchers to propose the IMM algorithm with a suitable compromise between the performance and complexity in MM systems [121]. Its computational cost is close to other methods such as those with small quadratic components, while its performance is similar to GPB2 [108]. The main feature of the IMM algorithm is the ability to estimate the state of a dynamic system with several operating modes, which can ‘switch’ from one mode to another. In this form, multiple state equations are used to describe each of the operating regimes. These regimes are typically referred to as linear models, where each model captures a particular operating point of a general nonlinear time-varying model. A Markov transition matrix is then used to determine the probability that the system is in one of the operating regimes [4].

Bar-Shalom et al. have conducted a significant amount of research to further develop the IMM estimator and its implementation in target tracking applications [21,107,122,110]. Mazoret et al. also presented an excellent survey on IMM approaches employed in the target tracking applications [108]. This survey contains new developments of the IMM method including the mode set adaptation, correlated measurement noise, square root algorithms [123], and probability data association filters (PDAF) [108]. The main advantage of the IMM over other MM approaches is due to the interacting action which mixes different modes that re-initialize each filter at the start of each cycle [118]. There has been a significant amount of research on target tracking algorithms while combining IMM with other filters, such as: the EKF [124], PF [125], and SVSF [126]. Other research has been conducted to study performance evaluation [110], model set adaptation [127] and the model group switching algorithm [21].

In order to formulate the IMM filter, assume a hybrid linear system described by equations (2-139) and (2-140). The IMM filter consists of three steps as follows [110]:

1. Interaction Step: The mixing probabilities are calculated, which refer to the probability of an event when mode m_i was in effect at time $k-1$, given that the mode m_j is in effect at time k conditioned on Z^{k-1} . The mixing probability is outlined as [110]:

$$\mu_{ij}(k-1|k-1) \triangleq P\{m_i(k-1)|m_j(k), Z^{k-1}\} = \frac{1}{\bar{\mu}_j} \pi_{ij} \mu_i(k-1), \quad (2.143)$$

where $\bar{\mu}_j$ is the predicted mode probability for r different modes and is given by [110]:

$$\bar{\mu}_j \triangleq P\{m_j(k)|Z^{k-1}\} = \sum_{i=1}^r \pi_{ij} \mu_i(k-1). \quad (2.144)$$

The mixed initial condition is then calculated using the previous state and covariance estimates, namely $\hat{x}_i(k-1|k-1)$ and $P_i(k-1|k-1)$ respectively. These parameters are filter outputs computed from r different Kalman (or other) filters corresponding to the r different operation modes. The mixed initial state and covariance are given for the filter m_j at time k , as [110]:

$$\hat{x}_{0j}(k-1|k-1) \triangleq E\{x(k-1)|m_j(k), Z^{k-1}\} = \sum_{i=1}^r \hat{x}_i(k-1|k-1) \mu_{ij}, \quad (2.145)$$

$$\hat{P}_{0j}(k-1|k-1) = \sum_{i=1}^r P_i(k-1|k-1) \mu_{ij} + \sum_{i,l=1}^r X_{ilj}, \quad (2.146)$$

where X_{ilj} is the weighted squared difference, given by [110]:

$$X_{ilj} \triangleq [\hat{x}_l(k-1|k-1) - \hat{x}_i(k-1|k-1)][\hat{x}_l(k-1|k-1) - \hat{x}_i(k-1|k-1)]^T (k-1|k-1) \triangleq \mu_{ilj} \mu_{lj}. \quad (2.147)$$

2. Filtering Step: In this step, mode-matched filtering is performed. The likelihood function associated to each of the r filters is also computed. Any estimation method or

filter may be used during this step; however, the most commonly implemented method is the KF. The mixed initial state and covariances are used as inputs to the Kalman (or other) filter matched to mode $m_j(k)$. The filtering step starts by predicting the state and covariance of each mode as [110]:

$$\hat{x}_j(k|k-1) = F_j(k-1)\hat{x}_{0j}(k-1|k-1) + G_j(k-1)u_j(k-1) + \Gamma_j(k-1)\bar{w}_j(k-1), \quad (2.148)$$

$$\hat{P}_j(k|k-1) = F_j(k-1)\hat{P}_{0j}(k-1|k-1)F_j(k-1)^T + \Gamma_j(k-1)Q_j(k-1)\Gamma_j(k-1)^T. \quad (2.149)$$

The residual and its corresponding covariance for each mode are also given [110]:

$$v_j(k) = z(k) - H_j(k)\hat{x}_j(k|k-1), \quad (2.150)$$

$$S_{rc,j}(k) = H_j(k)\hat{P}_j(k|k-1)H_j^T(k) + R_j(k). \quad (2.151)$$

The filter gain is computed, based on the residual and its covariance as follows [110]:

$$W_j(k) = \hat{P}_j(k|k-1)H_j^T(k)S_{rc,j}^{-1}(k). \quad (2.152)$$

It is now possible to update the state and corresponding covariance as follows [110]:

$$\hat{x}_j(k|k) = \hat{x}_j(k|k-1) + W_j(k)v_j(k), \quad (2.153)$$

$$\hat{P}_j(k|k) = \hat{P}_j(k|k-1) - W_j(k)S_{rc,j}(k)W_j(k)^T. \quad (2.154)$$

For updating the mode probability, the likelihood functions for the j^{th} mode are given by:

$$\Lambda_j(k) \triangleq N[v_j, 0, S_j] = \frac{e^{-\frac{1}{2}v_j(k)^T S_j^{-1}(k)v_j(k)}}{\sqrt{2\pi S_j(k)}}, \quad (2.155)$$

where the updated mode probability or weight is outlined [110]:

$$\mu_j(k) = \frac{\bar{\mu}_j \Lambda_j(k)}{\sum_{i=1}^r \bar{\mu}_i \Lambda_i(k)}. \quad (2.156)$$

3. Combination Step: In order to determine the overall estimates of state mean and covariance, the model conditioned estimates and covariance are respectively combined as follows [110]:

$$\hat{x}(k|k) \triangleq E[x(k)|Z^k] = \sum_{i=1}^r \hat{x}_i(k|k) \mu_j, \quad (2.157)$$

$$\hat{P}(k|k) \triangleq E\left[[x(k) - \hat{x}(k|k)][x(k) - \hat{x}(k|k)]^T | Z^k\right] = \sum_{j=1}^r P_j(k|k) \mu_j + \sum_{i,j=1}^r X_{ij}, \quad (2.158)$$

where the weighted square difference is given by [110]:

$$X_{ij}(k) \triangleq [x_i(k|k) - \hat{x}_j(k|k)][\hat{x}_i(k) - \hat{x}_j(k|k)]^T \mu_i \mu_j. \quad (2.159)$$

Figure 2.12 shows a block diagram representation of one cycle of an IMM estimation filter. The aforementioned IMM strategy has a fixed structure that means the selected models will not change over time. From the IMM filter, a newer filter, known as the variable structure multiple model (VSMM) has been developed. The VSMM strategy is one which uses variable model sets instead of fixed model sets [122]. The motivation for proposing this strategy is because of consideration given to the computation cost of the IMM filter. The cost of the IMM filter increases drastically with the number of local models. Therefore, it is desirable to neglect some of the inactive models from model sets to decrease the overall computational cost and time.

the filters operates based on a reduced order, linearized model derived from a general nonlinear uncertain system for each operational mode. A number of studies have been conducted, looking at implementing a number of different filters including the extended Kalman filter (EKF) [19,113], the unscented Kalman filter (UKF) [19], and the particle filter (PF) [130,90,131]. Unlike the IMM method, there is no model interaction in the MMAE method; therefore the re-initialization action is not necessary. However, the MMAE uses a conditional hypothesis probability evaluator engine to select the closet hypothesis that matches reality. Similar to other MM approaches, there is a bank of elemental filters, which use the control and measurement vector as inputs, as well as provides a state estimate and a residual.

In order to formulate the MMAE, assume the parameter a denotes the vector of uncertain parameters in a given stochastic system model. The hypothesis conditional probability $p_k(t_i)$ is the output, and is defined as the probability that it has the value of a_k at time step k , conditioned on the measurement at time t_i , as follows [116]:

$$p_k(t_i) = \Pr[a = a_k | Z(t_i) = Z_i]. \quad (2.160)$$

Note, $p_k(t_i)$ may be computed using the following recursive equation [132]:

$$p_k(t_i) = \frac{f_{z(t_i)|a, Z(t_{i-1})}(z_i | a_k, Z_{i-1}) p_k(t_{i-1})}{\sum_{j=1}^K f_{z(t_i)|a, Z(t_{i-1})}(z_i | a_j, Z_{i-1}) p_j(t_{i-1})}, \quad (2.161)$$

Where [132]:

$$f_{z(t_i)|a, Z(t_{i-1})}(z_i | a_k, Z_{i-1}) = \frac{1}{(2\pi)^{m/2} |A_k(t_i)|^{1/2}} \exp\left(-\frac{1}{2} r_k(t_i)^T A_k^{-1}(t_i) r_k(t_i)\right) \frac{f_{z(t_i)|a, Z(t_{i-1})}(z_i | a_k, Z_{i-1}) p_k(t_{i-1})}{\sum_{j=1}^K f_{z(t_i)|a, Z(t_{i-1})}(z_i | a_j, Z_{i-1}) p_j(t_{i-1})}. \quad (2.162)$$

Where $f_{z(t_i)|a,Z(t_{i-1})}(z_i | a_k, Z_{i-1})$ is the probability density of the current measurement $z(t_i)$ conditioned on the hypothesized failure status ($a = a_k$), and the previously observed measurement $Z(t_{i-1})$, based on the residuals r_k and the predetermined residual covariance A_k . Additionally, m denotes the dimension of the measurement vector. The equation: $f_{z(t_i)|a,Z(t_{i-1})}(z_i | a_k, Z_{i-1})$ has a normal distribution function in a number of applications. A block-diagram scheme of the MMAE strategy is presented in Figure 2.13. As shown, instead of producing a control vector u_k , a weighted state estimate is produced probabilistically. When the control and measurement vectors are applied to the bank of estimators, it is possible to determine the state estimate vector and subsequently the residual vector [115,116,119].

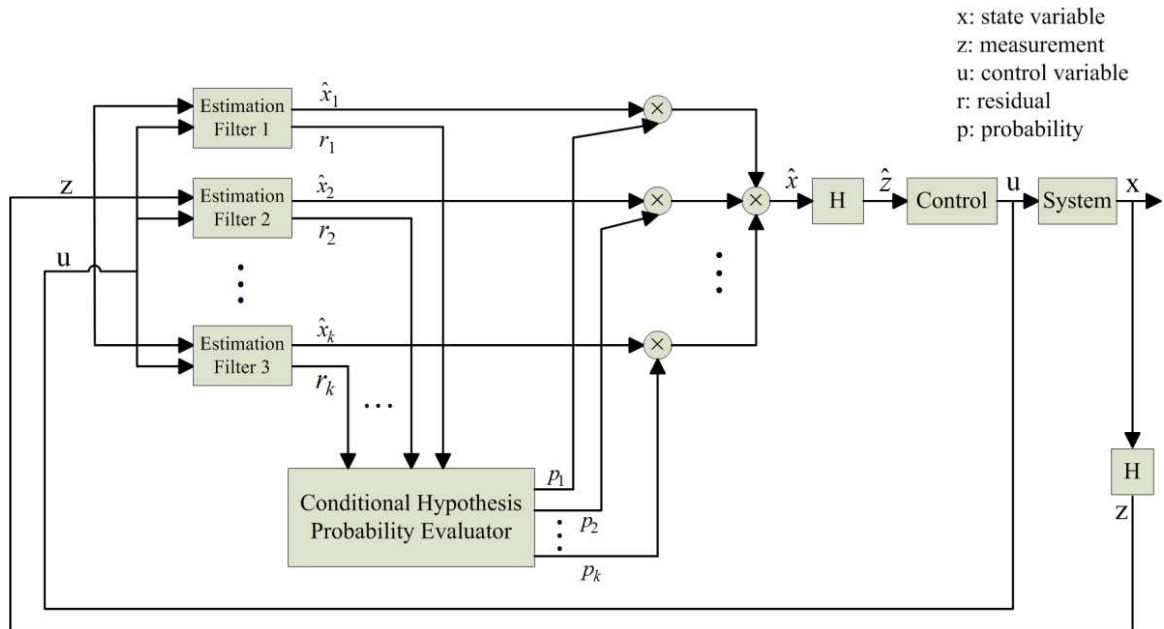


Figure 2.13: Block-diagram scheme of the multiple model adaptive estimation (MMAE) [115]

Research conducted by Maybeck and Hanlon employed the time correlation of the KF residuals instead of its scaled magnitude [133]. The conditional probabilities were assigned to the various hypotheses that were augmented in the KF bank within the MMAE. In this approach, a hypothesis testing algorithm (HTA) was designed that uses the residuals to calculate conditional probabilities p_k of the various hypotheses, conditioned on the measurement history. The HTA simultaneously tests the residuals of the KF bank under multiple hypotheses. The conditional probability was used to provide the best estimate of the fault condition and weight the individual state estimates, and calculate the probability weighted average of the state estimates \hat{x}_{MMAE} [133].

The spectral estimator outputs are essentially estimates of the power spectral density of each residual from the KFs. When the system is working without a fault, the residual is a white sequence with zero mean [133]. Kay introduced two methods for the spectral estimation techniques that include the periodogram and modified hypothesis testing algorithm (MHTA) [134]. In the periodogram method, the autocorrelation of the residual is estimated and then the Fourier transform of it is computed in order to estimate the power spectral density [133]. In the MHTA, the HTA is modified by filtering the generated residuals with a band-pass filter, sampling the output, and determining the squared magnitude. The primary advantage of this combined method over the standard MMAE is that it can identify faults at small input levels, where the standard MMAE does not operate. A disadvantage of the combined method is the increased amount of time required to collect sufficient samples and calculate the relevant spectral estimates [133]. A block diagram scheme of the MMAE algorithm using the residual correlation KF bank is shown in Figure 2.14.

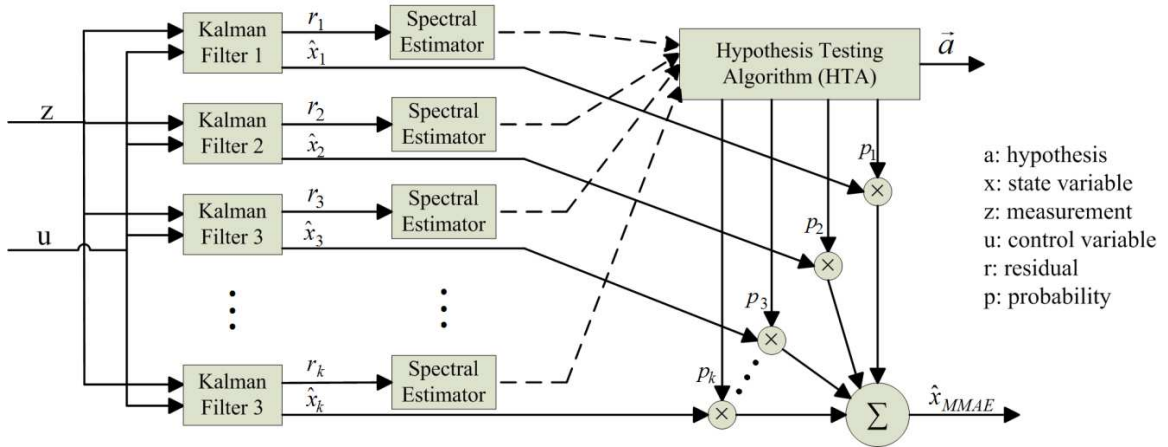


Figure 2.14: Combination of MMAE with residual correlation KF bank [133]

2.4.4. The Nonlinear Robust Filtering

In this section, the two main approaches used for robust state estimation of nonlinear stochastic systems are reviewed. The first approach, referred to as the variable structure filtering (VSF), was introduced by Habibi and Burton [135]. The VSF is a model-based filter and benefits from the robustness characteristic of the variable structure systems. The VSF-type filters provide robust state estimates against a large amount of structural and parametric uncertainties. The second approach is referred to as H_∞ filtering. It is based on the robust H_∞ control concept that has been introduced by Zames in 1980 [136]. The H_∞ filtering approach focuses on the worst-case energy gain design that produces estimation error with small energies for all small disturbance energies.

2.4.4.1. The Variable Structure-Type Filtering

The variable structure filter (VSF) is a model-based state estimation strategy that was introduced and implemented by Habibi and Burton in 2003 [135]. The VSF-type filters use the variable structure system's concept to preserve stability given bounded parametric uncertainties. Thus, the main objective is to increase stability and convergence

of the filter for situations with higher degrees of modeling or parametric uncertainties. In such situations the performance of common estimators such as Kalman-type filters may degrade considerably. The degradation occurs as a result of filter instability, modeling uncertainties, measurement noise, and inappropriate definition of initial conditions.

It is essential to note that in the Kalman-type filtering, the modeling uncertainties and measurement noise are characterized through the covariance matrices. These have a significant effect on the stability and convergence of the filter. Furthermore, even though characterization of the measurement noise is relatively simple, it is very difficult to characterize the process uncertainties. In order to improve the performance of such filters, the covariance matrices need to be tuned by trial and error which requires a lot of time and experiments. The VSF is a unique tool for explicitly defining modeling uncertainties in the filter's model. It alleviates the difficulties of tuning by trial and error. This is an advantage of using the VSF [135].

The VSF-type filtering and its newer extension (e.g., the Smooth Variable Structure Filter (SVSF) [3] utilizes the robustness property of the variable structure concept that results in stability within an upper bound for uncertainties and noise levels. In variable structure systems, the control input often contains a discontinuous term, called the sliding variable s , that is defined as a function of the state variable in the following form [3]:

$$u(x,t) = \begin{cases} u^+(x,t) & \text{if } s(x) > 0 \\ u^-(x,t) & \text{if } s(x) < 0 \end{cases}, \quad (2.163)$$

where $u^+(x,t)$ and $u^-(x,t)$ are continuous functions. Following the variable structure theory, the VSF's gain contains a discontinuous corrective term that preserves stability given bounded noise and uncertainties. It refines the *a priori* state estimates into the *a*

posteriori state estimates. In order to formulate the VSF method, the sliding variable is defined as: $S = \Lambda e_{z_k|k}$, where $e_{z_k|k} = z_k - \hat{z}_k$ is the estimation error and $\Lambda \in \mathbb{R}^{n \times n}$ is a diagonal matrix with constant positive elements. Here, the objective is to cancel the sliding variable S and satisfy the sliding condition given by $S=0$. This condition decreases the estimation error even in uncertain noisy situations. In this approach, Slotine, Hedrick, and Misawa [137] designed a nonlinear observer using the sliding mode theory that is robust to modeling errors and sensor noise. Walcott and Zak [138] also introduced a combined observer-controller structure for a class of uncertain nonlinear systems based on the variable structure concept. Edwards and Spurgeon [139] used the variable structure concept to develop a robust discontinuous observer for uncertain systems. They proved that their method is numerically tractable based on some examples.

In this section, the first generation of the variable structure filter family, namely VSF [135], is described. Following this, a more efficient version of the VSF, referred to as the smooth variable structure filter (SVSF) [3] will be described in detail. Newer versions of this filter such as the SVSF with covariance derivation [140,8], SVSF with a variable boundary layer (SVSF-VBL) [8,12], will be presented and compared.

2.4.4.1.1. The Variable Structure Filtering (VSF)

Habibi and Burton introduced the simplest generation of the VSF in 2003 [135]. In order to implement the VSF for state estimation, the system must be completely observable. One may assume the state-space model of equations (2-21) and (2-22) represents the linearized system and measurement models, respectively. One cycle of the VSF method contains following steps [135]:

1. Prediction Step:

- Calculation of *a priori* state and measurement estimates [135]:

$$\hat{x}_{k+1|k} = F_k \hat{x}_{k|k} + G_k u_k, \quad (2.164)$$

$$\hat{z}_{k+1} = H_{k+1} \hat{x}_{k+1} + v_{k+1}. \quad (2.165)$$

2. Update Step:

- Calculation of the VSF's corrective gain that is stated as [135]:

$$K_k = F_k^{-1} H_k^+ \left\{ \left[\left[H_k F_k \mid (\Upsilon \mid H_k^+ e_{z_{k|k-1}} \mid + (I \mid F_k^{-1} \mid) \mid H_k^+ \mid V_{\max} + \mid F_k^{-1} \mid W_{\max}) \right] \circ \text{sgn}(e_{z_{k|k-1}}) \right] \right\}. \quad (2.166)$$

- Refine the *a priori* state estimate into the *a posteriori* state estimate [135]:

$$\hat{x}_{k+1|k+1} = \hat{x}_{k+1|k} + K_{k+1}. \quad (2.167)$$

Note that sgn is the signum function, \circ is the Schur product, and $+$ is the pseudo-inverse transform. V_{\max} and W_{\max} also denote the upper bound for measurement noise and modeling uncertainties, respectively. Furthermore, Υ is a diagonal matrix with positive elements that contain the convergence rate γ_{ii} for each measurement z_i [135].

The discontinuous formulation of K_k produces high frequency chattering that degrades the estimation performance. In order to reduce these unwanted effects, the smoothing boundary layer concept may be considered. Utilizing the smoothing boundary layer concept, outside the smoothing layer Ψ the signum function may be applied to satisfy stability, when inside the layer a saturation function is applied to approximate the signum function and suppress high frequency chattering [135]:

$$\text{sat}(e_{z_k|k-1}, \Psi) = \begin{cases} e_{z_k|k-1} / \Psi & \text{if } |e_{z_k|k-1} / \Psi| \leq 1 \\ \text{sgn}(e_{z_k|k-1} / \Psi) & \text{if } |e_{z_k|k-1} / \Psi| > 1 \end{cases} \quad (2.168)$$

The width of the boundary layer indicates the level of uncertainties in the estimation process. However, in order to alleviate chattering, the width of the smoothing boundary layer should be sufficiently large. However, increasing the smoothing layer's width decreases the average level of accuracy in state estimates and hence, there needs to be a compromise between the level of uncertainties and the VSF's performance [135]. Stability of the VSF is proven based on the Lyapunov's second law of stability [135]. Habibi has also presented the derivation of the VSF corrective gain with explicit consideration of modeling uncertainties [135]. In subsequent research, Habibi also introduced an extension to the VSF that is used for estimating state variables of nonlinear systems. This is referred to as the extended variable structure filter (EVSF) [141]. The EVSF formulation is similar to the extended Kalman filter method. It is applied to a nonlinear system of a robotic arm successfully [141].

2.4.4.1.2. The Smooth Variable Structure Filter (SVSF)

The smooth variable structure filter (SVSF) is a more advanced generation of the variable structure filters, introduced and implemented by Habibi in 2007 [3]. Similar to the VSF concept, the SVSF is a model-based robust state estimation method that can be used to estimate state variables of smooth nonlinear dynamic systems. It has an inherent switching action that ensures convergence of the state estimates to within a region of the real values. The switching characteristic of the SVSF is due to the variable structure formulation of the discontinuous gain, which provides robustness to bounded uncertainties. Most filters only provide the estimation error (filter innovation) and its

covariance as measures of performance. The SVSF also provides another indicator that is linked to modeling uncertainties [3].

A schematic representation of the SVSF estimation concept is shown in Figure 2.15. The system state trajectory, estimated state trajectory, and existence subspace versus time are also presented in this representation. In order to start the estimation process, an initial value is selected for the state estimation process based on a prior knowledge of the systems. Thereafter, the estimated state is pushed towards a neighborhood of the system's true value referred to as the existence subspace. Once the value enters into the existence subspace, the estimated state is forced into switching along the system state trajectory via the SVSF's gain. The estimated state trajectory remains within the existing subspace that has a width proportional to modeling uncertainties, measurement noise, and disturbances. There have been lots of research to improve the SVSF and prepare it as a useful tool for FDI applications [3,135,141,8].

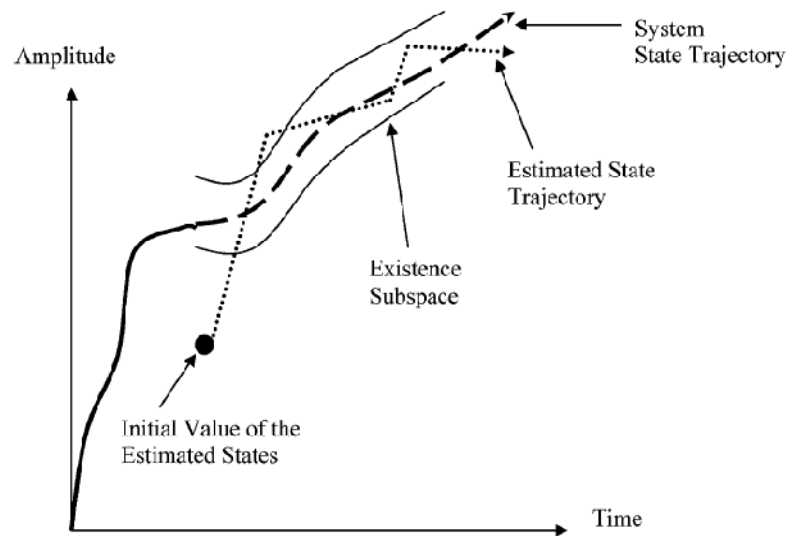


Figure 2.15: Representation of the SVSF estimation concept (Taken from [3])

The SVSF method differs with the VSF method in the derivation approach and the corrective gain formulation. The derivation of the VSF's gain is based on the explicit consideration of the upper bounds for modeling uncertainties and measurement noise. The derivation of the SVSF's gain is based on introducing a positive definite Lyapunov candidate that contains squared value of the estimation error as: $V = e_{z,k|k}^2$. Stability is then achieved by proving that the negative definiteness of the Lyapunov time-derivative. It is proven that the SVSF estimation process is stable and convergent if [3]:

$$|e_{k|k}| < |e_{k-1|k-1}|. \quad (2.169)$$

The SVSF estimation process has the same steps as the VSF process, but its corrective gain formulation is different. For a linear system with one measurement corresponding to each of the state variables, the SVSF's gain is stated as [3]:

$$K_{k+1} = H^+ \left(|e_{z,k+1|k}| + \gamma |e_{z,k|k}| \right) \circ \text{sat} \left(\psi^+ e_{z,k+1|k} \right), \quad (2.170)$$

where \circ denotes the Schur product (element-by-element multiplication) and ψ^+ is the pseudo-inverse of the smoothing boundary layer widths matrix with constant entries [3]. The saturation function is defined by [3]:

$$\text{sat} \left(\psi^{-1} e_{z_{k+1|k}} \right) = \begin{cases} 1, & e_{z_i,k+1|k} / \psi_i \geq 1 \\ e_{z_i,k+1|k} / \psi_i & -1 < e_{z_i,k+1|k} / \psi_i < 1. \\ -1, & e_{z_i,k+1|k} / \psi_i \leq -1 \end{cases} \quad (2.171)$$

It is proven that the corrective gain of (2.170) pushes the estimated states across the switching hyper plane and preserves stability. By adopting the Luenberger observer into

the SVSF method, the SVSF method may be applied to systems with fewer measurements than states [3].

Note that there are two different boundary layers in the SVSF concept including the existence layer, and the smoothing layer. The existence layer is referred to as the neighborhood of the estimated state trajectory in which the stability of the estimation process is preserved. The width of the existence layer varies in time as a function of the modeling uncertainties. Although the width of the existence layer is unknown, it is possible to obtain an upper boundary β for it. The smoothing boundary layer is defined to approximate the sign function in the corrective gain formulation and filter out chattering. Its width is known as ψ and outside this layer the sign function is applied to achieve the stability, while inside the smoothing layer the discontinuity of K_k is interpolated by the saturation function to provide smooth state estimates. As presented in Figure 2.16 (a), when the smoothing layer width is larger than the existence layer width $\psi > \beta$, chattering is filtered out. Otherwise as presented in Figure 2.16 (b), if the smoothing layer width is smaller than the existence layer width $\psi < \beta$, then the smoothing layer will be ineffective and chattering will appear [3].

Generally speaking, the filter gain construction is the main difference between the KF and SVSF. The KF gain depends on the *a priori* and the *a posteriori* measurements error values, whereas the SVSF gain depends on the smoothing boundary layer widths, convergence rate γ , and the measurement matrix H [3]. A significant amount of research has been conducted to improve the SVSF's performance. Gadsden et al. combined the SVSF with other filters such as the PF [142], the cubature Kalman filter (CKF) [143], and the IMM filter [144]. New research concentrated on the derivation of a state error covariance term for the SVSF [140], formulating a continuous-time form of the SVSF

[145], and defining an optimal smoothing boundary layer [12]. Further details and developments on the SVSF may be found in [8], and [146].

The main features of the SVSF that make it a unique and attractive tool for state estimation may be summarized as follows:

- a) It provides robustness and preserves stability within a predefined boundary layer for bounded uncertainties and noise levels [3].
- b) Other estimation techniques such as the KF, UKF, CKF, and PF provide the innovation and the error covariance as measures of performance. However, the SVSF also provides a secondary indicator of performance based on the chattering function [146], which explicitly relates to uncertainties and modeling errors [3].

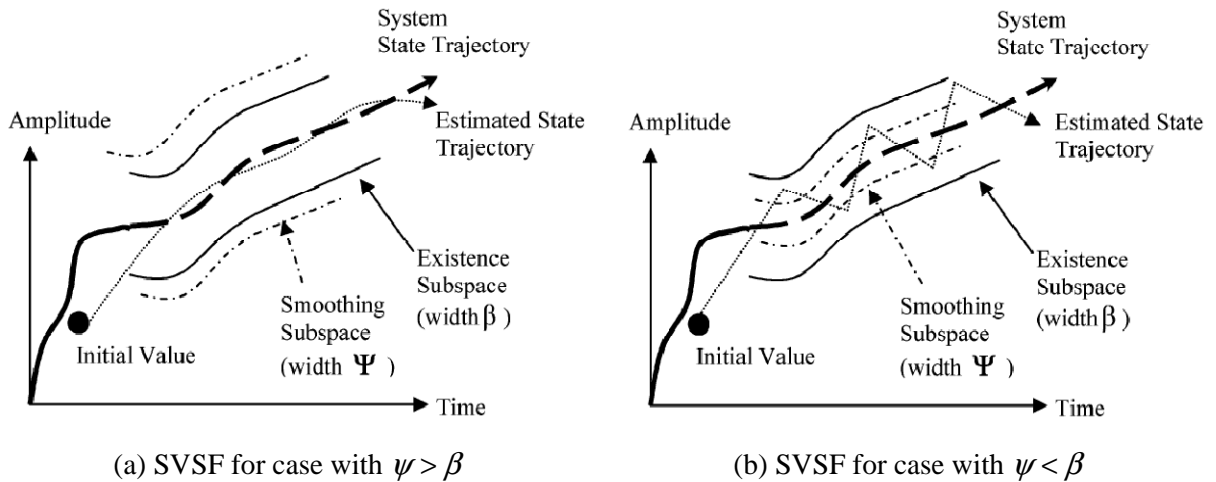


Figure 2.16: Effect of the smoothing layer width ψ on the SVSF performance (Taken from [3])

2.4.4.1.3. The SVSF with Variable Boundary Layer (SVSF-VBL)

The former version of the SVSF is introduced when the width of the smoothing boundary layer remains constant. As discussed, the width of the smoothing boundary

layer is selected based on available knowledge of the upper bound of modeling uncertainties and maximum levels of measurement noise and parametric errors. However, considering a constant width for this layer is a conservative choice that decreases the accuracy of state estimations. A more efficient smoothing boundary layer may be obtained when its width is changing as a function of uncertainty and noise levels. Gadsden introduced the state error covariance matrix for the SVSF and then used it to derive an optimal time-varying width for the smoothing boundary layer [11].

The calculation process of the error covariance matrix is similar to that of Kalman filtering [140]. The key idea for specifying the boundary layer width ψ is to take the partial derivative of the *a posteriori* error covariance matrix with respect to ψ . This idea is similar to calculating an optimal gain for the Kalman filter. This leads to an optimal formulation of the SVSF that optimizing the diagonal elements of the state error covariance matrix. Hence, a time-varying smoothing boundary layer is given by [11]:

$$\frac{\partial(\text{trace}[P_{k+1|k+1}])}{\partial \psi} = 0. \quad (2.172)$$

It is proven that the optimal time-varying smoothing layer for the SVSF leads to the well-known Kalman filter solution for linear systems. Following this, Gadsden proposed a method entitled the SVSF-VBL. It is a combination of the SVSF and KF. In this method, the SVSF preserves stability for estimates that are outside the smoothing boundary layer and provides optimality for estimates inside the boundary layer [11]. Figure 2.17 (a) presents the SVSF-VBL concept.

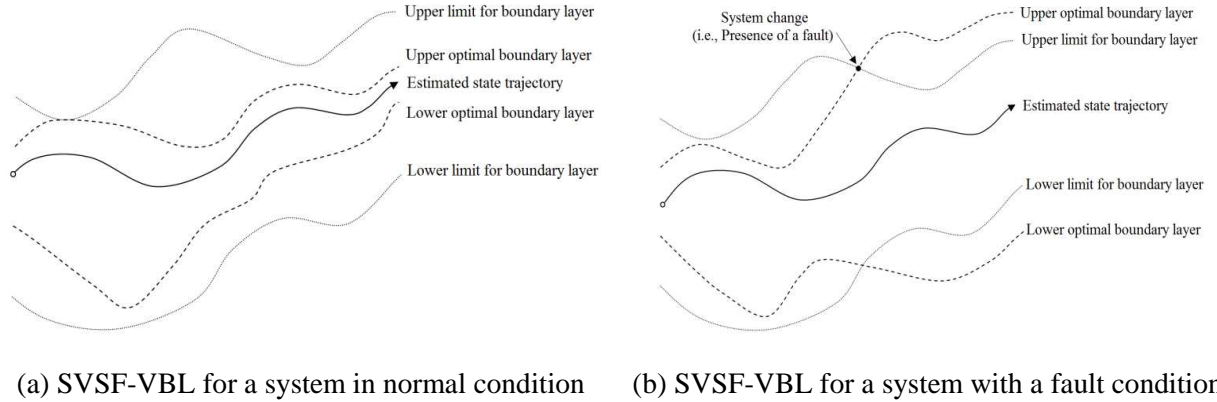


Figure 2.17: Main concept of SVSF-VBL for a system in normal and faulty conditions [11]

In the SVSF method, the smoothing boundary layer width is equal to the limit. It results in the loss of optimality demonstrated as the difference between the limit and the optimal boundary layer. However, the SVSF-VBL (KF) gain should be applied to provide efficient estimates. Figure 2.17 (b) presents the SVSF-VBL concept for estimating systems with high amount of uncertainties such as a system with a fault condition. In this case, the optimal smoothing boundary layer is larger than the limit enforced by the SVSF method. Hence, the SVSF-VBL gain is made equal to the SVSF gain to use its robust characteristic and preserve stability in uncertain conditions [11]. Inside the limit, the SVSF-VBL optimal boundary layer is used.

One cycle of the SVSF-VBL state estimation contains the following steps [11]:

1. Prediction Step [11]:

- Calculation of the predicted (*a priori*) state and covariance estimates respectively as:

$$\hat{x}_{k+1|k} = F_k \hat{x}_{k|k} + G_k u_k, \quad (2.173)$$

$$P_{k+1|k} = AP_{k|k}A^T + Q_k. \quad (2.174)$$

- Derivation of the predicted (*a priori*) measurement and error [11]:

$$\hat{z}_{k+1|k} = C\hat{x}_{k+1|k}, \quad (2.175)$$

$$e_{z_{k+1|k}} = z_{k+1} - \hat{z}_{k+1|k}. \quad (2.176)$$

2. Update Step [11]:

- Calculation of the innovation covariance and combined error vector respectively as:

$$S_{rc,k+1} = CP_{k+1|k}C^T + R_{k+1}, \quad (2.177)$$

$$E_{k+1} = |e_{z_{k+1|k}}| + \gamma |e_{z_{k|k}}|. \quad (2.178)$$

- Derivation of the smoothing boundary layer matrix given by [11]:

$$\psi_{k+1} = (\bar{E}_{k+1}^{-1}CP_{k+1|k}C^T S_{rc,k+1}^{-1})^{-1}. \quad (2.179)$$

- Calculation of the SVSF-VBL gain given by [11]:

$$K_{k+1} = C_k^{-1} \bar{E}_{k+1} \psi_{k+1}^{-1}. \quad (2.180)$$

- Refinement of the *a priori* state and covariance estimates into the *a posteriori* estimates that are respectively obtained by [11]:

$$\hat{x}_{k+1|k+1} = \hat{x}_{k+1|k} + K_{k+1}e_{z_{k+1|k}}, \quad (2.181)$$

$$P_{k+1|k+1} = (I - K_{k+1}C)P_{k+1|k}(I - K_{k+1}C)^T + K_{k+1}R_k K_{k+1}^{-1}. \quad (2.182)$$

2.4.4.2. The H_∞ Filtering

The first systematic approach into the robustness concept was firstly introduced by Zames in 1980 [136]. He presented the H_∞ theory for design and implementation of robust controllers that are insensitive to modeling uncertainties, and lack of statistical knowledge of inputs. The H_∞ theory may be considered as an extension to the linear quadratic Gaussian (LQG) theory introduced in 1960's [147]. The LQG design was performed based on a perfect model of the system and complete knowledge of input statistics. In contrast to the LQG concept, the H_∞ method was proposed to negate the necessity of a perfect model or complete knowledge of the input statistics. The H_∞ theory is designed based on tracking the energy of signal for the worst possible values of modeling uncertainties w and measurement noise v [147].

In order to clarify the H_∞ concept, one may define a measure of how good the estimator is as: $\min_{\hat{x}} \max_{w,v} J$, where w and v are the noise terms that try to degrade the state estimates. The main objective of the H_∞ filtering is to provide state estimates by minimizing the worst possible effect of w and v on the estimation error. The cost function J may be defined as [147]:

$$J = \frac{\text{ave} \|x_k - \hat{x}_k\|_Q}{\text{ave} \|w_k\|_W + \text{ave} \|v_k\|_V}, \quad (2.183)$$

where Q , W , and V , each denotes the weighting matrix corresponding to a parameter, when the averages are calculated on the weighted norms overall time steps k . Note that minimizing the cost function (2.183) means that the H_∞ filter tries to calculate the state estimates \hat{x}_k to be as close to x_k as possible, when noise terms make function J large. It is too difficult to mathematically find a solution for the described problem. It is possible

to solve the problem for $J < 1/\theta$, when θ is a constant parameter, and called the performance bound. It is chosen by the designer and its value depends on the case under study. However, by satisfying the condition $J < 1/\theta$ through the H_∞ filter, it is not important how large the magnitudes of noise terms w and v are. The H_∞ filter ensures that the ratio of the estimation error to noise will always remain less than $1/\theta$ [147].

In order to formulate the H_∞ filter recursively, based on the game theory approach [148], let us assume a linear stochastic system is represented as [41]:

$$x_{k+1} = F_k x_k + w_k, \quad (2.184)$$

$$y_k = H_k x_k + v_k, \quad (2.185)$$

$$z_k = L_k x_k, \quad (2.186)$$

where w_k and v_k are noise terms. They may be random with possibly unknown statistics or non-zero mean, or they may be deterministic. The objective is to estimate z_k as a linear combination of the state. Note that L_k is a full rank weighting matrix, and in the case of directly estimating the states, it is set $L_k = I$.

Similar to (2-183), the cost function J is defined as [41]:

$$J = \frac{\sum_{k=0}^{N-1} \|z_k - \hat{z}_k\|_{S_k}^2}{\|x_0 - \hat{x}_0\|_{P_0}^2 + \sum_{k=0}^{N-1} (\|w_k\|_{Q_k}^2 + \|v_k\|_{R_k}^2)}, \quad (2.187)$$

where P_0, Q_k, R_k , and S_k are symmetric and positive definite matrices chosen by the designer based on the case under study. As discussed, the cost function J should be

enforced to be less than $1/\theta$. The gain for the H_∞ estimation process may be calculated as [41]:

$$\bar{S}_k = L_k^T S_k L_k, \quad (2.188)$$

$$K_k = P_k \left[I - \theta \bar{S}_k P_k + H_k^T R_k^{-1} H_k P_k \right]^{-1} H_k^T R_k^{-1}. \quad (2.189)$$

Now, the state and covariance may be predicted as [41]:

$$\hat{x}_{k+1} = F_k \hat{x}_k + F_k K_k (y_k - H_k \hat{x}_k), \quad (2.190)$$

$$P_{k+1} = F_k P_k \left[I - \theta \bar{S}_k P_k + H_k^T R_k^{-1} H_k P_k \right]^{-1} F_k^{-1} + Q_k. \quad (2.191)$$

The following condition needs to be satisfied during the state estimation process [41]:

$$P_k^{-1} - \theta \bar{S}_k + H_k^T R_k^{-1} H_k > 0. \quad (2.192)$$

The following issues are addressed by comparing the H_∞ filter with the KF [41]:

- In the H_∞ filter, P_0 , Q_k , and R_k are design parameters chosen by the engineer based on the prior knowledge of noise, uncertainties, and the initial error. The noise and uncertainties may be nonzero mean. In the Kalman filter, noise, uncertainties and the error must be zero mean, when Q_k , R_k , and P_0 are their corresponding covariances [41].
- One may assume that $L_k = S_k = I$ in the H_∞ filter formulation. If now the performance bound is set as $\theta=0$ for the estimation process, then the H_∞ filter reduces to the Kalman filter. It means that the Kalman filter is a minmax filter, when the performance bound is set $\theta=\infty$. Therefore, the H_∞ filter may be

considered as a robust version of the Kalman filter, but it is not optimal in the sense of MMSE [41].

- The Kalman filter may become more robust by increasing Q_k artificially, which enlarges the covariance P_{k+1} and gain K_k , alternatively. In the same way, by subtracting the term $\theta \bar{S}_k P_k$ from the H_∞ filter's gain, it makes P_{k+1} and gain K_k larger. It intuitively results in increasing the robustness of the H_∞ filter [41].

2.5. Summary

In this chapter, an exhaustive survey of Gaussian filters for the state estimation task was provided and recent trends and developments were discussed in detail. The state estimation task is firstly described based on the well-known Bayesian paradigm. Then, in order to obtain a general framework for the so-called Gaussian filter, the estimation paradigm was regenerated under the Gaussian assumption of process and measurement noise. The main Gaussian filters, presented in the literature, were then classified into several groups. Classification was based on certain characteristics that included linearity or nonlinearity of the process model, numerical integration techniques used for the state's PDF propagation, and methods for providing robustness or adaptive characteristics. The considered state estimation approaches were also compared in terms of accuracy, robustness, and computational cost. The main problem common to all of the filters discussed, centered on how to properly extract the states from uncertain, inaccurate and noisy measurements.

Chapter 3

The Novel 2nd-Order SVSF for State Estimation

In this chapter, a new robust state estimation method referred to as the second-order Smooth Variable Structure Filter (2nd-order SVSF) is proposed and designed to satisfy both the first and second sliding conditions. It is a model-based state estimation method and benefits from the robustness and chattering suppression characteristics of second order sliding mode systems. Even though adding a smoothing boundary layer to the 1st-order SVSF method can decrease chattering, it can nonetheless compromise accuracy and robustness. This is because the smoothing boundary layer interpolates the discontinuous corrective action within a small vicinity of the switching surface and hence alleviates chattering at the expense of robustness. In the 2nd-order SVSF formulation, chattering is prevented by satisfying the second sliding condition that results in decreasing the estimation error as well as smoothing state estimates. The 2nd-order SVSF is applied to the EHA system and its performance is then compared with other estimation methods.

3.1. Introduction

As discussed, the Smooth Variable Structure Filters (SVSF) is a new robust strategy for state estimation that is based on the variable structure system's concept [3]. The SVSF has a predictor-corrector structure and uses a discontinuous corrective gain to push state estimates towards their true values. The SVSF's discontinuous corrective action satisfies the first sliding condition and hence achieves robustness to bounded uncertainties. This filter alleviates the need for tuning by trial and error and presents a mechanism for an explicit consideration of modeling uncertainties within the filter formulations. The main concern of this type of filter is eliminating the unwanted chattering effects from state estimates. The chattering phenomenon arises from discontinuous corrective actions inherent in sliding mode and variable structure control systems.

A smoothing boundary layer is commonly used in order to suppress chattering in sliding mode control systems [5,4,149], and is integral to the SVSF's gain formulation. The implementation of the smoothing action is through a saturation function that interpolates the discontinuous corrective action with a smoothing boundary layer around the switching hyperplane. Outside the smoothing boundary layer the discontinuous correction is fully applied to maintain stability. The width of the smoothing boundary layer is defined as a function of the upper bound of noise, uncertainties and perturbations [3]. Note that by interpolating the switching function with the smoothing boundary layer, the accuracy and robustness of the sliding mode are compromised [6,7].

The Smooth Variable Structure Filter (SVSF) is an estimation method that uses the sliding mode concept. It has been used in a number of applications including target tracking [8,126], control as well as in parameter estimation for fault detection in an Electro-Hydrostatic Actuation (EHA) system [150]. Gadsden extended the SVSF by

deriving a state error covariance term for it and using that for obtaining an optimal smoothing boundary layer [12,11]. The SVSF with an optimal time-varying boundary layer results in an optimal filter within the smoothing boundary layer when applied to linear Gaussian problems [12]. However, the method still uses a smoothing boundary layer that interpolates the discontinuous corrective action in the vicinity of the switching surface at the expense of robustness.

The higher order sliding mode concept is a strong alternative to the smoothing boundary layer for chatter avoidance. This concept is based on forcing the higher order time-derivatives of the sliding variable to satisfy additional constraints related to sliding motion. Along with keeping the main advantages of the variable structure systems, this concept is capable of reducing and in some cases removing the chattering effect completely. The higher order sliding mode concept provides better accuracy without compromising robustness and without the need to approximate or relax the discontinuous corrective action. The sliding mode order implies the degree of dynamic smoothness in the vicinity of the switching surface [6,13,14]. There are many publications on the second-order sliding mode control method [14,15,16,17].

Other research on higher order sliding mode systems includes Sira-Ramirez's dynamic sliding mode technique based on augmenting the differential algebraic approach to system formulations. This approach presents switching surfaces that produce chatter-free sliding mode for a special class of nonlinear systems [16,17]. Olgac and Elmali employed the second-order sliding mode technique to develop a robust output tracking algorithm for nonlinear multi-input multi-output systems [151]. Its robustness against parameter uncertainties and unknown disturbances is achieved by considering the error dynamics in the controller formulation that operates like a frequency domain filter [151,152]. There has been considerable research in the last two decades in the use of

sliding mode concepts in discrete-time systems. Sarpturk, Istefanopulos, and Kaynak investigated the stability of discrete-time sliding mode control strategies and alternatively proposed a sliding condition for statically given upper and lower bounds on uncertainties [153]. Of particular interest to SVSF is research on the derivation and implementation of the discrete form of the second-order sliding mode systems [15,154,155,156].

In this chapter, a 2nd-order SVSF state estimation method is proposed and formulated. It can satisfy both the first and second sliding mode conditions. It is capable of estimating state variables both for linear and nonlinear systems in uncertain and noisy conditions in which the level, source and occurrence of uncertainties are unknown. The main advantage of the 2nd-order SVSF is that it alleviates chattering without the needs for approximation or interpolation. This capability leads to better accuracy and robustness in uncertain conditions. The 2nd-order SVSF derivation is based on a discrete Lyapunov function that contains the first and second-order derivatives of the sliding variable. The proposed stability condition also presents a general criterion for the reachability and existence of the second order sliding motion for discrete-time systems. The 2nd-order SVSF's gain is designed such that it satisfies the first and second sliding conditions during the state estimation process. Simulation results and the performance of the 2nd-order SVSF are then compared to the Kalman filter and the 1st-order SVSF in terms of the root-mean-squared-error (RMSE), bias and the standard deviations (STD) of the estimation error.

3.2. Sliding Mode Control Theory

Variable structure control was first proposed and implemented in the Soviet Union in the 1940's. The variable structure control and its special subset of the sliding mode control (SMC) have become a useful technique for a wide range of control systems,

including: nonlinear systems, discrete-time models, multivariable, large-scale, and stochastic systems. An important feature of SMC systems is their robust stability and insensitivity to modeling uncertainties and external noise. In an SMC, the control input forces the system states to slide along a hyperplane. The system as it slides along the hyperplane is referred to as be in a sliding mode. Figure 3.1 presents the main concept of a system under a SMC. The sliding hyperplane (surface) is defined as $S=0$ and the sliding mode along this surface is achieved when system trajectories have reached the surface in a finite time and remain along it [4]. Note that $S \in \mathbb{R}^{n \times 1}$ represents the vector of sliding variables, whereas $s \in \mathbb{R}$ shows the sliding variable.

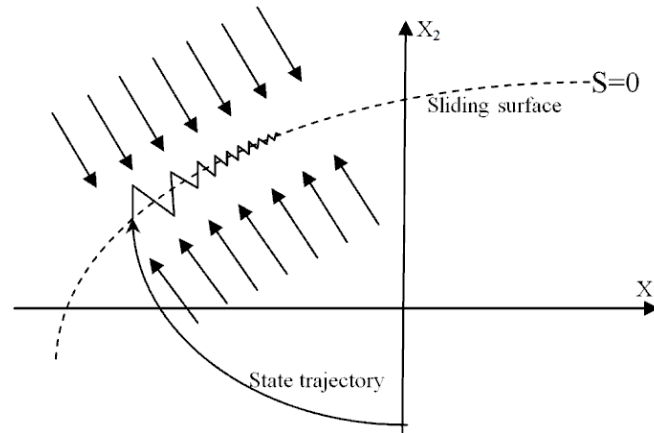


Figure 3.1: Main concept of system trajectories under a SMC

In order to design a standard SMC, there are two main steps [4]:

- 1- Design a switching surface $S(x,t)=0$ to represent the desired dynamics. Note that it should be of lower order than the system.
- 2- Design a control law $u(t,x)$ to force the state vector x to reach the switching surface in a finite period of time. To follow the desired system dynamics, the sliding mode will occur on the switching surface. The control is commonly defined as:

$$u(x,t) = \begin{cases} u^+(x,t) & \text{when } s(x) > 0 \\ u^-(x,t) & \text{when } s(x) < 0 \end{cases} \quad (3.1)$$

It has been shown that a properly designed SMC can be asymptotically stable. One of the main difficulties observed in the mathematical definition of SMC systems is the discontinuous nature of the control law. To overcome this drawback, several methods have been proposed. They mostly redefine the differential equation for the SMC system at points of discontinuous dynamics. The equivalent control technique is the most well-known approach. In this approach, it is assumed that the initial state vector is in the intersection of all discontinuous surfaces which is $S(x) = 0$. Thereafter, the sliding mode occurs with the state trajectories confined to this surface. Since the sliding motion results in $S(x) = 0$ for $t > 0$, it may be also assumed that $\dot{S}(x) = 0$. Hence, the first step of the equivalent control approach is to construct an input $u_{eq}(x)$ such that the state trajectory in the absence of modeling uncertainties would ideally remain on the switching surface $S(x) = 0$ without the need for the discontinuous control term of the SMC. The equivalent control is derived by considering the system's dynamics and the condition of $\dot{S}(x) = 0$. It alternatively leads to $\dot{S}(x) = G \cdot f(x, u) = 0$, where $G = \frac{\partial S}{\partial x}$ is an $p \times n$ matrix and represents gradients of the sliding function $S(x)$ [4].

Theoretically with SMC, system states stay confined to the switching surface, and the system trajectories slide along the switching surface. However, in real applications, SMC methods only approximate this theoretical behavior with a high frequency switching motion occurring in close vicinity of the switching surface. This high frequency switching of the system which is generally non-deterministic and unwanted is referred to as chattering. Although, the system is still stable and insensitive to various internal and

external disturbances, chattering is undesirable and much research was performed to eliminate or decrease its effects [14,15,157,158,159].

A commonly used strategy to suppress chattering is to change the sliding dynamics in a small vicinity of the discontinuity surface, while the main characteristics of the SMC system are preserved [5]. This results in partial loss in the accuracy and robustness of the SMC. More recently, higher order sliding mode theory has been proposed which helps to reduce the chattering effects. This approach not only maintains the main advantages of the standard sliding mode control, but also reduces the chattering amplitude and results in a higher trajectory following accuracy. A significant amount of research has been performed which shows the effect of using higher order sliding mode systems in reducing chattering [14,15,157,158,159].

In this context, assume a nonlinear dynamic system is defined as follows:

$$\dot{x} = F(x(t), u(t), t), \quad (3.2)$$

where $x \in \mathbb{R}^{n \times 1}$ is the state vector, $u \in \mathbb{R}^{p \times 1}$ is the input vector and $F : \mathbb{R}^{n+p} \rightarrow \mathbb{R}^n$ is a locally bounded and sufficiently smooth function. Under the ideal sliding mode condition, the sliding vector S , that is a measure of the distance of the states from the sliding hyperplane, would be zero such that:

$$S(x, t) = \left\{ \forall t \in [t_1, t_2], \forall x \in \mathbb{R}^{n \times 1} : S = 0 \right\}, \quad (3.3)$$

and its total time-derivatives $S^{(k)}$, $k = 0, 1, \dots, r-1$, along the system trajectories exist. This assumption indicates that there are no discontinuities in the first $r-1$ time-derivatives of the sliding vector S .

The sliding order presents the dynamic ‘smoothness degree’ in the neighborhood of the sliding surface. An r^{th} -order sliding mode regime exists if a SMC preserves [18]:

$$s = \dot{s} = \ddot{s} = \dots = s^{(r-1)} = 0, \quad (3.4)$$

where s represents the sliding variable. The standard sliding mode is based on the first order sliding motion, which means \dot{s} is discontinuous. The r -sliding mode realization preserves the r^{th} -order of sliding precision with respect to the measurement interval. The two main drawbacks for implementing higher order sliding mode controllers include the undesirable effect of the differentiation noise on the SMC and an increase in the amount of information required. For example, an r -sliding mode controller preserving $s=0$ also requires $s, \dot{s}, \dots, s^{(r-1)}$ to be available. Note that based on the relative degree of the SMC system, different conditions need to be satisfied [6]:

- 1) For relative degree $r=1$: $\frac{\partial}{\partial u} \dot{s} \neq 0$,
- 2) For relative degree $r \geq 2$: $\frac{\partial}{\partial u} s^{(i)} = 0$ ($i = 1, 2, \dots, r-1$), $\frac{\partial}{\partial u} s^{(r)} \neq 0$.

The first case defined above is the standard first order SMC, which keeps $s=0$. The second order sliding mode is a particular case of the type $r \geq 2$ and is used to avoid chattering effects. To achieve this condition, the control vector u is defined as an output of some first order dynamic system. In this approach, the time-derivative of the control vector \dot{u} is regarded as the actual control variable. The discontinuous control \dot{u} keeps the sliding variable s equal to zero and hence, the plant control remains continuous and the chattering will be suppressed. In fact, the second order SMC preserves the sliding motion on the sliding manifold by means of a continuous bounded input $u(t)$. This input is the continuous output of a suitable first order dynamic system controlled by a discontinuous

function. Figure 3.2 depicts a schematic of the second order sliding mode concept. The following relations are derived by differentiating the sliding variable s twice [6]:

$$\dot{s} = \frac{\partial}{\partial t} s(x, t) + \frac{\partial}{\partial x} s(x, t) f(x, u, t), \quad (3.5)$$

$$\ddot{s} = \frac{\partial}{\partial t} \dot{s}(x, u, t) + \frac{\partial}{\partial x} \dot{s}(x, u, t) f(x, u, t) + \frac{\partial}{\partial u} \dot{s}(x, u, t) \dot{u}(t) \quad (3.6)$$

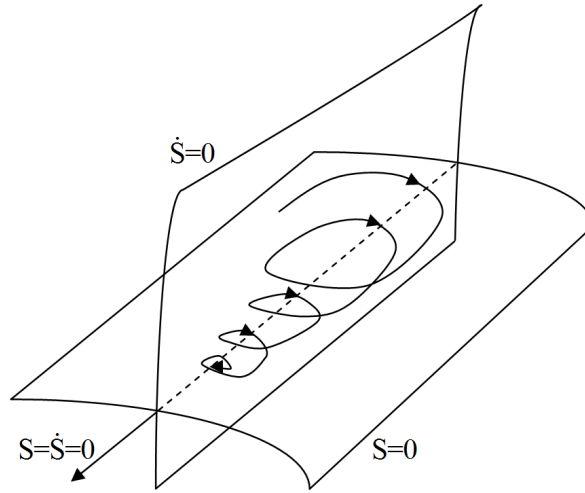


Figure 3.2: A scheme of the 2nd-order sliding mode regime [6]

Definition 3.1: Let a sliding mode system depend on a parameter $\varepsilon \in \mathbb{R}^m$, and the sliding condition occurs if $\varepsilon \rightarrow 0$, such that the constraint $S=0$ is satisfied. The sliding algorithm on $S=0$ is said to be of order r ($r > 0$), if for any bounded set of initial conditions, the following r equalities are satisfied [7]:

$$S^r(x, t) = \left\{ \forall t \in [t_1, t_2], \forall x \in \mathbb{R}^{n \times 1} : S = \dot{S} = \dots = S^{(r-1)} = 0 \right\}, \quad (3.7)$$

where the first r successive time derivatives of S are smooth functions and the r^{th} -order sliding set is not empty and is locally an integral set in the Filippov sense [7,160]. \square

Remark 3.1: The first order sliding mode exists for the dynamic system (3-2) if and only if the condition $s(x, t) = 0$ is satisfied. The necessary condition for the existence of the first sliding mode condition in the continuous time domain may be stated as [4]:

$$s(x, t)\dot{s}(x, t) < 0. \quad (3.8)$$

The sliding order r is defined as the number of continuous time-derivatives of the sliding variable. In this context, the size of the existence boundary layer would be up to r^{th} -order with respect to plant imperfections. The sliding order presents the dynamic ‘smoothness degree’ in the neighborhood of the sliding surface [7]. This smoothness is due to the higher order of constraints applied on the higher order time-derivatives of the sliding variable. At the same time, the system’s degree of robustness against modeling uncertainties, parameter variations and external disturbances is increased.

The above mentioned sliding conditions only preserve the sliding motion in continuous systems and are not directly applicable to discrete-time systems. Sarpturk, Istefanopulos and Kaynak have investigated the stability of sliding mode systems in discrete-time domain [153]. They proposed to replace the derivative in condition (3.8) with the difference operator based on the first-order Taylor expansion. This leads to: $s(k)[s(k+1) - s(k)] < 0$. Hence, the necessary condition for the existence of the first-order sliding mode in the discrete-time domain becomes [153]:

$$s(k)s(k+1) < s(k)s(k), \quad (3.9)$$

where \circ represents the Schur product and s denotes the sliding variable. This condition is necessary but not sufficient to ensure the existence of the sliding motion. If the sampling time is not small enough, condition (3-9) may lead to increased chattering that may result

in instability. Furthermore, Sarpturk, Istefanopulos, and Kaynak have proposed the following condition as a necessary and sufficient condition that preserves the reaching condition as well as the existence for the first sliding motion in discrete-time domain [153]:

$$|s(k+1)| < |s(k)|. \quad (3.10)$$

Spurgeon also introduced another approach for defining the reaching law stated as [161]:

$$S(k+1) = \Phi S(k), \quad (3.11)$$

where $S \in \mathbb{R}^{p \times 1}$ is the vector of sliding variables, $\Phi \in \mathbb{R}^{p \times p}$ is a diagonal matrix with all elements $0 \leq \Phi_{ii} \leq 1$; $\forall i = 1, \dots, p$ [161]. This condition is consistent with the reaching law given by Sarpturk in equation (3-10). Sira-Ramirez presented a similar reaching condition stated as: $|s(k+1)s(k)| < |s(k)s(k)|$ [17].

However, there is not any generalized rule to satisfy the reaching condition for r^{th} -order sliding systems. There has been only a few publications on the discrete-time second-order sliding mode system. Bartolini, Pisano, and Usai have presented new advances in the variable structure control of nonlinear sampled data systems via second-order sliding modes [162]. Furthermore, they have introduced the digital feedback sliding mode control for uncertain sampled data systems based on the Dead-Beat approach [162,163]. Acary, Brogliato, and Orlov also introduced and implemented a chattering free digital sliding mode control technique that compensates small effects of disturbances and perturbations. Mihoub, and Abdennour presented a discrete second-order sliding mode control for regulating the temperature of a chemical reactor [156]. They have employed the dynamic sliding mode approach to discretize the second-order sliding mode.

3.3. The 2nd-Order SVSF Estimation Process

The 2nd-order SVSF method has a predictor-corrector form (same as the Kalman filter and the 1st-order SVSF [3]) that involves prediction and update. In the prediction step, the *a priori* state estimate, $\hat{x}_{k+1|k}$, is calculated using knowledge of the system prior to step k . In the update step, the calculated *a priori* estimate is refined to produce an *a posteriori* state estimate $\hat{x}_{k+1|k+1}$. In this approach, a corrective gain is used to confine the estimated states and their first time-derivatives to within a neighborhood of a sliding hyperplane. This neighborhood is referred to as the existence subspace. To formulate the 2nd-order SVSF process, assume a class of nonlinear systems represented by the discrete-time state transition model:

$$x_{k+1} = \hat{F}(x_k, u_k, w_k), \quad (3.12)$$

where $\hat{F} : \mathbb{R}^{n+p} \rightarrow \mathbb{R}^n$ is the nonlinear state transition function, $x \in \mathbb{R}^{n \times 1}$ is the state vector, $u \in \mathbb{R}^{p \times 1}$ is the control vector, and $w \in \mathbb{R}^{n \times 1}$ is the process uncertainty vector. The measurement equation is assumed to be linear or piece-wise linear:

$$z_{k+1} = \hat{H} x_{k+1} + v_{k+1}, \quad (3.13)$$

where $z \in \mathbb{R}^{m \times 1}$ is the measurement vector, $v \in \mathbb{R}^{m \times 1}$ is the measurement noise, and $\hat{H} \in \mathbb{R}^{m \times n}$ is a known positive diagonal or pseudo-diagonal measurement matrix.

Assumption 3.1: The control vector $u \in \mathbb{R}^{p \times 1}$ is known and norm-bounded such that:

$$\|u_k\| \leq u_{\max}. \quad (3.14)$$

Assumption 3.2: Vectors w_k and v_k are mutually independent white processes and are norm-bounded by w_{\max} and v_{\max} as their upper limits such that:

$$\begin{cases} \|w_k\| \leq w_{\max}; \\ \|v_k\| \leq v_{\max}. \end{cases} \quad (3.15)$$

Assumption 3.3: It is assumed that the system with equations (3.12) and (3.13) is smooth and with continuous partial derivatives of any order. Furthermore, this system is completely observable and completely controllable [3].

The 2nd-order SVSF estimation process as applied to the system described by (3.12) and (3.13) is summarized by the following five steps:

- I. Prediction of the *a priori* state estimate vector is obtained based on the state transition model of the system described by (3.12) as:

$$\hat{x}_{k+1|k+1} = \hat{F}(\hat{x}_k, u_k, w_k), \quad (3.16)$$

where \hat{F} is an estimate of the exact state model F referred to in (3.12). This *a priori* estimate is produced by using the previous *a posteriori* state estimate $\hat{x}_{k|k}$. As such, an initial value for the state estimate $\hat{x}_0 \in \mathbb{R}^{n \times 1}$ is required to initialize the process. The *a priori* estimate of the measurement vector $\hat{z}_{k+1|k}$ is obtained using the estimated state vector and the linear measurement model of equation (3.13) as:

$$\hat{z}_{k+1|k} = \hat{H} \hat{x}_{k+1|k}, \quad (3.17)$$

where \hat{H} is an estimate of the exact measurement model H .

- II. The *a posteriori* and *a priori* measurement error vectors, $e_{z_k|k} \in \mathbb{R}^{m \times 1}$ and $e_{z_{k+1}|k} \in \mathbb{R}^{m \times 1}$ are respectively calculated as:

$$e_{z_k|k} = z_k - \hat{H} \hat{x}_{k|k}, \quad (3.18)$$

$$e_{z_{k+1}|k} = z_{k+1} - \hat{H} \hat{x}_{k+1|k}. \quad (3.19)$$

- III. The 2nd-order SVSF corrective gain vector, $K_{k+1} \in \mathbb{R}^{n \times 1}$, is obtained as a function of the *a priori* measurement error $e_{z_{k+1}|k}$ and the *a posteriori* measurement errors $e_{z_k|k}$ and $e_{z_{k-1}|k-1}$ as follows:

$$K_{k+1} = f(\hat{H}^+, e_{z_{k+1}|k}, e_{z_k|k}, e_{z_{k-1}|k-1}), \quad (3.20)$$

where \hat{H}^+ is the pseudo-inverse of the measurement matrix \hat{H} . Note that \hat{H} and H are initially assumed to be square matrices indicating that all states are measured, $m = n$. The 2nd-order SVSF without full state measurement $m \neq n$ is described later.

- IV. The *a priori* estimate is refined into the *a posteriori* estimate $\hat{x}_{k+1|k+1}$ such that:

$$\hat{x}_{k+1|k+1} = \hat{x}_{k+1|k} + K_{k+1}. \quad (3.21)$$

- V. Steps 1 to 4 are iteratively repeated for each sample time.

Remark 3.2: The 2nd-order SVSF method can be used to estimate states of linear or nonlinear systems that have a linear (or piecewise linear) measurement model. Further to *Definition 3.1* of Ref. [10], both the state and measurement transition models of equations (3.12) and (3.13) should be consecutive bijective, meaning that in the absence of modeling uncertainties and measurement noise, it is possible to find an inverse mapping

that generates x_k by consecutive time iterations of the output vector in the form of

$$x_{n_k} = F_n^{-1}(H^+ z_{k+1}, H^+ z_k, u_k) \quad [10].$$

The corrective gain K_{k+1} is a second-order Markov process that is formulated using the measurement error vector at different time steps, namely $e_{z_{k+1|k}}, e_{z_k|k}, e_{z_{k-1|k-1}}$. This formulation alleviates the chattering effects without the need for a smoothing boundary layer. In this context, the vector of sliding variables $S \in \mathbb{R}^{m \times 1}$ is defined as:

$$S_k = e_{z_k|k}, \quad (3.22)$$

where $e_{z_k|k}$ is the *a posteriori* measurement error vector at the time step k . The 2nd-order SVSF is formulated to satisfy both the first and the second sliding conditions. As such the *a posteriori* error and its first time-derivative must be forced to move towards a switching hyperplane such that $S_k = e_{z_k|k} = 0$ (first sliding condition) and $\Delta S_k = e_{z_k|k} - e_{z_{k-1|k-1}} = 0$ (second sliding condition) are satisfied at the same time. It is shown in Section 3.3 that the first and the second order sliding conditions are satisfied for the 2nd-order SVSF with a full diagonal measurement matrix $\hat{H} \in \mathbb{R}^{m \times n}$ ($m = n$), if:

$$K_{i,k+1} = \hat{h}_{ii}^{-1} \left[e_{z,i_{k+1|k}} - \frac{e_{z,i_{k|k}}}{2} - \gamma_{ii} \sqrt{\frac{e_{z,i_{k|k}}^2}{4} + \frac{\Delta e_{z,i_{k|k}}^2}{2}} \right], \quad (3.23)$$

where $e_{z,i_{k|k}}$ denotes an element of the error vector $e_{z_k|k}$, \hat{h}_{ii} denotes an element of the inverted measurement matrix \hat{H} , and $\gamma = \text{Diag}(\gamma_{ii}) \in \mathbb{R}^{m \times m}$ is a diagonal matrix with positive entries such that $0 < \gamma_{ii} < 1$. Section 3.6 presents the corrective gain for cases with fewer measurements than states, $m < n$.

3.4. A New Stability Rule for Second-Order Sliding Mode Systems

In order to prove stability of the 2nd-order SVSF, the first and second sliding conditions must be met. In this section, *Theorem 3.1* is presented for the proof of stability based on the Lyapunov's second law. It introduces a positive definite Lyapunov function that preserves the first and second sliding conditions. Further to the conceptual description of the 2nd-order SVSF, it is important to note that the measurement error and its difference ($s_{i,k}, \Delta s_{i,k} = e_{z,i_k|k} - e_{z,i_{k-1}|k-1}$) decrease in time until a 2-dimensional existence boundary layer is reached. Thereafter, the estimated trajectory is confined within the existence subspace, where it moves back and forth across the true state trajectory.

The width of the existence subspace Σ_e may be expressed in terms of two orthogonal directions of S_k and ΔS_k by $\Sigma_e(\varepsilon_{s_k}, \varepsilon_{\Delta s_k})$ in each time sequence. Note that ε_k is however unknown and may be calculated as a function of noise and uncertainties. If the noise and uncertainties are norm-bounded, as mentioned by *Assumption 3.2*, then ε_k is also norm-bounded. Note that the state estimation error $e_{x_k|k}$ generated from the 2nd-order SVSF contains two elements that are the error signal and noise. The width of the existence subspace ε_k cannot be decreased below a function of the random components of ε_k such as noise [3]. It is assumed that the noise random content η_k is norm-bounded such that $\|\eta_k\| < \varepsilon_k$. However, it is possible to calculate an upper bound for the width of the existence subspace in terms of ε_k . For discrete time SMC systems, the sampling time and switching imperfections will also affect and add to the value of ε_k [3].

Assumption 3.4: Let $\Delta s_{i,k} = s_{i,k} - s_{i,k-1}$ be the backward difference of the sliding variable $s_{i,k}$ at time k . It is assumed that $\Delta S_k : \mathbb{R}^m \rightarrow \mathbb{R}^m$ is a smooth differentiable function.

Definition 3.2: The ideal first-order sliding mode occurs for a discrete-time system if there exists a time sequence k_1 after which the state trajectory that belongs to the sliding manifold $S(x_k, k)$ satisfies [4]:

$$S_{1st} = \left\{ \forall x \in \mathbb{R}^n, \exists k \geq k_1 : S(x_k, k) = 0 \right\}. \quad (3.24)$$

Remark 3.3: Due to uncertainties, noise, and switching imperfections, however, the ideal sliding mode does not occur and the above condition needs to be met for a real sliding condition. The real first order sliding mode occurs if there is a time instance k_1 after which the state trajectory that belongs to the sliding hyperplane $S(x_k)$ preserves:

$$S_{1st} = \left\{ \forall x \in \mathbb{R}^n, \exists k \geq k_1, \varepsilon_s > 0 : \|S(x_k)\| < \varepsilon_s \right\}. \quad (3.25)$$

Further to *Remark 3.3*, if the first sliding condition is satisfied, then the sliding variables vector S_k will be bounded after the time sequence k_1 . Note that ε_s is the width of the existence subspace and is a function of modeling uncertainties, disturbances, and switching imperfections.

Definition 3.3: The ideal 2nd-order sliding mode occurs for a system if there exists a finite time $k_2 \geq k_1$ after which the state trajectory converges to the sliding manifold $S(x_k, k)$ such that:

$$S_{2nd} = \left\{ \forall x \in \mathbb{R}^n, \exists k \geq k_2 : S(x_k, k) = \Delta S(x_k, k) = 0 \right\}. \quad (3.26)$$

Remark 3.4: Note that *Definition 3.3* only describes the ideal 2nd-order sliding motion, but due to uncertainties and switching imperfections, the real 2nd-order sliding mode is produced. The real second-order sliding mode occurs if after a finite time sequence $k_2 \geq k_1$ the state trajectory that belongs to the sliding hyperplane $S(x_k, k)$ preserves:

$$S_{2nd} = \left\{ \forall x \in \mathbb{R}^n, \exists k \geq k_2, \varepsilon_s, \varepsilon_{\Delta s} > 0 : \|S(x_k, k)\| < \varepsilon_s, \|\Delta S(x_k, k)\| < \varepsilon_{\Delta s} \right\}. \quad (3.27)$$

Based on the above discussion, satisfaction of the first sliding condition is a necessary step for preserving the second sliding condition. Hence, the second order sliding motion occurs after the first order sliding motion, namely $k_2 \geq k_1$, and the second order sliding motion must satisfy all conditions corresponding to the first order sliding motion. *Theorem 3.1* presents a Lyapunov function that preserves the first and second sliding conditions based on *Definitions 3.2* and *3.3*, and under *Assumptions 3.1* to *3.4*.

Theorem 3.1: The second order sliding condition is preserved for a discrete-time system with the state and measurement models of equations (3.12) and (3.13), if it satisfies:

$$s_{i,k+1}(s_{i,k+1} - s_{i,k}) < \frac{1}{2} \Delta s_{i,k}^2, \quad (3.28)$$

where $\Delta s_{i,k} = s_{i,k} - s_{i,k-1}$.

Proof: Assume the following positive definite Lyapunov function that explicitly contains the first and second sliding conditions as:

$$V_k = s_{i,k}^2 + \Delta s_{i,k}^2, \quad (3.29)$$

where $s_k \subset S_k \in \mathbb{R}^{m \times 1}$ is the vector of sliding variables, and $\Delta s_k \subset \Delta S_k : \mathbb{R}^m \rightarrow \mathbb{R}^m$ is the backward difference operator generates the vector of sliding variable's difference. Based on the Lyapunov's second law, the system will be stable if: $\Delta V_{k+1} = V_{k+1} - V_k < 0$. The incremental difference of the proposed Lyapunov candidate (3.29) is now calculated as:

$$\Delta V_{k+1} = (s_{i,k+1}^2 + \Delta s_{i,k+1}^2) - (s_{i,k}^2 + \Delta s_{i,k}^2). \quad (3.30)$$

Simplifying the equality (3.30) leads to:

$$\Delta V_{k+1} = s_{i,k+1}^2 + (s_{i,k+1} - s_{i,k})^2 - [s_{i,k}^2 + (s_{i,k} - s_{i,k-1})^2]. \quad (3.31)$$

The above equality may be simplified as:

$$\Delta V_{k+1} = 2(s_{i,k+1}^2 - s_{i,k+1}s_{i,k}) - (s_{i,k} - s_{i,k-1})^2. \quad (3.32)$$

Note that the right side of equation (3.32) contains two terms and it is clear that the second term $-(s_{i,k} - s_{i,k-1})^2$ representing $-\Delta s_{i,k}^2$ is negative. Hence, if the first term $2(s_{i,k+1}^2 - s_{i,k+1}s_{i,k})$ is kept negative, stability and convergence of the second sliding motion is preserved. In this context, the sufficient condition for reaching the second sliding motion in discrete time is simply given by $s_{i,k+1}(s_{i,k+1} - s_{i,k}) < \frac{1}{2}(\Delta s_{i,k})^2$ that results in:

$$\Delta V_k < 0; \quad \forall s_{i,k} \in S_k, \forall \Delta s_{i,k} \in \Delta S_k. \quad (3.33)$$

It is easy to show that the proposed Lyapunov function of $V_k = s_{i,k}^2 + \Delta s_{i,k}^2$ preserves the first and second sliding conditions for discrete-time systems as follows. The Lyapunov function V_k contains two terms namely $s_{i,k}^2$ and $\Delta s_{i,k}^2$ that represent squared values of the sliding variable and its difference, respectively. Negative definiteness of the Lyapunov function's difference indicates that absolute values of $s_{i,k}^2$ and $\Delta s_{i,k}^2$ are decreasing over time such that after a finite time sequence $k_{2,sm}$, all trajectories that belong to the sliding hyperplane $S_k = e_{z_{k|k}}$ meet:

$$\|S(x_k, k)\| < \mathcal{E}_s, \|\Delta S(x_k, k)\| < \mathcal{E}_{\Delta s}; \quad \forall k \geq k_{2,sm}, \forall \mathcal{E}_s, \mathcal{E}_{\Delta s} > 0, \forall s_{i,k} \in S_k, \forall \Delta s_{i,k} \in \Delta S_k. \quad (3.34)$$

The above condition implies stability of a discrete-time sliding mode system under the second order sliding motion. □

Corollary 3.1: An intuitive result of *Theorem 3.1* is that if the condition (3.34) is preserved, then the measurement error $e_{z_{k|k}}$ and its difference $\Delta e_{z_{k|k}}$ are decreasing over time. However, due to modeling uncertainties, noise, and switching imperfections, this only occurs until they reach the existence subspace bounded by \mathcal{E}_s and $\mathcal{E}_{\Delta s}$.

3.5. Derivation of the 2nd-Order SVSF Corrective Gain

An important step in the 2nd-order SVSF estimation process is the update stage (3.21). Here, the corrective gain K_{k+1} is applied to the *a priori* state estimate to obtain the *a posteriori* state estimate. The corrective gain K_{k+1} must satisfy the Lyapunov function and the stability criterion presented in equations (3.29) and (3.28), respectively. It

contains some terms that restrict the *a posteriori* state estimate to within a close proximity of the actual state trajectory. In order to formulate the corrective gain, an explicit relation for refining the *a priori* measurement error into its *a posteriori* form is required. Later on, *Theorem 3.2* presents a corrective gain for the 2nd-order SVSF and shows its stability under the first and second sliding conditions.

Theorem 3.2: Consider a dynamic system with the state and measurement models of equations (3.12) and (3.13). The 2nd-order SVSF with the following corrective gain is stable and satisfies the first and second sliding conditions:

$$K_{i,k+1} = \hat{h}_{ii}^{-1} \left[e_{z,i_{k+1|k}} - \frac{e_{z,i_{k|k}}}{2} - \gamma_{ii} \sqrt{\frac{e_{z,i_{k|k}}^2}{4} + \frac{\Delta e_{z,i_{k|k}}^2}{2}} \right], \quad (3.35)$$

where $e_{z,i_{k|k}}$ denotes an element of the error vector $e_{z_{k|k}}$, \hat{h}_{ii} denotes an element of the inverted measurement matrix $\hat{H} \in \mathbb{R}^{m \times n}$ ($m = n$), $\Delta e_{z,i_{k|k}} = e_{z,i_{k|k}} - e_{z,i_{k-1|k-1}}$, and $\gamma = \text{Diag}(\gamma_{ii}) \in \mathbb{R}^{m \times m}$ is a diagonal matrix with positive entries such that $0 < \gamma_{ii} < 1$.

Proof: Consider a positive definite Lyapunov function such that it contains the first and second sliding mode conditions as follows:

$$V_k = s_{i,k}^2 + \Delta s_{i,k}^2, \quad (3.36)$$

where $s_{i,k} \in \mathbb{R}$ denotes an entry of the sliding variable vector for $i = 1, \dots, m$, where i denotes the row number of entries. Furthermore, $\Delta s_{i,k} \in \mathbb{R}$ represents the backward difference operator that generates the difference of the sliding variable vector. Based on the Lyapunov's second law of stability, the system will be stable if:

$\Delta V_{k+1} = V_{k+1} - V_k < 0$. In this context, let multiply both sides of the gain in equation (3.35) by \hat{h}_{ii} and consider the simplified result in terms of the elements as follows:

$$e_{z,i_{k+1|k}} - \hat{h}_{ii} K_{i,k+1} = \frac{e_{z,i_{k|k}}}{2} + \gamma_{ii} \sqrt{\frac{e_{z,i_{k|k}}^2}{4} + \frac{\Delta e_{z,i_{k|k}}^2}{2}}. \quad (3.37)$$

Following equation (3.21), since $\hat{x}_{k+1|k+1} = \hat{x}_{k+1|k} + K_{k+1}$, one can restate the gain as:

$K_{k+1} = \hat{x}_{k+1|k+1} - \hat{x}_{k+1|k}$. Substituting this relation into equality (3.37) yields:

$$e_{z,i_{k+1|k}} - \hat{h}_{ii} (\hat{x}_{i,k+1|k+1} - \hat{x}_{i,k+1|k}) = \frac{e_{z,i_{k|k}}}{2} + \gamma_{ii} \sqrt{\frac{e_{z,i_{k|k}}^2}{4} + \frac{\Delta e_{z,i_{k|k}}^2}{2}}. \quad (3.38)$$

The *a priori* and the *a posteriori* measurement errors at time step k are given by equations

(3.18) and (3.19) as: $e_{z,i_{k+1|k}} = \hat{h}_{ii} (\hat{x}_{i,k+1|k+1} - \hat{x}_{i,k+1|k})$ and $e_{z,i_{k+1|k+1}} = z_{i,k+1} - \hat{h}_{ii} \hat{x}_{i,k+1|k+1}$.

Subtracting the *a priori* error from the *a posteriori* error results in:

$$e_{z,i_{k+1|k+1}} - e_{z,i_{k+1|k}} = -\hat{h}_{ii} (\hat{x}_{i,k+1|k+1} - \hat{x}_{i,k+1|k}). \quad (3.39)$$

Using equation (3.39), equality (3.38) may be restated as follows:

$$e_{z,i_{k+1|k+1}} = \frac{e_{z,i_{k|k}}}{2} + \gamma_{ii} \sqrt{\frac{e_{z,i_{k|k}}^2}{4} + \frac{\Delta e_{z,i_{k|k}}^2}{2}}. \quad (3.40)$$

Transferring $e_{z,i_{k|k}}/2$ in equality (3.40) to the left side and squaring both sides, it becomes:

$$\left(e_{z,i_{k+1}|k+1} - \frac{e_{z,i_k|k}}{2} \right)^2 = \gamma_{ii}^2 \left(\frac{e_{z,i_k|k}^2}{4} + \frac{\Delta e_{z,i_k|k}^2}{2} \right). \quad (3.41)$$

Since $\lambda = \text{Diag}(\gamma_{ii})$ is defined such that $0 < \gamma_{ii} < 1$, the above equality is simply restated as follows:

$$\left(e_{z,i_{k+1}|k+1} - \frac{e_{z,i_k|k}}{2} \right)^2 < \left(\frac{e_{z,i_k|k}^2}{4} + \frac{\Delta e_{z,i_k|k}^2}{2} \right). \quad (3.42)$$

Expanding the above inequality leads to:

$$e_{z,i_{k+1}|k+1}^2 - e_{z,i_{k+1}|k+1} e_{z,i_k|k} < \Delta e_{z,i_k|k}^2 / 2. \quad (3.43)$$

Since $s_{i,k} = e_{z,i_k|k}$, inequality (3.43) may be restated in terms of the sliding variable entries $s_{i,k}$ as follows:

$$s_{i,k+1}^2 - s_{i,k+1} s_{i,k} < \Delta s_{i,k}^2 / 2. \quad (3.44)$$

Adding and subtracting $s_{i,k}^2$ into the left hand side of the above inequality and rearranging the resulting terms, it becomes:

$$2s_{i,k+1}^2 - 2s_{i,k+1} s_{i,k} + s_{i,k}^2 - s_{i,k}^2 - \Delta s_{i,k}^2 < 0. \quad (3.45)$$

Equality (3.45) may be restated such that:

$$s_{i,k+1}^2 + (s_{i,k+1} - s_{i,k})^2 - s_{i,k}^2 - (s_{i,k}^2 + \Delta s_{i,k}^2) < 0. \quad (3.46)$$

Based on the Lyapunov function candidate, given by $V_k = s_{i,k}^2 + \Delta s_{i,k}^2$, inequality (3.46) may be restated such that:

$$V_{k+1} - V_k < 0, \quad (3.47)$$

where it leads to:

$$\Delta V_k < 0; \quad \forall s_{i,k} \in S_k, \forall \Delta s_{i,k} \in \Delta S_k. \quad (3.48)$$

Since the Lyapunov function candidate V_k is a function of $s_{i,k}$ and $\Delta s_{i,k}$, it is deduced from equation (3.48) that the corrective gain (3.35) preserves stability and convergence of the 2nd-order SVSF for both the first and second order sliding mode regimes. \square

Corollary 3.2: Proper selection of the convergence rate matrix γ such that $0 < \gamma_{ii} < 1$ preserves the stability and convergence of the 2nd-order SVSF. Note that smaller values of γ_{ii} result in accelerating the Lyapunov decrement and subsequently increasing the convergence rate.

The 2nd-order SVSF gain is actually representing a second-order Markov process which is a function of the *a priori* measurement error vector $e_{i,z_{k+1|k}}$, the difference of the measurement error $\Delta e_{i,z_{k|k}} = e_{i,z_{k|k}} - e_{i,z_{k-1|k-1}}$, and the measurement matrix inverse \hat{h}_{ii}^{-1} . The term $(e_{i,z_{k|k}} - e_{i,z_{k-1|k-1}})^2 / 2$ in equation (3.35) arises by preserving the second order sliding condition. A block-diagram representation of the 2nd-order SVSF estimation process is presented in Figure 3.3. In the 2nd-order SVSF estimation process, an initial estimate of state variables is made albeit uncertain. The corrective gain pushes the estimated state trajectory towards the true state trajectory until it reaches the existence

k , the width of the existence boundary layer is obtained by calculating the two quantities $s_{i,k}$ and $\Delta s_{i,k}$ that are a measure of the distance from the switching hyperplane. Under the second sliding condition, these two variables converge to within an existence subspace with two upper bounds ε_s and $\varepsilon_{\Delta s}$.

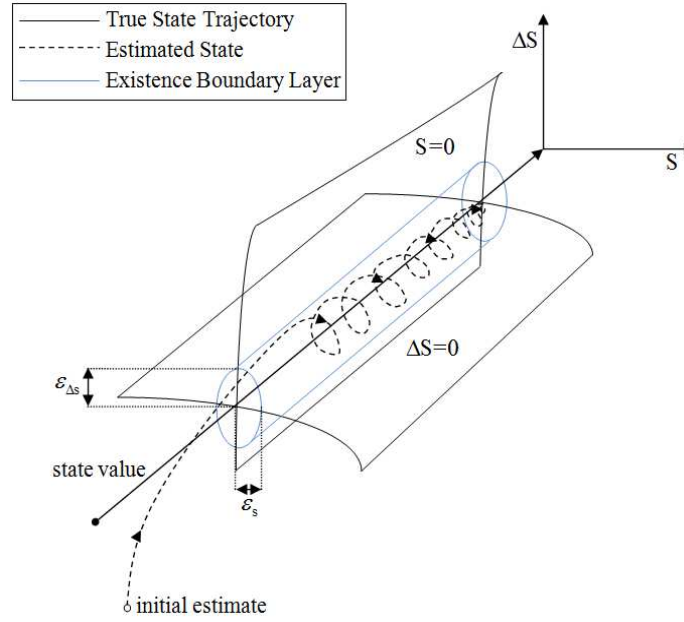


Figure 3.4: Main concept of the 2nd-order SVSF method for state estimation

Satisfaction of the second sliding condition by the 2nd-order SVSF will result in higher degrees of robustness in the estimated state trajectories. It is because the corrective gain of the 2nd-order SVSF applies separate constraints to the measurement error $\|e_{z_k|k}\| < \varepsilon_s$ and its difference $\|\Delta e_{z_k|k}\| < \varepsilon_{\Delta s}$ at the same time. It forces both the measurement error and its difference to remain in a close vicinity of the origin, $e_{z_k|k} = \Delta e_{z_k|k} = 0$, during the estimation process. In addition, regarding the equality (3.35), the corrective gain at $k+1$ computationally depends on the values of the measurement error at time k and $k-1$, namely $e_{z_k|k}$ and $e_{z_{k-1}|k-1}$. This means that the 2nd-order SVSF updates the *a priori*

state estimates at $k + 1$ based on information available from two time steps before. The corrective gain of the 2nd-order SVSF uses more information from the past in comparison to other first order filters.

Having access to more information of the sliding mode system alleviates undesirable effects of the chattering signal, unwanted spikes and other high frequency dynamics. It improves the performance of the 2nd-order SVSF in terms of accuracy, robustness, and smoothness. These are the main advantages of the 2nd-order SVSF over the Kalman filter and the former 1st-order SVSF. Figure 3.5 shows why preserving the second sliding condition helps the 2nd-order SVSF to increase accuracy. Accordingly, in the 2nd-order SVSF estimation process, the constraints are applied in two directions. The first sliding condition constrains the measurement error $e_{z_k|k}$ to within an upper bound \mathcal{E}_s and the second sliding condition constrains the error difference $\Delta e_{z_k|k} = e_{z_k|k} - e_{z_{k-1}|k-1}$ to within an upper bound $\mathcal{E}_{\Delta s}$. In contrast in the 1st-order SVSF, there exists only one constraint that applies an upper bound \mathcal{E}_s to only the measurement error $e_{z_k|k}$.

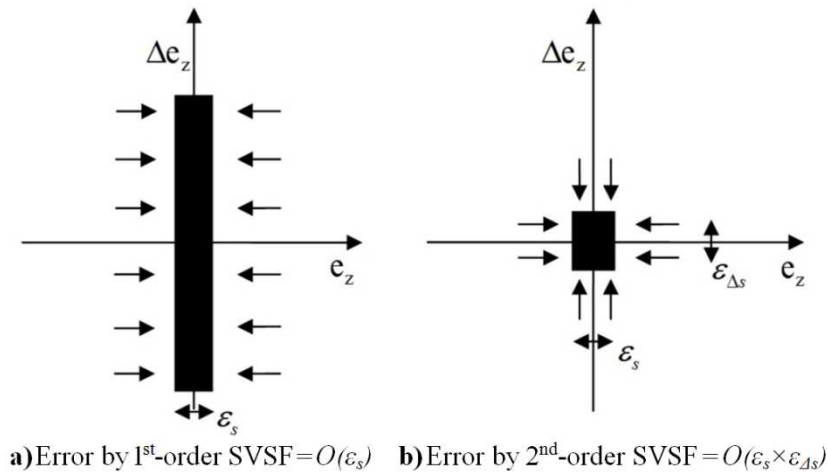


Figure 3.5: Main concept of increasing accuracy via the 2nd-order SVSF (upgraded from [7])

Remark 3.5: The 2nd-order SVSF can be applied to nonlinear systems without the need for linearization or approximation. This capability is one of the main advantages of the SVSF techniques over other estimation methods that are using the linearization or some form of approximation of nonlinear terms. The SVSF-type filtering does however require a linear or piecewise linear measurement model.

Remark 3.6: Pursuing the r^{th} -order sliding mode theory, it is possible to extend the 2nd-order SVSF concept to the n^{th} -order SVSF in which the n^{th} -order sliding mode condition is satisfied by $S_k = \Delta S_k = \dots = \Delta^{n-1} S_k = 0$. In order to preserve the stability of the n^{th} -order SVSF, the Lyapunov function may be defined as:

$$V_k = s_{i,k}^2 + \Delta s_{i,k}^2 + \dots + \Delta^{n-1} s_{i,k}^2, \quad (3.49)$$

where $\Delta^{n-1} s_{i,k} : \mathbb{R}^{m \times 1} \rightarrow \mathbb{R}^{m \times 1}$ is the $(n-1)^{\text{th}}$ order difference of the sliding variable vector and is a smooth function. The resulting sliding motion will be in an n -dimensional existence boundary layer. Alternatively, the corrective gain of the n^{th} -order SVSF is an n^{th} -order Markov process and formulated as a function of the measurement error vectors, from $e_{z_k|k}$ up to $e_{z_{k-(n-1)k-(n-1)}}$. Note that by increasing the order of the sliding mode condition, the amount of information that is required will increase.

3.6. The 2nd-Order SVSF for Linear Systems with Fewer Measurements than States

The 2nd-order SVSF can be applied to systems with fewer measurements than state variables. In this case, the corrective gain of the 2nd-order SVSF may be derived using the Luenberger's approach as presented in [3]. In this context, the nonlinear model of the system must be linearized. Now, consider a linear discrete state-space system as:

$$x_{k+1} = Ax_k + Bu_k + w_k, \quad (3.50)$$

$$z_{k+1} = Cx_{k+1} + v_{k+1}, \quad (3.51)$$

where $A \in \mathbb{R}^{n \times n}$ is the state transition matrix, $B \in \mathbb{R}^{p \times 1}$ is the control matrix, $C \in \mathbb{R}^{m \times n}$ is the measurement matrix, $w_k \in \mathbb{R}^{n \times 1}$ and $v_k \in \mathbb{R}^{m \times 1}$ are the process uncertainties and measurement noise, respectively. Note that in order to apply the 2nd-order SVSF to systems with fewer measurements than states, *Assumption 3.3* needs to be satisfied. The state variables may be decomposed into two parts $x_k = [x_{u_k} \quad x_{l_k}]^T$, where the upper part $x_{u_k} \in \mathbb{R}^{l \times 1}$ is directly measured and whereas the lower part $x_{l_k} \in \mathbb{R}^{(n-l) \times 1}$ is not [3].

Using the Luenberger's transformation (refer to [3]), a revised state vector is obtained in terms of measurements such that $y_k = [z_k \quad y_{l_k}]^T$, where $z_k \in \mathbb{R}^{l \times 1}$ denotes the direct measurement vector and $y_{l_k} \in \mathbb{R}^{(m-l) \times 1}$ denotes an artificial measurement vector. The problem is to obtain values for entries of y_{l_k} based on the partitioned model [3]. The measurement model is presented as:

$$\begin{bmatrix} z_{k+1} \\ y_{l_{k+1}} \end{bmatrix} = \begin{bmatrix} \Phi_{11} & \Phi_{12} \\ \Phi_{21} & \Phi_{22} \end{bmatrix} \begin{bmatrix} z_k \\ y_{l_k} \end{bmatrix} + \begin{bmatrix} G_1 \\ G_2 \end{bmatrix} u_k + \begin{bmatrix} \bar{w}_{1_k} \\ \bar{w}_{2_k} \end{bmatrix}, \quad (3.52)$$

where $\Phi = T^{-1}AT$, $G = T^{-1}B$, and $\bar{w}_k = T^{-1}w_k - [\Phi_{11} \quad \Phi_{21}]^T v_k$ [3]. Further to (3.52), the *a priori* state estimate may be obtained as [3]:

$$\begin{bmatrix} \hat{z}_{k+1|k} \\ \hat{y}_{l_{k+1}|k} \end{bmatrix} = \begin{bmatrix} \hat{\Phi}_{11} & \hat{\Phi}_{12} \\ \hat{\Phi}_{21} & \hat{\Phi}_{22} \end{bmatrix} \begin{bmatrix} z_k \\ \hat{y}_{l_k|k} \end{bmatrix} + \begin{bmatrix} \hat{G}_1 \\ \hat{G}_2 \end{bmatrix} u_k. \quad (3.53)$$

As presented in [3], the *a priori* and *a posteriori* measurement error vectors for the hidden measurement vector y_{l_k} are calculated as:

$$e_{y_{l_k|k}} = \hat{\Phi}_{12}^{-1} e_{z_{k+1|k}} - \hat{\Phi}_{12}^{-1} \bar{w}_{l_k}, \quad (3.54)$$

$$e_{y_{l_{k+1|k}}} = \hat{\Phi}_{22} \hat{\Phi}_{12}^{-1} e_{z_{k+1|k}} - \hat{\Phi}_{22} \hat{\Phi}_{12}^{-1} \bar{w}_{l_k} + \bar{w}_{2_k}, \quad (3.55)$$

where $e_{y_l} \in \mathbb{R}^{(m-l) \times 1}$ is the artificial measurement error vector and $e_z \in \mathbb{R}^{l \times 1}$ is the measurement error vector corresponding to measurable states. Equations (3.54) and (3.55) present a mapping of the measurement error vector that is used according to Luenberger's method for deriving a switching hyperplane and in calculating the filter gain.

In order to derive the 2nd-order SVSF gain for the lower partition of states, the switching hyperplane for the lower partition relies on a projection using measurement errors such that [3]:

$$S_l = \hat{\Phi}_{22} \hat{\Phi}_{12}^{-1} e_{z_{k|k}}, \quad (3.56)$$

where $S_l \in \mathbb{R}^{(m-l) \times 1}$. Further to equation (3.35), the 2nd-order SVSF corrective gain for the lower partition of states is derived as:

$$K_{i,k+1} = \hat{\Phi}_{22,ij} \hat{\Phi}_{12,ij}^{-1} e_{z,i_{k+1|k}} - \frac{\hat{\Phi}_{12,ij}^{-1} e_{z,i_{k|k}}}{2} - \gamma_{ii} \sqrt{\frac{(\hat{\Phi}_{12,ij}^{-1} e_{z,i_{k|k}})^2}{4} + \frac{(\hat{\Phi}_{12,ij}^{-1} \Delta e_{z,i_{k|k}})^2}{2}}, \quad \text{for } i, j = l+1, \dots, m. \quad (3.57)$$

By combining the gains of each partition of the state vector, the 2nd-order SVSF gain is restated for linear systems with fewer measurements than states as:

$$K_{i,k+1} = \begin{cases} K_{i,k+1} = \hat{h}_{ii}^{-1} \left[e_{z,i_{k+1|k}} - \frac{e_{z,i_{k|k}}}{2} - \gamma_{ii} \sqrt{\frac{e_{z,i_{k|k}}^2}{4} + \frac{\Delta e_{z,i_{k|k}}^2}{2}} \right], \text{ for } i, j = 1, \dots, l \\ \hat{\Phi}_{22,ij}^{-1} \hat{\Phi}_{12,ij}^{-1} e_{z,i_{k+1|k}} - \frac{\hat{\Phi}_{12,ij}^{-1} e_{z,i_{k|k}}}{2} - \gamma_{ii} \sqrt{\frac{(\hat{\Phi}_{12,ij}^{-1} e_{z,i_{k|k}})^2}{4} + \frac{(\hat{\Phi}_{12,ij}^{-1} \Delta e_{z,i_{k|k}})^2}{2}}, \text{ for } i, j = l+1, \dots, m. \end{cases} \quad (3.58)$$

where $\hat{h}^{-1} \subset \hat{H}^+$ is the pseudo-inverse of the measurement matrix $\hat{H} \in \mathbb{R}^{m \times n}$ that is not square.

Hence, the vector of sliding variables may be defined as: $S_k = \left[e_{z_{k|k}} \quad \hat{\Phi}_{22}^{-1} \hat{\Phi}_{12}^{-1} e_{z_{k+1|k}} \right]^T$.

Note that the squared terms in equation (3.58) are calculated using the Schur product. The gain formulation that can be used for nonlinear systems is provided in [3].

3.7. Comparative Analysis of the 2nd-Order SVSF

The 2nd-order SVSF method is compared with other estimation methods by its application to an electro-hydrostatic actuation (EHA) system with a model described in [3]. This comparison is made between the Kalman filter, the 1st-order SVSF and the proposed 2nd-order SVSF. These methods are applied to the EHA model under two different scenarios that include: 1) the safe condition with no modeling uncertainties; and 2) the faulty condition with a higher level of modeling uncertainties. The EHA model has three state variables including the position $x_1 = x$, velocity $x_2 = dx_1/dt$, and acceleration $x_3 = d^2x_1/dt^2$, where position is the only measurable state [3]. The linear discrete-time state and measurement models of the EHA are given by equations (3.50) and (3.51), respectively. Numerical values of the state, control and measurement matrices of the EHA model are presented as [3]:

$$A = \begin{bmatrix} 1 & 0.001 & 0 \\ 0 & 1 & 0.001 \\ -557.02 & -28.616 & 0.9418 \end{bmatrix}, \quad B = \begin{bmatrix} 0 \\ 0 \\ 557.02 \end{bmatrix}, \quad C = [1 \ 0 \ 0]. \quad (3.59)$$

Note that w_k and v_k are multivariate white normal random vectors with the mean of zero and standard deviation vectors equal to [3]:

$$w_{std} = [0.05 \quad 0.1 \quad 0.1]^T, \quad v_{std} = [0.05]. \quad (3.60)$$

The EHA system is third order with a single measurement that is the position. To produce the augmented measurement vector, the state space is partitioned based on equation (3.53) as [3]:

$$\hat{\Phi}_{11} = [1], \quad \hat{\Phi}_{12} = [0.001 \quad 1], \quad \hat{\Phi}_{21} = \begin{bmatrix} 0 \\ -877.02 \end{bmatrix}, \quad \hat{\Phi}_{22} = \begin{bmatrix} 1 & 0.001 \\ -32.616 & 0.8418 \end{bmatrix}. \quad (3.61)$$

For simulation purpose, the 2nd-order SVSF's gain is derived for the case with the convergence rate equal to $\gamma = [0.1]$. Hence, the gain is obtained for the EHA system using equation (3.35) for the measurable state and equation (3.57) for the rest as:

$$K_{k+1} = \begin{cases} e_{z_{k+1|k}} - \frac{e_{z_{k|k}}}{2} - \gamma \sqrt{\frac{e_{z_{k|k}}^2}{4} + \frac{\Delta e_{z_{k|k}}^2}{2}}, \\ 0.002e_{z_{k+1|k}} - 0.0005e_{z_{k+1|k}} - 1e - 4\sqrt{\frac{e_{z_{k+1|k}}^2}{4} + \frac{\Delta e_{z_{k+1|k}}^2}{2}}, \\ 0.809e_{z_{k+1|k}} - 0.5e_{z_{k+1|k}} - \sqrt{\frac{e_{z_{k+1|k}}^2}{4} + \frac{\Delta e_{z_{k+1|k}}^2}{2}}. \end{cases} \quad (3.62)$$

To check the robustness of the 2nd-order SVSF, a large degree of unknown uncertainties is injected into the model by changing the state matrix after 0.5 sec of simulation to [3]:

$$A_2 = \begin{bmatrix} 1 & 0.001 & 0 \\ 0 & 1 & 0.001 \\ -240 & -28 & 0.9418 \end{bmatrix}. \quad (3.63)$$

Note that element a_{31} of matrix A_1 is multiplied by 0.5 in order to simulate uncertainties.

The input u to the EHA system is a random signal with the amplitude in the range of -1 to 1, superimposed on a step input that occurs at 0.5 sec. The initial values of states are assumed to be zero and the sampling time for discretization is 0.001 sec. For the Kalman filter, the process noise, measurement noise and initial error covariance are respectively obtained as: $Q = \text{diag}([1 \ 10 \ 50])$, and $P_0 = 20Q$. Additionally, $R = 0.1 \text{cm}^2$ is obtained by calculating variance of the innovation signal for a time period. For the 1st-order SVSF and the 2nd-order SVSF methods, the convergence rate γ is 0.5. Furthermore, for the 1st-order SVSF, the smoothing boundary layer is set to $\psi = [5 \ 5 \ 5]^T \times v_{std}$, where v_{std} is the standard deviation of the measurement noise. Simulations are performed using the MATLAB and after 10^3 Monte-Carlo runs. Note that using a larger number of Monte-Carlo runs only increases the running time, when simulation results do not change.

Tables 3.1 to 3.3 compare some numerical performance indicators calculated by the three estimation methods (Kalman filter, 1st-order SVSF, and the 2nd-order SVSF) for a normal and an uncertain EHA model. For the normal model, it is assumed that the EHA model is known when there exist bounded process and measurement noise. For the uncertain EHA model, high amount of modeling uncertainties are injected after 0.5 sec. The uncertainties are applied to examine the performance and the robustness of the three estimation techniques given added uncertainties. The actual trajectories are also provided by solving state trajectories of the EHA system with state matrices A , B , and C . The state estimation error is the difference between values of the actual and estimated state.

In order to compare these state estimators, some indicators such as the root mean squared error (RMSE), bias and standard deviations (STD) of the state estimation error are used. The RMSE of a state estimator is an indicator of the difference between state estimate values \hat{x}_i and the actual values x_i that are only available through simulation.

Note that the individual difference is referred to as the state estimation error e_x , but the RMSE serves to summarize these differences into a single indicator of the estimator performance. In simulations, measurements of the state variables x_i are artificially produced by using the state and measurement models, and injecting measurement noise v_k and process uncertainties w_k . The RMSE value for an estimator is calculated as:

$$RMSE = \sqrt{\frac{\sum_{i=1}^n (x_i - \hat{x}_i)^2}{n}}, \quad (3.64)$$

where n denotes the number of time steps. Furthermore, the state estimation error is defined as the difference between the actual state values x_i and the estimated state values \hat{x}_i . Mean of the state estimation error (Bias) of an estimator is obtained as [1]:

$$Bias = E[x] - E[\hat{x}(k, Z_k)], \quad (3.65)$$

where $E[\]$ represents the expected value operator. For a discrete realization, Bias of a state estimator is calculated by:

$$Bias = \frac{1}{n} \sum_{i=1}^n (x_i - \hat{x}_i). \quad (3.66)$$

The standard deviation (STD) is an indicator that represents how much variation or dispersion from the average exists in a data set or statistical population. A low STD shows that the data points tend to be very close to the mean value (or the expected value), and a high STD represents that the data points are spread out over a large range of values [1]. STD of the state estimation error of an estimator is given by (\bar{e}_x denotes the mean value of the state estimation error):

$$STD = \sqrt{E[(e_x - \bar{e}_x)^2]} = \sqrt{E[e_x^2] - (E[\bar{e}_x])^2}, \quad (3.67)$$

For a discrete realization, the STD of the state estimation error is calculated as:

$$STD = \sqrt{\frac{1}{n} \sum_{i=1}^n (e_{x,i} - \bar{e}_{x,i})^2}. \quad (3.68)$$

Tables 3.1 through 3.3 respectively present numeric values of the RMSE, Bias, and STD of the state estimation error generated by the above mentioned state estimators. Table 3.1 presents the RMSE value of the state estimation error $e_{x_{k|k}}$ for both normal and uncertain conditions. Further to Table 3.1, the Kalman filter produces the most accurate state estimates in terms of the RMSE for the known model of the EHA system subject to white noise, followed by the 2nd-order SVSF and the 1st-order SVSF. It is because for normal conditions, the Kalman filter is optimal in terms of the RMSE. In spite of the normal case, it is observed that for the uncertain case, the 2nd-order SVSF produces the most accurate state estimates in terms of the RMSE. This accuracy is due to the robustness of the 2nd-order SVSF to uncertainties. Using the second order sliding condition instead of the smoothing boundary layer is the main reason why the 2nd-order SVSF is more accurate over the 1st-order SVSF for both normal and uncertain cases.

Table 3.2 compares state estimates in terms of the bias (mean of the state estimation error $e_{x_{k|k}}$) for both normal and uncertain conditions. Table 3.3 compares state estimates in terms of the standard deviation (STD) of the state estimation error $e_{x_{k|k}}$. For the normal case, the Kalman filter produces the smallest bias, followed by the 2nd-order SVSF and the 1st-order SVSF. But for the uncertain case, the 2nd-order SVSF generates the smallest bias, followed by the 1st-order SVSF and the Kalman filter. Furthermore, the 2nd-order SVSF has the smallest values pertaining to the standard deviation of the state estimation error $e_{x_{k|k}}$. Having the smallest value of the standard deviation for both normal and

uncertain models indicates the smoothness characteristic of the 2nd-order SVSF in comparison to other methods that reduces the amount of dispersion in the error signal. The 2nd-order SVSF produces state estimates with minimum values of bias and dispersion in the error $e_{z_{k|k}}$ for uncertain conditions.

Table 3.1: Comparison between RMSE of three estimation methods applied to the EHA model

	Kalman Filter		1 st -order SVSF		2 nd -order SVSF	
	Normal	Uncertain	Normal	Uncertain	Normal	Uncertain
RMSE of Position (cm)	1.01×10^{-2}	0.31	1.10×10^{-2}	1.13×10^{-2}	1.05×10^{-2}	1.08×10^{-2}
RMSE of Velocity (cm/s)	1.046	21.66	1.060	15.50	1.05	14.49
RMSE of Accel. (cm/s²)	167.24	2206.06	170.31	1341.53	168.91	1335.18

Table 3.2: Comparison between Biases of the three estimation methods applied to the EHA model

	Kalman Filter		1 st -order SVSF		2 nd -order SVSF	
	Normal	Uncertain	Normal	Uncertain	Normal	Uncertain
Bias in Position (m)	-2.53×10^{-5}	-9.94×10^{-3}	-2.58×10^{-4}	-3.15×10^{-4}	-1.57×10^{-4}	-2.12×10^{-4}
Bias in Velocity (m/s)	-1.95×10^{-3}	5.63	-2.77×10^{-3}	3.78	-4.70×10^{-3}	3.78
Bias in Accel. (m/s²)	9.84	27.32	10.04	20.86	9.98	20.76

Table 3.3: Comparison between STD of the estimation methods applied on the EHA model

	Kalman Filter		1 st -order SVSF		2 nd -order SVSF	
	Normal	Uncertain	Normal	Uncertain	Normal	Uncertain
STD of Position Error (m)	9.63×10^{-2}	0.30	1.05×10^{-2}	2.09×10^{-2}	7.51×10^{-3}	9.86×10^{-3}
STD of Velocity Error (m/s)	1.09	22.29	1.12	17.95	1.11	11.63
STD of Accel. Error (m/s²)	183.55	2867.9	186.16	1823.9	185.37	1674.60

Figure 3.6 presents the actual profile and the estimated state profile using the Kalman filter and the 2nd-order SVSF for the EHA in normal condition. Figure 3.7 compares the actual and the estimated state trajectories using the Kalman filter and the

2nd-order SVSF for the EHA system with modeling uncertainties. Comparing Figures 3.6 and 3.7 confirm the better performance of the 2nd-order SVSF in estimating state variables of the EHA system in the uncertain condition.

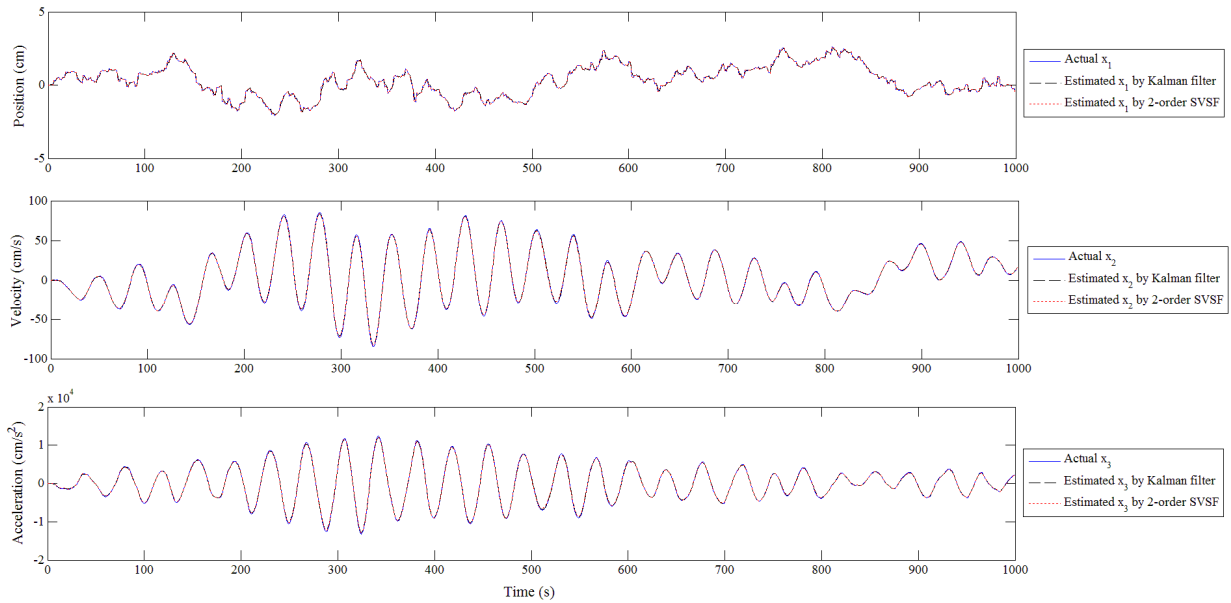


Figure 3.6: State estimations by the Kalman filter and 2nd-order SVSF for the normal EHA system

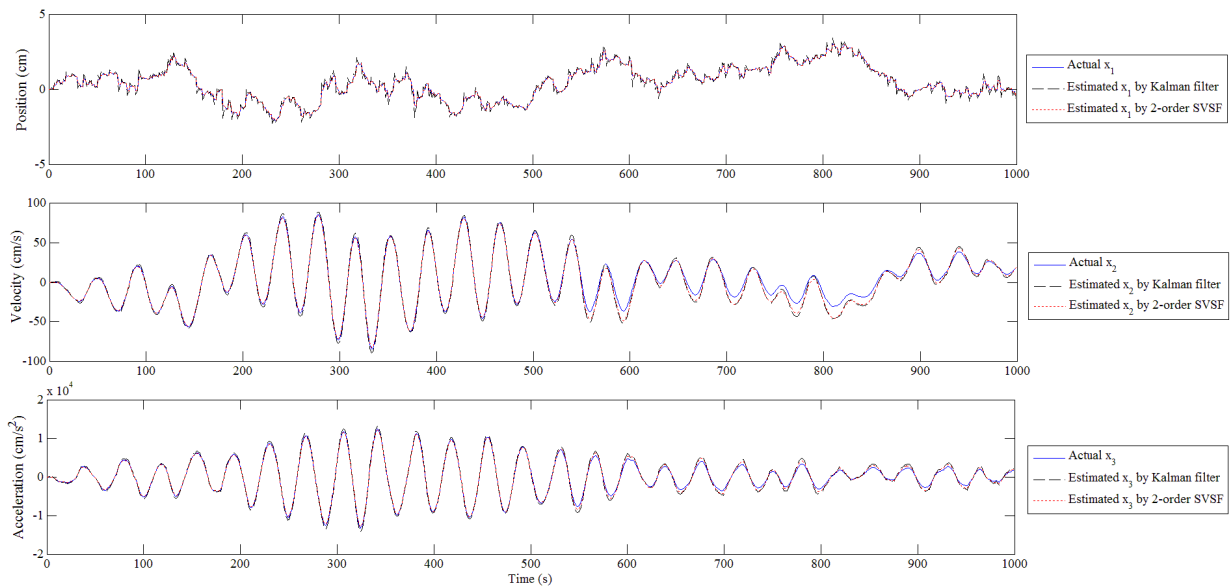


Figure 3.7: State estimations by the Kalman filter and 2nd-order SVSF for the faulty EHA system

The position's estimation error signal obtained from these three methods is presented in Figure 3.8. It is clear that the 2nd-order SVSF produces the smoothest state estimates with the smallest variation for both normal and uncertain cases. These profiles with numeric values of Table 3.3 demonstrate that satisfaction of the second sliding condition provides higher degrees of smoothness in estimates over other approaches based on approximation.

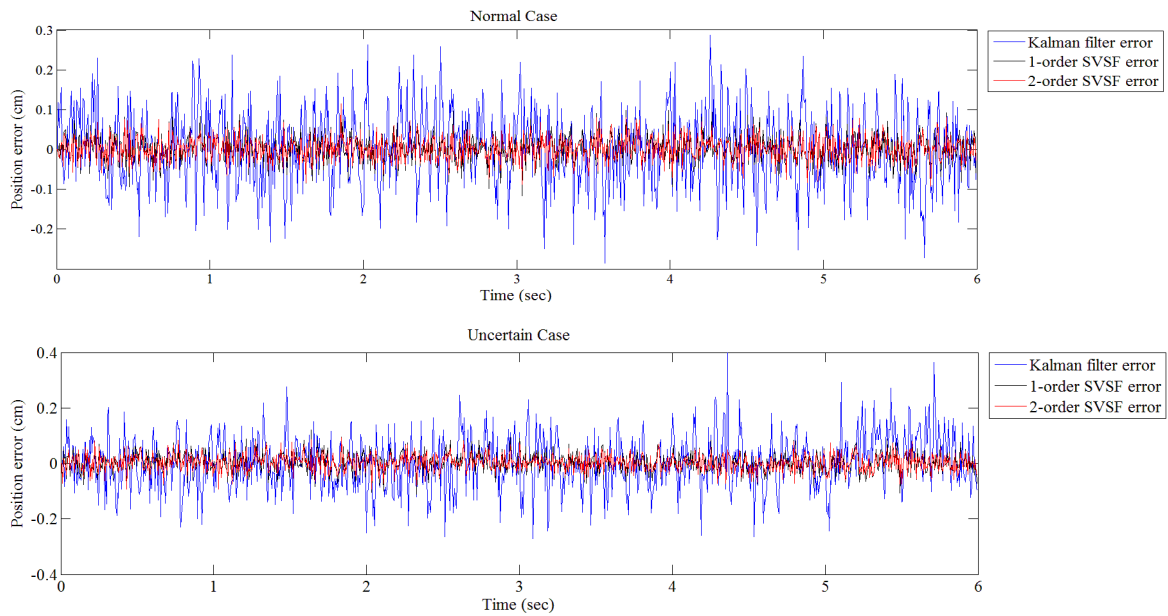


Figure 3.8: Profiles of measurement errors by different estimators for normal and faulty EHA

Figure 3.9 presents the phase portrait of the measurement error and its first difference obtained by the 1st-order SVSF under the normal and faulty scenarios. Moreover, Figure 3.10 presents the same phase portrait obtained by the 2nd-order SVSF. It is observed that for the 2nd-order SVSF in both normal and uncertain scenarios, the measurement error and its difference are decreasing in time until the estimates reach the existence subspace. This is due to the stability of corrective gain formulation for the 2nd-order SVSF and its ability to satisfy both the first and second sliding mode conditions.

For the 1st-order SVSF, it is observed that the measurement error and its difference are larger than ones obtained by the 2nd-order SVSF, but they still remain norm-bounded. As expected, stability of the 2nd-order SVSF results in finding an upper bound ε_s for the measurement error $e_{z_{k|k}}$ and another bound $\varepsilon_{\Delta s}$ for its difference $e_{z_{k|k}} - e_{z_{k-1|k-1}}$.

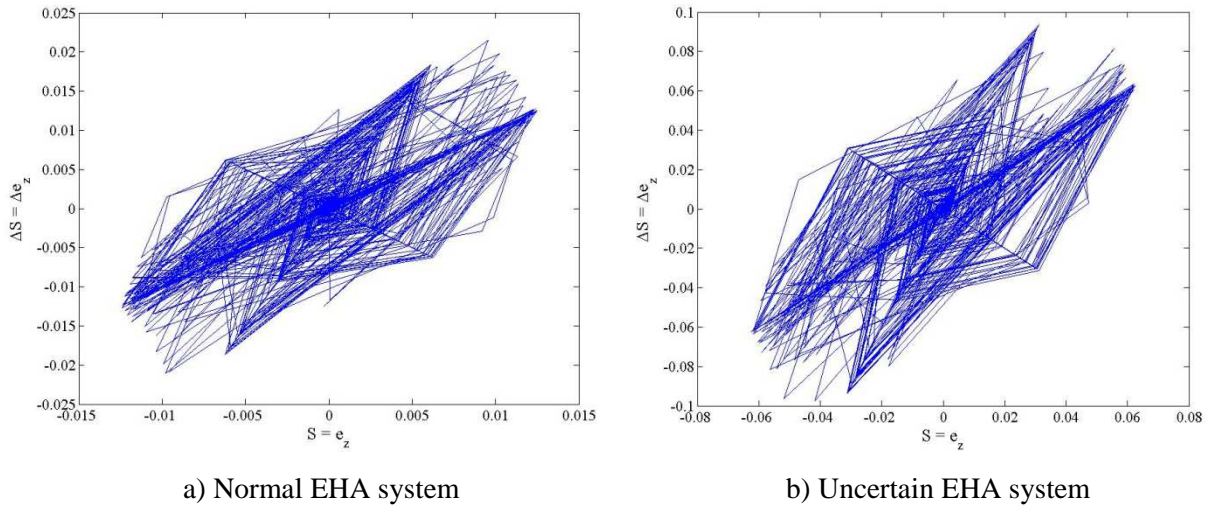


Figure 3.9: Phase portrait of the measurement error and its difference obtained by the 1st-order SVSF

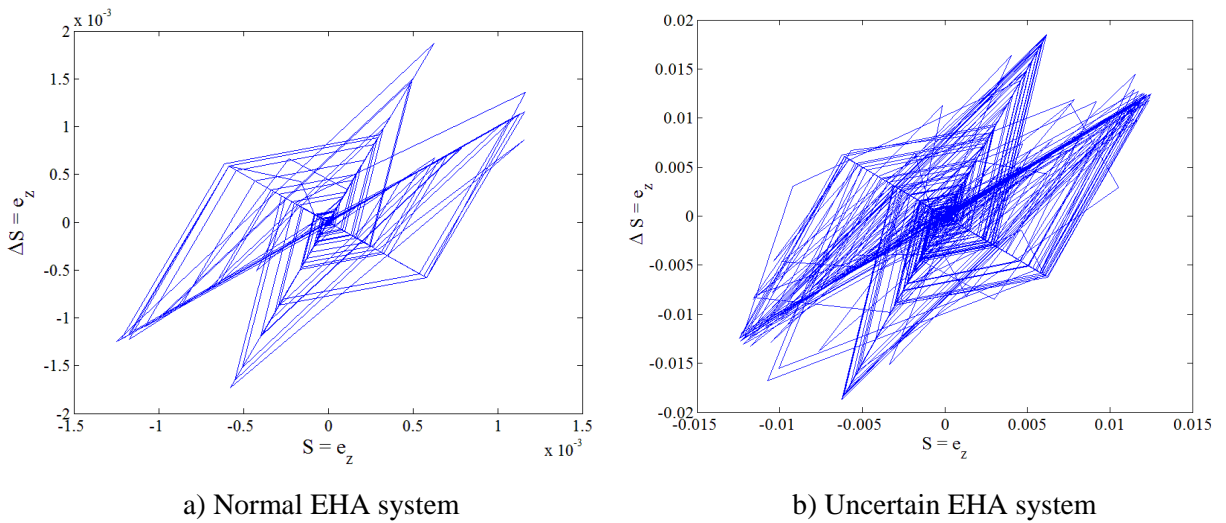


Figure 3.10: Phase portrait of the measurement error and its difference obtained by the 2nd-order SVSF

The main advantages of the 2nd-order SVSF over the Kalman filter and 1st-order SVSF are its greater accuracy and robustness in uncertain conditions. These are directly due to preserving the second order sliding condition which forces not only the estimated state trajectories to slide along the switching hyperplane, but also their derivatives to slide along a tangential hyperplane. Note that the corrective gain of the 2nd-order SVSF in each step updates the *a priori* state estimates based on available information of the measurement error from two steps back. This helps the 2nd-order SVSF to create smoother state estimates with smaller bias and dispersions in the estimation error.

3.8. Summary

A new state estimation strategy referred to as the second-order smooth variable structure filter (2nd-order SVSF) is introduced and implemented in this chapter. It is formulated in a predictor-corrector form and uses a corrective gain to satisfy both the first and second sliding conditions during the estimation process. The filter uses a corrective gain that is derived to satisfy Lyapunov's second law of stability. The 2nd-order SVSF can be applied to linear as well as nonlinear systems (without a need for linearization for the latter). Satisfaction of the second sliding condition results in higher degrees of robustness and smoothness in the estimated trajectory. This is achieved because the corrective gain of the 2nd-order SVSF has access to more information from past measurements that in this case are two previous time steps.

The 2nd-order SVSF formulation not only helps to produce smoother state estimates, but also improves performance compared to 1st-order SVSF in terms of accuracy and robustness. Simulation results indicate that when there are modeling uncertainties, the 2nd-order SVSF produces the most accurate state estimates and provides the smallest

RMSE, bias and standard deviations in the state estimation error compared to the other two filters. Satisfying the first and second sliding conditions, the 2nd-order SVSF alleviates chattering without the need for a smoothing boundary layer.

Main advantages of the 2nd-order SVSF with respect to other state estimation methods may be summarized as follows:

- the filter is robust and produces accurate state estimates in uncertain situations where the level, source and occurrence of uncertainties are unknown;
- the filter can be applied to systems with a nonlinear state model without any need for linearization or approximation;
- there is no need to use saturation or any type of approximation to alleviate discontinuities and prevent chattering;
- the filter produces smoother state estimates (with smaller STD of the error) when higher amount of information is available for the update stage; and
- the 2nd-order SVSF may be used for analysis of chattering as a secondary measure of the filter performance

The disadvantages of the 2nd-order SVSF are:

- it is not optimal in the mean square error sense; and
- more information in the form of past measurements are needed at each time step.

Chapter 4

The Optimal 2nd-Order SVSF based on a Dynamic Sliding Manifold

This chapter introduces the dynamic 2nd-order SVSF state estimation method that is designed based on the dynamic sliding mode concept. The dynamic 2nd-order SVSF produces state estimates by satisfying the first and second order sliding conditions that result in preserving the stability of the filter. Later on, the optimal version of this filter, referred to as the optimal 2nd-order SVSF, is calculated by minimizing the trace of the error covariance matrix. The corrective gain of the optimal 2nd-order SVSF is based on a dynamic sliding manifold that introduces a cut-off frequency coefficient into the filter formulation. The optimal value of the cut-off frequency coefficient is then calculated at each sample time such that the state's *a posteriori* error covariance is minimized. It is shown that the corrective gain of the optimal 2nd-order SVSF collapses to the Kalman filter gain. Hence, a combined strategy is introduced that includes the optimal 2nd-order SVSF for systems with a perfect model and the dynamic 2nd-order SVSF for systems with huge uncertainties. Simulation results demonstrate the performance benefits of the combined strategy over other methods such as the Kalman filter, the 1st-order SVSF, and the former 2nd-order SVSF.

4.1. Introduction

As discussed in the previous chapters, the main goals of state estimation are to minimize the estimation error as well as achieving robustness against modeling uncertainties, measurement noise and bounded disturbances. Optimality in estimation has usually been obtained by adjusting a filter's corrective gain to minimize the state error covariance matrix (trace). The Wiener-Kolmogorov filter was one of the first major contributions in optimal estimation that was proposed for stationary signals [20]. It assumes estimates with known spectral properties subject to white noise. The Kalman filter is a generalization of the Wiener-Kolmogorov filter and is applied to linear systems with non-stationary Gaussian signals [20]. The Kalman filter requires a dynamic model of the system, known control inputs, and measurements containing white Gaussian noise. Under these strict assumptions, it provides optimal estimates by recursively predicting the states, estimating the uncertainty of the predicted states, computing a weighted average of the predicted and measured values, and refining the predicted states.

Another important consideration in estimation is robustness to uncertainties and bounded disturbances. Common strategies found in the literature include the robust Kalman filter [50,57,53,2], the H_∞ filter [41,55,56], and the variable structure filtering (VSF) [3,135,141]. The robust Kalman filter may be designed for systems with bounded modeling uncertainties such that an upper bound of the mean square estimation error is minimized at each step [53]. Sayed [2] presented a general framework for robust state estimation of dynamic systems with modeling uncertainties. Zames [136] proposed the H_∞ method in 1980 that removes the necessity of a perfect model or complete knowledge of the input statistics. The H_∞ theory is designed based on tracking the energy of a signal for the worst possible values of modeling uncertainties and measurement noise [147].

More recently, the Smooth Variable Structure Filter (SVSF) was proposed as a model-based robust state estimation strategy [3]. It is based on the concept of variable structure systems that results in stability given an upper bound for uncertainties and noise levels. Its gain contains a discontinuous corrective term that refines the *a priori* state estimates into the *a posteriori* form. A smoothing boundary layer using the signum function was added to the gain formulation to alleviate high-frequency chattering. In this context, the signum function operates outside the smoothing layer to preserve robustness against uncertainties, while inside the smoothing layer it interpolates the gain to suppress unwanted chattering. The smoothing layer presents a compromise between accuracy versus smoothness [3].

Chapter 3 introduced the 2nd-order SVSF method as a new extension to the VSF-type filtering that satisfies the first and second order sliding conditions during the estimation process. It alleviates the unwanted chattering effects by decreasing the measurement error and its difference until reaching the existence subspace. Thereafter, it is proven that the measurement error and its difference remain bounded for situations with bounded noise and modeling uncertainties. By not using a smoothing boundary layer, the 2nd-order SVSF increases the accuracy of the standard SVSF [3] as well as its smoothness and robustness. The main issue with the 2nd-order SVSF method is that it is not however optimal in terms of the mean square error (MSE). This makes the 2nd-order SVSF to be conservative under the normal operating conditions in which the amount of uncertainties is small. Furthermore, the corrective gain of the 2nd-order SVSF is highly nonlinear and this yields to computational difficulties in the optimization process. In order to present the optimal version of the 2nd-order SVSF, a similar approach to the Kalman filter may be used. In this context, a linear formulation of the corrective gain that would satisfy the first and second order sliding conditions is required.

In this chapter, the dynamic 2nd-order SVSF method is firstly introduced based on a dynamic sliding mode manifold. The dynamic 2nd-order SVSF is applied to systems with linear state and measurement models that are subject to white additive noises. In this context, a linear sliding mode manifold is designed in terms of the sliding variable and its first difference. It is later proven that the slope of this linear manifold is effectively a cut-off frequency that filters chattering and can dynamically be updated at each time step. The Lyapunov's second law is used to provide the stability proof for the presented dynamic 2nd-order SVSF. In order to obtain the optimal derivation of the dynamic 2nd-order SVSF, the trace of the *a posteriori* state error covariance is minimized by finding the optimal value of the cut-off frequency at each step. It provides the cut-off frequency as a square matrix with time-varying entries. It is shown that the corrective gain of the optimal 2nd-order SVSF represents the Kalman filter gain. Therefore, a combined strategy is introduced by considering the optimal 2nd-order SVSF for systems with a known model and the dynamic 2nd-order SVSF for systems with huge uncertainties. This strategy is demonstrated by its application to an electro-hydrostatic actuator (EHA). Simulation results from the combined strategy are compared with results from the Kalman filter, 1st-order SVSF [3], and the former 2nd-order SVSF in terms of the root-mean-squared-error (RMSE), error's mean (Bias) and standard deviations (STD).

4.2. The Dynamic 2nd-Order SVSF Estimation Process

Consider a stochastic dynamic system defined by linear state and measurement models in discrete time as follows:

$$x_{k+1} = \hat{F} x_k + \hat{G} u_k + w_k, \quad (4.1)$$

$$z_{k+1} = \hat{H} x_{k+1} + v_k, \quad (4.2)$$

where $x_k \in \mathbb{R}^{n \times 1}$ is the state vector, $u_k \in \mathbb{R}^{p \times 1}$ is the control vector, and $z_k \in \mathbb{R}^{m \times 1}$ is the measurement vector. Furthermore, $\hat{F} \in \mathbb{R}^{n \times n}$ is the estimated state matrix, $\hat{G} \in \mathbb{R}^{n \times p}$ is the estimated control matrix, $\hat{H} \in \mathbb{R}^{m \times n}$ is the estimated measurement matrix (diagonal or pseudo-diagonal matrix), $w_k \in \mathbb{R}^{n \times 1}$ and $v_k \in \mathbb{R}^{m \times 1}$ are the process uncertainties and measurement noise, respectively. The following assumptions are made in the derivation of the dynamic SVSF.

Assumption 4.1: The control vector $u \in \mathbb{R}^{p \times 1}$ is known and norm-bounded such that:

$$\|u_k\| \leq u_{\max}. \quad (4.3)$$

Assumption 4.2: Vectors w_k and v_k are mutually independent white processes. They are norm-bounded by w_{\max} and v_{\max} as their upper limits such that:

$$\begin{cases} \|w_k\| \leq w_{\max}; \\ \|v_k\| \leq v_{\max}. \end{cases} \quad (4.4)$$

It is assumed that they are statistically independent with respect to the state vector.

The main benefit of higher order sliding mode condition is a reduction in the unwanted chattering effects. More specifically, the second order sliding mode condition not only retains the main advantages of the first order sliding mode systems such as robustness, but also reduces the chattering amplitude and results in a higher trajectory following accuracy. However, due to uncertainties, noise, and switching imperfections, the ideal conditions cannot be achieved and a real sliding regime needs to be considered. The real first and second order sliding mode conditions are described by the following definitions in discrete time.

Definition 4.1: The real first order sliding mode occurs if there is a time instance k_1 after which the state trajectory that belongs to the sliding hyperplane $S(x_k)$ preserves:

$$S_{1st} = \left\{ \forall x \in \mathbb{R}^n, \exists k \geq k_1, \varepsilon_s > 0: \|S(x_k)\| < \varepsilon_s \right\}. \quad (4.5)$$

Definition 4.2: The real second-order sliding mode occurs if after a finite time sequence $k_2 > k_1$, the state trajectory that belongs to the sliding hyperplane $S(x_k)$ preserves:

$$S_{2nd} = \left\{ \forall x \in \mathbb{R}^n, \exists k \geq k_2, \varepsilon_s, \varepsilon_{\Delta s} > 0: \|S(x_k)\| < \varepsilon_s, \|\Delta S(x_k)\| < \varepsilon_{\Delta s} \right\}. \quad (4.6)$$

In the dynamic 2nd-order SVSF, the corrective gain is a linear function of the *a priori* and the *a posteriori* measurement error multiplied by the cut-off frequency coefficient. The stability proof of the filter under this gain is then proven using the Lyapunov's second law of stability. The gain satisfies the first and second order sliding mode conditions that result in robust, smooth, and convergent state estimates. In order to optimize the dynamic 2nd-order SVSF in the mean squared error sense, the state and measurement models must be linearized. Hence, the optimal 2nd-order SVSF method is restricted to systems with linear state and measurement models. In order to apply the filter to systems with nonlinear state models, the state's *a posteriori* PDF may be predicted using techniques involving linearization or approximation, similarly to the EKF or UKF methods.

In this context, it is necessary to introduce the state error covariance matrix into the filter formulation. The error covariance matrix provides additional information about the state estimate's dispersion for the filter that in turns results in more accurate estimates. The error covariance matrix may also be interpreted as an indicator of the performance

that presents dispersions of the noise and outliers from the measurement data. Furthermore, derivation of the covariance matrix helps the optimal 2nd-order SVSF method to be combined with other estimation methods such as the interacting multiple models (IMM) filter. The combination of the IMM filter with the optimal 2nd-order SVSF will be used in Chapter 5 for fault detection and identification (FDI).

The calculation process of the *a priori* and *a posteriori* state error covariance for the new derivation is similar to what was presented by Gadsden and Habibi [140] for the 1st-order SVSF that followed a similar approach as the Kalman filter, [1,20]. In this context, the *a priori* state error covariance matrix is defined as the statistical expectation of the squared *a priori* state estimation error as follows [1]:

$$P_{k+1|k} = E \left\{ (x_{k+1} - \hat{x}_{k+1|k})(x_{k+1} - \hat{x}_{k+1|k})^T \right\}, \quad (4.7)$$

Since $x_{k+1} = \hat{F}x_k + \hat{G}u_k + w_k$, and $\hat{x}_{k+1|k} = \hat{F}\hat{x}_{k|k} + \hat{G}u_k$, it leads to [1]:

$$P_{k+1|k} = E \left\{ \hat{F}\tilde{x}_{k|k}\tilde{x}_{k|k}^T\hat{F}^T + \hat{F}\tilde{x}_{k|k}w_k^T + w_k\tilde{x}_{k|k}^T\hat{F}^T + w_kw_k^T \right\}, \quad (4.8)$$

where $\tilde{x}_{k|k} = x_k - \hat{x}_{k|k}$ is the state estimation error. Further to *Assumption 4.2* [1]:

$$E \{w_k\} = E \{w_k^T\} = 0, \quad (4.9)$$

$$E \left\{ \tilde{x}_{k|k}w_k^T \right\} = E \left\{ w_k\tilde{x}_{k|k}^T \right\} = 0, \quad (4.10)$$

$$E \left\{ w_kw_k^T \right\} = Q_k, \quad (4.11)$$

where Q_k is the process noise covariance matrix. Finally, the *a priori* state covariance matrix is formulated as [1]:

$$P_{k+1|k} = \hat{F}P_{k|k}\hat{F}^T + Q_k. \quad (4.12)$$

Similarly, the *a posteriori* state error covariance matrix is obtained as [1]:

$$P_{k+1|k+1} = (I - K_{k+1}H)P_{k+1|k}(I - K_{k+1}H)^T + K_{k+1}R_{k+1}K_{k+1}^T. \quad (4.13)$$

The dynamic 2nd-order SVSF estimation process is performed in a predictor-corrector form recursively. It applies to systems with linear state and measurement models (4.1-4.2). The estimation process may be summarized in six steps as follows:

I. Prediction of the *a priori* state estimate is obtained using initial conditions

$\hat{x}_0 \in \mathbb{R}^{n \times 1}$ or the previous *a posteriori* state estimate $\hat{x}_{k|k}$ as:

$$\hat{x}_{k+1|k} = \hat{F}\hat{x}_{k|k} + \hat{G}u_k. \quad (4.14)$$

Then, the *a priori* estimate of the measurement vector is calculated using the *a priori* state estimate and the linear measurement model of equation (4.2) as:

$$\hat{z}_{k+1|k} = \hat{H}\hat{x}_{k+1|k}. \quad (4.15)$$

II. The *a priori* state error covariance matrix is predicted using the linear state transition model and the previous *a posteriori* state error covariance matrix $P_{k|k}$ as:

$$P_{k+1|k} = \hat{F}P_{k|k}\hat{F}^T + Q_k. \quad (4.16)$$

III. The *a priori* and the *a posteriori* measurement error vectors, $e_{z_{k+1|k}} \in \mathbb{R}^{m \times 1}$ and

$e_{z_{k|k}} \in \mathbb{R}^{m \times 1}$ are calculated as follows:

$$e_{z_{k+1|k}} = z_{k+1} - \hat{H} \hat{x}_{k+1|k}, \quad (4.17)$$

$$e_{z_{k|k}} = z_k - \hat{H} \hat{x}_{k|k}. \quad (4.18)$$

IV. The corrective gain $K_{k+1} \in \mathbb{R}^{n \times 1}$ is obtained as a function of the *a priori* $e_{z_{k+1|k}}$ and the *a posteriori* $e_{z_{k|k}}$ and $e_{z_{k-1|k-1}}$ measurement errors, and the cut-off frequency matrix $\Lambda_k \in \mathbb{R}^{m \times m}$ as follows:

$$K_{k+1} = f(\Lambda_k, e_{z_{k-1|k-1}}, e_{z_{k+1|k}}). \quad (4.19)$$

The cut-off frequency matrix $\Lambda_k \in \mathbb{R}^{m \times m}$ is automatically calculated during the estimation process and represents the filter's bandwidth at each time step.

V. The *a priori* state estimate is updated into the *a posteriori* estimate as:

$$\hat{x}_{k+1|k+1} = \hat{x}_{k+1|k} + K_{k+1} e_{z_{k+1|k}}. \quad (4.20)$$

VI. The *a posteriori* state estimation is updated such that:

$$P_{k+1|k+1} = (I - K_{k+1} \hat{H}) P_{k+1|k} (I - K_{k+1} \hat{H})^T + K_{k+1} R_{k+1} K_{k+1}^T. \quad (4.21)$$

One of the main advantages of the dynamic 2nd-order SVSF over other approaches is the use of a switching hyperplane by introducing an internal filtering strategy with its own cut-off frequency coefficient. In this context, a cut-off frequency coefficient is assigned to each measurement that filters out the unwanted chattering and any other high frequency dynamics. This coefficient is formulated into the filter by defining the sliding manifold as $\sigma_k = \Delta S_k + C S_k$, where $C \in \mathbb{R}^{m \times m}$. The coefficient C referred to as the manifold cut-off frequency represents the slope of the sliding manifold in a phase plane

coordinated by S and ΔS . Its value affects the amount of chattering that needs to be filtered out from the state estimates.

For the optimal derivation of the dynamic 2nd-order SVSF, the entries of the cut-off frequency matrix $C_{ij,k}$ should be calculated such that the trace of the state error covariance matrix $P_{k+1|k+1}$ is minimized at each time step. In order to introduce the cut-off frequency term into the dynamic 2nd-order SVSF formulation, a linear sliding manifold is designed based on the concept of dynamic sliding mode systems. This concept was introduced and implemented by Sira-Ramirez [16,17].

Definition 4.3: Consider a polynomial P defined as following [17]:

$$P(s^{(r)}, \dots, \dot{s}, s, x, u^{(k)}, \dots, \dot{u}, u) = 0, \quad (4.22)$$

where the sliding function s may depend on the input u . A stable dynamic sliding manifold σ that preserves the r^{th} -order sliding condition may be formulated as [17]:

$$\sigma = s^{(r)} + a_1 s^{(r-1)} + \dots + a_{r-1} s = 0, \quad (4.23)$$

where the coefficients $\{a_1, a_2, \dots, a_{r-1}\}$ are defined such that the polynomial (4.22) is Hurwitz. The controller u may be a discontinuous function of σ such that it satisfies the polynomial P .

Regarding the dynamic sliding mode concept, a linear sliding manifold σ_k may be defined as a linear combination of S_k and ΔS_k in the following form:

$$\sigma_k = \Delta S_k + C S_k, \quad (4.24)$$

where $\sigma_k : \mathbb{R}^{m \times 1} \rightarrow \mathbb{R}^{m \times 1}$ is the new sliding mode manifold, $S_k \in \mathbb{R}^{m \times 1}$ is the vector of sliding variables, and $\Delta S_k : \mathbb{R}^{m \times 1} \rightarrow \mathbb{R}^{m \times 1}$ is the backward difference operator. Matrix $C = \text{Diag}(c_{ii}) \in \mathbb{R}^{m \times m}$ is a diagonal matrix with entries c_{ii} representing the cut-off frequency associated to a particular measurement error $e_{z_{i,k|k}}$.

Similar to the 1st-order SVSF [3] and the 2nd-order SVSF methods, the sliding variable is equal to the *a posteriori* measurement error $S_k = e_{z_k|k}$ and the difference of the sliding variable is also equal to the difference of the measurement error $\Delta S_k = e_{z_k|k} - e_{z_{k-1|k-1}}$. Therefore, by defining the sliding manifold as $\sigma_k = \Delta S_k + CS_k$ and proving the stability of state estimates about it, it is ensured that the estimation error and its difference are vanishing in finite time. A corrective gain $K_{k+1} \in \mathbb{R}^{n \times m}$ for the dynamic 2nd-order SVSF given a square measurement matrix $\hat{H} \in \mathbb{R}^{m \times n}$ is presented as follows:

$$K_{k+1} = \hat{H}^{-1} \begin{bmatrix} e_{z_{k+1|k}} - (\gamma + \Lambda_{k+1})e_{z_k|k} + \gamma \Lambda_{k+1}e_{z_{k-1|k-1}} \end{bmatrix} \begin{bmatrix} e_{z_{k+1|k}} \end{bmatrix}^+ \quad (4.25)$$

Where $\Lambda_{k+1} \in \mathbb{R}^{m \times m}$ is the cut-off frequency matrix, and $\gamma = \text{Diag}(\gamma_{ii}) \in \mathbb{R}^{m \times m}$ is a diagonal matrix with positive entries such that $0 < \gamma_{ii} < 1$ represents the convergence rate.

Note that $\begin{bmatrix} e_{z_{k+1|k}} \end{bmatrix}^+$ represents the pseudo-inverse of the *a priori* measurement error $e_{z_{k+1|k}}$ and inserted in the gain formulation in order to cancel the term $e_{z_{k+1|k}}$ in the update equation (4.20). It is shown later in Section 4.3 that the corrective gain (4.25) will satisfy the stability requirement. Furthermore, Section 4.6 presents a corrective gain for cases with fewer measurements than states. Figure 4.1 presents the main concept of the dynamic 2nd-order SVSF under the linear sliding mode manifold.

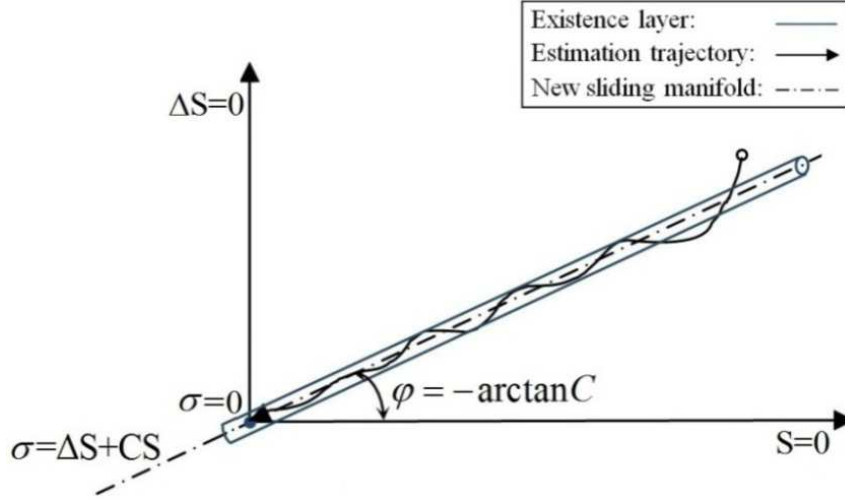


Figure 4.1: Main concept of the dynamic 2nd-order SVSF under the linear sliding manifold

Remark 4.1: The new sliding manifold $\sigma_k = \Delta S_k + CS_k$ presents a first-order low-pass filter, where C is referred to as the manifold cut-off frequency matrix. The entry c_{ii} is the cut-off frequency corresponding to the i^{th} element of the measurement error e_{z_i} . Taking the Z-transform of the manifold, the sliding variable s can be expressed as:

$$s_i(z) = \frac{\sigma_i(z)}{1 + c_{ii}z^{-1}}. \quad (4.26)$$

It is simply restated as: $s_i(z) = \frac{z\sigma_i(z)}{(1+c_{ii})z-1}$. Hence, the sliding variable $s_i(z)$ may be synthesized as the output of a first-order low-pass filter with a variable bandwidth that is a function of the manifold slope c_{ii} . Hence, by proper selection of the cut-off frequency matrix C , it is possible to establish a filtering strategy for the sliding variable. It is important to note that C determines the amount of chattering that needs to be filtered out.

4.3. Corrective Gain for the Dynamic 2nd-Order SVSF Method

This section presents the derivation of the corrective gain of equation (4.25) for the dynamic 2nd-order SVSF that is a linear function of the *a priori* and the *a posteriori* measurement errors. The corrective gain is calculated such that the dynamic 2nd-order SVSF under the linear sliding manifold $\sigma_k = \Delta S_k + C S_k$ remains stable. The manifold introduces the cut-off frequency coefficient $C \in \mathbb{R}^{m \times m}$ into the formulation of the filter gain. In the following, *Theorem 4.1* shows that the dynamic 2nd-order SVSF under the corrective gain (4.25) is stable based on the Lyapunov's second law.

Theorem 4.1: Assume a linear discrete system with the state and measurement models of equations (4.1) and (4.2). The dynamic 2nd-order SVSF with the following corrective gain is stable and produces convergent state estimates into the first and second order sliding mode hyperplanes (given a full measurement matrix $\hat{H} \in \mathbb{R}^{m \times n}$, $m = n$):

$$K_{k+1} = \hat{H}^{-1} \left[e_{z_{k+1|k}} - (\gamma + \Lambda_{k+1}) e_{z_{k|k}} + \gamma \Lambda_{k+1} e_{z_{k-1|k-1}} \right] \left[e_{z_{k+1|k}} \right]^+$$

Proof: Consider the following positive-definite Lyapunov function:

$$V_k = \sigma_{i,k}^2, \quad (4.27)$$

where $\sigma_{i,k} \in \mathbb{R}$ is an element of the linear sliding manifold and defined as: $\sigma_{i,k} = \Delta s_{i,k} + c_{ii} s_{i,k}$. Furthermore, $s_{i,k} \in \mathbb{R}$ denotes an element of the sliding variable vector, and $\Delta s_{i,k} \in \mathbb{R}$ denotes the difference of the sliding variable $s_{i,k}$ calculated using the backward difference operator as: $\Delta s_{i,k} = s_{i,k} - s_{i,k-1}$. The 2nd-order SVSF under the proposed gain (4.25) will be stable if $\Delta V_{k+1} = V_{k+1} - V_k < 0$. Substituting the Lyapunov

function in the last inequality yields: $\Delta V_{k+1} = (\Delta s_{i,k+1} + c_{ii} s_{i,k+1})^2 - (\Delta s_{i,k} + c_{ii} s_{i,k})^2$,

where $\Delta s_{i,k+1} = s_{i,k+1} - s_{i,k}$ and $\Delta s_{i,k} = s_{i,k} - s_{i,k-1}$. Substituting the above values and rearranging, ΔV_{k+1} is obtained as:

$$\Delta V_{k+1} = (1+c_{ii})^2 s_{i,k+1}^2 - 2(1+c_{ii})s_{i,k+1}s_{i,k} - 2c_{ii}(1+c_{ii})s_{i,k}^2 + 2(1+c_{ii})s_{i,k}s_{i,k-1} - s_{i,k-1}^2. \quad (4.28)$$

For simplicity let elements of the manifold's cut-off frequency matrix be defined as:

$$\lambda_{ii} = \frac{1}{1+c_{ii}}, \quad (4.29)$$

where $\Lambda = \text{Diag}(\lambda_{ii}) \in \mathbb{R}^{m \times m}$ is a diagonal matrix. This definition simplifies the calculation of the derivative of the error covariance with respect to the manifold cut-off frequency.

Multiplying the gain equation (4.25) from the left by \hat{H} , and then from the right by $e_{z_{k+1|k}}$, and rearranging:

$$e_{z_{k+1|k}} - \hat{H} K_{k+1} e_{z_{k+1|k}} = (\gamma + \Lambda_{k+1}) e_{z_{k|k}} - \gamma \Lambda_{k+1} e_{z_{k-1|k-1}}. \quad (4.30)$$

Since the estimated states are updated using equation (4.20), namely $\hat{x}_{k+1|k+1} = \hat{x}_{k+1|k} + K_{k+1} e_{z_{k+1|k}}$, it simply leads to: $K_{k+1} e_{z_{k+1|k}} = \hat{x}_{k+1|k+1} - \hat{x}_{k+1|k}$. Substituting this relation into (4.30) leads to:

$$e_{z_{k+1|k}} - \hat{H} (\hat{x}_{k+1|k+1} - \hat{x}_{k+1|k}) = (\gamma + \Lambda_{k+1}) e_{z_{k|k}} - \gamma \Lambda_{k+1} e_{z_{k-1|k-1}}. \quad (4.31)$$

The *a priori* and the *a posteriori* measurement errors at time step k are obtained from equations (4.17) and (4.18) as: $e_{z_{k+1|k}} = z_{k+1} - \hat{H} \hat{x}_{k+1|k}$ and $e_{z_{k+1|k+1}} = z_{k+1} - \hat{H} \hat{x}_{k+1|k+1}$.

Subtracting the *a priori* error from the *a posteriori* error leads to:

$$e_{z_{k+1|k+1}} - e_{z_{k+1|k}} = -\hat{H} (\hat{x}_{k+1|k+1} - \hat{x}_{k+1|k}). \quad (4.32)$$

From equation (4.32), it is possible to restate equality (4.31) as follows:

$$e_{z_{k+1|k+1}} = (\gamma + \Lambda_{k+1}) e_{z_{k+1|k}} - \gamma \Lambda_{k+1} e_{z_{k+1|k-1}}. \quad (4.33)$$

Since $s_k = e_{z_{k|k}}$, equality (4.33) can be restated in terms of sliding variable entries $s_{i,k}$ as:

$$s_{i,k+1} = (\gamma_{ii} + \lambda_{ii}) s_{i,k} - \gamma_{ii} \lambda_{ii} s_{i,k-1}. \quad (4.34)$$

In order to show negative definiteness of the Lyapunov function candidate (4.27), equality (4.34) is substituted into the first difference of the Lyapunov function (4.28). Expanding the result:

$$\Delta V_{k+1} = (\gamma_{ii}^2 - 1)(1 + \lambda_{ii})^2 s_{i,k}^2 - 2(\gamma_{ii}^2 - 1)(1 + \lambda_{ii}) s_{i,k} s_{i,k-1} + (\gamma_{ii}^2 - 1) s_{i,k-1}^2. \quad (4.35)$$

Rearranging equality (4.35) results in:

$$\Delta V_{k+1} = (\gamma_{ii}^2 - 1) \left[(1 + \lambda_{ii}) s_{i,k} - s_{i,k-1} \right]^2. \quad (4.36)$$

Since the convergence rate matrix $\gamma = \text{Diag}(\gamma_{ii}) \in \mathbb{R}^{m \times m}$ is defined such that $0 < \gamma_{ii} < 1$, it leads to $\Delta V_{k+1} < 0$ that indicates the stability of the 2nd-order SVSF under the corrective gain (4.25). Given that the Lyapunov function V_k is a function of S_k as well as ΔS_k , it

can be concluded from equation (4.36) with $\Delta V_{k+1} < 0$ that convergence is attained for both the first and second order sliding mode conditions. \square

Remark 4.2: Note that due to modeling uncertainties, noise, and switching imperfections, however the ideal second order sliding motion does not occur, and real second order sliding regime is obtained.

Corollary 4.1: If the Lyapunov function (4.27) is satisfied, then $|\sigma_{k+1}| < |\sigma_k|$. Since $\sigma_k = \Delta S_k + C S_k$, where $S_k = e_{z_k|k}$ and $\Delta S_k = \Delta e_{z_k|k}$, it means that the measurement error and its corresponding rate of change are decreasing over time while $\sigma_k > \varepsilon_\sigma$. Due to measurement noise and modeling uncertainties, σ_k only decreases until it reaches the existence subspace bounded ε_σ . However, under ideal sliding mode condition: $\sigma_k = 0$.

Remark 4.3: The corrective gain (4.25) actually represents a second-order Markov process that is formulated in terms of the *a priori* measurement error terms at time step k : $e_{z_k|k}$, and time step $k-1$: $e_{z_{k-1}|k-1}$, and the *a posteriori* measurement error $e_{z_{k+1}|k}$. Using a second-order corrective gain in the update step results in updating the state estimates based on information available from the last two steps. Having access to higher amounts of information however increases the smoothness and the robustness of the dynamic 2nd-order SVSF in comparison to first-order filters like the Kalman filter, or the 1st-order SVSF.

Remark 4.4: Proper selection of the convergence rate matrix $\gamma \in \mathbb{R}^{m \times m}$ such that $0 < \gamma_{ii} < 1$ preserves the stability and convergence of the dynamic 2nd-order SVSF. Note that the main reason for calling the coefficient γ as the convergence rate is because of

the Lyapunov stability criterion that leads to: $V_{k+1} = \gamma V_k$. This alternatively results in $\Delta V_{k+1} = (\gamma - 1)V_k$, and hence, smaller values of γ_{ii} leads to a faster convergence rate for the dynamic 2nd-order SVSF method.

4.4. Derivation of an Optimal Cut-Off Frequency Matrix

In order to minimize the mean squared error and extract the optimal state estimates using the dynamic 2nd-order SVSF, the optimal value of the cut-off frequency coefficient must be found at each time step. The proposed strategy for finding the optimal cut-off frequency matrix is to calculate the partial derivative of the state's *a posteriori* error covariance matrix (trace) $P_{k+1|k+1}$ with respect to the cut-off frequency Λ_k . It results in determining the optimal value of the cut-off frequency at each time step and calculates the filter's bandwidth as a function of uncertainties in an optimal sense. In a geometrical sense, this strategy leads to finding the optimal value of the sliding manifold's slope for filtering out chattering at each time step (Refer to Figure 4.1).

In the Kalman filtering process, the gain is calculated to directly minimize the state's *a posteriori* error covariance matrix (trace). In the dynamic 2nd-order SVSF, the filter's corrective gain is firstly derived to within a range that preserves the Lyapunov's second law, nonetheless the cut-off frequency matrix is assumed to be unknown and time-varying. In the next step, the optimal value of the cut-off frequency matrix (filter's bandwidth) is calculated by using optimization. The process is iterative and similar in steps to the Kalman filter. The optimization process is directly applicable to systems with a square measurement matrix \hat{H} . For the case involving fewer measurements than states, the Luenberger's observer [3,164] or any other reduced-order observer is used.

In the stability-oriented design of the dynamic 2nd-order SVSF, the cut-off frequency matrix is set to be diagonal. Each diagonal entry λ_{ii} represents the cut-off frequency corresponding to a measurement error and this makes the cut-off frequency coefficients become independent of each other. The consequence is that the measurement error of each state $e_{z_k|k}$ is directly filtered out with a pre-determined bandwidth. The filtered data are used later to calculate the corrective gain. Note that however due to the diagonal consideration of the cut-off frequency matrix, coupling effects were neglected in the derivation of the dynamic 2nd-order SVSF. Hence, only diagonal entries of the state error covariance matrix are minimized and the off-diagonal entries are neglected [11,165]. Diagonal consideration of the cut-off frequency matrix on their own does not lead to an optimal solution.

As such, for optimizing the dynamic 2nd-order SVSF, the cut-off frequency matrix $\Lambda_k \in \mathbb{R}^{m \times m}$ needs to be full with diagonal and off-diagonal entries as follows:

$$\Lambda_k = \begin{bmatrix} \lambda_{11,k} & \lambda_{12,k} & \cdots & \lambda_{1m,k} \\ \lambda_{21,k} & \lambda_{22,k} & \cdots & \lambda_{2m,k} \\ \vdots & \vdots & \ddots & \vdots \\ \lambda_{m1,k} & \lambda_{m2,k} & \cdots & \lambda_{mm,k} \end{bmatrix}, \quad (4.37)$$

where $\lambda_{ii,k}$ is a diagonal entry and represents the cut-off frequency applied on $e_{z_k|k}$. Otherwise, $\lambda_{ij,k}$ is an off-diagonal entry that represents a geometrical relation between two independent cut-off frequencies $\lambda_{ii,k}$ and $\lambda_{jj,k}$ corresponding to measurement errors $e_{i,z_k|k}$ and $e_{j,z_k|k}$. *Theorem 4.2* is presented to introduce the optimal value of the cut-off frequency matrix at each time step.

Theorem 4.2: Assume a linear discrete-time system described by the state and measurement models of equations (4.1) and (4.2). The optimal 2nd-order SVSF minimizes the trace of the state's error covariance matrix $P_{k+1|k+1}$ for this system, if the cut-off frequency matrix is given by:

$$\Lambda_{k+1} = \left[\text{diag}(e_{z_{k+1|k}} - \gamma e_{z_{k|k}}) S_{rc,k+1} - \hat{H} P_{k+1|k} \hat{H}^T \right] \left[\text{diag}(e_{z_{k|k}} - \gamma e_{z_{k-1|k-1}}) S_{rc,k+1} \right]^{-1} \text{diag}(e_{z_{k+1|k}}). \quad (4.38)$$

Proof: In order to minimize $P_{k+1|k+1}$ with optimal selection of the cut-off frequency Λ_{k+1} , its partial derivative (trace) with respect to Λ_{k+1} is needed such that:

$$\frac{\partial [\text{trace}(P_{k+1|k+1})]}{\partial \Lambda_{k+1}} = 0. \quad (4.39)$$

The error covariance matrix $P_{k+1|k+1}$ is presented by equation (4.13) as follows:

$$P_{k+1|k+1} = (I - K_{k+1} \hat{H}) P_{k+1|k} (I - K_{k+1} \hat{H})^T + K_{k+1} R_{k+1} K_{k+1}^T. \quad (4.40)$$

It contains the corrective gain K_{k+1} given by equation (4.25). For calculating the partial derivative of equation (4.39), some relations from the gradient matrix rules are required, including [166]:

$$\frac{\partial [\text{trace}(AXB)]}{\partial X} = A^T B^T, \quad (4.41)$$

$$\frac{\partial [\text{trace}(AX^T B)]}{\partial X} = BA, \quad (4.42)$$

$$\frac{\partial [\text{trace}(AXBX^T C)]}{\partial X} = A^T C^T X B^T + C A X B. \quad (4.43)$$

Note that some matrices like $P_{k+1|k}$ are symmetric and this simplifies calculations. Substituting the corrective gain (4.25) into the error covariance equation (4.40) and expanding the resulting terms lead to the following four parts:

$$\text{Part 1: } P_{k+1|k}, \quad (4.44)$$

$$\text{Part 2: } -\hat{H}^{-1}[\text{diag}(e_{z_{k+1|k}} - \gamma e_{z_{k|k}}) - \Lambda_{k+1} \text{diag}(e_{z_{k|k}} - \gamma e_{z_{k-1|k-1}})] [\text{diag}(e_{z_{k+1|k}})]^{-1} \hat{H} P_{k+1|k}, \quad (4.45)$$

$$\text{Part 3: } -P_{k+1|k} \hat{H}^T [\text{diag}(e_{z_{k+1|k}} - \gamma e_{z_{k|k}})]^T - \text{diag}(e_{z_{k|k}} - \gamma e_{z_{k-1|k-1}})]^T \Lambda_{k+1}^T [\text{diag}(e_{z_{k+1|k}})]^{-1} \hat{H}^{-T}, \quad (4.46)$$

$$\begin{aligned} \text{Part 4: } & \hat{H}^{-1}[\text{diag}(e_{z_{k+1|k}} - \gamma e_{z_{k|k}})]^T - \Lambda_{k+1} \text{diag}(e_{z_{k|k}} - \gamma e_{z_{k-1|k-1}})]^T [\text{diag}(e_{z_{k+1|k}})]^{-1} S_{rc,k+1} \\ & [\text{diag}(e_{z_{k+1|k}})]^{-1} [\text{diag}(e_{z_{k+1|k}} - \gamma e_{z_{k|k}})]^T - \text{diag}(e_{z_{k|k}} - \gamma e_{z_{k-1|k-1}})]^T \Lambda_{k+1}^T \hat{H}^{-T}. \end{aligned} \quad (4.47)$$

The partial derivative in equation (4.39) may be calculated as a summation of the partial derivative of the four parts presented by (4.44-4.47). These derivatives are separately calculated as follows:

$$\frac{\partial \{\text{trace}(\text{Part 1})\}}{\partial \Lambda_{k+1}} = 0, \quad (4.48)$$

$$\frac{\partial \{\text{trace}(\text{Part 2})\}}{\partial \Lambda_{k+1}} = \hat{H}^{-T} P_{k+1|k} \hat{H}^T [\text{diag}(e_{z_{k+1|k}})]^{-1} \text{diag}(e_{z_{k|k}} - \gamma e_{z_{k-1|k-1}})]^T, \quad (4.49)$$

$$\frac{\partial \{\text{trace}(\text{Part 3})\}}{\partial \Lambda_{k+1}} = \hat{H}^{-T} P_{k+1|k} \hat{H}^T [\text{diag}(e_{z_{k+1|k}})]^{-T} \text{diag}(e_{z_{k|k}} - \gamma e_{z_{k-1|k-1}})]^T, \quad (4.50)$$

$$\begin{aligned} \frac{\partial \{\text{trace}(\text{Part 4})\}}{\partial \Lambda_{k+1}} = & 2\hat{H}^{-1}[\Lambda_{k+1} \text{diag}(e_{z_{k|k}} - \gamma e_{z_{k-1|k-1}})] S_{rc,k+1}^T [\text{diag}(e_{z_{k+1|k}})]^{-1} \text{diag}(e_{z_{k|k}} - \gamma e_{z_{k-1|k-1}})]^T \\ & - \text{diag}(e_{z_{k+1|k}} - \gamma e_{z_{k|k}})]^T S_{rc,k+1} [\text{diag}(e_{z_{k+1|k}})]^{-1} \text{diag}(e_{z_{k|k}} - \gamma e_{z_{k-1|k-1}})]^T. \end{aligned} \quad (4.51)$$

where $S_{rc,k+1} \in \mathbb{R}^{m \times m}$ is a symmetric matrix, called the innovation covariance matrix, and given by (similar to the Kalman filtering):

$$S_{rc,k+1} = \hat{H} P_{k+1|k} \hat{H}^T + R_k. \quad (4.52)$$

Adding equations (4.48-4.51) and rearranging them, the partial derivative of $P_{k+1|k+1}$ is obtained as:

$$\begin{aligned} P_{k+1|k} \hat{H}^T - \hat{H}^{-1} [\text{diag}(e_{z_{k+1|k}} - \gamma e_{z_{k|k}})] S_{rc,k+1} = \\ -\hat{H}^{-1} \Lambda_{k+1} [\text{diag}(e_{z_{k+1|k}})]^{-1} \text{diag}[(e_{z_{k|k}} - \gamma e_{z_{k-1|k-1}})] S_{rc,k+1} = 0. \end{aligned} \quad (4.53)$$

Solving equality (4.53) in terms of Λ_{k+1} results in the optimal cut-off frequency matrix as:

$$\Lambda_{k+1} = \left[\text{diag}(e_{z_{k+1|k}} - \gamma e_{z_{k|k}}) S_{rc,k+1} - \hat{H} P_{k+1|k} \hat{H}^T \right] \left[\text{diag}(e_{z_{k|k}} - \gamma e_{z_{k-1|k-1}}) S_{rc,k+1} \right]^{-1} \text{diag}(e_{z_{k+1|k}})$$

that is equal to equation (4.38). □

Corollary 4.2: Following *Theorem 4.2*, the value of the cut-off frequency matrix is directly affected by the level of modeling uncertainties. Each entry is calculated as a function of the measurement error $e_{z_{k|k}}$, its covariance $P_{k+1|k}$, and the state error covariance $S_{rc,k+1}$. Hence, Λ_{k+1} needs to be calculated at each step and then used for evaluating the filter's corrective gain.

The optimal 2nd-order SVSF method is summarized in three main steps as follows:

I. Prediction of the *a priori* state, measurement and state error covariance as:

$$\begin{aligned} \hat{x}_{k+1|k} &= \hat{F} \hat{x}_{k|k} + \hat{G} u_k, \\ \hat{z}_{k+1|k} &= \hat{H} \hat{x}_{k+1|k}, \\ P_{k+1|k} &= \hat{F} P_{k|k} \hat{F}^T + Q_k. \end{aligned} \quad (4.54)$$

II. Calculation of the innovation covariance, cut-off frequency and corrective gain as:

$$\begin{aligned}
 S_{rc,k+1} &= \hat{H}P_{k+1|k}\hat{H}^T + R_k, \\
 \Lambda_{k+1} &= \left[\text{diag}(e_{z_{k+1|k}} - \gamma e_{z_{k|k}})S_{rc,k+1} - \hat{H}P_{k+1|k}\hat{H}^T \right] \left[\text{diag}(e_{z_{k|k}} - \gamma e_{z_{k-1|k-1}})S_{rc,k+1} \right]^{-1} \text{diag}(e_{z_{k+1|k}}), \\
 K_{k+1} &= \hat{H}^{-1} \left[\text{diag}[e_{z_{k+1|k}} - (\gamma + \Lambda_{k+1})e_{z_{k|k}}] + \gamma \Lambda_{k+1} \text{diag}(e_{z_{k-1|k-1}}) \right] \left[\text{diag}(e_{z_{k+1|k}}) \right]^{-1}.
 \end{aligned} \quad (4.55)$$

III. Update of the *a priori* state and covariance into the *a posteriori* estimates as:

$$\begin{aligned}
 \hat{x}_{k+1|k+1} &= \hat{x}_{k+1|k} + K_{k+1}e_{z_{k+1|k}}, \\
 P_{k+1|k+1} &= (I - K_{k+1}\hat{H})P_{k+1|k}(I - K_{k+1}\hat{H})^T + K_{k+1}R_{k+1}K_{k+1}^T.
 \end{aligned} \quad (4.56)$$

Figure 4.2 presents a block-diagram of the optimal 2nd-order SVSF estimation process.

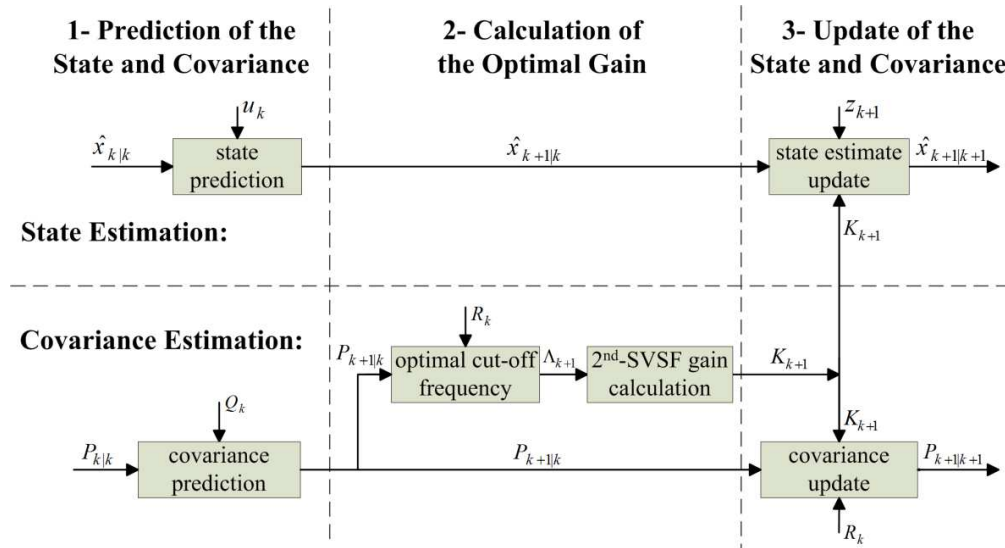


Figure 4.2: A block-diagram scheme of the optimal 2nd-order SVSF estimation process

Remark 4.5: In order to apply the optimal 2nd-order SVSF to systems with nonlinear state models, the state's *a posteriori* PDF needs to be predicted using techniques involving linearization or approximation, similarly to the extended Kalman or unscented Kalman filters.

Remark 4.6: A potential difficulty with the optimal 2nd-order SVSF method for state estimation is related to the term $\left[\text{diag}(e_{z_{k|k}} - \gamma e_{z_{k-1|k-1}}) S_{rc,k+1} \right]^{-1}$ that is appearing in the denominator of the cut-off frequency formulation. This term may cause numerical taken in implementing matrix inversion.

It is interesting to note that the corrective gain of the optimal 2nd-order SVSF with the introduced cut-off frequency coefficient represents the Kalman filter gain. In order to show that, let substitute the cut-off frequency coefficient (4.38) into the corrective gain of the optimal 2nd-order SVSF (4.25) such that:

$$K_{k+1} = \hat{H}^{-1} \left\{ \text{diag}(e_{z_{k+1|k}} - \gamma e_{z_{k|k}}) - \left[\text{diag}(e_{z_{k+1|k}} - \gamma e_{z_{k|k}}) S_{rc,k+1} - \hat{H} P_{k+1|k} \hat{H}^T \right] \right. \\ \left. \left[\text{diag}(e_{z_{k|k}} - \gamma e_{z_{k-1|k-1}}) S_{rc,k+1} \right]^{-1} \text{diag}(e_{z_{k|k}} - \gamma e_{z_{k-1|k-1}}) \right\} \text{diag}(e_{z_{k+1|k}}) \left[\text{diag}(e_{z_{k+1|k}}) \right]^{-1}. \quad (4.57)$$

Rearranging (4.57), it becomes:

$$K_{k+1} = \hat{H}^{-1} \left\{ \text{diag}(e_{z_{k+1|k}} - \gamma e_{z_{k|k}}) - \left[\text{diag}(e_{z_{k+1|k}} - \gamma e_{z_{k|k}}) S_{rc,k+1} - \hat{H} P_{k+1|k} \hat{H}^T \right] \right. \\ \left. S_{rc,k+1}^{-1} \left[\text{diag}(e_{z_{k|k}} - \gamma e_{z_{k-1|k-1}}) \right]^{-1} \text{diag}(e_{z_{k|k}} - \gamma e_{z_{k-1|k-1}}) \right\}, \quad (4.58)$$

where equality (4.58) may be restated as follows:

$$K_{k+1} = \hat{H}^{-1} \left[\text{diag}(e_{z_{k+1|k}} - \gamma e_{z_{k|k}}) - \text{diag}(e_{z_{k+1|k}} - \gamma e_{z_{k|k}}) + \hat{H} P_{k+1|k} \hat{H}^T S_{rc,k+1}^{-1} \right]. \quad (4.59)$$

Simplifying equality (4.59), the corrective gain of the optimal 2nd-order SVSF becomes:

$$K_{k+1} = P_{k+1|k} \hat{H}^T S_{rc,k+1}^{-1}, \quad (4.60)$$

where it is equal to the Kalman filter gain. Hence, the optimal 2nd-order SVSF produces an optimal solution for well-defined linear systems while its gain formulation represents the Kalman filter gain.

As presented, the corrective gain of the optimal 2nd-order SVSF collapses to the Kalman filter’s gain and hence, its robustness to modeling uncertainties is lost. In order to overcome this issue and preserving robustness as well as optimality, a combined strategy is proposed that is similar to the Gadsden’s combined approach introduced in [8]. In this combined strategy, the dynamic 2nd-order SVSF with the corrective gain of (4.25) applies to systems with huge uncertainties. Besides, the optimal 2nd-order SVSF (Kalman filter) applies to systems with a known model. This strategy preserves optimality for systems with a known model and at the same time preserves robustness for systems with huge uncertainties. The decision on the level of uncertainties is made by comparing the current amplitude of the measurement noise with the noise amplitude of the system in the normal condition. Following Gadsden’s approach [8], a limit for the measurement noise may be set equal to 5 times the maximum system noise, or approximately equal to the measurement noise. Figure 4.3 presents the main concept of the combined strategy that selects one of the dynamic or optimal 2nd-order SVSF methods based on current level of uncertainties.

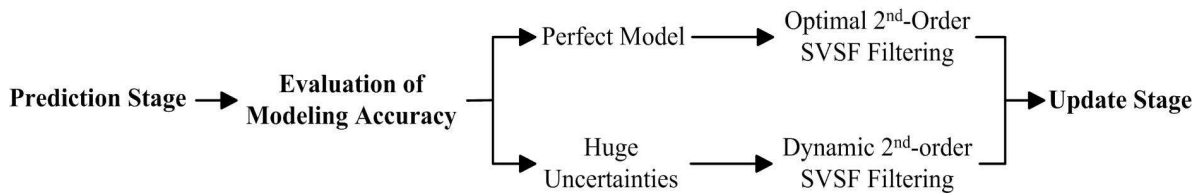


Figure 4.3: Main concept of combined strategy based on the dynamic and optimal 2nd-order SVSF

4.5. Geometrical Interpretation of the Cut-Off Frequency Matrix

An important feature of the optimal 2nd-order SVSF is its time-varying manifold cut-off frequency matrix Λ_k and its use in the gain formulation. This effectively results in an adaptive bandwidth that filters out chattering such that the state error covariance (trace) is minimized. At the same time, it preserves the first and second sliding conditions that yields the linear sliding manifold $\sigma_{i,k} = \Delta s_{i,k} + c_{ii}s_{i,k}$ converges to zero under the ideal sliding motion, such that $\sigma_k = 0$. This equality shows that each diagonal entry $c_{ii,k}$ represents the slope of a corresponding sliding manifold $\sigma_{i,k}$. Note that the cut-off frequency c_{ii} is simply obtained from equality (4.29) such that $c_{ii} = (1 - \lambda_{ii}) / \lambda_{ii}$. Figure 4.4 presents a geometrical depiction of the cut-off frequency matrix C with its entries.

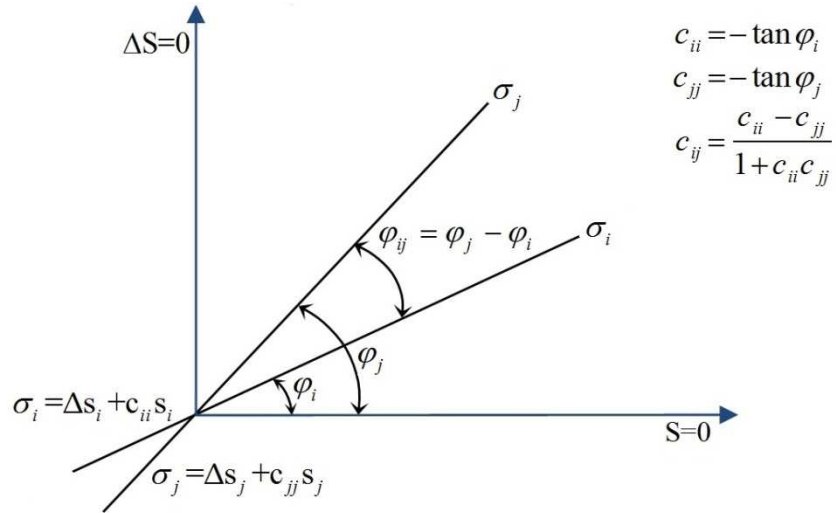


Figure 4.4: A geometrical depiction of the cut-off frequency matrix with its entries

In this figure, $\varphi_{i,k}$ is the angle between the linear manifold $\sigma_{i,k} \in \sigma_k$ and the horizontal axis. The cut-off frequency matrix $C \in \mathbb{R}^{m \times m}$ is a square matrix with time-varying diagonal and off-diagonal entries as follows:

$$C_k = \begin{bmatrix} c_{11,k} & c_{12,k} & \cdots & c_{1m,k} \\ c_{21,k} & c_{22,k} & \cdots & c_{2m,k} \\ \vdots & \vdots & \ddots & \vdots \\ c_{m1,k} & c_{m2,k} & \cdots & c_{mm,k} \end{bmatrix}. \quad (4.61)$$

The diagonal entry $c_{ii,k}$ represents the slope of the linear manifold $\sigma_{i,k}$ defined for the measurement $z_{i,k}$. Its numeric value is simply calculated as: $c_{ii,k} = -\tan \varphi_{i,k}$. However, the off-diagonal entry $c_{ij,k}$ does not imply any physical meaning and only correlates two entries $c_{ii,k}$ and $c_{jj,k}$. These entries are respectively pertaining to the two independent measurements vector z_i and z_j at the time step k . Hence, the off-diagonal entry c_{ij} may be used to mathematically correlate diagonal entries (e.g. c_{ii} and c_{jj}) of the cut-off frequency matrix. In this context, $c_{ij,k}$ may be interpreted as the angle between the two linear manifolds $\sigma_{i,k}$ and $\sigma_{j,k}$, and obtained by $\varphi_{ij,k} = \varphi_{j,k} - \varphi_{i,k}$ as follows:

$$c_{ij,k} = \tan(\tan^{-1} c_{ii,k} - \tan^{-1} c_{jj,k}) = \frac{c_{ii,k} - c_{jj,k}}{1 + c_{ii,k} c_{jj,k}}. \quad (4.62)$$

4.6. The Optimal 2nd-SVSF for Systems with Fewer Measurements than States

Similar to the 2nd-order SVSF method, its optimal version may be applied to systems with fewer measurements than state variables. In this case, the corrective gain of the optimal 2nd-order SVSF may be derived using the Luenberger's approach [3]. It is furthermore assumed that the linear dynamic system with equations (4-1) and (4-2) is completely observable. Similar to section 3.5, the state variables may be decomposed into two parts $x_k = [x_{u_k} \quad x_{l_k}]^T$, where the upper part $x_{u_k} \in R^{l \times 1}$ is directly measured and whereas the lower part $x_{l_k} \in \mathbb{R}^{(n-l) \times 1}$ is not [3]. Using the Luenberger's transformation, a

revised state vector is obtained in terms of measurements such that $y_k = [z_k \quad y_{l_k}]^T$, where $z_k \in \mathbb{R}^{l \times 1}$ denotes the direct measurement vector and $y_{l_k} \in \mathbb{R}^{(m-l) \times 1}$ denotes an artificial projected measurement vector. The problem is to calculate values for entries of y_{l_k} based on the partitioned model [3]. The measurement model is presented as:

$$\begin{bmatrix} z_{k+1} \\ y_{l_{k+1}} \end{bmatrix} = \begin{bmatrix} \Phi_{11} & \Phi_{12} \\ \Phi_{21} & \Phi_{22} \end{bmatrix} \begin{bmatrix} z_k \\ y_{l_k} \end{bmatrix} + \begin{bmatrix} G_1 \\ G_2 \end{bmatrix} u_k + \begin{bmatrix} \bar{w}_{1k} \\ \bar{w}_{2k} \end{bmatrix}, \quad (4.63)$$

where $\Phi = T^{-1}AT$, $G = T^{-1}B$, and $\bar{w}_k = T^{-1}w_k - [\Phi_{11} \quad \Phi_{21}]^T v_k$ [3]. Now, the *a priori* state estimate is given by [3]:

$$\begin{bmatrix} \hat{z}_{k+1|k} \\ \hat{y}_{l_{k+1}|k} \end{bmatrix} = \begin{bmatrix} \hat{\Phi}_{11} & \hat{\Phi}_{12} \\ \hat{\Phi}_{21} & \hat{\Phi}_{22} \end{bmatrix} \begin{bmatrix} z_k \\ \hat{y}_{l_k|k} \end{bmatrix} + \begin{bmatrix} \hat{G}_1 \\ \hat{G}_2 \end{bmatrix} u_k. \quad (4.64)$$

As presented in [3], the *a priori* and *a posteriori* measurement error vectors for the projected measurement vector y_{l_k} are calculated as:

$$e_{y_{l_k|k}} = \hat{\Phi}_{12}^{-1} e_{z_{k+1|k}} - \hat{\Phi}_{12}^{-1} \bar{w}_{l_k}, \quad (4.65)$$

$$e_{y_{l_{k+1}|k}} = \hat{\Phi}_{22} \hat{\Phi}_{12}^{-1} e_{z_{k+1|k}} - \hat{\Phi}_{22} \hat{\Phi}_{12}^{-1} \bar{w}_{l_k} + \bar{w}_{2k}, \quad (4.66)$$

where $e_{y_l} \in \mathbb{R}^{(m-l) \times 1}$ is the projected measurement error vector and $e_z \in \mathbb{R}^{l \times 1}$ is the measurement error vector corresponding to measurable states. Equations (4.65) and (4.66) present a mapping of the measurement error vector that is used according to Luenberger's method for deriving a switching hyperplane and in calculating the filter gain.

In order to calculate a corrective gain for the lower partition of states, the switching hyperplane for the lower partition may be formulated by projecting the measurement error as follows [3]:

$$S_l = \hat{\Phi}_{22} \hat{\Phi}_{12}^{-1} e_{z_k|k}, \quad (4.67)$$

where $S_l \in \mathbb{R}^{(m-l) \times l}$. Further to equation (4.25), the corrective gain of the optimal 2nd-order SVSF for the lower partition of states is derived as:

$$K_{l_{k+1}} = \left[\hat{\Phi}_{22} \hat{\Phi}_{12}^{-1} e_{z_{k+1}|k} - (\gamma + \Lambda_{k+1}) \hat{\Phi}_{12}^{-1} e_{z_{k+1}|k} + \gamma \Lambda_{k+1} \hat{\Phi}_{12}^{-1} e_{z_k|k-1} \right] \left[\hat{\Phi}_{22} \hat{\Phi}_{12}^{-1} e_{z_{k+1}|k} \right]^+. \quad (4.68)$$

By combining the gains of each partition of the state vector, the optimal 2nd-order SVSF gain is obtained for linear systems with fewer measurements than states as follows:

$$K_{k+1} = \begin{cases} \hat{H}^+ \left[e_{z_{k+1}|k} - (\gamma + \Lambda_{k+1}) e_{z_k|k} + \gamma \Lambda_{k+1} e_{z_{k-1}|k-1} \right] \left[e_{z_{k+1}|k} \right]^+, \\ \left[\hat{\Phi}_{22} \hat{\Phi}_{12}^{-1} e_{z_{k+1}|k} - (\gamma + \Lambda_{k+1}) \hat{\Phi}_{12}^{-1} e_{z_{k+1}|k} + \gamma \Lambda_{k+1} \hat{\Phi}_{12}^{-1} e_{z_k|k-1} \right] \left[\hat{\Phi}_{22} \hat{\Phi}_{12}^{-1} e_{z_{k+1}|k} \right]^+. \end{cases} \quad (4.69)$$

where \hat{H}^+ is the pseudo-inverse of the measurement matrix H where it is not squared. Hence, the vector of sliding variables may be defined as: $S_k = \begin{bmatrix} e_{z_k|k} & \hat{\Phi}_{22} \hat{\Phi}_{12}^{-1} e_{z_{k+1}|k} \end{bmatrix}^T$. The formulation that can be applied for estimation of nonlinear systems is presented in [3].

4.7. Comparative Analysis of the Combined Method (Dynamic & Optimal 2nd-SVSF)

In order to study the performance of the combined strategy (including the dynamic and optimal 2nd-order SVSF) for state estimation, it is applied to the EHA model introduced in section 3.6. Later on, its performance is compared to other estimation methods such as the well-known Kalman filter, 1st-order SVSF [3], and the former 2nd-order SVSF. Two main scenarios are considered for comparisons that are the normal

condition with a known model but including white noise, and a faulty condition with a large degree of modeling uncertainties. The EHA system is described by a discrete third-order model. The three state variables include the actuator position $x_1 = x$, velocity $x_2 = dx_1/dt$, and acceleration $x_3 = d^2x_1/dt^2$, with position being the only measurable state [3]. The linear state and measurement model of the EHA are restated here from Section 3.7 and are given by equations (4.1) and (4.2), respectively. Numeric values of the state, control and measurement matrixes of the EHA model are as follows [3]:

$$\hat{F} = \begin{bmatrix} 1 & 0.001 & 0 \\ 0 & 1 & 0.001 \\ -557.02 & -28.616 & 0.9418 \end{bmatrix}, \quad \hat{G} = \begin{bmatrix} 0 \\ 0 \\ 557.02 \end{bmatrix}, \quad \hat{H} = [1 \ 0 \ 0]. \quad (3.59)$$

Furthermore, w_k and v_k are the process uncertainties and measurement noise. They are multivariate white normal random vectors with the mean of zero and standard deviation vectors equal to (same as equation (3.60) from Section 3.7) [3]:

$$w_{std} = [0.05 \ 0.1 \ 0.1]^T, \quad v_{std} = [0.05]. \quad (3.60)$$

In order to apply the optimal 2nd-order SVSF to states that are not measured directly, it is combined with the Luenberger's observer [164]. In this context, the state space is partitioned based on equation (3.61) from Section 3.7 as follows [3]:

$$\hat{\Phi}_{11} = [1], \quad \hat{\Phi}_{12} = [0.001 \ 1], \quad \hat{\Phi}_{21} = \begin{bmatrix} 0 \\ -877.02 \end{bmatrix}, \quad \hat{\Phi}_{22} = \begin{bmatrix} 1 & 0.001 \\ -32.616 & 0.8418 \end{bmatrix}. \quad (3.61)$$

In simulation, the corrective gain is calculated for the case with the convergence rate equal to $\gamma = [0.5]$. Hence, the gain is obtained for the EHA system using equation (4.25) for the measurable state and equation (4.68) for the rest as following:

$$K_{k+1} = \begin{cases} \left[\begin{array}{c} e_{z_{k+1|k}} - (0.5 + \Lambda_{k+1})e_{z_{k|k}} + 0.5\Lambda_{k+1}e_{z_{k-1|k-1}} \\ e_{z_{k+1|k}} - 0.25(0.5 + \Lambda_{k+1})e_{z_{k+1|k}} + 0.125\Lambda_{k+1}e_{z_{k|k-1}} \\ e_{z_{k+1|k}} - 0.4(0.5 + \Lambda_{k+1})e_{z_{k+1|k}} + 0.2\Lambda_{k+1}e_{z_{k|k-1}} \end{array} \right] \left[e_{z_{k+1|k}} \right]^+, \\ \left[e_{z_{k+1|k}} \right]^+, \\ \left[e_{z_{k+1|k}} \right]^+. \end{cases} \quad (4.70)$$

In simulation, it is assumed that the initial state error covariance for the Kalman filter and the combined strategy (dynamic and optimal 2nd-order SVSF) are equal. For both the Kalman filter and the combined strategy, the process noise, measurement noise and the initial error covariance are respectively obtained as: $Q = \text{diag}([1 \ 10 \ 100])$, and $P_0 = 20Q$. Furthermore, $R = 0.1 \text{ cm}^2$ is obtained by calculating variance of the innovation signal for a time period. For the 1st-order SVSF [3], the width of the smoothing boundary layer is set to $\psi = [5 \ 5 \ 5]^T \times v_{std}$, where v_{std} is the standard deviation of the measurement noise. For all the 1st-order SVSF, the 2nd-order SVSF and the combined strategy, the convergence rate used in the corrective gain is set to $\gamma = [0.5]$. To compare the robustness characteristic of these three methods, a large degree of uncertainties is injected into the model by changing the state matrix after 0.5 sec of simulation to [3]:

$$\hat{F}_2 = \begin{bmatrix} 1 & 0.001 & 0 \\ 0 & 1 & 0.001 \\ -240 & -28 & 0.9418 \end{bmatrix}. \quad (4.71)$$

The input to the EHA system is a random signal with the amplitude in the range of -1 to 1, superimposed on a step input that occurs at 0.5 sec. The initial values of states are assumed to be zero and the sampling time for discretization is 0.001 sec. All the other inputs are considered the same for the four estimation methods. Simulations are performed using the MATLAB and under the 10^3 Monte-Carlo runs. Tables 1 to 3 compare a select number of numerical performance indicators generated from the four estimation methods for the above mentioned normal and uncertain EHA models. For the

normal model, it is assumed that the EHA model is known but is subject to white noise. For the uncertain EHA model case, large modeling uncertainties are injected after 0.5 sec of simulation. This amount of uncertainties is applied in order to examine the performance of the estimation techniques.

In order to compare these estimators, their RMSE, as well as the bias and STD of their state estimation error are calculated and compared. The RMSE indicator is calculated based on equation (3.64) from section 3.7 as follows:

$$RMSE = \sqrt{\frac{\sum_{i=1}^n (x_i - \hat{x}_i)^2}{n}}, \quad (3.64)$$

where x_i denotes the actual state value, \hat{x}_i denotes the estimated state value, and n is the number of time steps. Note that the actual state values are obtained by solving state trajectories of the EHA system with state matrices. Furthermore, the bias index is obtained based on equation (3.66) as:

$$Bias = \frac{1}{n} \sum_{i=1}^n (x_i - \hat{x}_i). \quad (3.66)$$

The STD of the state estimation error for a discrete realization is given by:

$$STD = \sqrt{\frac{1}{n} \sum_{i=1}^n (e_{x,i} - \bar{e}_{x,i})^2}. \quad (3.68)$$

Table 4.1 presents the root mean squared error (RMSE) value of the state estimation error $e_{x_{k|k}}$ for both normal and uncertain conditions. Further to Table 4.1, the Kalman filter, as well as the optimal 2nd-order SVSF, produces the most accurate state estimates in terms of the RMSE for the normal model of the EHA system subject to white noise, followed by the 2nd-order SVSF and the 1st-order SVSF. This is because for a known

model the Kalman filter and the optimal 2nd-order SVSF are optimal in terms of the RMSE. Since these two methods minimize the state's error covariance matrix (trace), their RMSEs are smaller than the 2nd-order SVSF and the 1st-order SVSF. In the uncertain case, the dynamic 2nd-order SVSF and the 2nd-order SVSF produce more accurate state estimates in terms of the RMSE. This accuracy is due to preserving the first and second order sliding conditions that increases their robustness to uncertainties.

Table 4.1: Comparison between RMSE values of the four estimation methods applied to the EHA model

	Kalman Filter		1 st -order SVSF		2 nd -order SVSF		Combined Dynamic and Optimal 2 nd SVSF	
	Normal	Uncertain	Normal	Uncertain	Normal	Uncertain	Normal	Uncertain
RMSE of Position (cm)	1.01×10^{-2}	0.31	1.10×10^{-2}	1.13×10^{-2}	1.05×10^{-2}	1.08×10^{-2}	1.01×10^{-2}	1.06×10^{-2}
RMSE of Velocity (cm/s)	1.045	21.66	1.060	15.50	1.05	14.49	1.045	12.66
RMSE of Accel. (cm/s²)	167.24	2206.06	170.31	1341.53	168.91	1335.18	167.24	1328.02

Note that satisfying the second order sliding condition instead of using the smoothing boundary layer is the main reason why the dynamic 2nd-order SVSF and the 2nd-order SVSF are more accurate than the 1st-order SVSF for both normal and uncertain cases. In the 1st-order SVSF chattering is alleviated by defining a smoothing boundary layer in a vicinity of the sliding hyperplane. In this context, the signum function is replaced with a smoother function such as saturation function [3]. This however approximates the sliding motion in a close vicinity of the sliding hyperplane and reduces the ultimate accuracy and robustness of the SVSF-type filtering. The second order sliding condition not only removes the need for approximation, but also alleviates higher degrees of chattering.

Table 4.2 compares state estimates in terms of the bias (mean of the state estimation error $e_{x_{k|k}}$) for both the normal and uncertain conditions. Table 4.3 compares the state

estimates in terms of the standard deviation (STD) of the state estimation error $e_{x_{k|k}}$. For the normal case, the Kalman filter and the optimal 2nd-order SVSF produce the smallest bias, followed by the 2nd-order SVSF and the 1st-order SVSF. But for the uncertain case, the dynamic 2nd-order SVSF and the 2nd-order SVSF generate the smallest bias, followed by the 1st-order SVSF and the Kalman filter. Following Table 4.3, the dynamic 2nd-order SVSF and the 2nd-order SVSF have the smallest values pertaining to the standard deviation (STD) of the state estimation error $e_{x_{k|k}}$.

Table 4.2: Comparison between bias values of the four estimation methods applied to the EHA model

	Kalman Filter		1 st -order SVSF		2 nd -order SVSF		Combined Dynamic and Optimal 2 nd SVSF	
	Normal	Uncertain	Normal	Uncertain	Normal	Uncertain	Normal	Uncertain
Bias in Position (cm)	2.53×10^{-5}	-9.94×10^{-3}	-2.58×10^{-4}	-3.15×10^{-4}	-1.57×10^{-4}	-2.12×10^{-4}	2.53×10^{-5}	-2.08×10^{-4}
Bias in Velocity (cm/s)	-1.95×10^{-3}	6.83	-2.77×10^{-3}	3.78	-4.70×10^{-3}	3.44	-1.95×10^{-3}	2.85
Bias in Accel. (cm/s²)	9.84	27.32	10.04	20.86	9.98	20.76	9.84	18.71

Table 4.3: Comparison between STD of the four estimation methods applied to the EHA model

	Kalman Filter		1 st -order SVSF		2 nd -order SVSF		Combined Dynamic and Optimal 2 nd SVSF	
	Normal	Uncertain	Normal	Uncertain	Normal	Uncertain	Normal	Uncertain
STD of Position (cm)	9.63×10^{-2}	0.30	1.05×10^{-2}	2.09×10^{-2}	7.51×10^{-3}	9.86×10^{-3}	9.63×10^{-2}	7.41×10^{-3}
STD of Velocity (cm/s)	1.09	22.29	1.12	17.95	1.11	11.63	1.09	11.14
STD of Accel. (cm/s²)	183.55	2867.9	186.16	1823.9	185.37	1674.60	183.55	1654.37

Having smaller values of the standard deviation (STD) for uncertain models implies a higher degree of smoothness for the dynamic 2nd-order SVSF and the 2nd-order SVSF. These two methods produce state estimates with the lowest values of bias and dispersion in the error $e_{z_{k|k}}$ for uncertain conditions. The performance of the Kalman filter, as well as

the optimal 2nd-order SVSF, is the best in the normal case with no uncertainties and Gaussian noise, followed by the 2nd-order SVSF. For the second case that includes modeling uncertainties, the performance of the dynamic 2nd-order SVSF is best, closely followed by the 2nd-order SVSF, as both methods achieve stability through the second order sliding condition.

Figure 4.5 presents the actual and estimated state trajectories using the Kalman filter and the optimal 2nd-order SVSF for the EHA under the normal condition. Figure 4.6 compares the actual and estimated state trajectories using the Kalman filter and the dynamic 2nd-order SVSF for the EHA system with modeling uncertainties. Comparing Figures 4.4 and 4.5 confirms the better performance of the combined strategy in estimating the state variables of the EHA in the uncertain condition.

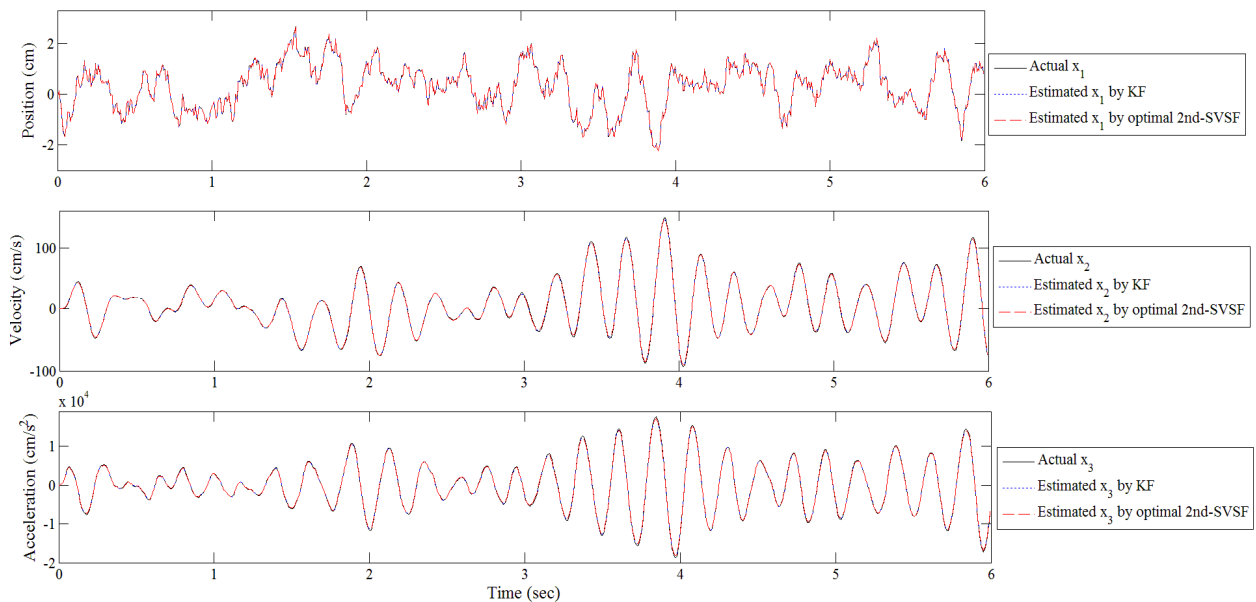


Figure 4.5: State estimations by the Kalman filter and optimal 2nd-order SVSF for the normal EHA

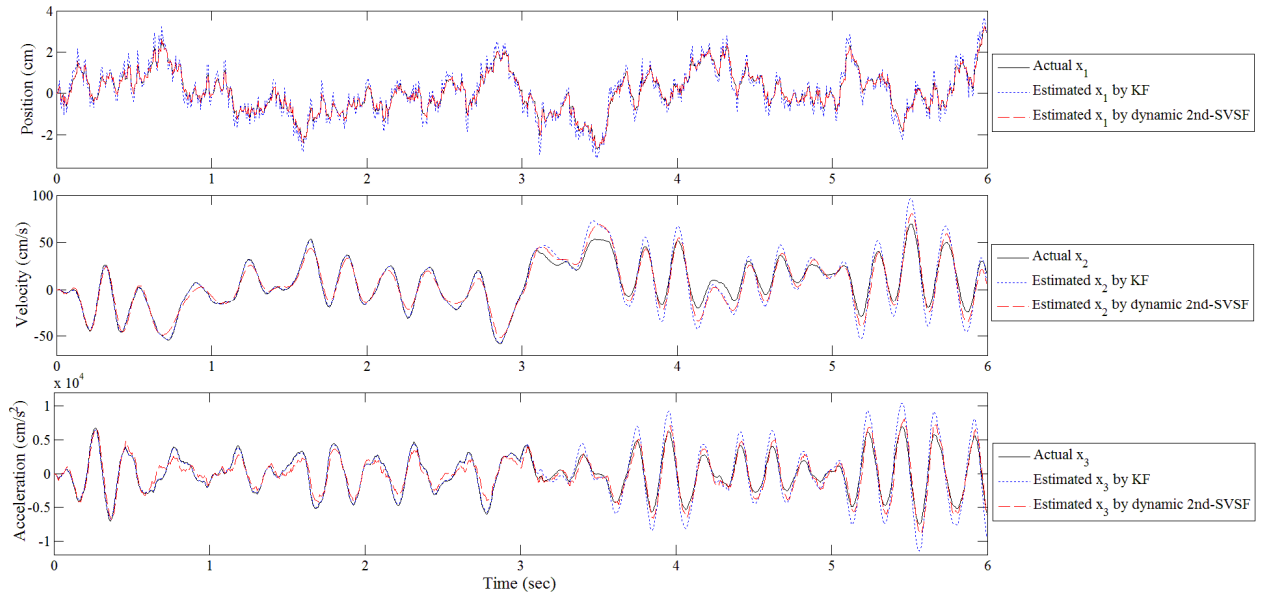


Figure 4.6: State estimations by the Kalman filter and dynamic 2nd-SVSF for the uncertain EHA system

The position's estimation error signals obtained from the combined strategy (dynamic and optimal 2nd-order SVSF) and the Kalman filter are presented in Figure 4.7. It is deduced from Figure 4.7 that the combined strategy produces the smoothest state estimates with the smallest variation for both normal and uncertain cases. Figure 4.8 presents the phase portrait of the measurement error and its first difference for the normal and faulty EHA systems using the optimal and dynamic 2nd-order SVSF method, respectively. As demonstrated, in both cases the measurement error and its difference are decreasing in time until they reach the existence subspace. Figure 4.9 also presents profiles of the sliding variable s and the dynamic sliding manifold σ for both the normal and uncertain cases using the optimal and dynamic 2nd-order SVSF method, respectively. In both cases, σ is decreasing in time until it reaches the existence subspace such that $|\sigma| \leq \varepsilon_\sigma$. Figures 4.8 and 4.9 illustrate convergence of the dynamic and optimal 2nd-order SVSF under the dynamic sliding manifold given bounded noise and uncertainties. Figure 4.10 also presents profiles of the cut-off frequency coefficients for these scenarios.

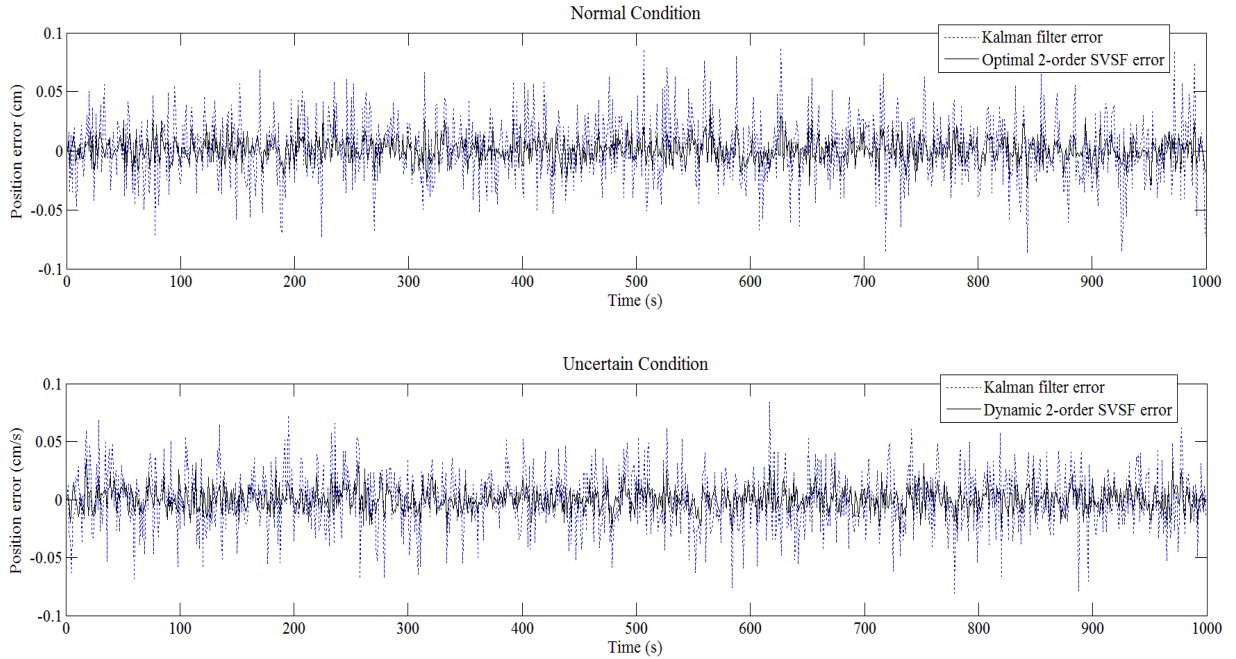


Figure 4.7: Measurement errors by the Kalman filter and the combined strategy (optimal 2nd-order SVSF for the normal condition and dynamic 2nd-order SVSF for the uncertain condition)

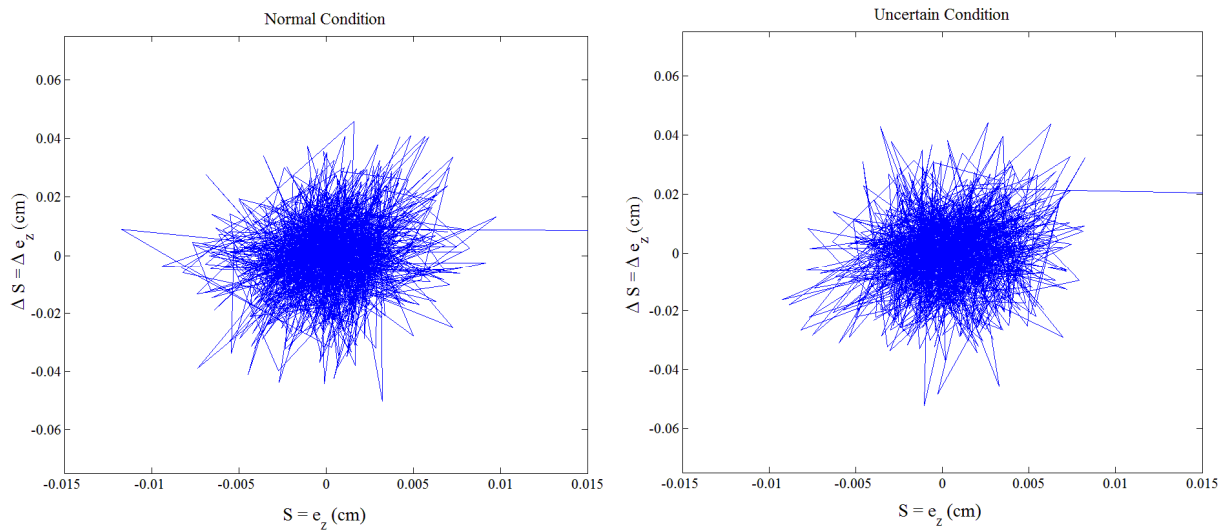


Figure 4.8: Phase portrait of the measurement error and its difference produced by the combined strategy (optimal 2nd-order SVSF for the normal condition and dynamic 2nd-order SVSF for the uncertain condition)

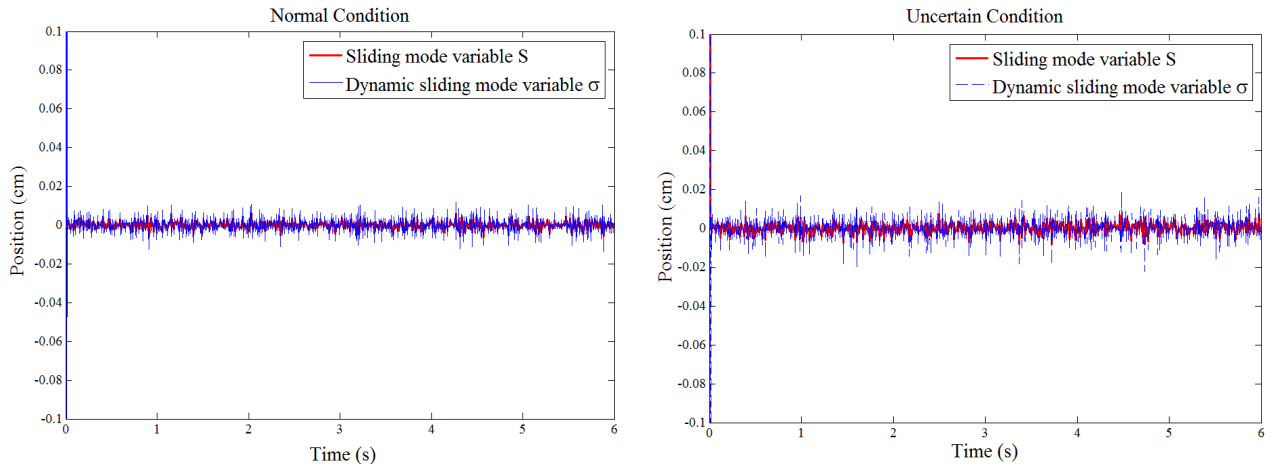


Figure 4.9: Sliding variable and dynamic sliding variable produced by the combined strategy (optimal 2nd-order SVSF for the normal condition and dynamic 2nd-order SVSF for the uncertain condition)

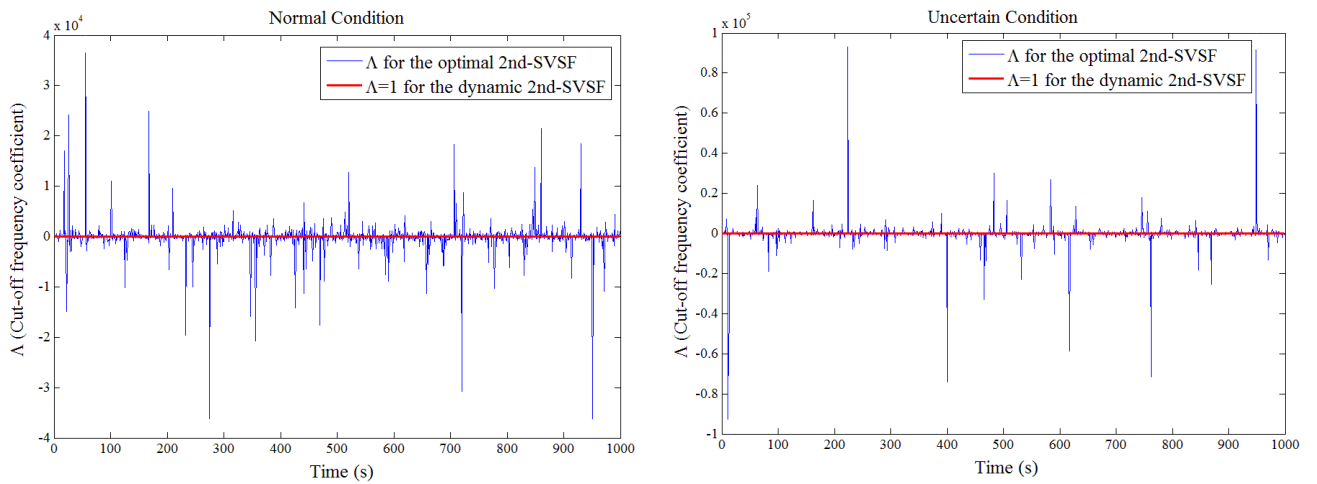


Figure 4.10: Profiles of the cut-off frequency coefficients produced by the combined strategy (optimal 2nd-order SVSF for the normal condition and dynamic 2nd-order SVSF for the uncertain condition)

4.8. Robustness Analysis with an Explicit Consideration of Uncertainties

In this section, the robustness characteristic of the dynamic 2nd-order SVSF is numerically evaluated and compared with the Kalman filter, and the 1st-order SVSF methods. The analysis is based on a research performed by Yan and Wang for comparing robustness of some deterministic state observers [167]. Their approach is developed here

in order to estimate state variables of stochastic dynamic systems with an explicit consideration of the source of uncertainties. In this context, modeling uncertainties are considered as an additive perturbation to the nominal state matrix. The nominal model is the known model of the system that is represented by:

$$\hat{H} \in \mathbb{R}^{m \times n} (m = n) \quad (4.72)$$

$$z_{k+1} = \hat{H} x_{k+1} + v_k, \quad (4.73)$$

where the system's actual state matrix \hat{F} is represented to \hat{F}_0 by:

$$\hat{F} = \hat{F}_0 + \Delta\hat{F}. \quad (4.74)$$

The perturbed system is subjected to the following assumption.

Assumption 4.3: It is assumed that the perturbation in the state model $\Delta\hat{F} \in \mathbb{R}^{n \times n}$ is bounded by $\delta \in \mathbb{R}^{n \times n}$ such that:

$$|\Delta\hat{F}_{ij}| < \delta_{ij}, \quad \text{where } \delta_{ij} > 0. \quad (4.75)$$

Remark 4.7: Note that $\|x_k\|$ represents the Euclidean norm of vector x_k given by [167]:

$$\|x_k\| = \sqrt{x_k^T x_k}. \quad (4.76)$$

Also, $\|x_k\|_\infty$ represents the supremum norm of a discrete sequence x_k given by [167]:

$$\|x_k\|_\infty = \sup_{k>0} \|x_k\|. \quad (4.77)$$

Wang and Yan introduced an index for evaluating robustness properties of model-based state observers, whereas they remain stable given bounded noise and modeling

uncertainties [167]. Following their approach, when $|\Delta\hat{F}_{ij}| < \delta_{ij}$, the state estimation error

$e_{x,k} = x_k - \hat{x}_k$ may be stated as follows [167]:

$$e_{x,k+1} = \zeta(K_k, \hat{F}, \hat{H}, k)e_{x,k} + v(\Delta\hat{F}, \Delta\hat{G}, k), \quad (4.78)$$

where K_k is the filter's corrective gain. Note that ζ_k and v_k are unknown functions and need to be calculated for each state estimation method. Furthermore, it is presented by Wang and Yan [167] that for a stable state observer, there exist a function β and a positive quantity α such that the state estimation error $e_{x,k} = x_k - \hat{x}_k$ is bounded as follows [167]:

$$\|e_{x,k}\| \leq \beta(\|e_{x,0}\|, k) + \alpha \|v_k\|_{\infty} \quad \forall k, \quad (4.79)$$

where α is an index of the robustness property and calculated by [164]:

$$\alpha = 1/(1-c), \quad (4.80)$$

with $c = \sup_{\forall k} (|\lambda_{\max}(\zeta_k)|)$ and $\lambda_{\max}(\zeta_k)$ is the maximum eigenvalue of the matrix ζ_k .

Note that a smaller α represents a better robustness property of the filter. The proof of this theorem is presented and discussed in [167]. This approach may be developed and applied for the robustness analysis of the Kalman filter, the 1st-order SVSF, and the dynamic 2nd-order SVSF. For each filter, the matrix ζ_k should be initially calculated as a function of the filter's gain and the state model.

For the dynamic 2nd-order SVSF, the *a posteriori* state estimation error $e_{x,k+1|k+1}$ may be calculated as follows:

$$e_{x,k+1|k+1} = x_{k+1} - \hat{x}_{k+1|k+1}, \quad (4.81)$$

where $x_{k+1} = \hat{F}x_k + \hat{G}u_k + w_k$, $\hat{x}_{k+1|k+1} = \hat{x}_{k+1|k} + K_k e_{z,k+1|k}$, and $\hat{x}_{k+1|k+1} = \hat{F}\hat{x}_{k|k} + \hat{G}u_k + K_k e_{z,k+1|k}$.

Note that in the case of systems with modeling uncertainties: $F = \hat{F} + \Delta\hat{F}$. Substituting these terms in equality (4.81), the *a posteriori* estimation error $e_{x,k+1|k+1}$ is obtained by:

$$e_{x,k+1|k+1} = \hat{F}e_{x,k|k} + \Delta\hat{F}x_k - K_{k+1}e_{z,k+1|k} + w_k. \quad (4.82)$$

For the dynamic 2nd-order SVSF method, the corrective gain is given by:

$$K_{k+1} = \hat{H}^{-1} \left[e_{z,k+1|k} - (\gamma + \Lambda_{k+1})e_{z,k|k} + \gamma\Lambda_{k+1}e_{z,k-1|k-1} \right] \left[e_{z,k+1|k} \right]^+. \quad (4.83)$$

Since $e_{z,k|k} = \hat{H}e_{x,k|k} + v_k$, equality (4.83) may be simply restated in terms of $e_{x,k|k}$.

Substituting the corrective gain term in equality (4.82) and simplifying the resulting terms, it leads to:

$$\begin{aligned} e_{x,k+1|k+1} = & \left[\hat{F} + \hat{H}^{-1}(\gamma + \Lambda_{k+1})\hat{H} \right] e_{x,k|k} - e_{x,k+1|k} - \hat{H}^{-1}\gamma\Lambda_{k+1}\hat{H}e_{z,k-1|k-1} \\ & + \Delta\hat{F}x_k + w_k - \hat{H}^{-1}v_{k+1} + \hat{H}^{-1}(\gamma + \Lambda_{k+1})v_k - \hat{H}^{-1}\gamma\Lambda_{k+1}v_{k-1}. \end{aligned} \quad (4.84)$$

Comparing equality (4.84) to equality (4.78), the matrix ζ is obtained for the dynamic 2nd-order SVSF method as follows:

$$\zeta_{2nd-SVSF} = \hat{F} + \hat{H}^{-1}(\gamma + \Lambda_{k+1})\hat{H}. \quad (4.85)$$

The process of calculation ζ for the 1st-order SVSF and the Kalman filter is similar to the above calculations. For the 1st-order SVSF method, the matrix ζ is calculated by:

$$\zeta_{1st-SVSF} = \hat{F} - \hat{H}^{-1}\gamma\hat{H} \operatorname{sgn}(e_{x,k|k}). \quad (4.86)$$

Similarly, for the Kalman filter method, the matrix ζ is obtained by:

$$\zeta_{Kalman} = \hat{F} - K_{k+1} \hat{H}. \quad (4.87)$$

where the Kalman filter's gain is given by:

$$K_{k+1} = P_{k+1|k+1} \hat{H}^T \left[\hat{H} P_{k+1|k} \hat{H}^T + R_{k+1} \right]^{-1}. \quad (4.88)$$

In order to numerically evaluate robustness properties of each filter, the uncertain model of the EHA system is used for simulation and comparison. Following equality (4.80) and calculating the maximum eigenvalue of the ζ_k matrix for each filter, the numeric value of α is obtained for each filter (see Table 4.4). As can be seen, the smallest value of the robustness index α is obtained for the dynamic 2nd-order SVSF, followed by the 1st-order SVSF and the Kalman filter. Following the Yan's approach [167], it is deduced that the dynamic 2nd-order SVSF shows the best robustness property, followed by the 1st-order SVSF, and the Kalman filter.

Table 4.4: Numeric values of the robustness index α for each filter

	Kalman Filter	1 st -Order SVSF	Dynamic 2 nd -Order SVSF
α	1.971	1.334	1.135

4.9. Summary

In this chapter, the dynamic 2nd-order SVSF estimation method is firstly introduced based on the dynamic sliding mode concept. Its corrective gain is obtained using a linear sliding manifold defined in terms of the sliding variable and its first difference, where the sliding variable represents the *a posteriori* measurement error. The stability and convergence of the dynamic 2nd-order SVSF method is then proven using the Lyapunov's second law of stability. The linear dynamic manifold introduces a cut-off frequency coefficient matrix into the filter formulation that alleviates the unwanted chattering effect.

It operates like a first-order low-pass filter with a cut-off frequency that is equal to the slope of the linear sliding manifold. Furthermore, the corrective gain of the dynamic 2nd-order SVSF in each step updates the *a priori* state estimates based on available information of the measurement error from two steps back. This yields to smoother state estimates with smaller bias and dispersions in comparison to the Kalman filter. In order to optimize the dynamic 2nd-order SVSF method, the optimal value of the cut-off frequency matrix is calculated at each time step such that the trace of the error covariance matrix is minimized.

It was shown that the corrective gain of the optimal 2nd-order SVSF represents the Kalman filter gain. Hence, a combined strategy is used that includes both the dynamic and optimal 2nd-order SVSF methods. This strategy applies the optimal 2nd-order SVSF to systems with a known model and applies the dynamic 2nd-order SVSF to systems with huge uncertainties when the level, source and occurrence of uncertainties are unknown. The combined strategy is implemented on an electro-hydrostatic actuator (EHA) model for estimation in normal and uncertain conditions. Its performance is then compared with other estimation methods, including the Kalman filter, the 1st and the 2nd-order SVSF.

The main advantages of the combined strategy over the Kalman filter and 1st-order SVSF are its greater accuracy, and robustness in uncertain conditions with a higher level of smoothness in state estimation. These are directly due to preserving the first and second order sliding conditions which push not only the estimated state trajectories to slide along the switching hyperplane, but also their derivatives to slide along a tangential hyperplane. Yan's robustness analysis shows the superior robustness performance of the dynamic 2nd-order SVSF in comparison to the Kalman filter and the 1st-order SVSF.

Chapter 5

Application to Fault Detection and Diagnosis

This chapter presents applications of the combined strategy (including the dynamic and optimal 2nd-order SVSF methods) for model-based fault detection and identification (FDI). For fault identification, the dynamic 2nd-order SVSF is combined with the interacting multiple models (IMM) filter such that the mode probability estimate represents the current operating regime (normal or faulty) of the system. An experimental setup of an electro-hydrostatic actuator (EHA) is used for experimentations. The performance of the combined strategy is then compared with the extended Kalman filter (EKF) and the 1st-order SVSF in terms of robustness, and accuracy.

5.1. Introduction

Due to the growing desire for higher performance as well as for increasing safety and reliability, fault diagnosis systems are being increasingly used in the last decade. Fault Detection and Identification (FDI) is in general a subfield of Control engineering which concerns itself with monitoring a system's health condition, identifying the time of fault occurrence, and pinpointing the type of fault and its location. A fault is an abnormal condition or defect at the component, equipment, or sub-system level which leads to deviation of the system from its normal mode of operation.

FDI tasks can be performed using both hardware redundancy and/or analytical redundancy methods. In hardware redundancy, hardware instrumentations are replicated and repeated such as computers, sensors, actuators and other instruments, and their outputs compared for consistency. Analytical redundancy is performed using analytical or functional information of the process being monitored. Analytical or functional models are obtained and various measured signals are used to estimate unmeasured quantities [168]. Two main approaches are commonly used in analytical redundancy-based FDI, namely signal-based and model-based approaches. Both approaches require *a priori* knowledge of the dynamic process. In signal-based approaches, the *a priori* knowledge includes a large quantity of historical process data, observations, and measurements [168].

Signal-based techniques usually require signal processing tools (e.g., fast Fourier transform (FFT) and wavelet analysis), statistical techniques (e.g., statistical classifiers, partial least squares (PLS), and principle component analysis (PCA)), and intelligent decision making techniques (e.g., artificial neural networks) [168]. In the model-based approaches, the *a priori* knowledge is in the form of a model of the system that describes

its dynamic behavior. Model-based FDI approaches usually involve the use of observer, state estimation, and system identification techniques [168]. In this chapter, the state estimation-based FDI is considered for fault detection and diagnosis of an EHA setup.

5.2. State Estimation-Based FDI

State estimation-based FDI is based on evaluating the residual or innovation that is the difference between measurements and estimated outputs at each sample time. In order to estimate the system states or outputs, it is necessary to select an estimation filter such as the KF, EKF, PF, etc, in conjunction with a mathematical model. Figure 5.1 presents a block-diagram of the state estimation-based FDI strategy. It involves two main stages as [168]:

1. Residual generation stage in which the system inputs and outputs are used to produce a mathematical model of the process, when the difference between the model process output and the measurement is referred to as the estimation residual or innovation.
2. Decision making stage in which the generated residuals are checked for the likelihood of faults, and a decision rule is then made to recognize if any fault has occurred. The knowledge of process normal operation is required in this stage.

It is important to note that the residual is just a quantity that represents the inconsistency between the actual process measurement and the mathematical model output and thus it may include both system noise as well as the fault signature. Hence, in order to perform a more accurate FDI task, it is necessary to filter out the noise from the residual signal.

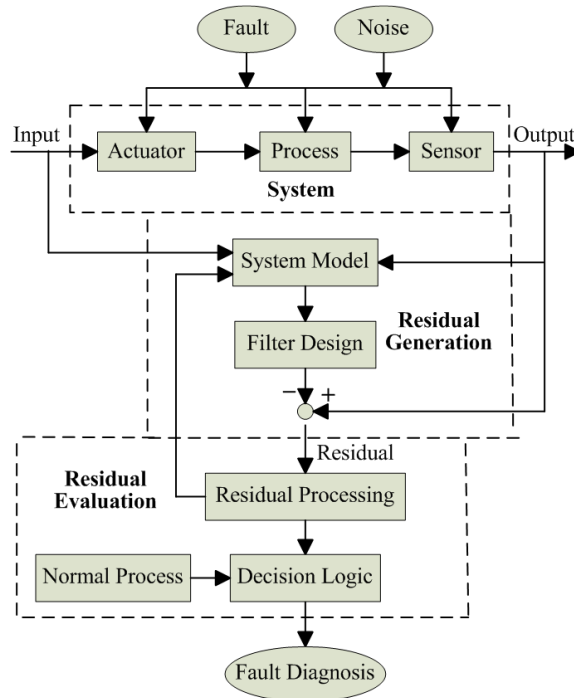


Figure 5.1: A block-diagram scheme of the state estimation-based FDI task

State estimation has become increasingly popular in model-based FDI systems in the last two decades. Note that the Kalman-type filtering methods assume a known system model with known parameters. In real applications however there may be considerable uncertainties about the model structure, the physical parameters, the level of noise, and the initial conditions. In some situations, the system dynamic is too complex to be modeled exactly, or there is no *a priori* knowledge about parameters as well as noise levels or distributions. In other situations, the system structure or parameters may change with time or due to fault conditions unpredictably. Hence, Kalman-type filtering methods may diverge or present an unacceptable performance. To overcome such potential difficulties, a robust state estimation approach is recommended. Examples of the robust state estimation are the robust Kalman (H_2) filter [53], the H_∞ filter [137], and the Smooth Variable Structure Filter (SVSF) [3].

In this chapter, an experimental setup of an Electro-Hydrostatic Actuator (EHA) prototype is used to demonstrate an SVSF based FDI. Several experiments are performed in order to examine the accuracy and robustness of the 2nd-order SVSF and its dynamic version under the normal and uncertain faulty conditions. Results are then compared with other state-of-the-art methods such as the Kalman Filter (KF) and the 1st-order SVSF in terms of the root-mean-squared-error (RMSE), the error's mean (Bias), and the standard deviations (STD). There are two sets of experiments that are respectively performed for fault detection and fault identification purposes. In the fault detection experiments, the objective is to figure out whether the system is operating under the normal condition or faulty condition. In the fault identification experiments, the objective is to determine the type of fault conditions. There are two types of faults that can be physically simulated on the EHA setup. These include friction and internal leakage faults with various degrees of severity. The next section describes the experimental setup of the EHA prototype with the two types of faults.

5.3. The Experimental Electro-Hydrostatic Actuator (EHA) Setup [165,10]

The experimental setup of the electro-hydrostatic actuator (EHA) has been designed and manufactured in the Center for Mechatronics and Hybrid Technology (CMHT) at McMaster University. This setup is used for doing experimentations on control, state estimation, and fault detection and diagnosis applications. Figure 5.2 presents the EHA experimental setup. Furthermore, the circuit diagram of the EHA setup with numbered elements is shown in Figure 5.3. The EHA uses pumping action (10) to create pressure and move piston *A* (3) and piston *B* (4). The EHA system is currently being used in aerospace applications and therefore its reliability and performance are highly important. Hence, health monitoring is an important element in designing EHA systems.



Figure 5.2: Experimental setup of the electro-hydrostatic actuator (EHA): The piston on the right is referred to as piston *A* (3) and the piston connected to it on the left is referred to as piston *B* (4). An optical linear encoder (12) attached to piston *A* is used to provide position measurements (which are differentiated to obtain velocity measurements). The gear pump (10) and electric motor (13) are located in the rear (middle) of the table.

The EHA is composed of several components including a symmetric linear actuator (8), a variable-speed electric motor (13), a bi-directional gear pump (10), a pressure relief valve (7), an accumulator (2), connecting tubes, and safety circuits for fault simulations. The EHA set up includes complementary circuits that allow a physical simulation of friction and leakage faults. The variable-speed servomotor, which is a SIEMENS 1FK7080-5AF71-1AG2 electric motor, drives the bi-directional gear pump (10) and forces oil into the cylinder (8). Thereby, the gear pump (10) can adjust the actuation performance by changing the fluid flow rate. An accumulator (12) is used to avoid cavitation and to collect the case drain leakage from the gear pump (10). The pressure relief valve (7) is used to limit the maximum system pressure to 500 psi in this case study [165,10].

The hydraulic circuit of the EHA setup has two main parts. The first part is the inner low-pressure circuit that filters the oil and preserves the minimum system pressure at 40 *psi*, by using an accumulator (2) as well as filters and check valves (6). The inner circuit prevents cavitation and supplies fluid for compensating leakage. The second part of the hydraulic circuit is the outer high-pressure circuit that performs actuation. EHA’s input is the voltage to the electric motor (13) that regulates the direction and the speed of the pump (10). This results in controlling the value of the fluid flow rate in the outer circuit and correspondingly adjusts the piston’s position, velocity, and acceleration [10].

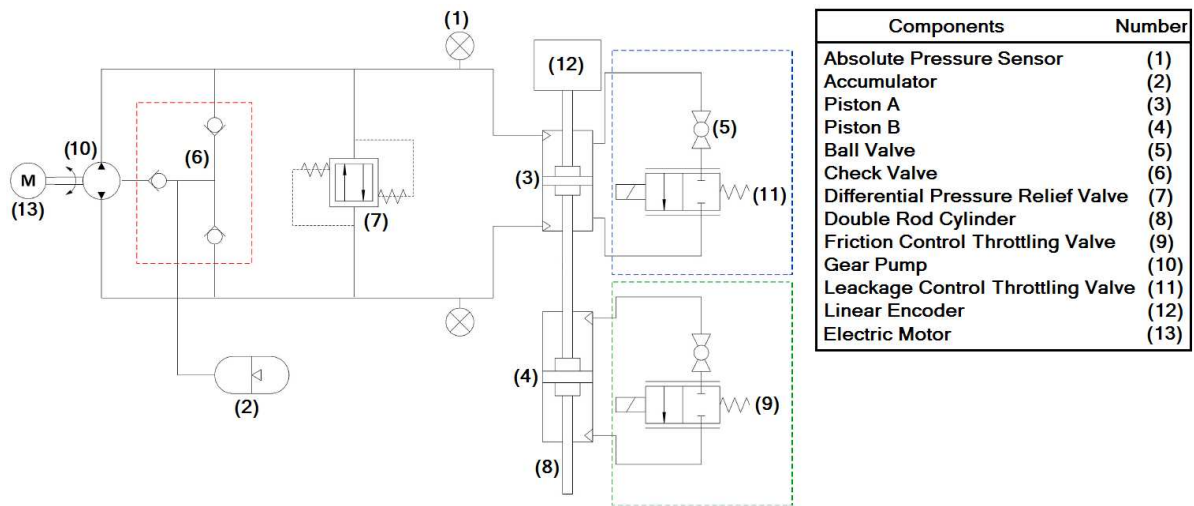


Figure 5.3: The circuit diagram of the EHA experimental setup (Taken from [165,10])

The piston at the top is referred to as piston A (3) and the below piston connected to it is referred to as piston B (4). An optical linear encoder (12) attached to piston A is used to obtain position measurements. The state resolution of this encoder is 1 nm. Two types of fault conditions can be physically induced: internal leakage and friction. To implement a friction fault in the system, piston A in Figure 5.3 was used as the driving mechanism while piston B acted as a load. To simulate internal leakage faults across the circuit, the piston A throttling valve is used (where the piston A throttle blocking valve is open). The

piston A throttling valve produces cross-port leakage between both chambers of the corresponding cylinder. Based on this fault condition, the output response of the cylinder (8) is affected [10,169].

Table 5.1: Numeric values of the EHA parameters [10]

Parameter	Physical Meaning	Parameter Values
A_E	Piston Area	$1.52 \times 10^{-3} \text{ m}^2$
D_p	Pump Displacement	$5.57 \times 10^{-7} \text{ m}^3/\text{rad}$
L	Leakage Coefficient	$4.78 \times 10^{-12} \text{ m}^3/(\text{sec} \times \text{Pa})$
M	Load Mass	7.376 Kg
Q_{L0}	Flow Rate Offset	$2.41 \times 10^{-6} \text{ m}^3/\text{sec}$
V_0	Initial Cylinder Volume	$1.08 \times 10^{-3} \text{ m}^3$
β_e	Effective Bulk Modulus	$2.07 \times 10^8 \text{ Pa}$

The EHA dynamics may be described using three state variables including the actuator position $x_1 = x$, velocity $x_2 = \dot{x}$, and acceleration $x_3 = \ddot{x}$. Gadsden, Song, and Habibi [10] investigated the dynamic model of the EHA using the physical modeling approach. They presented a nonlinear state-space model of the EHA system as follows:

$$x_{1,k+1} = x_{1,k} + T x_{2,k}, \quad (5.1)$$

$$x_{2,k+1} = x_{2,k} + T x_{3,k}, \quad (5.2)$$

$$x_{3,k+1} = \left[1 - T \frac{a_2 V_0 + M \beta_e L}{M V_0} \right] x_{3,k} - T \frac{(A_E^2 + a_2 L) \beta_e}{M V_0} x_{2,k} + T \frac{A_E \beta_e}{M V_0} - T \frac{2a_1 V_0 x_{2,k} x_{3,k} + \beta_e L (a_1 x_{2,k}^2 + a_3)}{M V_0} \text{sgn}(x_{2,k}), \quad (5.3)$$

where A_E denotes the piston cross-sectional area, β_e denotes the effective bulk modulus, L denotes the leakage coefficient, M denotes the load mass, and V_0 denotes the initial

cylinder volume. Moreover, T is the sample time and is set at $T=1$ ms. Table 5.1 presents numeric values of the aforementioned parameters. The differential pressure of the EHA may be calculated based on the actuator friction that is modeled as a second order quadratic function related to the actuator velocity [10]:

$$(P_1 - P_2)A_E = a_2\dot{x} + (a_1\dot{x}^2 + a_3)\text{sgn}(\dot{x}). \quad (5.4)$$

In this context, the differential pressure ΔP may be calculated based on the actuator friction that is modeled as a second-order quadratic function as follows [10]:

$$\Delta P_{k+1} = \frac{a_2}{A_E}x_{2,k} + \frac{(a_1x_{2,k}^2 + a_3)}{A_E}\text{sgn}(x_{2,k}) + \frac{M}{A_E}x_{3,k}, \quad (5.5)$$

The input to the EHA system relates to flow and in a simplified form as given by [10]:

$$u = D_p \omega_p - \text{sgn}(P_1 - P_2)Q_{L0}, \quad (5.6)$$

where D_p is the pump displacement, Q_l is the leakage flow rate, and Q_{l_0} is the parameter used to adjust offsets (see Ref. [10] for detailed information). It is important to notice that there are two types of parameters that are affected by the fault condition: the leakage coefficient L and the friction coefficients a_1 , a_2 , and a_3 . Hence, for accurately modeling the EHA system, numeric values of these parameters are required under different operating conditions. Table 5.2 lists numerical values of the friction coefficients for different operating conditions measured by experimentation as reported on [10]. Table 5.3 also presents numerical values of the leakage coefficients and flow rate offsets for these conditions [10]. In this research, three scenarios of the EHA setup are used for experimentation and comparison. They include the normal EHA, the EHA with major friction and the EHA with major internal leakage.

Table 5.2: Numeric values of the friction coefficients [10]

Condition	a_1	a_2	a_3
Normal	6.589×10^4	2.144×10^3	436
Major Friction	1.162×10^6	-7.440×10^3	500
Minor Friction	4.462×10^6	1.863×10^4	551

Table 5.3: Numeric values of the leakage coefficients and flow rate offsets [10]

Condition	Leakage (L)	Flow Rate (Q_{L0})
Normal	$4.78 \times 10^{-12} \text{m}^3/(\text{sec} \times \text{Pa})$	$2.41 \times 10^{-6} \text{m}^3/\text{s}$
Major Leakage	$2.52 \times 10^{-11} \text{m}^3/(\text{sec} \times \text{Pa})$	$1.38 \times 10^{-5} \text{m}^3/\text{s}$
Minor Leakage	$6.01 \times 10^{-11} \text{m}^3/(\text{sec} \times \text{Pa})$	$1.47 \times 10^{-5} \text{m}^3/\text{s}$

5.4. State Estimation under the Normal and Faulty Conditions

This section presents state estimation of the EHA experimental setup under the normal and faulty conditions. The nonlinear model of equations (5.1) through (5.3) is used for modeling the EHA system. In order to compare the robust performance of the dynamic 2nd-order SVSF with the 1st-order SVSF and the extended Kalman filter (EKF), the EHA normal model is used for state estimation under the normal and faulty conditions. Comparisons are made in terms of accuracy, robustness and smoothness of the generated state estimates. Initial values of states are assumed zero and the sample time for discretization is set to $T=1 \text{ ms}$. Furthermore, in order to update the state error covariance matrix of the 1st-order SVSF and the dynamic 2nd-order SVSF, the linearized model of the EHA is used (An approach similar to the covariance update in the EKF).

There are two different scenarios for the EHA experiment; the EHA in the normal situation and the faulty EHA with friction or internal leakage. Accuracy, robustness, and smoothness of state estimates provided by the combined strategy (dynamic and optimal 2nd-order SVSF) are compared with those obtained by the extended Kalman Filter (EKF)

and the 1st-order SVSF method. Note that the EHA model is third order, and position is the only measurable state. In order to estimate other states, the 1st-order and the dynamic 2nd-order SVSF need to be combined with the Luenberger observer. Simulations are performed using the MATLAB and all the inputs and initial conditions are assumed the same for the three estimators. The initial state estimates \hat{x}_{00} and error covariance matrix P_{00} for the EKF and the dynamic 2nd-order SVSF are the same and defined as follows:

$$\hat{x}_{00} = [0 \ 0 \ 0], \quad P_{00} = 10 \times \text{eye}(4). \quad (5.7)$$

The convergence rate factor for the 1st-order SVSF, and the dynamic 2nd-order SVSF are set to $\gamma = 0.5$. For the 1st-order SVSF, the smoothing boundary layer is also set to $\varphi = [5 \ 5 \ 5]^T \times v_{std}$, where v_{std} is the standard deviation of the measurement noise. The system uncertainty matrix Q for the EKF and the dynamic 2nd-order SVSF are obtained by tuning and they are respectively equal to:

$$Q_{EKF} = \begin{bmatrix} 10^{-12} & 0 & 0 \\ 0 & 10^{-10} & 0 \\ 0 & 0 & 10^{-9} \end{bmatrix}, \quad Q_{2nd-SVSF} = \begin{bmatrix} 10^{-12} & 0 & 0 \\ 0 & 10^{-9} & 0 \\ 0 & 0 & 5 \times 10^{-9} \end{bmatrix}. \quad (5.8)$$

For the EKF and the dynamic 2nd-order SVSF, the measurement noise R is obtained by calculating variance of the innovation signal for a time period that is equal to $R = 10^{-12} m^2$.

In order to compare these state estimation methods, some indicators including the root mean square error (RMSE), and standard deviation of the state estimation error $e_{x_k|k}$ are used. Note that the state estimation error represents the difference between the state estimate values \hat{x}_k and the measured values x_k (for only the measurable state x_1 that is position). Note that however for an intuitive comparison of state estimation profiles, the

values of the actuator velocity x_2 and acceleration x_3 may be obtained by taking the first and the second time-derivatives of the position measurement signal respectively. Since differentiation results in added noise, a Butterworth filter is used to filter out the velocity and acceleration signals that are obtained by differentiation and filtering. *Remark 5.1* presents more details about design and implementation of the Butterworth filter on the EHA data (refer to the McCullough¹ thesis [169]).

Remark 5.1: In order to design a filter for real-time control applications, the filter's order must be low such that it removes as much of the noise as possible without adding a significant phase shift [169]. In this context, McCullough [169] used a second-order Butterworth filter with a cut-off frequency of 350 rad/sec (55.7 Hz). A second-order Butterworth filter provides sufficient filtering of the signal without producing too much phase shift that however degrades the filtering performance. The cut-off frequency for the Butterworth filter should be five to ten times the values of the system's bandwidth. The best value for the filter's cut-off frequency, which was obtained by trial and error, is equal to 350 rad/sec. The resultant Butterworth filter in discrete time is represented by [169]:

$$J(z) = \frac{5.28E - 2z^{-1} + 4.39E - 2z^{-2}}{1 - 1.514z^{-1} + 0.61z^{-2}}. \quad (5.9)$$

The RMSE index for estimated values of a measurable state is calculated by:

$$RMSE = \sqrt{\frac{\sum_{i=1}^n (x_i - \hat{x}_i)^2}{n}}, \quad (5.10)$$

¹K. McCullough, "Design and characterization of a dual electro-hydrostatic actuator," M.Sc. Thesis, Department of Mechanical Engineering, McMaster University, Hamilton, Ontario, Canada, 2011.

where x_i denotes the measured state values (for measurable states), \hat{x}_i denotes the estimated state values generated by each state estimator, and n denotes the number of time steps. The state estimation error of a measurable state (actuator position) is the difference between the measured state values x_i and the estimated ones \hat{x}_i . The STD of the state estimation error for a measurable state variable is obtained by:

$$STD = \sqrt{\frac{1}{n} \sum_{i=1}^n (e_{x,i} - \bar{e}_{x,i})^2}, \quad (5.11)$$

where $\bar{e}_{x,i}$ denotes the mean value of the state estimation error.

Table 5.4 presents the RMSE and the STD indicators generated by the EKF, 1st-order SVSF, and the combined strategy (dynamic and optimal 2nd-order SVSF methods). Experiments are performed for the normal setup and the faulty EHA setup with two types of faults including the major friction and the major leakage separately. As observed earlier from simulation results, for the normal setup, the optimal 2nd-order SVSF and the EKF produce the most accurate state estimates in terms of the RMSE, followed by the 1st-order SVSF. The reason is that under normal conditions, the optimal 2nd-order SVSF and the EKF estimates are optimal in the mean squared error sense. In the faulty EHA setups, the dynamic 2nd-order SVSF provided the most accurate state estimates in terms of the RMSE. Due to preserving higher orders of robustness via the dynamic 2nd-order SVSF, its RMSE under the faulty condition is smaller compared with the 1st-order SVSF and the EKF estimation methods.

Preserving the second order sliding mode condition instead of approximating the sliding motion via the smoothing boundary layer provides the dynamic 2nd-order SVSF with more accurate state estimates in comparison to the 1st-order SVSF under the normal

and faulty EHA operations. As shown in Table 5.4, for the normal and faulty scenarios, the combined strategy produced the smallest STD, followed by the 1st-order SVSF, and the KF. This confirms that the dynamic 2nd-order SVSF can achieve higher degrees of smoothness in state estimates with respect to other estimation methods. However, the RMSE values of state estimates for major leakage are larger than those for the major friction and the normal condition.

Table 5.4: Indicator values of different estimators under the normal and faulty scenarios

	Indicator	Normal	Friction	Leakage
Extended Kalman Filter (EKF)	RMSE of Position (m)	1.76×10^{-5}	2.39×10^{-4}	3.74×10^{-4}
	Position Error STD (m)	2.03×10^{-5}	6.88×10^{-4}	8.54×10^{-4}
1st-order SVSF	RMSE of Position (m)	1.89×10^{-5}	2.89×10^{-5}	3.65×10^{-5}
	Position Error STD (m)	2.03×10^{-5}	7.50×10^{-5}	8.79×10^{-5}
Combined Strategy (Dynamic & Optimal 2nd- SVSF)	RMSE of Position (m)	1.76×10^{-5}	2.03×10^{-5}	2.93×10^{-5}
	Position Error STD (m)	2.03×10^{-5}	6.53×10^{-7}	8.74×10^{-7}

Figure 5.4 compares the state estimation profiles generated by the EKF, and the optimal 2nd-order SVSF with the state trajectories under the normal EHA condition. Furthermore, Figures 5.5 and 5.6 present the state estimation profiles generated by the EKF, and the dynamic 2nd-order SVSF but under the faulty EHA setups with the major friction and internal leakage, respectively. Experimental results demonstrate that under the normal condition, the optimal 2nd-order SVSF and the EKF provide the most accurate results, followed by the 1st-order SVSF. However, for the EHA under the friction or leakage fault condition, the dynamic 2nd-order SVSF produces the most accurate state estimates, followed by the 1st-order SVSF and then the EKF. Furthermore, it is demonstrated that the dynamic 2nd-order SVSF also generates state estimates with a smaller STD. As discussed, in order to intuitively compare the state estimation trajectories with measurement, the measured values for the velocity and acceleration are respectively

obtained by taking the first and second order time-derivatives of the position (measurement) trajectory. As discussed in *Remark 5.1*, they are also filtered by using a Butterworth filter in order to alleviate the differentiation noise and other unwanted spikes.

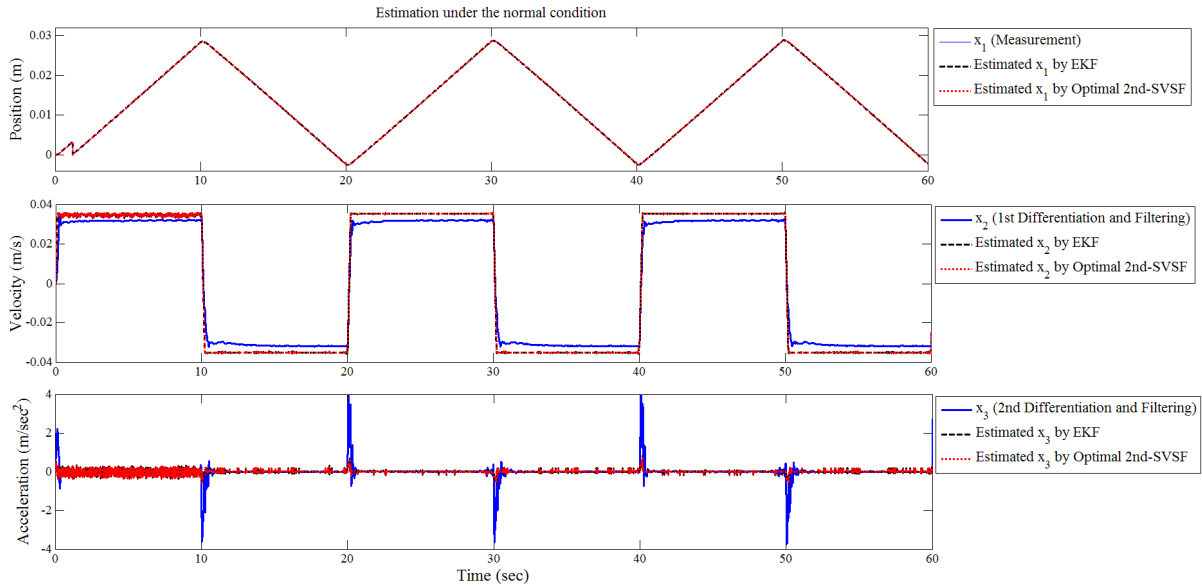


Figure 5.4: State estimate profiles generated by different estimators for the normal EHA setup

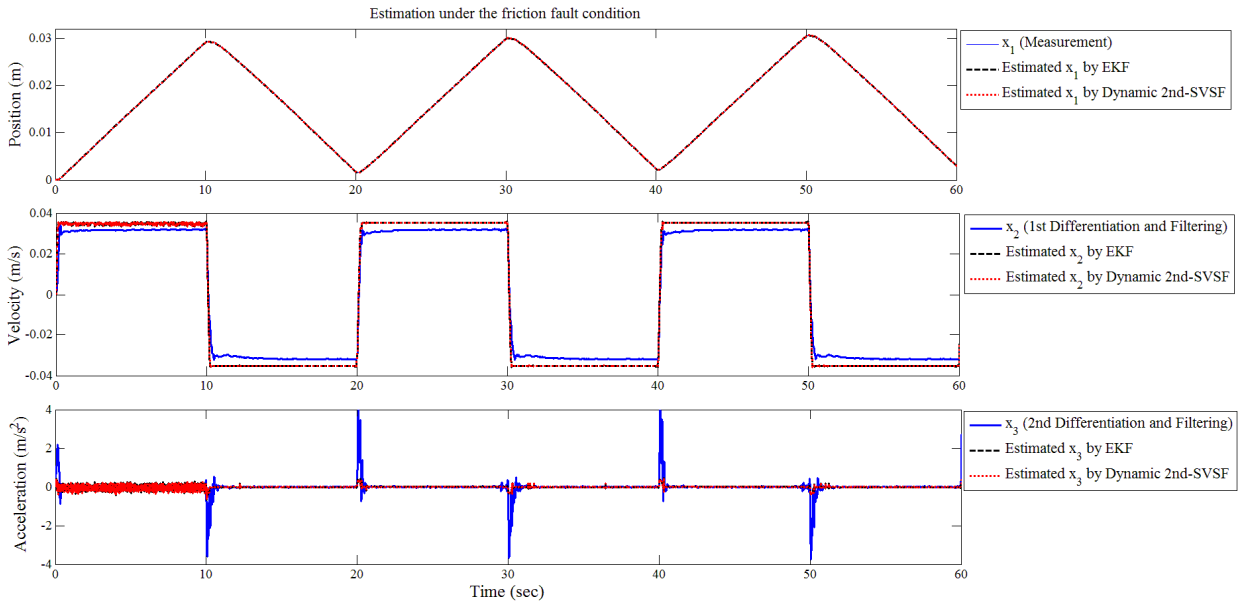


Figure 5.5: State estimate profiles generated by different estimators for the EHA setup under friction

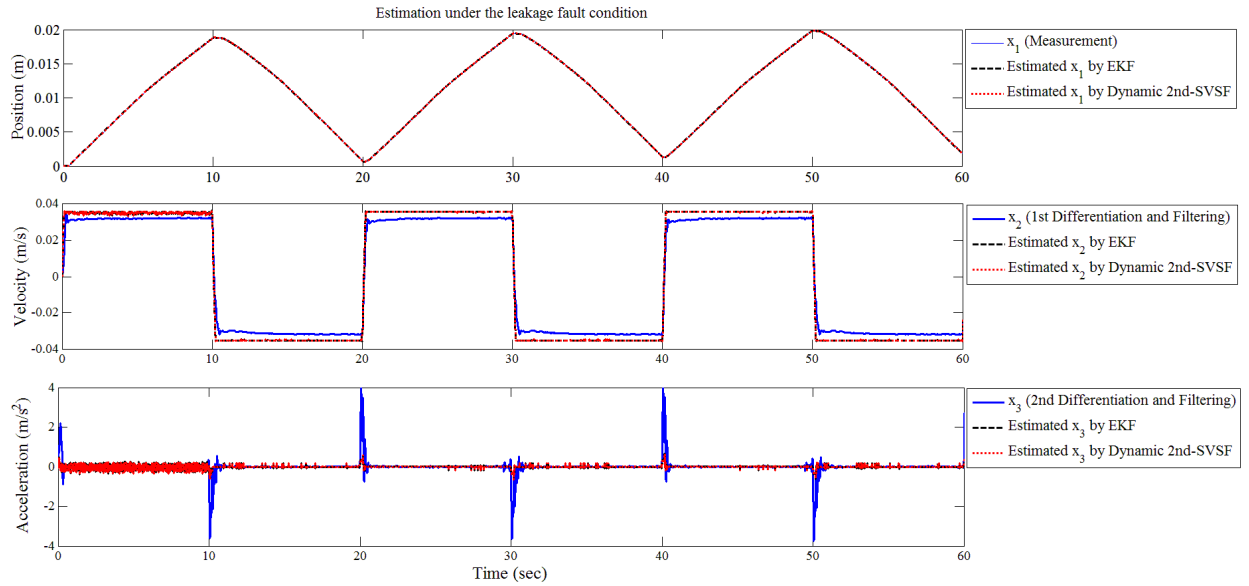


Figure 5.6: State estimate profiles generated by different estimators for the EHA setup under leakage

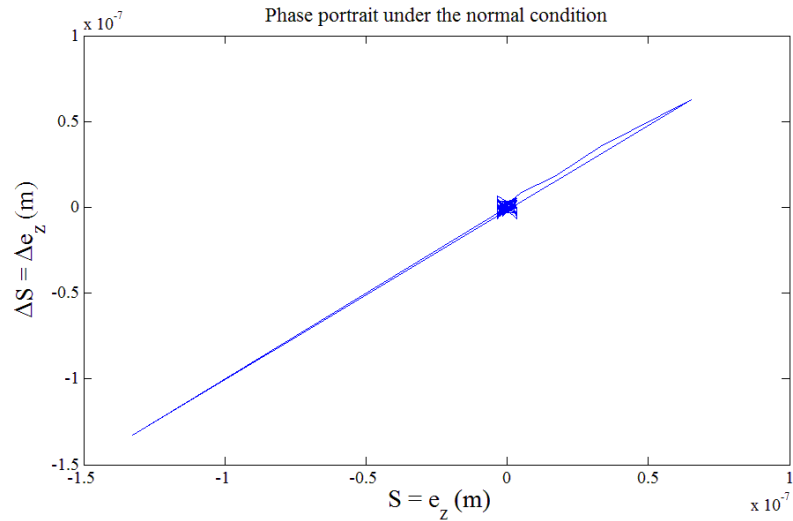


Figure 5.7: Phase portrait of the sliding variable and its difference for the normal EHA setup

Figure 5.7 depicts the phase portrait of the sliding variable (measurement error) versus its time difference generated by the optimal 2nd-order SVSF for the normal EHA setup. Furthermore, Figures 5.8 and 5.9 present the phase portraits generated by the dynamic 2nd-order SVSF for the EHA setup under the friction and leakage fault

conditions. According to these phase portraits of these three scenarios, both the measurement error and its difference are decreasing with time until the existence subspace is reached. However, due to noise, uncertainties, and discretization errors, the ideal sliding mode does not occur and real sliding condition is achieved.

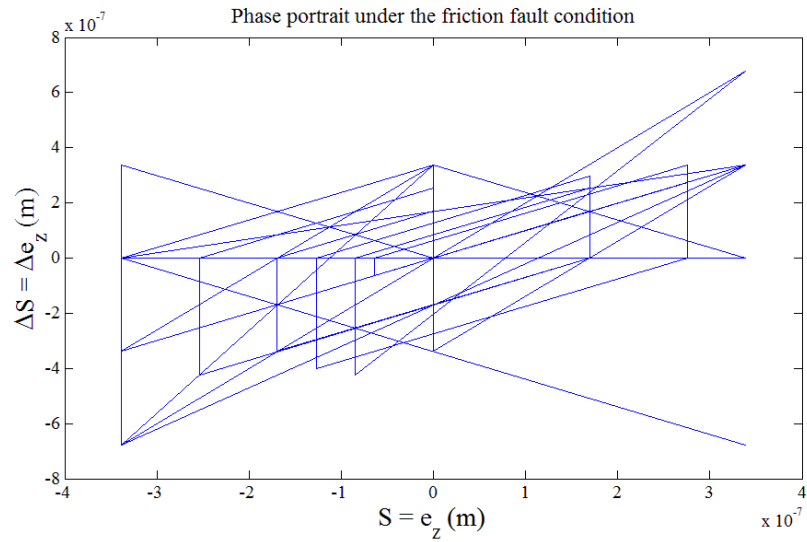


Figure 5.8: Phase portrait of the sliding variable and its difference for the EHA under friction

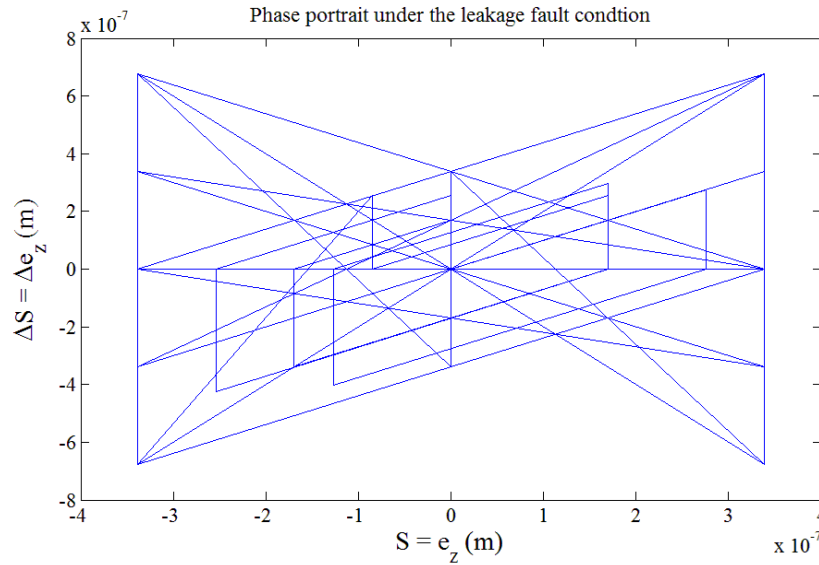
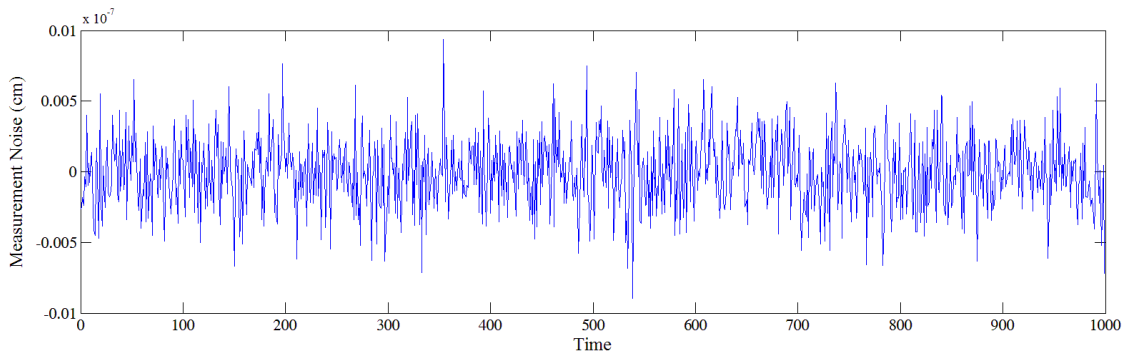
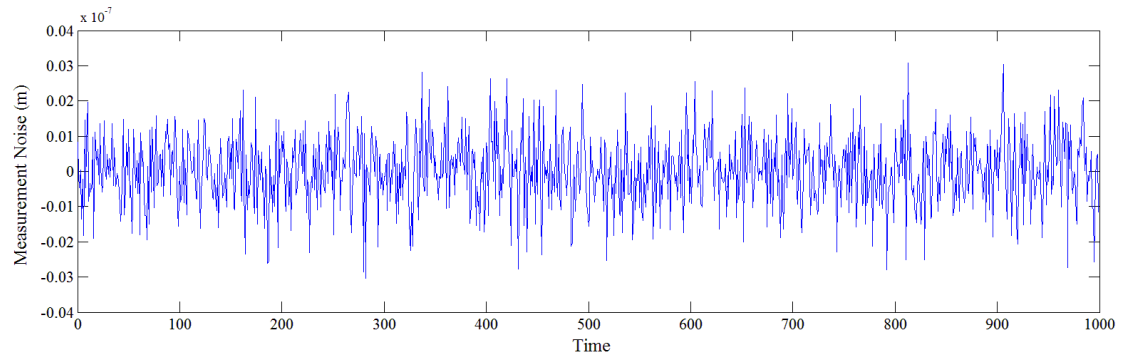


Figure 5.9: Phase portrait of the sliding variable and its difference for the EHA under leakage

State estimation results demonstrate the superior performance of the combined strategy (dynamic and optimal 2nd-order SVSF) over the extended Kalman Filter (EKF) and the 1st-order SVSF in terms of accuracy and smoothness under the faulty EHA setup. In order to find the type, location or severity of the fault, a fault identification task is implemented. The next section introduces a fault detection and identification (FDI) structure that is based on combining the dynamic 2nd-order SVSF with the IMM filter. In order to select one of the optimal or dynamic 2nd-order SVSF methods by the combined strategy, the measurement noise is studied. Figure 5.10 shows the measurement noise profiles for the normal EHA and EHA with major friction. As presented, for the EHA with major friction, the measurement noise has larger amplitude in comparison to the measurement noise of the normal EHA setup.



a) Measurement noise for the normal EHA setup



b) Measurement noise for the EHA with friction setup

Figure 5.10: Measurement noise profiles for the normal and faulty EHA setups

5.5. FDI of the EHA Setup Using the State Estimation Approach

This section presents fault detection and identification (FDI) of the experimental EHA setup using different state estimators (Kalman filter, 1st-order SVSF and the dynamic 2nd-order SVSF) combined with the interacting multiple model (IMM) filter. A typical FDI structure formulated by combining the dynamic 2nd-order SVSF and the IMM filter is initially described. Thereafter, a comparative analysis is performed based on experimental data and different state estimators in order to evaluate and compare the robust performance of each estimation method under uncertain faulty scenarios.

5.5.1. FDI Structure Using the Dynamic 2nd-Order SVSF and the IMM Filter

The Interacting Multiple Model (IMM) estimator is a suboptimal hybrid filter that can be combined with other state estimators. The main feature of this algorithm is the ability to estimate the states of a dynamic system under several operating modes that can transition from one mode to another. In this strategy, multiple models are used to describe the different operational modes of the system. A linear or nonlinear state model is used to describe each operating mode. The combination of these models is used to describe the dynamics of the nonlinear time-varying system. A Markov transition matrix is used to calculate the probability of the system being in one of the operational modes. In this section, the combination of the dynamic 2nd-order SVSF with the IMM filter is described.

The IMM filter can be used for modeling and estimation of complex nonlinear systems using a finite number of possible operating regimes. In this context, assume a hybrid linear system with different operating modes, using the state and measurement equations such that [1]:

$$x_{k+1} = \hat{F}_{k,m_k} x_k + \hat{G}_{k,m_k} u_{k,m_k} + w_{k,m_k}, \quad (5.12)$$

$$z_k = \hat{H}_{k,m_k} x_k + v_{k,m_k}. \quad (5.13)$$

where k is the time index and m_k denotes the current system mode. Furthermore, the operating mode in which the i^{th} model operates is represented by $M_{k,i} = \{m_k = m_i\}$, where M denotes the set of all modes in the multiple models framework.

It is assumed that the system model sequence is a homogenous Markov chain with transition probabilities represented as follows [1]:

$$\Pr\{m_{j,k+1} | m_{i,k}\} = \pi_{ij,k}, \quad \forall i, j \in M \quad (5.14)$$

where π_{ij} is the Markov transition probability from mode i to mode j , when $\sum_{j=1}^r \pi_{ij,k} = 1$.

Mode probabilities are updated at each new measurement, and weighting factors are used to calculate the state variables. Figure 5.11 presents a block-diagram scheme of the IMM-based dynamic 2nd-order SVSF structure. As demonstrated, this structure applies to a hybrid system with m different operating modes. The framework of the IMM filter combined with the dynamic 2nd-order SVSF consists of three main steps as follows:

I. Interaction Step [1]:

In this step, the mixing probability that is the probability of the system currently in mode i , and switching to mode j at the next step is calculated. The mixing probability, $\mu_{i|j,k-1|k-1} = \Pr\{M_{i,k-1} | M_{j,k}, Z^{k-1}\}$, is obtained as follows [1]:

$$\mu_{i|j,k-1|k-1} \triangleq \frac{1}{\bar{\mu}_j} \pi_{ij} \mu_{i,k-1}, \quad (5.15)$$

where π_{ij} is the mode transition probability that is set by the designer. Furthermore, $\bar{\mu}_j$ is the predicted mode probability for r different modes and calculated by [1]:

$$\bar{\mu}_j \triangleq \Pr\{M_{j,k} | Z^{k-1}\} = \sum_{i=1}^r \pi_{ij} \mu_{i,k-1}. \quad (5.16)$$

The mixed initial condition is calculated using previous state and covariance estimates $\hat{x}_{i,k-1|k-1}$ and $P_{i,k-1|k-1}$, respectively. They are outputs of r different dynamic 2nd-order SVSF filters that are based on r different models. The mixed initial state and covariance matrix are calculated for the filter M_j at time k as follows [1]:

$$\hat{x}_{0j,k-1|k-1} \triangleq E\{x_{k-1} | M_{j,k}, Z^{k-1}\} = \sum_{i=1}^r \hat{x}_{i,k-1|k-1} \mu_{i|j}, \quad (5.17)$$

$$\hat{P}_{0j,k-1|k-1} = \sum_{i=1}^r \mu_{i|j,k-1|k-1} [\hat{P}_{i,k-1|k-1} + (\hat{x}_{i,k-1|k-1} - \hat{x}_{0j,k-1|k-1})(\hat{x}_{i,k-1|k-1} - \hat{x}_{0j,k-1|k-1})^T]. \quad (5.18)$$

II. Filtering Step [1]:

Mode-matched filtering is applied in this step and the likelihood function corresponding to each filter is determined. The calculated mixed initial state and covariance are set as inputs to the dynamic 2nd-order SVSF which is matched to mode $M_j(k)$. The filtering step starts by predicting the state and the error covariance matrix of each mode are provided as follows [1]:

$$\hat{x}_{j,k|k-1} = \hat{F}_{j,k-1} \hat{x}_{0j,k-1|k-1} + \hat{G}_{j,k-1} u_{j,k-1} + \bar{w}_{j,l-1}, \quad (5.19)$$

$$\hat{P}_{j,k|k-1} = \hat{F}_{j,k-1} \hat{P}_{0j,k-1|k-1} \hat{F}_{j,k-1}^T + Q_{j,k-1}. \quad (5.20)$$

The residual and its covariance for each mode are respectively calculated as follows [1]:

$$e_{j,k} = z_k - \hat{H}_{j,k} \hat{x}_{j,k|k-1}, \quad (5.21)$$

$$S_{rc_{j,k}} = \hat{H}_{j,k} \hat{P}_{j,k-1|k} \hat{H}_{j,k}^T + R_{j,k}. \quad (5.22)$$

Later on, the corrective gain of the dynamic 2nd-order SVSF is applied such that:

$$\begin{aligned} K_{j,k} = & \hat{H}_j^+ \left[\text{diag}(e_{j,k|k-1}) - (\gamma + \Lambda_j) \text{diag}(e_{j,k-1|k-1}) \right. \\ & \left. + \gamma \Lambda_j \text{diag}(e_{j,k-2|k-2}) \right] \left[\text{diag}(e_{j,k|k-1}) \right], \end{aligned} \quad (5.23)$$

where \hat{H}_j^+ is the pseudo-inverse of the measurement matrix \hat{H}_j , and Λ_j is the constant cut-off frequency matrix. State and covariance updates are respectively given by:

$$\hat{x}_{j,k|k} = \hat{x}_{j,k|k-1} + K_{j,k} e_{j,k|k-1}, \quad (5.24)$$

$$\hat{P}_{j,k|k} = \hat{P}_{j,k|k-1} - K_{j,k} S_{rc_{j,k}} K_{j,k}^T. \quad (5.25)$$

Based on the innovation matrix (residual covariance) $S_{rc_{j,k}}$, and the *a priori* measurement error $e_{j,k|k-1}$, a corresponding likelihood function $\Lambda_{j,k}$ may be calculated as follows [1]:

$$\Lambda_{j,k} = N[e_{j,k}, 0, S_{rc_{j,k}}] = \frac{e^{-\frac{1}{2} e_{j,k}^T S_{rc_{j,k}}^{-1} e_{j,k}}}{\sqrt{2\pi S_{rc_{j,k}}}} \quad (5.26)$$

The likelihood function is used to calculate the mode probability update given by [1]:

$$\mu_{j,k} = \frac{\bar{\mu}_j \Lambda_{j,k}}{\sum_{i=1}^r \bar{\mu}_i \Lambda_{i,k}}. \quad (5.27)$$

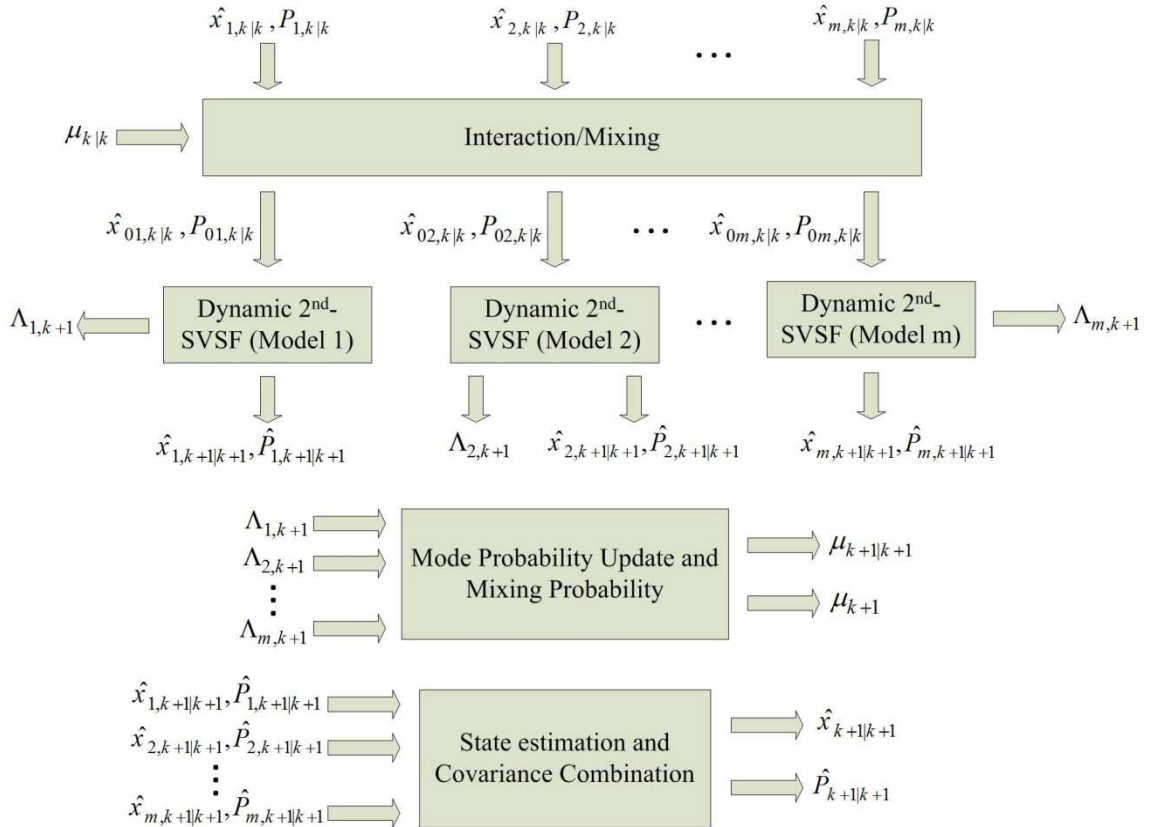
III. Combination Step [1]:

The *a posteriori* state and covariance matrix are estimated by combining the mode conditioned estimates and covariance as follows [1]:

$$\hat{x}_{k|k} \triangleq E \left[x_k | Z^k \right] = \sum_{i=1}^r \hat{x}_{i,k|k} \mu_j, \quad (5.28)$$

$$P_{k|k} = \sum_{i=1}^r \mu_{i,k} \left[\hat{P}_{i,k|k} + (\hat{x}_{i,k|k} - \hat{x}_{k|k})(\hat{x}_{i,k|k} - \hat{x}_{k|k})^T \right]. \quad (5.29)$$

It is important to note that using the dynamic 2nd-order SVSF within the IMM structure does not affect the stability and convergence of the IMM filter. It is because, similar to the IMM-Kalman filter structure, at the step time k the dynamic 2nd-order SVSF only applies to one particular model of the system. If the operating regime changes at time $k+q$, then the dynamic 2nd-order SVSF method will apply to another particular model of the system that describes it more accurately.


 Figure 5.11: Block-diagram of the IMM-based dynamic 2nd-order SVSF structure

5.5.2. Comparative Analysis Using the Experimental EHA Setup

In this section, the FDI task is performed by combining some of the extended Kalman filter, as well as the 1st-order SVSF and the dynamic 2nd-order SVSF, within an Interacting Multiple Models (IMM) structure. The experimental EHA setup is used to study and compare the IMM strategies. The software used to communicate with the EHA setup is MATLAB's Real-Time Windows Target environment. Two types of fault conditions were physically induced to the EHA setup: internal leakage and friction. Hence, there are three main scenarios for experimentations including the EHA under the normal condition, the EHA with major friction and the EHA with internal leakage. Each scenario applies within 2 sec separately.

The normal, leakage, and friction operating conditions of the EHA have been extensively studied and modeled in [10]. As demonstrated, Tables 5.2 lists numerical values of the friction coefficients for the EHA setup under different friction fault conditions. Furthermore, Table 5.3 presents numerical values of the leakage coefficients and flow rate offsets for the EHA setup under different leakage fault conditions. These numeric values are obtained by experimentations and reported in [10]. The actuator position is the only measurable state, such that the measurement matrix is given by:

$$C = [1 \ 0 \ 0]. \quad (5.30)$$

In order to apply the 1st-order SVSF, as well as the dynamic 2nd-order SVSF method, to the EHA setup with one measurement available (actuator position), the Luenberger's observer is used (refer to section 3.5) [3]. Note that this however increases the amount of noise experienced by the SVSF estimation strategies. For all strategies, the initial state estimate and state error covariance matrix are defined as follows:

$$\hat{x}_{00} = [0 \quad 0 \quad 0]^T, \quad (5.31)$$

$$P_{00} = \begin{bmatrix} 1 & 0 & 0 \\ 0 & 10 & 0 \\ 0 & 0 & 50 \end{bmatrix}. \quad (5.32)$$

The process noise covariance Q and the measurement noise covariance R for the EKF, the 1st-order SVSF and the dynamic 2nd-order SVSF methods are given by:

$$Q = \text{diag} \left([10^{-12} \quad 10^{-10} \quad 10^{-9}] \right), \quad (5.33)$$

$$R = 10^{-12}. \quad (5.34)$$

In an effort to minimize the estimation error, the convergence rate for the 1st-order SVSF and the dynamic 2nd-order SVSF are set to $\gamma=0.5$. For the 1st-order SVSF, the smoothing boundary layer vector is set to:

$$\psi = [3.5 \times 10^{-3} \quad 1 \times 10^4 \quad 1 \times 10^6]. \quad (5.35)$$

For the IMM settings, the initial mode probability was defined as follows:

$$\mu_{i,0} = [0.90 \quad 0.05 \quad 0.05]^T. \quad (5.36)$$

The mode transition matrix P_{ij} is defined as a 3-by-3 diagonal matrix with 0.90 along the diagonal and 0.05 on the off-diagonal, as follows:

$$P_{ij} = \begin{bmatrix} 0.90 & 0.05 & 0.05 \\ 0.05 & 0.90 & 0.05 \\ 0.05 & 0.05 & 0.90 \end{bmatrix}. \quad (5.37)$$

It states, for example, that there is a 90% probability that the EHA will stay in mode 1 (normal operation) if it was in mode 1 at the current time step (i.e., $P_{1,1} = 0.90$). The

scenario that was studied involved the EHA operating normally for two seconds, a leakage fault for two seconds, followed by a friction fault for the last two seconds. Profiles of the input into the EHA setup (motor velocity) and the output (position measurement) are shown in Figures 5.12, and 5.13, respectively. The input to the EHA system is a square wave signal fluctuates between +5 and -5 rad/sec. A linear encoder is used to measure the only measurable state that is the actuator position.

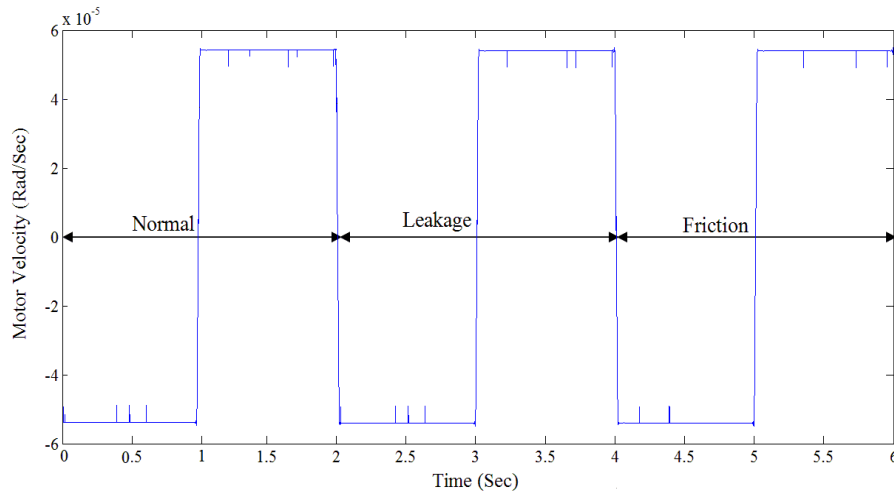


Figure 5.12: Profile of the input into the EHA setup (motor velocity)

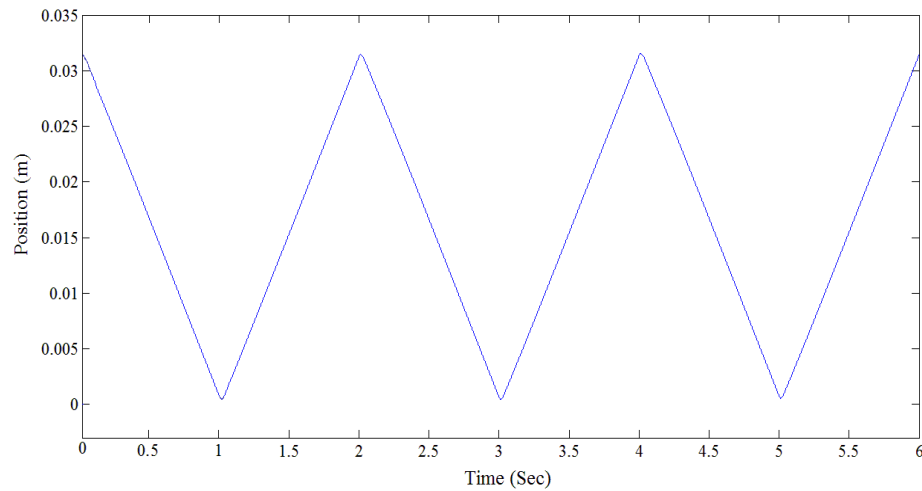


Figure 5.13: Measurement profile of the EHA setup (actuator position)

In this section, the extended Kalman filter (EKF), the 1st-order SVSF and the dynamic 2nd-order SVSF were combined with the IMM method and applied to the EHA setup for fault detection and diagnosis. Tables 5.5 through 5.7 summarize the probability results for each method. These are referred to as confusion matrices, and provide an indication of how accurate the models were in detecting the correct operating mode. Following confusion matrices, it is deduced that all of the methods successfully detected the correct operating mode (a diagonal probability of 50% or greater); however, with varying degrees of confidence. The IMM-based dynamic 2nd-order SVSF strategy correctly identified the EHA operating normally with the highest probability level (93.33%), followed by the IMM-1st order SVSF, and the IMM-EKF.

The IMM-based dynamic 2nd-order SVSF also detected the leakage fault with the highest level (90.05%), followed by the IMM-1st order SVSF, and the IMM-EKF. Furthermore, the IMM-based EKF strategy correctly identified the friction fault with the highest confidence level (93.29%), followed by the IMM-1st order SVSF, and the IMM-dynamic 2nd-order SVSF. It is interesting to note that another important factor to study includes cross-detection errors or misclassifications. For example, when the EHA was operating normally, the IMM-EKF strategy detected a leakage fault with 40.51% probability. This is a high cross-detection error, as the IMM-EKF method detected normal operation with only 59.31% probability. If these values were closer, it would be difficult to properly diagnose the fault with a high level of confidence. Note that a comparative analysis of some other state estimation methods including the unscented Kalman filter (UKF), the cubature Kalman filter (CKF), and the particle filter (PF), when combined within an Interacting Multiple Models (IMM) structure, is presented in Appendix.

Table 5.5: Confusion matrix for the IMM-based EKF

		Actual Condition		
		Normal	Leakage	Friction
Predicted Condition	Normal	59.31%	27.65%	3.18%
	Leakage	40.51%	66.94%	3.53%
	Friction	0.18%	5.41%	93.29%

Table 5.6: Confusion matrix for the IMM-based 1st-order SVSF

		Actual Condition		
		Normal	Leakage	Friction
Predicted Condition	Normal	91.93%	7.16%	4.07%
	Leakage	7.73%	86.41%	3.66%
	Friction	0.34%	6.43%	92.27%

Table 5.7: Confusion matrix for the IMM-based dynamic 2nd-order SVSF

		Actual Condition		
		Normal	Leakage	Friction
Predicted Condition	Normal	93.33%	4.14%	3.06%
	Leakage	6.53%	90.05%	4.75%
	Friction	0.14%	5.81%	92.19%

Another interesting factor to study is the overall correct detection probability. This can be studied by referring to the confusion matrices and Figure 5.14. Note that the summation of the diagonal elements in the matrices is equal to the total mode probability. Ideally, the perfect detection strategy would correctly identify the operating modes and thus, the total mode probability would be 3 or 300%. Overall, the IMM-dynamic 2nd-order SVSF yielded the best results in terms of maximizing the correct mode detection and minimizing the misclassifications. The IMM-dynamic 2nd-order SVSF had a total mode

probability of 281.53%, followed by the IMM-1st order SVSF with a total mode probability of 270.61%, followed by the IMM-EKF with a total mode probability of 219.54%. Hence, it appears that the IMM-dynamic 2nd-order SVSF method provides the best method for fault detection and diagnosis. This may be due to its unique gain calculation, which preserves robustness during the state estimation process.

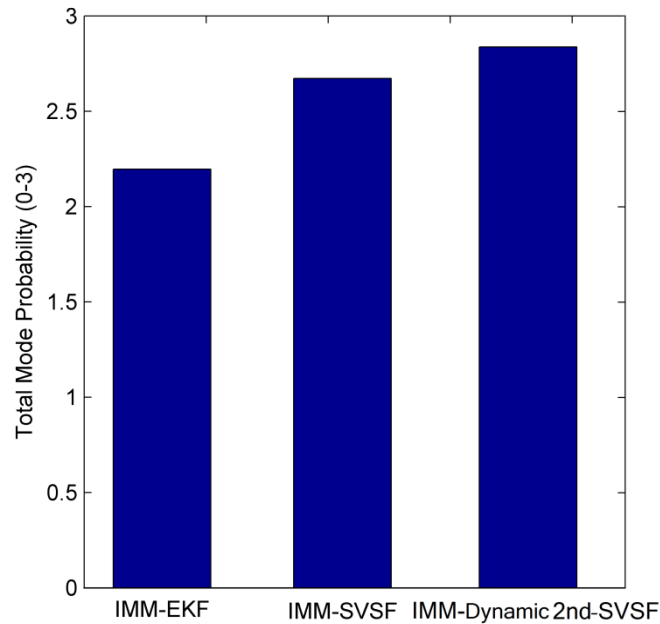


Figure 5.14: Total mode probability detections by different methods

For more clarity in comparison, the mode probability profiles of the IMM-dynamic 2nd-order SVSF, the IMM-1st order SVSF and the IMM-EKF strategies are respectively presented in Figures 5.15 through 5.17. It is observed from these figures that the IMM-based dynamic 2nd-order SVSF produces the largest mode probability value, followed by the IMM-based 1st-order SVSF, and the IMM-based EKF structures. Mode probability profiles demonstrate the superior performance of the dynamic 2nd-order SVSF in identifying the operating mode of the EHA under the normal and uncertain conditions.

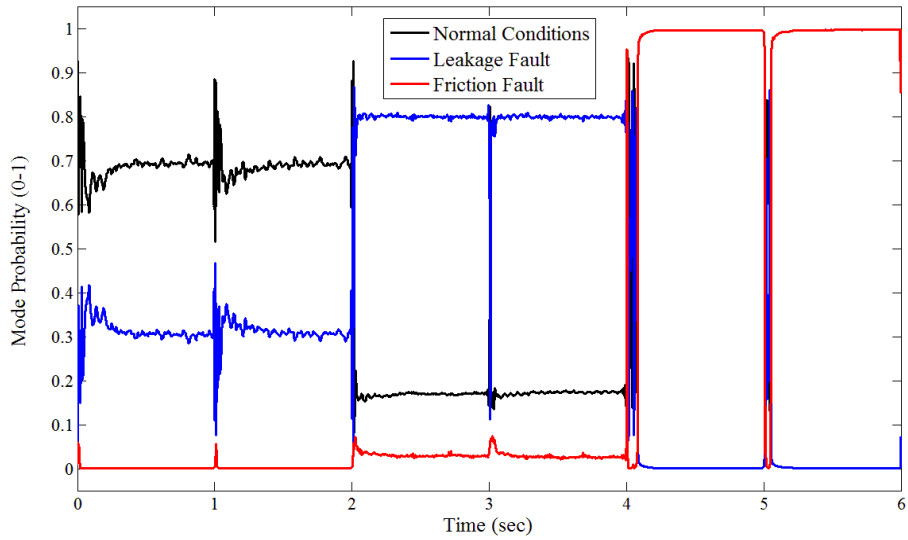


Figure 5.15: Mode probability estimate generated by the IMM-based EKF

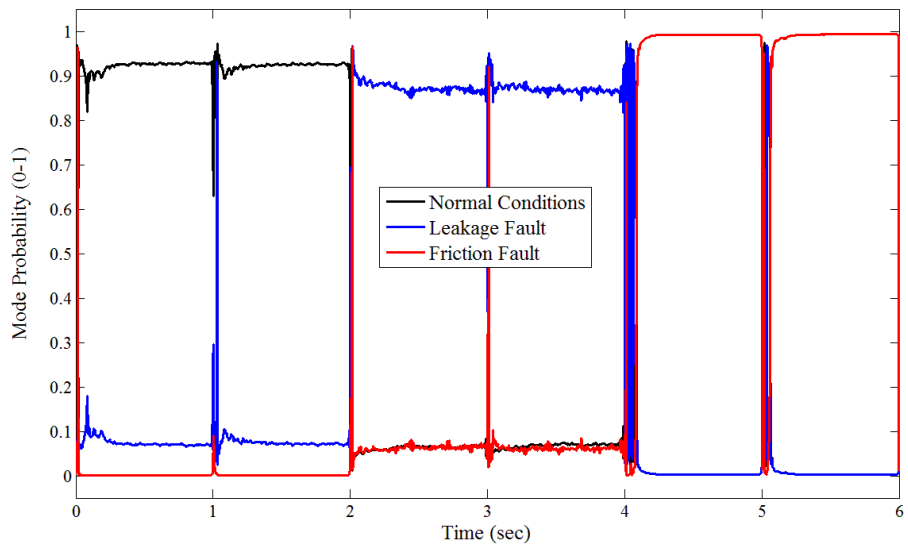


Figure 5.16: Mode probability estimate generated by the IMM-based 1st-order SVSF

Figure 5.18 furthermore presents profiles of the measured (obtained by the measurement or differentiation) and estimated state trajectories using the IMM-based dynamic 2nd-order SVSF structure. Note that the differentiated and filtered data for the velocity and acceleration are respectively obtained by taking the first and second order time-derivatives of the position (measurement) trajectory. As discussed in *Remark 5.1*,

these signals are later filtered out through a Butterworth filter in order to filter out the differentiation noise and other spikes. Fig. 5.18 demonstrates that state estimation trajectories successfully follow measured (obtained by measurement or differentiation) state trajectories in the normal and faulty scenarios.

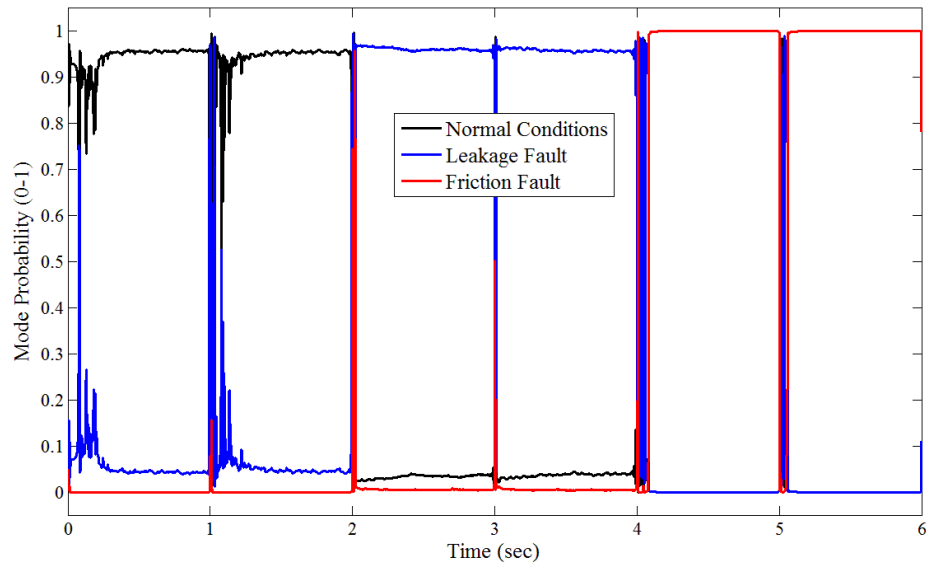


Figure 5.17: Mode probability estimate given by the IMM-based dynamic 2nd-order SVSF

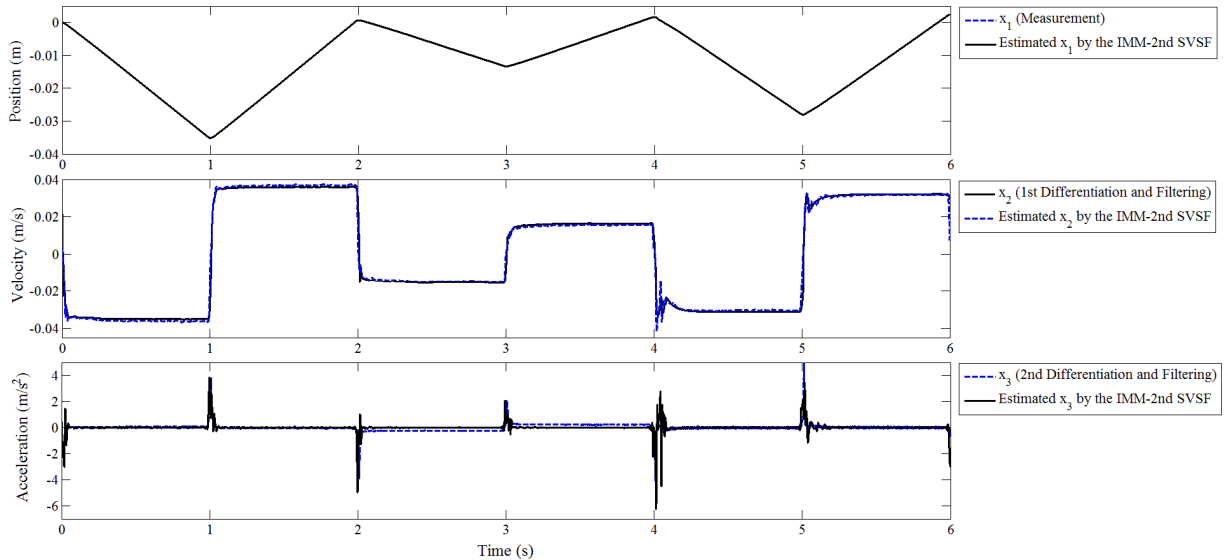


Figure 5.18: Actual and estimated state trajectories using the IMM-dynamic 2nd-order SVSF method

Table 5.8 presents the RMSE values of the four state estimators (the EKF, the 1st-order SVSF, and the dynamic 2nd-order SVSF) combined with the IMM filter for the described scenario. It is deduced from Table 5.8 that the IMM-based dynamic 2nd-order SVSF strategy provide the more accurate state estimates, followed by the IMM-based 1st-order SVSF. This however confirms the superior performance of the combined strategy (including the dynamic and optimal 2nd-order SVSF) for state estimation under the normal condition and its robust performance under the uncertain faulty conditions. Numeric values of Tables 5.7 and 5.8 present the superior performance of the combined strategy over other estimation approaches for fault detection and diagnosis.

Table 5.8: RMSE values of different state estimators combined with the IMM filter

States	EKF	1 st -order SVSF	Dynamic 2 nd -order SVSF
\mathbf{x}_1 (m)	6.59×10^{-4}	4.10×10^{-5}	1.85×10^{-5}

5.6. Summary

This chapter presents applications of the combined strategy (dynamic and optimal 2nd-order SVSF methods) for fault detection and diagnosis using an experimental EHA setup. Fault detection is performed by comparing the RMSE of state estimates with their values under normal condition. Moreover, fault diagnosis is performed by combining the dynamic 2nd-order SVSF with the IMM filter. The mode probability estimate represents the current operating regime (normal or faulty) of the EHA. This structure successfully identified the correct operating regime with smaller values of RMSE and higher values of the mode probability.

Chapter 6

Summary and Concluding Remarks

This chapter presents the main contributions of this PhD research and the relevant conclusions. It also provides recommendations for future research.

6.1. Summary of the PhD Research

Kalman-type filtering methods assume a known model with uncertainties being represented as white noise. In real applications, there are considerable amount of uncertainties about the model structure, physical parameters, level of noise, and initial conditions that make white noise representation invalid. In order to overcome such difficulties, robust state estimation techniques are widely used. The SVSF filter is a new robust state estimation approached introduced in 2007. The SVSF-type filtering benefits from the robust stability of variable structure systems and results in a robust state estimation algorithm with an inherent switching action. This PhD research presents three main contributions that are mainly based on using the second order sliding mode theory for control and state estimation of uncertain dynamic systems. The higher accuracy and robustness of these methods over other conventional methods are proven in computer simulation and experimentation. An experimental setup of an Electro-Hydrostatic Actuator (EHA) is used in order to verify computer simulations.

The first contribution of this PhD thesis is the design and implementation of the 2nd-order SVSF in which the chattering effects are suppressed by satisfying the second order sliding condition. The 2nd-order SVSF applies to systems with nonlinear state model and linear or at least piece-wise measurement model. It satisfies both the first and second order sliding mode conditions using the Lyapunov's second law of stability. Furthermore, in order apply the 2nd-order SVSF, there is no need to linearize or even approximate the nonlinear state model. In the 2nd-order SVSF method, the estimation error and it first difference are decreasing over time until reaching the existence subspace. Hence, along with keeping the main advantages of the former 1st-order SVSF [3], it alleviates the unwanted chattering effect considerably. It also produces more accurate state estimates without compromising its robustness and even without the need to approximate or relax

the discontinuous corrective action. Simulation results present the superior performance of the 2nd-order SVSF over other methods such as the Kalman filter and the 1st-order SVSF method given uncertainties.

The second contribution of this research is the optimal 2nd-order SVSF method for state estimation. The corrective gain formulation of the 2nd-order SVSF is highly nonlinear, making optimization difficult. In order to avoid such computational difficulties, the dynamic 2nd-order SVSF is firstly designed based on a linear dynamic sliding mode manifold. It is defined as a linear combination of the sliding variable and its first derivative. The new sliding manifold introduces a cut-off frequency matrix into the filter formulation. The cut-off frequency coefficient operates like a first-order low-pass filter with an adjustable bandwidth. Stability and convergence of this new derivation for the first and second order sliding motions are proven using a discrete-time Lyapunov function candidate.

In order to formulate the optimal 2nd-order SVSF, the error covariance matrix at each iteration needs to be obtained. The optimization process is then performed to calculate the optimal value of the cut-off frequency by minimizing the error covariance matrix (trace). It is shown that the corrective gain of the optimal 2nd-order SVSF restates the Kalman filter gain and hence, a combined strategy includes the dynamic 2nd-order SVSF for uncertain systems and the optimal 2nd-order SVSF for normal systems is introduced. The main advantages of the combined strategy over other state estimation methods include robustness to noise and modeling uncertainties, low computational cost, and ease of implementation. In order to compare the performance of the 2nd-order SVSF and its dynamic version with other estimation methods such as the well-known Kalman filter and the 1st-order SVSF, they are simulated using a model of an electro-hydrostatic actuator (EHA). Simulations are performed for the normal and uncertain scenarios when

in the uncertain scenario the level, source and occurrence of uncertainties are unknown. These methods are then compared in terms of robustness, accuracy and smoothness of the state estimates.

An experimental setup of an electro-hydrostatic actuator (EHA) is used for verifying the robust performance of the 2nd-order SVSF and its dynamic version. These methods are implemented in a FDI strategy. Fault detection is performed by comparing the RMSE of state estimates with ones under normal condition. Moreover, fault diagnosis is performed by combining the dynamic 2nd-order SVSF with the IMM filter. The mode probability estimate represents the current operating regime (normal or faulty) of the system. The IMM-based dynamic 2nd-order SVSF successfully identified the correct regime with smaller values of RMSE and higher values of mode probabilities. Experimentations confirm the superior performance of the combined strategy in comparison with other state estimators such as the Kalman filter, and the 1st-order SVSF.

6.2. Concluding Remarks

Concluding remarks on the 2nd-order SVSF and its optimal version for state estimation may be summarized as follows.

- Simulation and experimentation results demonstrate that the 2nd-order SVSF and its dynamic version produce more accurate, robust and smoother state estimates in uncertain situations in comparison to the Kalman filter, and the 1st-order SVSF.
- The 2nd-order SVSF applies to systems that have a nonlinear state model but with a measurement model without the need to linearization or approximation. It is one of the main advantage of the 2nd-order SVSF over conventional state estimation methods that are mainly based on linearization or approximation of the state model.

- Due to the low computational cost of the 2nd-order SVSF and its dynamic version, they may be simply applied for the real-time state estimation task.
- Stability of the 2nd-order SVSF and its dynamic version are proven by using the discrete-time Lyapunov stability criteria.
- In spite of the 2nd-order SVSF, its optimal version only applies to systems with a linear state model. For implementing the optimal 2nd-order SVSF to nonlinear systems, the state's *a posteriori* PDF can be predicted using approximation or linearization techniques, similarly to the extended Kalman filter.
- In the 2nd-order SVSF and its dynamic version, there is no need to use the saturation function or any type of approximation to alleviate discontinuities and prevent chattering. They use the 2nd-order sliding mode concept such that the measurement error and its difference decrease in time until the existence subspace is reached.
- The corrective gain of the dynamic 2nd-order SVSF is designed based on a dynamic sliding mode manifold which preserves the first and second sliding mode conditions. This dynamic manifold formulation introduces a first-order low-pass filter with an adjustable cut-off frequency coefficient. The cut-off frequency coefficient determines the filter's bandwidth. The optimization process is then performed to find the optimal value for the cut-off frequency at each time step.
- The 2nd-order SVSF and its dynamic version are primarily designed for estimating state variables of systems with a square measurement matrix. In order to apply them to systems with fewer measurements than states, Luenberger's observer needs to be applied as was done in [3].
- The 2nd-order SVSF alleviates the need for tuning by trial and error that saves time and efforts. However for the optimal version, the system and measurement covariance matrices need to be tuned similarly to the Kalman filter.

- The corrective gain of the 2nd-order SVSF and its optimal version represent a second order Markov process. They refine the *a priori* state estimates into the *a posteriori* ones based on the available values of the measurement error from the last two steps. Updating estimates based on this higher amount of information will improve their performance with smoother state estimates.
- The main concern with the 2nd-order SVSF state estimation method is that it is however not optimal in the mean square error sense. In order to overcome this, the optimal 2nd-order SVSF is introduced that minimizes the covariance of the state estimation error at each step. It is shown that the corrective gain of the optimal 2nd-order SVSF collapses to the Kalman filter gain and hence robustness is lost. To preserve robustness, a combined strategy is used that benefits from optimality of the optimal 2nd-order SVSF as well as robustness of the dynamic 2nd-order SVSF.

6.3. Recommendations for Future Research

This PhD research introduced and discussed a number of contributions on the SVSF-type filtering with applications to an electro-hydrostatic actuator setup. Since the SVSF-type filtering is still new, a considerable amount of research still remains. Additionally, the 2nd-order SVSF presented a new field of research relevant to robust state estimation based on preserving the first and second order sliding conditions. The main recommendations for future studies include the following.

1. **Chattering analysis:** In the sliding mode context, the second order sliding regime has been frequently used for the numerical analysis of chattering [157,159,14]. Moreover, in the SVSF-type filtering, frequency and amplitude of chattering are related to the level of modeling uncertainties. During the fault condition, the amount of uncertainties in system states and parameters increases significantly.

Hence, the energy of the corresponding chattering signal starts to increase as long as the uncertainty continues to grow. This property of the SVSF-type filtering can be considered as a strong tool for analyzing dynamics of faulty components, when it is difficult to analyze the residual (innovation sequence) signal. Chattering signal can then be used to diagnose fault conditions. There has been a lot of research on chattering in SMC systems [57, 58]. The most well-known methods are the averaging approach [56], describing function [59], state dependent gain method [59], singular perturbation theorem [60] and the Poincare map technique [59]. Numerical analysis of chattering as well as evaluating the innovation sequence (measurement error) will improve health monitoring.

- 2. Design a discrete-time 2nd-order sliding mode controller:** An interesting topic for the future research is to design and implement a discrete-time 2nd-order sliding mode controller (SMC) that is robust against modeling uncertainties. Note that conventional digital 2nd-order SMCs are mainly designed based on direct digitization of continuous-time controllers that only approximates formulations of the continuous SMCs using the Taylor series integration. In contrast, the mentioned discrete 2nd-order SMC would be designed for discrete-time linear systems based on a discrete-time Lyapunov stability criterion. The controller has two main elements that include an equivalent control part and a switching control part. The equivalent control is a model-based feed-forward compensation of the plant's dynamics and can be formulated based on the second order differentiation of the sliding variable. Meanwhile, a switching control term is added for robustness to modeling uncertainties and disturbances. The total control law needs to satisfy the first and second sliding conditions and in turns the Lyapunov's stability condition defined in discrete-time.

Bibliography

- [1] Y. Bar-Shalom, X. R. Li, and T. Kirubarajan, *Estimation with Applications to Tracking and Navigation.*: John Wiley & Sons Inc, 2001.
- [2] A. H. Sayed, "A framework for state-space estimation with uncertain models," *IEEE Transactions on Automatic Control*, vol. 46, no. 7, pp. 998-1013, 2001.
- [3] S. R. Habibi, "The smooth variable structure filter," *Proceedings of the IEEE*, vol. 95, no. 5, pp. 1026-1059, 2007.
- [4] V. Utkin, J. Gulner, and J. Shi, *Sliding Mode Control in Electro-mechanical Systems*, 2nd ed., Taylor & Francis Group, Ed.: CEC Press, 2009.
- [5] J. J. Slotine and S. S. Sastry, "Tracking control of nonlinear systems using sliding surfaces, with application to robot manipulators," *International Journal of Control*, vol. 38, pp. 465-492, 1993.
- [6] W. Perruquetti and J.P. Barbot, *Sliding Mode Control in Engineering.*: Marcel Dekker Inc., 2002.
- [7] A. Levant, "Sliding order and sliding accuracy in sliding mode control," *International Journal of Control*, vol. 58, no. 6, pp. 1247-1263, 1993.
- [8] S. A. Gadsden, "Smooth variable structure filter: theory and applications," Departemnt of Mechanical Engineering, McMaster University, PhD Thesis 2011.
- [9] Dunne D., Habibi S., and Kirubarajan T., Gadsden S. A., "Nonlinear estimation techniques applied on target tracking problems," *Transactions of the ASME, Journal of Dynamic Systems, Measurement, and Control*, vol. 134, no. 5, 2012.
- [10] S.A. Gadsden, Y. Song, and S. Habibi, "Novel Model-based Estimators for the Purpose of Fault Detection and Diagnosis," *IEEE Transactions on Mechatronics*, vol. 18, no. 4, pp. 1237-1249, 2013.
- [11] S. A. Gadsden and S. R. Habibi, "A new robust filtering strategy for linear systems," *Journal of Dynamic Systems, Measurement, and Control*, vol. 135, no. 1, p. 014503, 2013.
- [12] S. A. Gadsden, M. El Sayed, and S. R. Habibi, "Derivation of an optimal boundary layer width for the smooth variable structure filter," in *American CONTROL*

Conference, San Francisco, United States, 2011.

- [13] A. Levant, "Arbitrary-order sliding modes with finite time convergence," in *Proceedings of the 6th IEEE Mediterranean Conference on Control and Systems*, Sardinia, Italy, 1998.
- [14] A. Levant, "Chattering analysis," *IEEE Transactions on Automatic Control*, vol. 55, no. 6, pp. 1380-1389, 2010.
- [15] G. Bartolini, A. Ferrara, and E. Usai, "Chattering Avoidance by Second-order Sliding Mode Control," *IEEE Transactions on Automatic Control*, vol. 43, no. 2, pp. 241-246, 1998.
- [16] H. Sira-Ramirez, "Non-linear discrete time variable structure systems in quasi-sliding mode," *International Journal of Control*, vol. 54, pp. 1171-1187, 1991.
- [17] H. Sira-Ramirez, "On the dynamical sliding mode control of nonlinear systems," *International Journal of Control*, vol. 57, no. 5, pp. 1039-1061, 1993.
- [18] A. Gelb, *Applied Optimal Estimation*. Cambridge, MA: MIT Press, 1974.
- [19] B. Ristic, S. Arulampalam, and N. Gordon, *Beyond the Kalman Filter: Particle Filters for Tracking Applications*. Boston, United States: Artech House, 2004.
- [20] M. S. Grewal and A. P. Andrews, *Kalman Filtering: Theory and Practice Using MATLAB*, 2nd ed. New York, United States, NY: John Wiley & Sons, INC, 2001.
- [21] Y. Bar-Shalom, X. Rong Li, and T. Kirubarajan, *Estimation with Application to tracking and navigation*. New York, United States: John Wiley and Sons, INC, 2004.
- [22] H. Haykin, *Adaptive filter theory*, 3rd ed. Upper Saddle River, NJ, United States: Prentic-Hall, 1996.
- [23] N. Wiener, *Extrapolation, Interpolation, and Smoothing of Stationary Time Series*. Cambridge, Massachusetts, United States: MIT Press, 1964.
- [24] A. Kolmogorov, *Interpolation and Extrapolation of Stationary Random Sequences*. Dordrecht, Netherlands: Kluwer Academic Publishers, 1941.

- [25] H. W. Sorenson, "Least-Squares Estimation: From Gauss to Kalman," *IEEE Spectrum*, pp. 63-68, 1970.
- [26] R. Kalman and R. Bucy, "New Results in Linear Filtering and Prediction Theory," *ASME Journal of Basic Engineering*, vol. 83, pp. 95-108, March 1961.
- [27] I. Arasaratnam and S. Haykin, "Square-root quadrature Kalman filtering," *IEEE Transactions on Signal Processing*, vol. 95, no. 6, pp. 953-977, 2008.
- [28] I. Arasaratnam, S. Haykin, and R. J. Elliott, "Discrete-time nonlinear filtering algorithms using Gauss-Hermite quadrature," *Proceedings of IEEE*, vol. 95, no. 5, pp. 953-977, 2007.
- [29] R. Chen and J. Liu, "Mixture Kalman Filters," *Journal of the Royal Statistical Society, Series B*, vol. 62, no. 3, pp. 493-508, 2000.
- [30] I. Arasaratnam and S. Haykin, "Cubature Kalman filters," *IEEE Transactions on Automatic Control*, vol. 54, no. 6, pp. 1254-1269, 2009.
- [31] L. S. Wang, Y. T. Chiang, and F. R. Chang, "Filtering method for nonlinear systems with constraints," *IEE Proceedings, Control theory and Application*, vol. 149, no. 6, pp. 525-531, 2002.
- [32] Y. C. Ho and R. C. Lee, "A Bayesian approach to problems in stochastic estimation and control," *IEEE Transactions on Automatic Control*, vol. 9, no. 4, pp. 333-339, 1964.
- [33] R. L. Stratonovich, "On the theory of optimal non-linear filtering of random functions," *Theory of Probability and its applications*, vol. 4, pp. 223-225, 1959.
- [34] R. L. Stratonovich, "Application of the Markov processes theory to optimal filtering," *Radio Engineering and Electronic Physics*, vol. 5, no. 11, pp. 1-19, 1960.
- [35] T. Kailath, "An innovation approach to least-squares estimation, Part I: linear filtering in additive white noise," *IEEE Transactions on Automatic Control*, vol. 13, no. 6, pp. 646-655, 1968.
- [36] Y. Chinniah, R. Burton, and S. R. Habibi, "Failure monitoring in a high performance hydrostatic actuation system using the extended Kalman filter,"

- Mechatronics*, vol. 16, no. 10, pp. 643-653, 2006.
- [37] N. J. Gordon, D. J. Salmond, and A. F. Smith, "Novel approach to nonlinear/non-Gaussian Bayesian state estimation," *IEE Proceedings, Part F: Radar and Sonar Navigation*, vol. 140, no. 2, pp. 107-113, 1993.
- [38] X. Shao, B. Haung, and J. M. Lee, "Constrained Bayesian state estimation - A comparative study and a new particle filter based approach," *Journal of Process Control*, vol. 20, pp. 143-157, 2010.
- [39] T. Kailath, "A view of three decades of linear filtering theory," *IEEE Transactions of Information Theory*, vol. 20, no. 2, pp. 146-181, 1974.
- [40] B. D. O. Anderson and J. B. Moore, *Optimal Filtering*. Englewood Cliffs, NJ: Prentice-Hall, 1979.
- [41] D. Simon, *Optimal State Estimation: Kalman, H-Infinity, and Nonlinear Approaches*.: Wiley-Interscience, 2006.
- [42] R. E. Kalman, "A new approach to linear filtering and prediction problems," *ASME Transactions of Basic Engineering*, vol. 82, pp. 35-45, 1960.
- [43] S. J. Julier, J. K. Uhlmann, and H. F. Durrant-Whyte, "A New Method for Nonlinear Transformation of Means and Covariances in Filters and Estimators," *IEEE Transactions on Automatic Control*, vol. 45, pp. 472-482, March 2000.
- [44] V. Awasthi and K. Raj, "A survey on the algorithms of Kalman filter and its variants in state estimation," *VSRD Technical & Non-Technical Journal*, vol. 2, no. 2, pp. 73-88, 2011.
- [45] N. A. Carlson, "Fast triangular formulation of the square root filter," *AIAA Journal*, vol. 11, no. 9, pp. 1259-1265, 1973.
- [46] W. H. Press, S. A. Teukolsky, W. T. Vetterling, and B. P. Flannery, *Numerical recipes: The art of scientific computing*. New York, USA: Cambridge University Press, 2007, vol. , Numerical Recipes: The.
- [47] C. L. Thornton and G. J. Bierman, "Givens transformation techniques for Kalman filtering," *Acta Astronautica*, vol. 4, no. 7-8, pp. 847-863, 1977.

- [48] A. Andrews, "A square root formulation of the Kalman covariance equations," *AIAA Journal*, vol. 6, pp. 1165-1166, 1968.
- [49] M. Verhaegen and P. V. Dooren, "Numerical aspects of different Kalman filter implementations," *IEEE Transactions on Automatic Control*, vol. 31, no. 10, pp. 907-917, 1986.
- [50] L. Xie, C. Soh, and C. E. Souza, "Robust Kalman Filtering for Uncertain Discrete-Time Systems," *IEEE Transactions on Automatic Control*, vol. 39, no. 6, pp. 1310-1314, 1994.
- [51] M. A. Gandhi and L. Mili, "Robust Kalman filter based on a generalized maximum-likelihood-type estimator," *IEEE Transactions on Signal Processing*, vol. 58, no. 5, pp. 2509-2520, 2010.
- [52] J. Y. Ishihara, M. H. Terra, and J. T. Campos, "Robust Kalman filter for Descriptor Systems," *IEEE Transactions on Automatic Control*, vol. 51, no. 8, pp. 1354-1358, 2006.
- [53] F. Wang and V. Balakrishnan, "Robust Kalman filters for linear time-varying systems with stochastic parameter uncertainties," *IEEE Transactions on Signal Processing*, vol. 50, no. 4, pp. 803-813, 2002.
- [54] C. S. Hsieh, "Robust two-stage Kalman filtering for systems with unknown inputs," *IEEE Transactions on Automatic Control*, vol. 45, no. 12, pp. 2347-2378, 2000.
- [55] C. E. De Souza, "H-infinity and robust estimation," Department of Electrical and Computer Engineering, University of Newcastle, NSW, Australia,.
- [56] B. Hassibi, A. H. Sayed, and T. Kailath, *Indefinite Quadratic Estimation and Control: A Unified Approach to H2 and H-infinity Theories*. Philadelphia, PA, USA: SIAM Studies in Applied and Numerical Mathematics, 1999.
- [57] T. H. Lee, W. S. Ra, T. S. Yoon, and J. B. Park, "Robust Kalman Filtering Via Krein Space Estimation," *IEEE Proceedings of Control Theory Application*, vol. 151, no. 1, pp. 59-63, January 2004.
- [58] D. P. Bertsekas and I. B. Rhodes, "Recursive state estimation for a set membership description of uncertainty," *IEEE Transactions on Automatic Control*, vol. 16, no.

- 2, pp. 117-128, 1999.
- [59] I. R. Petersen and A. V. Savkin, *Robust Kalman Filtering for Signals and Systems with Large Uncertainties*. Birkhauser, Boston, USA: Springer, 1999.
- [60] C. J. Masreliez and R. D. Martin, "Robust Bayesian estimation for the linear model and robustifying the Kalman filter," *IEEE Transactions on Automatic Control*, vol. 22, no. 3, pp. 361-371, 1977.
- [61] P. K. Kitanidis, "Unbiased minimum-variance linear state estimation," *Automatica*, vol. 23, no. 6, pp. 775–778, 1987.
- [62] A. Benavoli, M. Zaffalon, and E. Miranda, "Robust filtering through coherent lower previsions," *IEEE Transactions on Automatic Control*, vol. 56, no. 7, pp. 1567-1581, 2011.
- [63] A. V. Savkin and I. R. Petersen, "Robust state estimation and model validation for discrete-time uncertain systems with a deterministic description of noise and uncertainty," *Automatica*, vol. 34, no. 2, pp. 271-274, 1998.
- [64] T. S. Schei, "A finite difference method for linearizing in nonlinear estimation algorithms," *Automatica*, vol. 33, no. 11, pp. 2051-2058, 1997.
- [65] M. Norgaard, N. K. Poulsen, and O. Ravn, "New developments in state estimation of nonlinear systems," *Automatica*, vol. 36, pp. 1627-1638, 2000.
- [66] M. Simandl, J. Kralovec, and T. Soderstrom, "Advanced point-mass method for nonlinear state estimation," *Automatica*, vol. 42, no. 7, pp. 1133-1145, 2006.
- [67] D. L. Alspach and H. W. Sorenson, "Nonlinear Bayesian estimation using Gaussian sum approximation," *IEEE Transactions of Automatic Control*, vol. 17, no. 4, pp. 439-448, 1972.
- [68] Y. Wu, M. Wu, and X. Hu, "A numerical-integration perspective on Gaussian filters," *IEEE Trnasactions on Signal Processing*, vol. 54, no. 8, pp. 2910-2921, 2006.
- [69] A. H. Stroud, *Gaussian quadrature formulas*. New Jercy, USA: Prentice Hall, 1966.

- [70] S. J. Julier and J. K. Uhlmann, "Unscented filtering and nonlinear estimation," *Proceeding of the IEEE*, vol. 92, no. 3, pp. 401-422, 2004.
- [71] K. Ito and K. Xiong, "Gaussian filters for nonlinear filtering problem," *IEEE Transactions on Automatic Control*, vol. 45, no. 5, pp. 910-927, 2000.
- [72] J. S. Liu, *Monte Carlo strategies in scientific computing.*: Springer, 2001.
- [73] H. Niederreiter, "Quasi-Monte Carlo methods and pseudo-random numbers," *Bulletin of American Mathematics Society*, vol. 84, pp. 957-1041, 1978.
- [74] S. Sloan, and I. H. Joe, *Lattice methods for multiple integration*. Oxford: Oxford University Press, 1994.
- [75] M. Griebel, and T. Gerstner, "Numerical integration using sparse grids," *Numerical Algorithms*, vol. 18, no. 4, pp. 209-232, 1998.
- [76] J. H. Kotecha and P. A. Djuric, "Gaussian particle filtering," *IEEE Transactions on Signal Processing*, vol. 51, no. 10, pp. 2592–2601, 2003.
- [77] M. S. Arulampalam, S. Maskell, N. Gordon, and T. Clapp, "A tutorial on particle filters for online nonlinear/non-Gaussian Bayesian tracking," *IEEE Transactions on Signal Processing*, vol. 59, no. 2, pp. 174-188, 2002.
- [78] R. Van der Merwe, "Sigma-Point Kalman Filters for Probabilistic Inference in Dynamic State Space Models," OGI School of Science and Engineering, Oregon Health and Science Univeristy, PhD Thesis 2004.
- [79] J. Ambadan and Y. Tang, "Sigma-point Kalman filter data assimilation methods for strongly nonlinear systems," *Journal of the Atmospheric Sciences*, vol. 66, no. 2, 2009.
- [80] E. A. Wan and R. Van der Merwe, "The unscented Kalman filter for nonlinear estimation," in *IEEE Symposium on Adaptive Systems for Signal Processing, Communications, and Control*, Lake Louise, Canada, 2000, pp. 153-158.
- [81] S. Julier and J. k. Uhlmann, "A general method for approximating nonlinear transformations of probability distributions," *Transformation, Robotics Research Group, Oxford University*, vol. 4, no. 7, pp. 1-27, 1996.

- [82] S. Julier, "The Spherical Simplex Unscented Transformation," in *Proceedings of the American Conference Conference*, 2003, pp. 2430-2434.
- [83] G. Steiner, D. Watzenig, C. Magel, and U. Baumgaetner, "Statistical robust design using the unscented transformation," *The International Journal for Computation and Mathematics in Electrical and Electronic Engineering*, vol. 24, no. 2, pp. 606-619, 2005.
- [84] S. A. Smolyak, "Quadrature and interpolation formulas for tensor products of certain classes of functions," *Soviet. Math. Dokl.*, vol. 4, pp. 240-243, 1963.
- [85] S. L. Sobolev, "Formulas of mechanical cubature on the surface of a sphere," *Sibirsk. Math. (Russian)*, vol. Z 3, pp. 769-796, 1981.
- [86] R. Cools, "Constructing cubature formulas: the science behind the art," *Acta Numerica*, Cambridge University Press, vol. 6, pp. 1-54, 1997.
- [87] B. Jia, M. Xin, and Y. Cheng, "High-degree cubature Kalman filter," *Automatica*, vol. 49, pp. 510-518, 2013.
- [88] A. J. Haug, "A tutorial on Bayesian estimation and tracking techniques applicable to nonlinear and non-Gaussian processes," The MITRE Corporation, McLean, Virginia, Technical Report MTR 05W0000004, 2005.
- [89] A. Doucet, J. F. G. de Freitas, and N. J. Gordon, *Sequential Monte Carlo methods in practice*. New York, USA: Springer-Verlag, 2001.
- [90] A. Doucet, S. Godsill, and C. Andrieu, "On sequential monte carlo sampling methods for Bayesian filtering," *Statistics and Computing*, vol. 10, pp. 197-208, 2000.
- [91] D. L. Alspach and H. W. Sorenson, "Nonlinear Bayesian estimation using Gaussian sum approximation," *IEEE transactions on Automatic Control*, vol. 17, pp. 439-448, 1972.
- [92] S. C. Kramer and H.W. Sorenson, "Recursive Bayesian estimation using piece-wise constant approximations," *Automatica*, vol. 24, pp. 789-801.
- [93] B. Hassibi, "On the robustness of LMS filters," Department of Electrical Engineering, California Institute of Technology, Pasadena, CA, USD, PhD Thesis

2003.

- [94] N. Shimkin, "Estimation and identification in dynamical systems," Israel Institute of Technology, Department of Electrical Engineering, Lecture Notes of "Estimation and Identification in Dynamical Systems" course 2009.
- [95] R. F. Stengel, *Optimal control and estimation*. Mineola, New York, USA: Wiley, 1994.
- [96] M. W. Hofbar and B. C. Williams, "Hybrid estimation of complex systems," *IEEE Transactions on Systems, Man, and Cybernetics*, vol. 34, no. 5, pp. 2178-2191, 2004.
- [97] J. K. Tugnait, "Detection and estimation for abrupt changing systems," *Automatica*, vol. 18, no. 5, pp. 607-615, 1982.
- [98] D. T. Magill, "Optimal adaptive estimation of sampled stochastic processes," *IEEE Transactions on Automatic Control*, vol. 10, no. 5, pp. 434-439, 1965.
- [99] X. Rong Li, "Hybrid Estimation Technique," in *Control and Dynamic Systems*. New York, United States: Academic Press, 1996, ch. Volume 76, pp. 213–287.
- [100] D. G. Lainiotis, "Partitioning: a unifying framework for adaptive systems, I: estimation," *Proceeding of the IEEE*, vol. 64, no. 8, pp. 1126-1143, 1976.
- [101] D. G. Lainiotis, "Optimal adaptive estimation: Structure and parameter adaptation," *IEEE Transactions on Automatic Control*, vol. 16, no. 2, pp. 160–170, 1971.
- [102] P. S. Maybeck, "Application of multiple model adaptive algorithms to reconfigurable flight control," *Control, Dynamics and System*, vol. 52, pp. 291-320, 1992.
- [103] P. S. Maybeck, "Multiple model adaptive algorithms for detecting and compensating sensor and actuator/surface failures in aircraft flight control systems," *International Journal of Robust and Nonlinear Control*, vol. 9, pp. 1051-1070, 1999.
- [104] P. S. Maybeck, *Stochastic Model, Estimation and Control, Vol. II*. New York, United States: Academic Press, 1982.

- [105] P. S. Maybeck, *Stochastic Models, Estimation, and Control, Vol. I*. New York, United States: Academic Press, 1979.
- [106] M. J. Stepaniak and P. S. Maybeck, "Model-based control redistribution applied to the Vista F-16," *IEEE Transactions on Aerospace and Electronic System*, vol. 34, no. 4, pp. 1249-1260, 1998.
- [107] H. A. P. Bloom and Y. Bar-Shalom, "The interacting multiple model algorithm for systems with Markovian switching coefficients," *IEEE Transactions on Automatic Control*, vol. 33, no. 8, pp. 780-783, 1988.
- [108] E. Mazor, A. Averbuch, Y. Bar-Shalom, and J. Dayan, "Interacting multiple model method in target tracking: a survey," *IEEE Transactions on Aerospace and Electronic Systems*, vol. 34, no. 1, pp. 103-123, 1998.
- [109] X. Rong Li and Y. Bar-Shalom, "A recursive multiple model approach to noise identification," *IEEE Transactions on Aerospace and Electronic Systems*, vol. 30, no. 3, pp. 671-684, X. Rong Li, and Y. Bar-Shalom, "", , Vol. 30, No. 3, , 1994. 1994.
- [110] X. Rong Li and Y. Bar-Shalom, "Performance prediction of the interacting Multiple Model algorithm," *IEEE Transactions on Aerospace and Electronic Systems*, vol. 29, no. 3, pp. 755-771, 1993.
- [111] X. Rong Li and Y. Zhang, "Multiple Model estimation with variable structure, part V: likely-model set algorithm," *IEEE Transactions on Aerospace and Electronic Systems*, vol. 36, no. 2, pp. 448-466.
- [112] X. Rong Li, Z. Zhao, and X. B. Li, "General model-set design methods for Multiple Model approach," *IEEE Transactions on Automatic Control*, vol. 50, no. 9, pp. 1260-1276, [108] X. Rong Li, Z. Zhao, and X.B. Li, 2005.
- [113] Y. Bar-Shalom and W. D. Blair, *Multi-Target Multi Sensor tracking: Applications and Advances, Volume III.*: Artech House, INC, 1991.
- [114] R. L. Moose, "An adaptive state estimation solution to the maneuvering target problem," *IEEE Transactions on Automatic Control*, vol. 20, no. 3, pp. 359-362, 1975.

- [115] P. Eide and P. Maybeck, "An MMAE failure detection system for the F-16," *IEEE Transaction on Aerospace and Electronic Systems*, vol. 32, no. 2, pp. 1125-1135, 1996.
- [116] T. E. Menke and P. S. Maybeck, "Sensor/actuator failure detection in the Vista F-16 by multiple model adaptive estimation," *IEEE Transactions on Aerospace and Electronic Systems*, vol. 31, no. 4, pp. 1218-1229, 1995.
- [117] E. Phelps, P. Willett, T. Kirubarajan, and C. Brideau, "Predicting time to failure using the IMM and excitable tests," *IEEE Transactions on Systems, Man, and Cybernetics-Part A: Systems and Humans*, vol. 37, no. 5, pp. 630-642, 2007.
- [118] J. Ru and X. Rong Li, "Variable-structure multiple-model approach to fault detection, identification, and estimation," *IEEE Transactions on Control Systems Technology*, vol. 16, no. 5, pp. 1029-1038, 2008.
- [119] M. Athans, "The stochastic control of the F-8C aircraft using a multiple model adaptive control (MMAC) method - Part I: Equilibrium flight," *IEEE Transactions on Automatic Control*, vol. 22, no. 5, pp. 768-780, 1977.
- [120] P. S. Maybeck and R. D. Stevens, "Reconfigurable flight control via multiple model adaptive control methods," *IEEE Transactions on Aerospace and Electronic Systems*, vol. 27, no. 3, pp. 470-480, 1991.
- [121] H. A. P. Bloom, "An efficient filter for abruptly changing systems," in *Proceedings of the 23rd Conference on Decision and Control*, Las Vegas, NV, United States, 1984, pp. 656-658.
- [122] X. Rong Li and Y. Bar-Shalom, "Multiple Model estimation with variable structure," *IEEE Transactions on Automatic Control*, vol. 41, no. 4, pp. 478-493, 1996.
- [123] M. Lu, X. Qiao, and G. Chen, "A parallel square root algorithm for modified extended Kalman filter," *IEEE Transactions on Aerospace and Electronic Systems*, vol. 28, no. 1, pp. 153-163, 1992.
- [124] S. M. Aly, R. El Fouly, and H. Braka, "Extended Kalman filtering an dinteracting multiple model for tracking maneuvering targets in sensor networks," in *IEEE 17th Workshop on Intelligent Solution in Embedded Systems*, 2009, pp. 149-156.

- [125] D. Crisan and A. Doucet, "A survey of convergence results on particle filtering for practitioners," *IEEE Transactions on Signal Processing*, vol. 50, no. 3, pp. 736-746, 2002.
- [126] S. A. Gadsden, S. R. Habibi, and t. Kirubarajan, "A novel interacting multiple model method in target tracking," in *13th Conference on Information Fusion*, Edinburg, UK, 2010, pp. 1-8.
- [127] X. Rong Li, "Multiple-model estimation with variable structure-Part II: model-set adaptation," *IEEE Transactions on Automatic Control*, vol. 45, no. 11, pp. 2047-2060, 2000.
- [128] X. Rong Li, X. Zhi, and Y. Zhang, "Multiple Model estimation with variable structure, Part III: model-group switching algorithm," *IEEE Transactions on Aerospace and Electronics Systems*, vol. 35, no. 1, 1999.
- [129] X. Rong Li, V. P. Jilkov, and J. F. Ru, "Multiple-model estimation with variable structure-Part VI: expected-mode augmentation," *IEEE Transactions on Aerospace and Electronic Systems*, vol. 41, no. 3, pp. 853–867, 2005.
- [130] P. Li and V. Kadiramanathan, "Particle filtering based likelihood ratio approach to fault diagnosis in nonlinear stochastic systems," *IEEE Transactions on Systems, Man, and Cybernetics, Part C: Applications and Reviews*, vol. 31, no. 3, pp. 337-343, 2001.
- [131] V. Kadiramanathan, P. Li, M. H. Jaward, and S. G. Fabri, "A sequential Monte-Carlo filtering approach to fault detection and isolation in nonlinear systems," in *Proceedings of the IEEE Conference on Decision and Control*, Sydney, Australia, 2000, pp. 4341-4346.
- [132] M. Blanke, M. Kinnaert, J. Lunze, and M. Staroswiecki, *Diagnosis and Fault-Tolerant Control*. Berlin: Springer-Verlag, 2006.
- [133] P. D. Hanlon and P.S. Maybeck, "Multiple-model adaptive estimation using a residual correlation Kalman filter bank," *IEEE Transactions on Aerospace and Electronic System*, vol. 36, no. 2, pp. 393-406, 2000.
- [134] S. M. Kay, *Modern Spectral Estimation*. Englewood Cliffs, NJ, United States: Prentice Hall, 1988.

- [135] S. R. Habibi and R. Burton, "The variable structure filter," *ASME Journal of Dynamic Systems, Measurement and Control*, vol. 125, no. 3, pp. 287-293, 2003.
- [136] G. Zames, "Feedback and optimal sensitivity: model reference transformations, multiplicative seminorms and approximate inverses," *IEEE Transactions on Automatic Control*, vol. 26, pp. 301-320, 1981.
- [137] J. J. Slotine, J. K. Hedrick, and E. A. Misawa, "On sliding observers for nonlinear systems," *Journal of Dynamic Systems, Measurement, and Control*, vol. 109, pp. 245-252, 1987.
- [138] B. L. Walcott and S. H. Zak, "Combined observer-controller synthesis for uncertain dynamical systems with applications," *IEEE Transactions on Systems, Man, and Cybernetics*, vol. 18, no. 1, pp. 88-104, 1988.
- [139] C. Edwards and S. K. Spurgeon, "On the development of discontinuous observers," *International Journal of Control*, vol. 59, no. 5, pp. 1211-1229, 1994.
- [140] S. A. Gadsden and S. R. Habibi, "A new form of the smooth variable structure filter with a covariance derivation," in *IEEE Conference on Decision and Control*, Atlanta, United States, 2010.
- [141] S. R. Habibi, "The extended variable structure filter," *ASME Journal of Dynamic Systems, Measurements and Control*, vol. 128, no. 2, pp. 341-351, 2006.
- [142] S. A. Gadsden, D. Dunne, S. R. Habibi, and T. Kirubarajan, "Combined particle and smooth variable structure filtering for nonlinear estimation problems," in *14th International Conference on Information Fusion*, Chicago, United States, 2011.
- [143] S. A. Gadsden, M. Al-Shabi, and S. R. Habibi, "Estimation of an electro-hydrostatic actuator using a combined cubature Kalman and smooth variable structure filter," in *ASME International Mechanical Engineering Congress and Exposition*, Vancouver, Canada, 2010.
- [144] S. A. Gadsden, K. McCullough, and S. R. Habibi, "Fault detection and diagnosis of an electro-hydrostatic actuator using a novel interacting multiple model approach," in *American Control Conference*, San Francisco, United States, 2011.
- [145] S. A. Gadsden, M. El Sayed, and S. R. Habibi, "The continuous-time smooth variable structure filter," in *23rd Canadian Congress of Applied Mechanics*,

Vancouver, Canada, 2011.

- [146] M. A. Al-Shabi, "The genral toeplitz/observability smooth variable structure filter," Department of Mechanical Engineering, McMaster University, PhD Thesis 2011.
- [147] D. Simon, "From here to infinity," *Embeded Systems Programming*, vol. 14, no. 11, pp. 20-32, 2000.
- [148] R. Banavar, "A game theoretic approach to linear dynamic estimation," University of Texas at Austin, Austin, Texas, USA, PhD Thesis 1992.
- [149] J. J. Slotine, "Sliding controller design for nonlinear systems," *International Journal of Control*, vol. 40, pp. 421-434, 1984.
- [150] S. R. Habibi and R. Burton, "Parameter identification for a high performance hydrostatic actuation system using the variable structure filter concept," *ASME Journal of Dynamic Systems, Measurement and Control*, vol. 129, no. 2, pp. 229-235, 2007.
- [151] H. Elmali, and N. Olgac, "Robust output tracking control of nonlinear MIMO systems via sliding mode technique," *Automatica*, vol. 28, no. 1, pp. 145-151, 1992.
- [152] L. W. Chang, "A versatile sliding control with a second-order sliding condition," in *American Control Conference*, Boston, MA, USA, 54-55, 1991 1991, pp. 54-55.
- [153] Istefanopulos Y., and Kaynak O. Sarpturk S. Z., "On the stability of discrete-time sliding mode control systems," *IEEE Transactions on Automatic Control*, vol. 32, no. 10, pp. 930-932, 1987.
- [154] Brogliato B., and Orlov Y. V. Acary V., "Chattering-free digital sliding-mode control with state observer and disturbance rejection," *IEEE Transactions on Automatic Control*, vol. 57, no. 5, pp. 1087-1101, 2012.
- [155] A. Bartoszewicz, "Discrete-time quasi-sliding-mode control strategies," *IEEE Transactions on Industrial Electronics*, vol. 45, no. 4, pp. 633-637, 1998.
- [156] A. S. Nouri, R. B. Abdenmour, M. Mihoub, "A second order discrete sliding mode observer for the variable structure control of a semi-bat reactor," *Control Engineering Practice*, vol. 19, pp. 1216-1222, 2011.

- [157] L. M. Fridman, "An averaging approach to chattering," *IEEE Transactions on Automatic Control*, vol. 46, no. 8, pp. 1260-1265, 2001.
- [158] L. Fridman, "Singularly perturbed analysis of chattering in relay control system," *IEEE Transactions on Automatic Control*, vol. 47, no. 12, pp. 2078-2084, 2002.
- [159] Fridman L., Pisano A., and Usai E. Boiko I., "Analysis of chattering in systems with second-order sliding modes," *IEEE Transactions on Automatic Control*, vol. 52, no. 11, pp. 2085-2102, 2007.
- [160] A. F. Filippov, *Differential equations with discontinuous right-hand sides.*: Springer, 1998.
- [161] S. K. Spurgeon, "Hyperplane design techniques for discrete-time variable structure control systems," *International Journal on Control*, vol. 55, no. 2, pp. 445–456, 1992.
- [162] A. Pisano, and E. Usai Bartolini, "Variable structure control of nonlinear sampled data systems by second order sliding modes," in *Variable structure systems, sliding mode and nonlinear control, Lecture Notes in Control and Information Sciences.*: Springer, p. Vol. 247/19.
- [163] A. Pisano, and E. Usai, G. Bartolini, "Direct discretization of second order sliding mode control for uncertain nonlinear systems," in *Proceedings of the 37th IEEE Conference on Decision & Control*, Florida, USA, 1998, pp. 2398-2403.
- [164] G. Luenberger, *Introduction to Dynamic Systems*. New York, USA: Wiley, 1979.
- [165] S. A. Gadsden, "Smooth Variable Structure Filtering: Teory and Applications," McMaster University - Department of Mechanical Engineering, Hamilton, PhD Thesis 2011.
- [166] M. S. Pedersen, and K. B. Petersen, *The Matrix Cookbook*. Copenhagen, Denmark: Technical University of Denmark, 2008.
- [167] F. Yan and J. Wang, "Design and robustness analysis of discrete observers for diesel engine in cylinder oxygen mass fraction cycle-by-cycle estimation," *IEEE Transactions on Control Systems Technology*, vol. 20, no. 1, pp. 72-83, 2012.

- [168] R. Isermann, *Fault Diagnosis Systems*. Berlin, Germany: Springer-Verlag, 2006.
- [169] K. McCullough, "Design and Characterization of a Dual Electro-Hydrostatic Actuator," Department of Mechanical Engineering, McMaster University, Hamilton, Ontario, M.A.Sc. Thesis 2011.

Appendix

In this section, some of the state estimation methods including the unscented Kalman filter (UKF), the cubature Kalman filter (CKF), and the particle filter (PF) are combined within an Interacting Multiple Models (IMM) structure for fault detection and identification. Experimentations are performed using the EHA setup with the same properties and inputs presented in Chapter 5. Note that for the PF, the effective threshold (Neff) is set to 0.8, and 350 particles are used in total. Furthermore, the UKF parameter \mathcal{K} is defined as: 1×10^{-3} .

The EHA dynamics are described by equations 5.1 through 5.3. For all strategies, the initial state estimate and state error covariance matrix are defined as follows:

$$\hat{x}_{0|0} = [0 \quad 0 \quad 0]^T, \quad (\text{A.1})$$

$$P_{0|0} = \begin{bmatrix} 1 & 0 & 0 \\ 0 & 10 & 0 \\ 0 & 0 & 50 \end{bmatrix}. \quad (\text{A.2})$$

The system and measurement noise covariance's Q and R are also given by:

$$Q = \text{Diag} \left(\left[10^2 \quad 10^3 \quad 10^5 \right] \right), \quad (\text{A.3})$$

$$R = 10^{-1}. \quad (\text{A.4})$$

For the IMM settings, the initial mode probability was defined as follows:

$$\mu_{i,0} = [0.90 \quad 0.05 \quad 0.05]^T. \quad (\text{A.5})$$

The mode transition matrix P_{ij} is defined as a 3-by-3 diagonal matrix with 0.90 along the diagonal and 0.05 on the off-diagonal. Similar to experimentations of Chapter 5, the experimental scenario involves the EHA operating normally for two seconds, a leakage fault for two seconds, followed by a friction fault for the last two seconds. Tables A.1 through A.3 present the mode probability results (confusion matrices) for the IMM-based UKF, IMM-based CKF, and the IMM-based PF strategies. They provide an indication of how accurate the models are in detecting the correct operating mode.

Table A.1: Mode probability results for the IMM-UKF

		Actual Condition		
		Normal	Leakage	Friction
Predicted Condition	Normal	70.28 %	16.67 %	2.72 %
	Leakage	29.63 %	80.33 %	3.60 %
	Friction	0.09 %	3.00 %	93.68 %

Table A.2: Mode probability results for the IMM-CKF

		Actual Condition		
		Normal	Leakage	Friction
Predicted Condition	Normal	96.82 %	27.19 %	13.63 %
	Leakage	2.98 %	65.66 %	1.02 %
	Friction	0.21 %	7.14 %	85.35 %

Table A.3: Mode probability results for the IMM-PF

		Actual Condition		
		Normal	Leakage	Friction
Predicted Condition	Normal	59.31 %	1.59 %	9.07 %
	Leakage	21.94 %	97.77 %	9.05 %
	Friction	18.75 %	0.63 %	81.88 %

All of the methods successfully detected the correct operating mode (a diagonal probability of 50% or greater); however, with varying degrees of confidence. The IMM-CKF strategy correctly identified the EHA operating normally with the highest probability level (96.82%). The IMM-PF detected the leakage fault with the highest level (97.77%), and the IMM-UKF correctly identified the friction fault with the highest confidence level (93.68%). Another interesting factor to study is the overall correct detection probability. This can be studied by referring to the confusion matrices and Figure A.1. The overall correct detection probability for these three estimation methods and some other methods of Chapter 5 are compared in Figure A.1. It is observed that the IMM-based dynamic 2nd-order SVSF has the largest probability, followed by the IMM-based 1st-order SVSF.

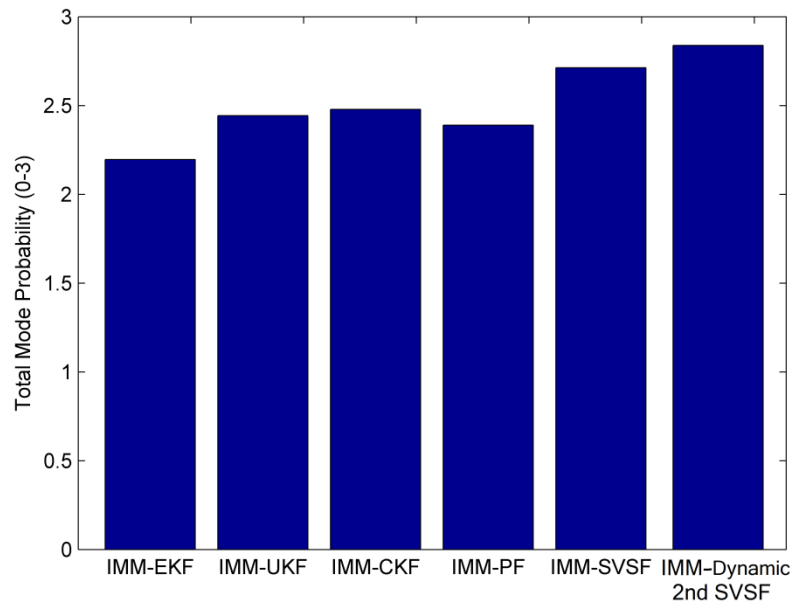


Figure A.1: Total mode probability detections by different estimation methods

Note that the summation of the diagonal elements in the matrices is equal to the total mode probability. Ideally, the perfect detection strategy would correctly identify the

operating modes and thus, the total mode probability would be 3 or 300%. The IMM-CKF provides the best results in terms of maximizing the correct mode detection and minimizing the misclassifications. The IMM-CKF has a total mode probability of 247.83%, followed by the IMM-UKF with a total mode probability of 247.83%, and the IMM-PF with a total mode probability of 238.96%. Figures A.2 through A.4 present the mode probability profiles for the EHA setup under the normal condition, internal leakage and friction fault conditions, respectively. Compared with other popular IMM methods, it appears that the IMM-based SVSF method provides the best method for FDI, followed by the IMM-based CKF.

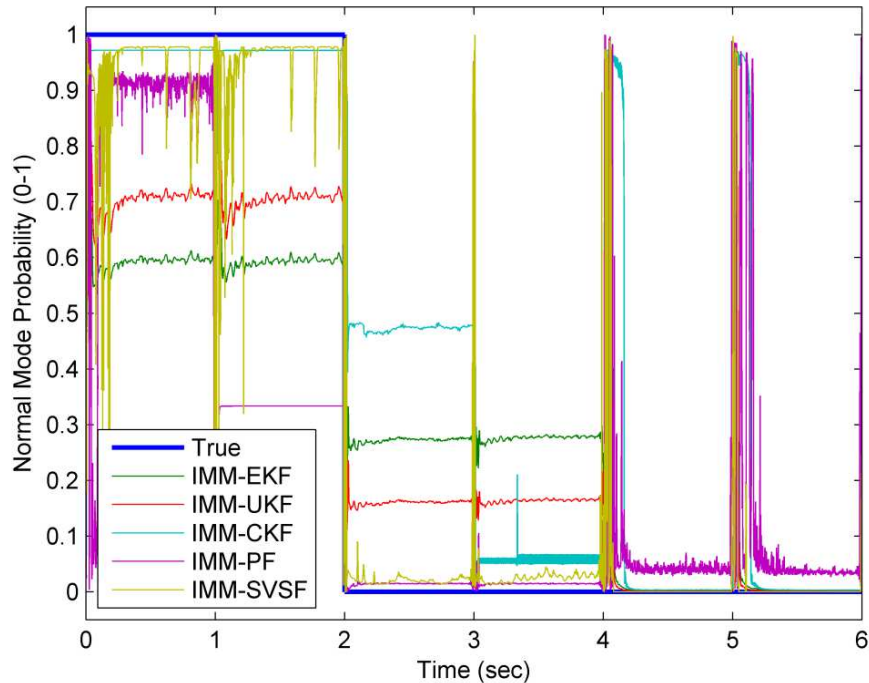


Figure A.2: Normal mode probability results by different estimation methods

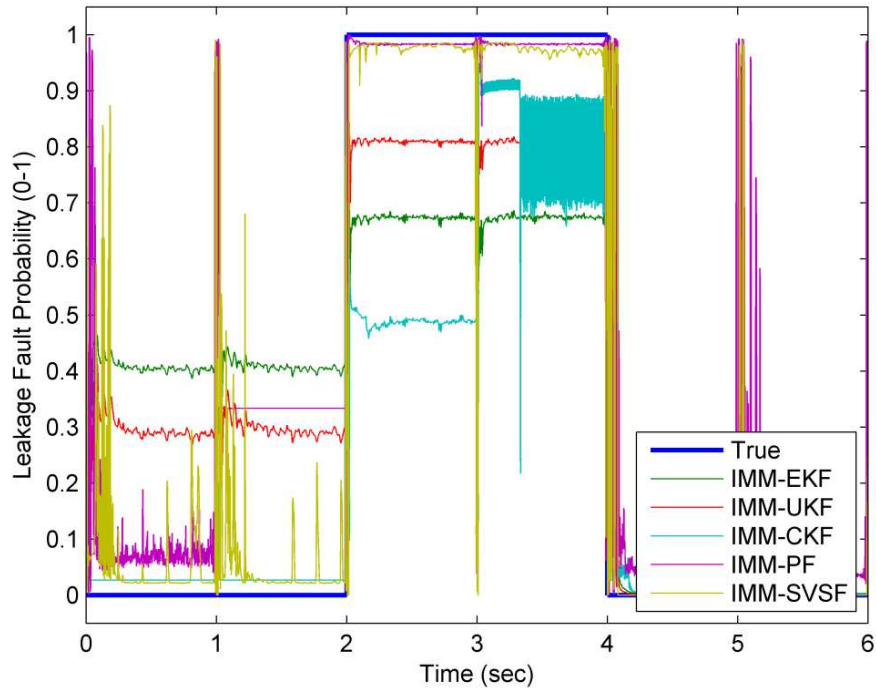


Figure A.3: Leakage fault mode probability results by different estimation methods

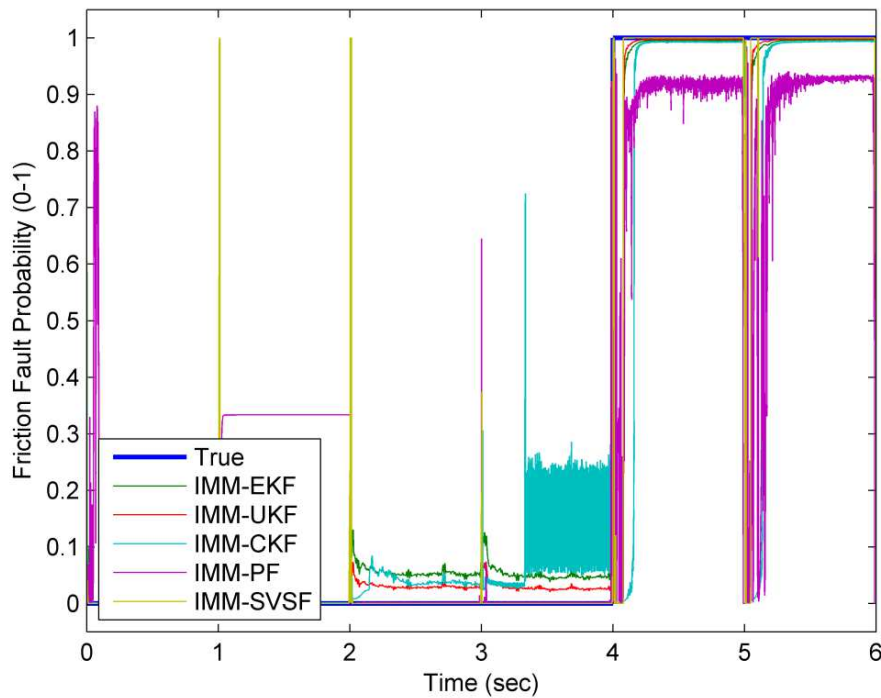


Figure A.4: Friction fault mode probability results by different estimation methods